OS-GE 85-03
August 1985

Double Beta Decay and Majorana Neutrino

M. Doi

Osaka College of Phamacy, Matsubara, Osaka 580, Japan

T. Kotani and E. Takasugi

Institute of Physics, College of General Education

Osaka University, Toyonaka 560, Japan

Abstruct

This review consists of three parts: Various properties of the quantized neutrino fields are summarized in part I from the viewpoint that a Dirac neutrino consists of two Majorana neutrinos with a degenerate mass but with opposite CP signs. It is shown why the Dirac neutrino has a freedom of the phase transformation to guarantee the lepton number conservation, while the Majorana neutrino does not.

The part II is devoted to the theoretical investigation of the double beta decay and the analysis on the experimental data. Various corrections due to the vanishing terms in the closure approximation and the higher spherical waves of leptons are estimated. The constraints on the effective neutrino mass and the effective right-handed weak interaction parameters are derived from the present experimental data. In part III, the above bounds are compared with those from other processes like the ^{3}H decay, the neutrino oscillation, the π-μ-e decay etc. The possible mixing schems of the neutrino system are explored.

Contents

§1 Introduction

§1.1 Finite neutrino mass and the V+A current

(i) Motivations:

Questions whether neutrinos have finite mass and whether the right-handed weak charged current exists are of great interest. They are the important issues to provide evidence for possible new physics beyond the minimum standard model of electroweak interaction by Glashow, Weinberg and Salam: The main assumptions of this model can be summarized as follows:

(1) The gauge group is $SU(2)_L \times U(1)$, i.e., only the V-A interaction.

(2) There are left-handed fermion doublets and right-handed fermion singlets for three generations of quarks and leptons in $SU(2)_L$.

(3) There is no right-handed neutrinos, i.e., no Dirac type mass term.

(4) Only one doublet of Higgs bosons is assumed, which induces masses for charged fermions and gauge bosons, but does not give the Majorana type mass term for neutrinos.

(5) The CP violating phase is introduced solely through the Kobayashi-Maskawa (generalized Cabbibo) mixing matrix for the quark sector.

At present, all known experimental results, such as lepton and baryon number conservations, lepton-quark universality, the absence of neutrino masses and their mixing, etc., do not show any large deviations from the minimum standard model. On the other hand, neutrino mass seems to play a crucial role in astrophysics as well as in cosmology. In this paper, we shall examine the first, third and fourth assumptions mainly, though some models beyond other assumptions are considered as generalized cases.

Let us express our questions in more explicit forms:

[Q1] Are neutrinos really massless ($m_\nu = 0$)? If not, why is the observed limit or value of the electron neutrino mass much smaller than the electron mass (m_e)?

[Q2] If $m_\nu \neq 0$, are neutrinos Dirac or Majorana particles?

[Q3] If $m_\nu \neq 0$, do the weak eigenstate neutrinos differ from the mass eigenstate ones? Are there neutrino mixings and the new CP violating phases similarly to the quark mixing?

[Q4] Why does the Nature favor only the left-handed (V-A) current, i.e., $SU(2)_L$ only? Isn't it natural to consider[1] that the V-A current appears at the present low energy region, but there should be the left-right symmetry above some higher energy?

These questions could shed light on the validity of more encompassing theoretical schemes such as grand unified theories.

(ii) Why do we consider the Majorana neutrino?

In the Dirac description of spin 1/2 fermion (Dirac particle), there exist the negative energy states which lead to the symmetric description of particles and antiparticles. In 1937, Majorana showed that it is possible to construct the theory without negative energy state by using the real representation of the classical spinor field, which is called the Majorana field. In this scheme, particle is assigned to be equal to its antiparticle and four freedoms of one Dirac particle are reduced to two, i.e. two spin states. Therefore, the Majorana scheme is used only for neutral fermions such as neutrinos.

The V-A theory of charged current interaction was established in 1957. Neutrinos were assumed to be massless so that they are

in the definite helicity state (Weyl neutrinos) to assure the V-A structure of leptonic current. Ryan and Okubo, Pauli, and Gürsey[2] showed that the Majorana description of massless neutrinos is equivalent to the Weyl (Dirac) description, if the interaction of neutrino is restricted to the V-A interaction; that is, for a Majorana neutrino, the helicity h works as an indicator to identify particle ($h = -1/2$) or antiparticle ($h = 1/2$) in the Weyl description with the V-A leptonic current. As a result, the questions whether neutrinos are Majorana or Weyl (Dirac) particles had not been considered seriously.

In the middle of 1970's, the interest in the neutrino mass revived in accord with the progress of grand unified theories (GUTs) of strong and electroweak interactions. In this scheme, leptons and quarks are treated on the same basis, so that there seems to be no reason to discriminate neutrinos from other massive fermions and thus to protect massive neutrinos. If neutrinos are massive, the question [Q2] becomes an important and fundamental one. In the gauge theories with both the left- and right-handed weak interactions, if neutrinos are massless, there is no distinction between the Majorana and Weyl (Dirac) descriptions, because the left- and right-handed neutrinos represent the independent degree of freedoms.

There are two motivations to consider neutrinos to be Majorana particles. One is that a Dirac neutrino consists of a pair of mass degenerate Majorana neutrinos.[3),4),5)] [see §2.1 and Eq.(2.5.1)] On the other hand, within the framework of the gauge theory, the conservation of electric charge forces the charged fermions to be Dirac particles. The origin of the phase freedom for the Dirac field to introduce the charge and lepton number conservation will be explained in Eq.(2.5.8). Since no such strong symmetry is required for neutrinos,

their description as Majorana particles seems to be more fundamental. The other is based on the argument to understand why the "observed left-handed" electron neutrinos are so light [Q1], even though they are treated similarly to quarks and charged leptons. One beautiful and attractive idea is the so-called "see-saw" mechanism, proposed by Gell-Mann, Ramond and Slansky and by Yanagida[6] in 1979. In this mechanism, it takes advantage of the fact that the left- and right-handed Majorana neutrinos can acquire the small and large masses separately, instead of forming a Dirac neutrino, as will be explained in § 2.6.1. From these standpoints, neutrinos are likely to be Majorana particles, if they are massive at all.

(iii) The neutrino mass and the V+A interaction:

The idea of the see-saw mechanism to explain the smallness of the electron neutrino mass can be realized in the models which include the $SU(2)_L \times SU(2)_R \times U(1)$ gauge group.[1] That is, the existence of the right-handed (V+A) current [Q4] should be confirmed experimentally to utilize the see-saw mechanism.

As for the neutrino mixing [Q3], since there exists the Kobayashi-Maskawa (generalized Cabibbo) mixing in the quark sector, it is natural to assume the corresponding neutrino mixing in the lepton sector, if neutrinos are massive. Although there is no definite indication of the neutrino oscillation at present,[7] except the Bugey experiment,[8] we shall take account of the neutrino mixing in our analysis [§§3.1,9and10]. If neutrinos are Majorana particles, there are some special properties for their mixing matrix in contrast with the Dirac neutrino case, e.g. the additional CP

violating phases [9),10)] [§2.3]. Even in the CP conserving case, it is possible to formulate two different descriptions of the quantized Majorana field, so that the presentations of mixing matrix are different [§2.3.2 and §2.4.5]. In order to make these points clear, we shall summarize our description of Majorana neutrinos and compare it with other formulations [Part I].

In order to confirm the finite neutrino mass, there are various experiments such as the β decays of ^{3}H, ^{35}S and ^{63}Ni, the neutrino oscillation, the electron capture in ^{163}Ho and so on [§9]. Concerning the V+A charged current, the precise measurements on the β and μ decays have been performed [§10]. In addition to these problems, the question whether neutrinos are Dirac or Majorana [Q2] can be tested by the neutrinoless double β decay directly [§1.3].

§1.2 The neutrino emitting double β decay:

(i) General properties of the $\beta\beta$ decay:

The $\beta\beta$ decay can occur in the case where the single β decay of parent nucleus (A, Z-2) is forbidden energetically or at least strongly suppressed due to a large change of spin. As a typical example, the level structure of ^{76}Ge is shown in Fig. 1.1. The $\beta\beta$ transition takes place through two decay modes: The two neutrino emitting mode suggested by Mayer in 1935 is[11)]

$$(\beta\beta)_{2\nu}\ :\ N_i(A, Z-2) \longrightarrow N_f(A, Z) + 2e^- + 2\bar{\nu}_e , \qquad (1.2.1)$$

and the neutrinoless mode proposed by Furry in 1939 is[12)]

$$(\beta\beta)_{0\nu}\ :\ N_i(A, Z-2) \longrightarrow N_f(A, Z) + 2e^- . \qquad (1.2.2)$$

The former $(\beta\beta)_{2\nu}$ mode can occur as a second order perturbation of the weak interaction within the minimum standard model independently

of whether neutrinos are Dirac or Majorana and massive or massless, if it is allowed energetically. In Fig. 1.2, this mode is shown for the 2n-mechanism where the successive β transitions of two neutrons (n_1 and n_2) trigger the $\beta\beta$ decay, as first suggested by Mayer.[11)]

In Table 1.1, the $\beta\beta$ transitions are listed for naturally occurring isotopes with their total kinetic energy release T in units of KeV. On the third column, we list the comparative half-lives for the $(\beta\beta)_{2\nu}$ mode, $T_{2\nu}$, multiplied by $\left|M_{GT}^{(2\nu)}/\mu_0\right|^2$ which is of order of 10^{-2} and should be determined theoretically from the ratios of the nuclear matrix elements to the excitation energies due to the denominator of the second order perturbation theory [§3.2]. These numerical values are the inverses of the integrated kinematical factors defined in Eq.(3.2.11).

As it is clear from Table 1.1, if the half-life $T_{2\nu}$ of the $(\beta\beta)_{2\nu}$ mode is measured, then $\left|M_{GT}^{(2\nu)}/\mu_0\right|$ can be determined uniquely. It offers the quite interesting new information to the nuclear physics itself, because it is the weighted sum of contributions from all virtual intermediate nuclear states with $J = 1^+$, the Gamow-Teller states [§7.1 and §8.1].

All of the parent and daughter isotopes in Table 1.1 are even-even nuclei. The pairing force acting between like nucleons is responsible for the increase in the binding energy of these nuclei relative to the odd-odd isotopes, and prevents the single β decay. This same pairing force leads to 0^+ ground states for the daughter nuclei, so that all the g.s.$\rightarrow$g.s. transitions in Table 1.1 is the $0^+ \rightarrow 0^+$ transition. Generally 1^+ and J^- states are not populated, because of their greater excitation energies. Therefore, our theoretical formulae are restricted to the $0^+ \rightarrow J^+$ transitions,

and the detailed transition rates are given only for the $J = 0$ and 2 cases.

We find from Table 1.1 that there are eight pairs of parents for a given Z and a triad for Nd. Since the structure of nuclei differing by only one pair of neutrons may be similar, these pairs can be used to extract information about the $\beta\beta$ decay from ratios of total half lives independently of the absolute values of nuclear matrix elements. The available total kinetic energy T for the lighter isotope of the pair is so small to measure the half life by the direct counting experiemnt, except Nd. Pontecorvo[14] applied this idea to the ratio of $^{128}Te/^{130}Te$ based on the old data by Takaoka and Ogata,[15] who used the geochemical method. The recent experimental data on this ratio will be analyzed in §8.2.1. We would like to point out that the pair of ^{148}Nd and ^{150}Nd is expected to give the useful information, if both of their $(\beta\beta)_{0\nu}$ modes are measured.

(ii) Experimental methods:

Experiemnts on the $\beta\beta$ decay can be divided into three categories; (a) geochemical method, (b) direct counting method and (c) radiochemical method. In the geochemical method, the total $\beta\beta$ decay half life is determined by measuring the abundance of the daughter isotope in an old ore sample containing the parent nucleus. It has advantage such that the accumulation of decay products (daughter isotopes) for a long period can be used. Such an example is the ratio of $^{128}Te/^{130}Te$ mentioned above. The experimental data obtained by the geochemical method are summarized in the extensive review by Kirsten[16] and by Haxton and Stephenson.[17] We do not repeat it.

The direct counting methods have an advantage to discriminate the $(\beta\beta)_{0\nu}$ mode from the $(\beta\beta)_{2\nu}$ mode and the $0^+ \to 0^+$ transition from $0^+ \to 2^+$ by measuring the energy sum of two electrons [Fig. 6.2] and by detecting the γ-ray simultaneously, as shown in Fig. 1.1. The fundamental idea of the radiochemical method proposed by Haxton, Cowan and Goldhaber[18] is as follows: Among five unstable daughter nuclei in Table 1.1, the half-lives of ^{232}U and ^{238}Pu are relatively short such as 70 y and 87.74 y, so that the accumulation occurs over a known time interval in a carefully controlled environment. Since there are laborious reviews on the data obtained by these methods by Haxton and Stephenson,[17] by Zanotti, by Wu and by Zdesenko,[19] we shall not mention them. Only the recent results will be compared with theoretical estimates in §8.

There are six nuclei which emit two positrons accompanied by two neutrinos.[17),19] Although the search for this $\beta^+\beta^+$ decay has an advantage experimentally,[20] this decay has the long half-life relative to the $\beta^-\beta^-$ decay.[21),17] This is because the decay rate is reduced by the strong Coulomb repulsion, $\exp(-4\pi\alpha Z) \sim 10^{-2}$, and the kinetic energy release is relatively unfavorable due to the pairing force between two protons. [§11 and Table 11.1].

§1.3 Why do we consider the $(\beta\beta)_{0\nu}$ mode?

If neutrinos are assumed to be Majorana particles, then the $(\beta\beta)_{0\nu}$ mode can be proved to take place under some conditions, which will be explained later. Of course, this is the motivation for the $(\beta\beta)_{0\nu}$ mode by Furry in 1939.[12] However, the important question is whether the observation of the $(\beta\beta)_{0\nu}$ mode implies

at least the electron neutrino to be a massive Majorana particle. Schechter and Valle[22] and by extending their proof, Takasugi and Nieves have proved[23] that the answer is yes [§1.3 (iii)].

(i) Conditions required for the $(\beta\beta)_{0\nu}$ mode:

Let us consider, as an example, the $(\beta\beta)_{0\nu}$ mode in the 2n-mechanism shown in Fig. 1.3. If it is restricted to the minimum standard model, then an antineutrino ($\bar{\nu}_e$) with h = +1/2 is emitted from the n_1 vertex and a neutrino (ν_e) with h = -1/2 is absorbed at the n_2 vertex, as shown in Fig. 1.3a, where the main helicity states of leptons with large momentum are shown by short arrows. These two neutrino lines can not be connected within the minimum standard model; namely the $(\beta\beta)_{0\nu}$ mode does not take place. In order for the $(\beta\beta)_{0\nu}$ mode to occur, the following two conditions are necessary:

Condition (1): The electron neutrino (ν_e) should be the same particle as its antiparticle, i.e., this virtual neutrino should be the Majorana one [$\nu_e = \bar{\nu}_e$, *the lepton number non-conservation*].

Condition (2): Both neutrinos should have the same helicity component to connect these neutrino lines in Fig. 1.3 [*the requirement of the helicity matching*].

The latter condition is satisfied, if neutrinos are massive (the m_ν part)[25),26)] and/or if the right-handed (V+A) current coexists with the V-A current (the V+A part).[27),26)]

Let us express the second helicity matching condition more quantitatively. If $m_\nu \neq 0$, then the neutrino has the minor helicity state with h=+1/2, which is proportional to m_ν/ω, ω being the neutrino

energy, as shown in §2.4.1 (ii). Thus, the transition amplitude from the m_ν part should be proportional to (m_ν/m_e), where m_ν comes from the numerator of the neutrino propagator [Eq. (3.3.1)] and the electron mass m_e is introduced to represent the order of the typical energy in the $\beta\beta$ decay. If there is the neutrino mixing, then the weak eigenstate neutrino ν_{eL} appeared in the V-A interaction is replaced by a superposition of mass eigenstate Majorana neutrinos,

$$\nu_{eL} = \sum_j U_{ej} N_{jL}, \tag{1.2.1}$$

where N_j represents a Majorana neutrino with the mass m_j. Thus, in the $(\beta\beta)_{0\nu}$ mode, various neutrinos N_j propagate between two β decay vertecies. Since the electron neutrino mixing matrix U_{ej} appears at each vertex, the m_ν part of the transition amplitude becomes to be proportional to the effective neutrino mass such as

$$\langle m_\nu \rangle = \left| \sum_j{}' m_j U_{ej}^2 \right|, \tag{1.2.2}$$

where the primed sum extends over only the light neutrinos ($m_j \lesssim$ 10 MeV), which gives the Coulomb type potential due to the virtual neutrino propagation [§3.4 and Fig. 3.4]. The contributions from much heavier neutrinos ($m_j \gtrsim 10$ GeV) are suppressed due to the Yukawa type potentials and their small mixing parameters. If there are neutrinos with masses 10 MeV < m_j < 10 GeV, then the complicated m_j dependence should be taken into account, which will be discussed in §9. Anyhow, the m_ν part of the $(\beta\beta)_{0\nu}$ transition amplitude is suppressed by the order of $\langle m_\nu \rangle / m_e \sim 10^{-5}$, as it will be derived from the present experimental limits in Eqs.(8.2.10) and (8.2.13).

On the other hand, if the second vertex is the V+A interaction, the second neutron n_2 in Fig. 1.3b can absorb the neutrino with

$h = +1/2$. Thus, the condition (2), the helicity matching, is satisfied. The transition amplitude in this case is proportional to the V+A parameters, say λ and η, which are assumed to be zero in the minimum standard model. In the $SU(2)_L \times SU(2)_R \times U(1)$ model, these parameters λ and η are $\lambda_0 \approx (M_{WL}/M_{WR})^2$ and $\eta_0 \approx -\tan\zeta$, where M_{WL} and M_{WR} are masses of the left and right gauge bosons and ζ is the mixing angle between the mass eigenstates of W_L and W_R, as will be shown in Eq.(A.2.8) of Appendix A. If there is the neutrino mixing, then the weak eigenstate neutrino ν'_{eR} in the V+A interaction is expressed as

$$\nu'_{eR} = \Sigma_j V_{ej} N_{jR}, \tag{1.2.3}$$

where the mixing matrix V_{ej} is different from U_{ej} in Eq.(1.2.1) and satisfies the relation

$$\Sigma_j U_{ej} V_{ej} = 0, \tag{1.2.4}$$

which means that ν_{eL} and ν'_{eR} are independent each other. Since one vertex is V-A and another is V+A in Fig. 1.3b, the V+A part of the $(\beta\beta)_{0\nu}$ mode, for example the λ term, should be proportional to

$$\langle\lambda\rangle = \lambda \left| \Sigma'_j U_{ej} V_{ej} (\cos\theta'/\cos\theta) \right|, \tag{1.2.5}$$

where θ and θ' are the Cabibo angles of the left-and right-handed quark mixings, respectively. Here the primed sum means again the sum over only the light neutrinos similarly to the m_ν part. If all neutrinos are massless or light enough, then we have[28),29)]

$$\langle\lambda\rangle = 0 \tag{1.2.6}$$

from Eq.(1.2.4). It should be noted that if there is no neutrino mixing, then we have $\langle\lambda\rangle = 0$ also, beacuse, for example, $U_{ej} = \delta_{j1}$, and $V_{ej} = \delta_{jk}$ $(k \neq 1)$ in the gauge theory. In order to have some contributions from the V+A part to the $(\beta\beta)_{0\nu}$ mode, there should be some neutrino mixing between light and heavy Majorana neutrinos. Since neutrino mixing plays an important role, the detailed general structure will be discussed in §§2.2, 2.3 and 3.1.1.

Thus, it is clear that both m_ν and V+A parts should be considered simultaneously [§3.3].[26)] Then, a general form of the effective charged current weak interaction should be taken into consideration [Eq.(3.1.3)]. Parameters of the V+A interactions and neutrino mixing matrices are shown in the explicit forms for various gauge models, including the contributions from the mirror leptons, which transform as the ordinary leptons, but have the opposite chirality [§A.2.1]. The relation between the renormalized V-A and V+A hadronic currents will be established in §A.2.2.

Another N* mechanism is proposed by Primakoff and Rosen[27)] in 1969, where the $\beta\beta$ decay occurs through the transition of $\Delta(1232)$ inside the nucleus [§4]. Examples are shown in Fig. 1.4. As a modification of the N* mecahnism, the transitions like $\Delta^- + \Delta^+ + 2e^-$ are proposed,[17),14)] as shown in Fig. 1.5. This contribution is minor, because of the product of the nucleon -Δ trnasition probabilities [§4]. Within the conventional framework, it is possible to consider some process relating with the pion exchange current [Figs. 3.1 and 3.3].

(ii) Selection rules:

Let us first consider the case where both emitted electrons are in the S-wave state, so that the total angular momentum of two electron system is $J_{2e} = 0$ or 1, and the $0^+ \to 2^+$ transition is forbidden.

For the m_ν part, in practice, only the $0^+ \to 0^+$ transition takes place mainly, while the $0^+ \to 1^+$ transition is suppressed, because of no operator to change the nuclear spin in the closure approximation [§3.3.1]. Here the closure approximation means that the energy levels of the virtual intermediate nuclear states are replaced by one appropriate average value, so that the closure property is applied for these virtual nuclear states.

As for the V+A part, two different situations appear due to the energy (ω) and space momentum ($\vec{q}$) terms in the numerator of the virtual neutrino propagator, instead of the neutrino mass in the m_ν part [§3.3 and §3.3.2]. It should be noted that the average energy of virtual neutrino is of order of $\langle\omega\rangle \sim \langle q\rangle \sim (1/R) \sim 80\ m_e$, where R is the nuclear radius ($R = 1.2\sqrt[3]{A}$ fm). Therefore, it is expected that contributions from the kinematical factor of the V+A part are much larger than those from the m_ν part, because of the factor $\langle m_\nu\rangle/\langle\omega\rangle \sim 10^{-6}$. However, it is not so in reality. There is a large suppression originated from the smallness of the right-handed parameters themselves and/or the mixing matrix (V_{ej}) appeared at the V+A vertex.[26),21)] The latter is due to the fact that the weak eigenstate neutrinos appearing at the V-A and V+A vertices should be different in the gauge theory, as mentioned before.

In the case of the ω term of the V+A part, it is expected to have the similar features to the m_ν term, because ω behaves like m_ν. However, since the main helicities of two electrons are opposite as shown in Fig. 1.3b, their angular correlation should be the $(1 + \cos\theta)$ type to minimize J_{2e}, in contrast with the $(1 - \cos\theta)$ type for the m_ν part.[26)] The more important difference is the cancellation between two potentials due to the virtual neutrino propagation. This situation is originated from the Pauli principle for two electrons, i.e., the exchange of two emitting electrons gives the opposite signs for two amplitudes. In the case of the m_ν part, this sign change has been compensated by the sign change of the electron currents. This cancellation gives the suppression factor of order of 1/40 [§3.3.2]. For the parts of amplitude vanishing in the closure approximation, this cancellation does not occur, so that we have to examine the theoretical formulae from this viewpoint carefully. Therefore, formulae without using the closure approximation will be presented for the $(\beta\beta)_{2\nu}$ and $(\beta\beta)_{0\nu}$ modes in Appendices B and C, respectively.

On the other hand, for the $\vec{q}$ term of the V+A part, there is no cancellation between neutrino potentials, because of the parity odd character of $\vec{q}$ [§3.3.2]. But, this $\vec{q}$ acts as a parity odd and rank 1 tensor operator between the initial and final nuclear wave functions with the same parity. Therefore, as long as the $0^+ \to J^+$ transition is concerned, we need to have one more parity-odd operator: Namely, (a) one of emitted electrons should be in the P-wave state

or (b) the nucleon recoil effect should be taken into consideration. Let us first consider the P-wave case (a), where J_{2e} can take 0, 1 and 2. This is the first forbidden transition in the terminology of the single β decay, but it is expected that this contribution is larger kinematically, in comparison with the m_ν part and the ω term, because of the large $\langle q \rangle \sim 80\ m_e$ and no cancellation between neutrino potentials. Thus, we find two interesting results: (a1) The $0^+ \to 2^+$ transition is allowed only for this $\vec{q}$ term. In other words, if the $0^+ \to 2^+$ transition in the $(\beta\beta)_{0\nu}$ mode is observed, then we can say definitely that the V+A current exists in addition to the Majorana character of neutrino as pointed out by Doi, Kotani, Nishiura, Okuda and Takasugi[26] and by Rosen.[30] (a2): Of course, the $0^+ \to 0^+$ transition is also allowed, where the electron P-wave should be the one with $j = 1/2$, because $J_{2e} = 0$. This type of P-wave Coulomb wave function should be treated carefully, because the leading term of the Coulomb correction is $\alpha Z/2$ ($\sim 1/6$) in comparison with the ordinary P-wave term $pR/3 \sim 1/60$ [§3.1.3 and Appendix D]. Thus, this contribution should be large and is called the P-wave effect.[21),31] Furthermore, Doi et al.[21),31] pointed out that the small nucleon recoil terms (b) become important relatively, because they appear in the electron S-wave case, the recoil effect [§3.5.1]. This recoil effect is confirmed numerically by Tomoda, Faessler, Schmid, and Grümmer[32] and by Doi, Kotani and Takasugi.[33]

Summarizing these arguments, we can get the selection rules for various transitions and their order of magnitudes, which are shown in Table 1.2 [Table 3.3]. Here we have used the conservation laws of angular momemtum and parity for the nuclear transitions in the impulse approximation of the hadronic currents. The lowest necessary partial waves of electrons are taken into consideration.*) In the case of the N^*-mechanism, the SU(6) static model has been used for the wave functions of the nucleon and Δ.[27),26] Note that the contribution through this N^* mechanism is limited to the $0^+ \to 2^+$ transition [§4].

Now let us compare transition rates of the $(\beta\beta)_{2\nu}$ and $(\beta\beta)_{0\nu}$ modes quantitatively. Since they are five and three body decays respectively, the yields of the $(\beta\beta)_{0\nu}$ mode are favorable in comparison with the $(\beta\beta)_{2\nu}$ mode from the viewpoint of the phase space integration. In addition, when these decays are treated by the second order perturbation theory, the $(\beta\beta)_{2\nu}$ mode is suppressed by the energy denominator, $\mu_a m_e = E_a - (M_f + M_i)/2$, where E_a is the energy of the intermediate nucleus and M_f and M_i are masses of the final and initial nuclei, respectively. This suppression factor is represented by $\mu_0 m_e$ defined in Eq.(3.2.9), where μ_0 is some average of μ_a. This $\mu_0 \sim 20$ is taken out as the

*) If both electrons are P-wave, the $0^+ \to 2^+$ transition will take place even by the m_ν part. Here we do not list such possibility due to the higher spherical waves [Appendices B and C].

multiplication factor in the third column of Table 1.1. On the other hand, in the case of the $(\beta\beta)_{0\nu}$ mode, this energy denominator μ_0 is compensated by the momentum of the virtual neutrino, $(d^3\kappa/\omega) \sim \langle q \rangle^2 \sim (80 m_e)^2$ and the factor $\langle q \rangle^2/\mu_0 m_e^2$ works as the enhancement of the $(\beta\beta)_{0\nu}$ amplitude. Thus, the yields of the $(\beta\beta)_{0\nu}$ mode becomes larger by the order of $(80)^4/(20)^2 \sim 10^5$ than the $(\beta\beta)_{2\nu}$ mode. However, in the $(\beta\beta)_{0\nu}$ mode, there are large suppression factors; that is, $(\langle m_\nu \rangle/m_e)^2 \sim 10^{-10}$ for the m_ν part and $\langle \lambda \rangle^2$ or $\langle \eta \rangle^2$ for the V+A part. Thus, the half-life of the $(\beta\beta)_{0\nu}$ mode becomes in general larger than the $(\beta\beta)_{2\nu}$ mode, as shown in the fourth column of Table 1.1.

(iii) The need of massive Majorana neutrino for the $(\beta\beta)_{0\nu}$ mode

In the previous part (i), we discussed the conditions for the $(\beta\beta)_{0\nu}$ mode to take place in the 2n-mechanism. Here we shall give the general theorems which are valid in all order of perturbation and are independent of mechanisms for the $(\beta\beta)_{0\nu}$ mode. At first, we shall define the following terminology : Whenever the technical term "massive Majorana particle" is used, it includes the case of a superposition of massive Majorana neutrinos if there are neutrino mixings, but excludes the case where it consists of only Dirac neutrinos. Note that if there are mixings among Dirac and Majorana neutrinos, then Dirac neutrinos should become Majorana neutrinos in the higher order perturbation.

Theorem 1 : The electron neutrino ν_{eL} is the massive Majorana particle, if the $(\beta\beta)_{0\nu}$ decay takes place.

Theorem 2 (Converse of theorem 1): The $(\beta\beta)_{0\nu}$ decay takes place, if the electron neutrino ν_{eL} is the massive Majorana particle.

The following facts are used to prove these theorems; (a) the u and d quarks (constituents of nucleon) and electron are massive and (b) there exists at least the standard V-A interaction,

$$(g/2\sqrt{2})(\overline{\nu_{eL}}\gamma^\rho(1-\gamma_5)e + \bar{u}\gamma^\rho(1-\gamma_5)d)W_{L\rho}^{+} + \text{h.c.}, \qquad (1.3.1)$$

where W_L is the left gauge boson associated with $SU(2)_L$ symmetry. Since we are considering theorems valid in all order of perturbation, massive Majorana means that the Majorana type mass term in Eq. (2.1.14) is given in some order of perturbation.

Therefore, in order to prove the theorem 1, it is sufficient to show that the Majorana type mass term for ν_{eL} is induced if the $(\beta\beta)_{0\nu}$ mode takes place independently of whether ν_{eL} is massive or massless in the tree level. The theorem 2 may be understandable, because if ν_{eL} is massive, there is a non-vanishing contribution to the $(\beta\beta)_{0\nu}$ mode through the 2n-mechanism. Since it is hard to consider that this contribution is canceled out by others in all order of berturbation, the $(\beta\beta)_{0\nu}$ mode should take place in some order. The general proof of these theorems are presented in Appendix A.

From the theorem 1, we have the interesting corollary.

Corollary : If the electron neutrino ν_{eL} is massless in all order of perturbation, the $(\beta\beta)_{0\nu}$ decay does not take place independently of whether it is the Majorana or the Weyl (massless Dirac) particle.

This corollary is trivially derived by taking the negation of the

theorem 1 : Suppose that ν_{eL} is massless, but the $(\beta\beta)_{0\nu}$ mode occurs. Then by the theorem 1, the Majorana type mass term for ν_{eL} is induced in the higher order perturbation. This contradicts with the assumption of the massless electron neutrino. Therefore the $(\beta\beta)_{0\nu}$ mode is forbidden. Needless to say, the $(\beta\beta)_{0\nu}$ mode is also forbidden if ν_{eL} is the massive Dirac neutrino.

(iv) Present status of experimental results:

When we analyze the experimental results, we should note that the emitted two electrons are attracted by the Coulomb field of nucleus. Haxton, Stephenson and Strottman[34] and Nishiura[35] have pointed out that this attraction is substantial for the medium-heavy nuclei due to the overlap between wave functions of electrons and nucleus. By taking this enhancement into account, the comparative half lives from the m_ν part are listed on the fourth column of Table 1.1, where the effective mass $\langle m_\nu \rangle$ is measured in units of eV and $M_{GT}^{(0\nu)}$ is the unknown nuclear matrix element of order of unity and determined theoretically [§3.5]. In the V+A part, there are many nuclear matrix elements. Haxton and Stephenson,[17] Grotz and Klapdor[36] and many authors have estimated these nuclear matrix elements [§7.2]. The theoretical formulae to analyze the experimental results are presented in §8.2.

Besides the 2n and N^* mechanisms, we can consider various new mechanisms by taking into account varieties of Higgs bosons beyond the minimum standard models.[22] Among them, Vergados and Mohapatra[37] proposed the possible $(\beta\beta)_{0\nu}$ mode through doubly charged Higgs boson without virtual neutrinos, as shown in Fig. 1.6. This contribution has been found to be negligible[38),22] As the process which should be checked carefully, Georgi, Glashow and Nussinov[39]

pointed out the $(\beta\beta)_{0\nu,B}$ mode accompanied by the emission of a light pseudo-scalar (Majoron, Nambu-Goldstone boson[40]) or scalar boson, as shown in Fig.1.7. This process is important to extract the pure $\beta\beta$ decay experimentally [§5.1, §5.2 and Fig.6.11].

Until now, no definite observation of the $(\beta\beta)_{0\nu}$ mode has been reported. The upper limits on both the effective neutrino mass $\langle m_\nu \rangle$ and the effective right-handed parameters, $\langle \lambda \rangle$ and $\langle \eta \rangle$, have been derived [§8].

The constraint on $\langle m_\nu \rangle$ obtained from the $(\beta\beta)_{0\nu}$ mode is compared with the experimental information on m_ν from the tritium decay, the neutrino oscillation and other processes. Some possible schemes of neutrino masses and their mixings are discussed [§9]. Bounds on the effective right-handed current parameters $\langle \eta \rangle$ and $\langle \lambda \rangle$ from the $(\beta\beta)_{0\nu}$ mode are discussed with the other experimental constraints from the β, μ and K decays [§10]. It is argued that, if at least one right-handed neutrino is heavy, then the $(\beta\beta)_{0\nu}$ mode gives the most stringent bound on the right-handed parameters and the neutrino mixings.

As for the exploration of the Majorana character of neutrinos, there are two kinds of processes. One is the lepton number violating processes such as the neutrinoless $\beta^+\beta^+$ decay, the $e + e \to W_L + W_L$ reaction etc. Their observation means that neutrinos are Majorana particles [§11.1]. The other is the processes which occur independently of Majorana and Dirac character of neutrinos. But we may be able to find some clean signal of the Majorana character from them. As this kind of processes, the $\mu^- - e^+$ conversion, the μ decay etc. are discussed in §11.2.

Part I The Majorana neutrino

§2 General properties of the Majorana neutrino

The description of the Majorana particle has been formulated clearly in the classic papaer by Case and by many authors.[3),4),5)] Here the difference and relation between the Dirac and Majorana descriptions of neutrino and models of neutrino mass matrix are presented by summarizing these previous investigations.

§2.1 Dirac, Weyl and Majorana neutrinos

The Lagrangian density for a classical Majorana field will be introduced in this subsection.[3),4),5)]

First, we shall start from the Lagrangian density for a classical Dirac field $\psi(\vec{x}, t)$,

$$\mathcal{L} = \bar{\psi}(i\gamma^0\partial_t + i\vec{\gamma}\cdot\vec{\nabla} - m)\psi, \tag{2.1.1}$$

Hereafter, the Weyl representation of γ matrices is employed.*)

Let us rewrite ψ in the two component form,

$$\psi = \begin{pmatrix}\phi\\ \chi\end{pmatrix}, \quad \psi_L = \begin{pmatrix}0\\ \chi\end{pmatrix}, \quad \psi_R = \begin{pmatrix}\phi\\ 0\end{pmatrix}. \tag{2.1.2}$$

Then the Lagrangian becomes

$$\mathcal{L} = \phi^\dagger O_+\phi + \chi^\dagger O_-\chi - \phi^\dagger m\chi - \chi^\dagger m\phi, \tag{2.1.3}$$

where

$$O_\pm = i(\partial_t \pm \vec{\sigma}\cdot\vec{\nabla}). \tag{2.1.4}$$

*) $\gamma^0 = \begin{pmatrix}0 & 1\\ 1 & 0\end{pmatrix}$, $\vec{\gamma} = \begin{pmatrix}0 & -\vec{\sigma}\\ \vec{\sigma} & 0\end{pmatrix}$, $\gamma_5 = \begin{pmatrix}1 & 0\\ 0 & -1\end{pmatrix}$

$C = i\gamma^2\gamma^0 = \begin{pmatrix}-i\sigma_2 & 0\\ 0 & i\sigma_2\end{pmatrix}$, $L = (1-\gamma_5)/2$ and $R = (1+\gamma_5)/2$.

Note that the mass term consists of the mixing between χ and ϕ and it is called a Dirac type mass term. If $m = 0$, then χ and ϕ represent two different fields (two Weyl neutrinos). As the quantized field operator, χ with $m = 0$ includes both the annihilation of neutrino with the negative helicity ($h = -1/2$) and the creation of antineutrino with $h = 1/2$, because of the character of O_-.

Let us seek another expression of ψ by diagonalyzing the mass term in the two component form.[28),41)] Note that χ transforms as $(0, 1/2)$, while ϕ does as $(1/2, 0)$ under Lorentz transformation. Here (j_1, j_2) is the representation of the Lorentz group, $SO(1,3)$,[45)] ... Therefore, χ and ϕ can not be mixed each other. Then, we define

$$\tilde{\phi} = i\sigma_2\phi^*, \tag{2.1.5}$$

which transforms as $(0, 1/2)$ and has the O_- type kinetic energy term. With this notation, the mass term becomes $-m(\tilde{\phi}^T i\sigma_2\chi - \chi^\dagger i\sigma_2\tilde{\phi}^*)$ and can be diagonalized by the following unitary transformation;

$$\begin{aligned}\chi &= (\eta + i\tilde{\xi})/\sqrt{2},\\ \tilde{\phi} &= (\eta - i\tilde{\xi})/\sqrt{2}, \quad \phi = -i\sigma_2(\eta^* + i\tilde{\xi}^*)/\sqrt{2}.\end{aligned} \tag{2.1.6}$$

Now the Lagrangian is expressed as the combination of two $(0, 1/2)$ fields η and ξ.

$$\mathcal{L} = \mathcal{L}_L(\eta) + \mathcal{L}_L(\tilde{\xi}), \tag{2.1.7}$$

where

$$\mathcal{L}_L(\eta) = \eta^\dagger O_-\eta - \tfrac{1}{2}m(\eta^T i\sigma_2\eta - \eta^\dagger i\sigma_2\eta^*). \tag{2.1.8}$$

Hereafter we refer to η as the left-handed Majorana neutrino in the two component form. Defining ξ as

$$\xi = -i\sigma_2 \eta^*, \tag{2.1.9}$$

which transforms as (1/2, 0), we find

$$\mathcal{L}_L(\eta) = \mathcal{L}_R(\xi), \tag{2.1.10}$$

where

$$\mathcal{L}_R(\xi) = \xi^\dagger O_+ \xi + \frac{1}{2} m (\xi^T i\sigma_2 \xi - \xi^\dagger i\sigma_2 \xi^*). \tag{2.1.11}$$

We refer to ξ as the right-handed Majorana neutrino, because of operator O_+.[28]

Now we know from Eqs.(2.1.2), (2.1.6) and (2.1.9) that a Dirac field ψ consists of two independent Majorana neutrinos η and ξ as[5]

$$\psi = (N_1 + i N_2)/\sqrt{2}, \tag{2.1.12}$$

where N_1 and N_2 are Majorana neutrinos in the four component form defined by

$$N_1 = \begin{pmatrix} -i\sigma_2 \eta^* \\ \eta \end{pmatrix}, \quad N_2 = \begin{pmatrix} \xi \\ i\sigma_2 \xi^* \end{pmatrix}. \tag{2.1.13}$$

Fields N_1 and N_2 satisfy the Majorana (self-conjugate) condition $N_1^C = N_1$ and $N_2^C = N_2$, where $N^C = C\bar{N}^T$, C being the charge conjugation matrix.

Let us examine the properties of η and ξ. At first, we notice that η and ξ have opposite sign under the CP transformation because of the factor i in Eq.(2.1.12). ψ is required to have a definite CP sign. Next their mass terms are the $\eta^T i\sigma_2 \eta$ (or $\xi^T i\sigma_2 \xi$) type (Majorana type mass term) instead of $\phi^\dagger \chi$ type (Dirac type mass term) in

Eq.(2.1.3). These Majorana type mass terms mean that when the momentum representation is adopted, the positive and negative frequency parts can not be treated separately. Therefore, when $\eta(\xi)$ is interpreted as a quantized field operator, the particle and antiparticle creation operators can not be distinguished in contrast to the Dirac neutrino. This is the well-known character of Majorana neutrinos. Thus, the field $\eta(\xi)$ expresses the left-(right-)handed Majorana neutrino, because of the $O_{-(+)}$ character.

The natural expression for the Majorana field is the two component form, η and ξ, because they have only two freedoms (two spin states). The four component form $N_1(N_2)$ in Eq.(2.1.13) should be understood as a convention to express the weak charged current compactly. It should be noticed that a Dirac field ψ can also be expressed as a combination of two left-handed Majorana fields η and $\tilde{\xi}$, as seen from Eq.(2.1.7). This ψ will be refered to as the Konopinski-Mahmoud(KM) Dirac field, see § 2.5.1.[13]

The Lagrangians for the left- and right-handed Majorana fields are expressed in the four component form, N_1 and N_2 in Eq.(2.1.13), as

$$\mathcal{L}_L = \overline{N_{1L}}\, i\gamma^\mu \partial_\mu N_{1L} - \frac{1}{2} m \left(\overline{(N_{1L})^c}\, N_{1L} + \overline{N_{1L}}\, (N_{1L})^c \right), \tag{2.1.14a}$$

$$\mathcal{L}_R = \overline{N_{2R}}\, i\gamma^\mu \partial_\mu N_{2R} - \frac{1}{2} m \left(\overline{(N_{2R})^c}\, N_{2R} + \overline{N_{2R}}\, (N_{2R})^c \right). \tag{2.1.14b}$$

The mass terms in the above expressions are also called Majorana type mass terms for the left- and right-handed neutrinos.[42),43)]

§2.2 Types of neutrino mass terms and their diagonalization

Let us consider a system of n left-handed neutrinos $\nu_{\ell L}$ ($\ell = e, \mu, \cdots$). Since $\nu_{\ell L}$ transform as (0, 1/2) and $(\nu_{\ell L})^C$ as (1/2, 0), the only Lorentz invariant mass term is a Majorana type mass term in Eq.(2.1.14a),

$$\mathcal{L}_{m_L} = -\frac{1}{2}\sum_{l,l'}\overline{(\nu_{lL})^c}\, m_{Ll l'}\,\nu_{l'L} + h.c.) \qquad (2.2.1)$$

The n×n Majorana type mass matrix m_L is a symmetric one because[10] $\overline{(\nu_{lL})^c} = -\nu_{lL}^T C^{-1}$ and thus $\overline{(\nu_{lL})^c}\,\nu_{kL} = -\nu_{lL}^T C^{-1}\nu_{kL} = \overline{(\nu_{kL})^c}\,\nu_{lL}$.

The complex symmetrix matrix m_L is diagonalized by the unitary matrix U_ν as*),9),10),42)

$$U_\nu^T m_L U_\nu = D_\nu , \qquad (2.2.2)$$

where D_ν is a diagonal mass matrix with real positive eigenvalues. Note that the unitary matrix U_ν is determined completely including phases. Accordingly, ν_{lL} are related to n mass eigenstates N_{jL} as

$$\nu_{lL} = (U_\nu)_{lj} N_{jL} . \qquad (2.2.3)$$

Now the mass term becomes

$$\mathcal{L}_{m_L} = -\frac{1}{2}\left(\overline{(N_L)^c}\, D_\nu N_L + \overline{N_L}\, D_\nu (N_L)^c\right) = -\frac{1}{2}\overline{N}\, D_\nu N, \qquad (2.2.4)$$

where $N^T = (N_1^T, N_2^T, \cdots, N_n^T)$ and

$$N = N_L + (N_L)^c , \qquad (2.2.5)$$

represent Majorana neutrinos which satisfy the Majorana (self-conjugate) condition,

$$N^c = N. \qquad (2.2.6)$$

If n right-handed neutrinos ν_{lR} exist in addition, both the Majorana type mass term of right-handed neutrinos $\mathcal{L}_{mR}$ in Eq.(2.1.14b) and the Dirac type mass term $\mathcal{L}_D$ arise,

*) Any matrix m is diagonalized as $V^\dagger m U = D$, where U and V are unitary matrices which diagonalize hermitian matrices $m^\dagger m$ and $m m^\dagger$, respectively. If $m^T = m$, then $m^\dagger m = m^* m^T = (m^\dagger m)^*$ so that $V = U^*$ is concluded.

$$\mathcal{L}_{m_R} = -\frac{1}{2}\overline{(\nu_R)^c}\, m_R \nu_R + h.c., \qquad (2.2.7)$$

$$\mathcal{L}_D = -\overline{\nu_R}\, m_D \nu_L + h.c.. \qquad (2.2.8)$$

Again m_R is a n×n symmetric matrix. Now the mass term of neutrinos is expressed as

$$\mathcal{L}_M = \mathcal{L}_{m_L} + \mathcal{L}_{m_R} + \mathcal{L}_D$$
$$= -\frac{1}{2}\left(\overline{(\nu_L)^c},\ \overline{\nu_R}\right) m \begin{pmatrix}\nu_L \\ (\nu_R)^c\end{pmatrix} + h.c., \qquad (2.2.9)$$

$$m = \begin{pmatrix} m_L & m_D^T \\ m_D & m_R \end{pmatrix}, \qquad (2.2.10)$$

where the identity $\overline{\nu_R} m_D \nu_L = \overline{(\nu_L)^c} m_D^T (\nu_R)^c$ has been used. The ν_L and $(\nu_R)^c$ can be mixed because they behave as (0, 1/2). The matrices m_L and m_R are symmetric and so is true for m. Therefore, m is diagonalized by the unitary matrix U_ν as[43),42)]

$$\begin{pmatrix}\nu_L \\ (\nu_R)^c\end{pmatrix} = U_\nu N_L = \begin{pmatrix} U_I \\ V_I^* \end{pmatrix} N_L = \begin{pmatrix} U_{\nu I} & U_{\nu II} \\ V_{\nu I}^* & V_{\nu II}^* \end{pmatrix}\begin{pmatrix} N_{IL} \\ N_{IIL} \end{pmatrix}, \qquad (2.2.11)$$

$$U_\nu^T m U_\nu = D_\nu . \qquad (2.2.12)$$

Then the mass term takes the form as that in Eq.(2.2.4) with the definition of Eq.(2.2.5). Now we have 2n mass eigenstate Majorana neutrinos, i.e., $(N_I)^T = (N_1^T, N_2^T, \cdots, N_n^T)$ and $(N_{II})^T = (N_{n+1}^T, N_{n+2}^T, \cdots, N_{2n}^T)$.

§2.3 The CP violating phases

§2.3.1 The CP violation case

Let us consider the system of n left-handed neutrinos first. The neutrino mixing matrix among n Majorana neutrinos in a SU(2)×U(1) model with n left-handed lepton doublets is expressed as

$$U = U_\ell^+ U_\nu, \tag{2.3.1}$$

where U_ν is defined in Eq.(2.2.2) and U_ℓ is a unitary matrix to diagonalize the charged lepton mass matrix. Hereafter, U_ν and U_ℓ are referred to as the transformation matrices for neutrinos and the left-handed charged leptons, respectively. The unitary matrix U has n^2 parameters in which n(n-1)/2 parameters are for the orthogonal transformation. Out of the remaining n(n+1)/2 phases, n phases are absorbed by the phase redefinition of charged leptons. Thus the number of the CP violating phases for n Majorana neutrino system is [9),10)]

$$n(n-1)/2. \tag{2.3.2}$$

The number of CP violating phases is larger than the Kobayashi-Maskawa phases (n-2)(n-1)/2 for n Dirac neutrino case. The extra n-1 phases appear because the phase redefinition for neutrinos is not allowed due to the Majorana condition $N = N^C$.

For the simple <u>two generation mixing case</u> with only 2 left-handed neutrinos, the mixing matrix is expressed as[10)]

$$U = \begin{pmatrix} \cos\theta & e^{i\beta}\sin\theta \\ \sin\theta & -e^{i\beta}\cos\theta \end{pmatrix}, \tag{2.3.3}$$

where β is the extra phase intrinsic to Majorana neutrinos. It is instructive to note that the extra n-1 phases appear only in the

processes characterized by Majorana neutrinos, that is, the total lepton number violating processes.

The physical significance of these extra CP violating phases was first discussed by Doi, Kotani, Nishiura, Okuda and Takasugi[10)] for the process of the neutrinoless double beta decay $(\beta\beta)_{0\nu}$. In this process, the contribution from neutrino mass part appears in the form of

$$\langle m_\nu \rangle = \left| \sum{}' m_j U_{ej}^2 \right|, \tag{2.3.4}$$

as it was explained in Eq.(1.2.2). By using the parametrization of the mixing matrix in Eq.(2.3.3) and assuming its first low to be U_{ej}, $\langle m_\nu \rangle$ is expressed as

$$\langle m_\nu \rangle = \left[(m_1 \cos^2\theta - m_2 \sin^2\theta)^2 + m_1 m_2 \sin^2 2\theta \cos^2\beta \right]^{1/2}. \tag{2.3.5}$$

This has the following features: The effective neutrino mass $\langle m_\nu \rangle$ takes the maximum values for $\beta = 0 \pmod{\pi}$ and decreases with β until reaching to $\pi/2$ where the maximum destructive interference occurs. The complete cancellation takes place when $\beta = \pi/2$ and $\tan(\theta) = \sqrt{m_1/m_2}$. It was argued that the $(\beta\beta)_{0\nu}$ decay rate depends on β, because $m_1 = m_2$ and $\theta = \pi/4$ are expected for the maximum mixing case between two neutrinos belonged to different generations, which will be called the pseudo Dirac (P D) neutrino in § 2.5.2. In their paper,[10)] there is a confusion for the interpretation of the $\beta = \pi/2$ case (called the maximum CP violation case). It was solved by Wolfenstein[44)] who showed that the cases $\beta = 0$ or $\pi/2 \pmod{\pi}$ occur in the CP conserving case, as will be discussed in the next subsection.

The extension to models with left- and right-handed neutrinos is straightforward. In the $SU(2)_L \times SU(2)_R \times U(1)$ models with n left- and n right-handed doublet leptons, the neutrino mixing matrix is expressed as

$$U_{LR} = \begin{pmatrix} U_\ell^\dagger U_{\nu I} & U_\ell^\dagger U_{\nu II} \\ V_\ell^T V_{\nu I}^* & V_\ell^T V_{\nu II}^* \end{pmatrix}, \tag{2.3.6}$$

where $U_{\nu i}$ and $V_{\nu i}$ are defined in Eq.(2.2.11), and U_ℓ and V_ℓ are the transformation matrices for left- and right-handed charged leptons. Since U_{LR} is a unitary matrix of $2n \times 2n$, the total phases are $n(2n+1)$ out of which n phases are absorbed by the phase redefinition of charged leptons. Therefore, $2n^2$ phases appear as the CP violating phases.[35] As an example, the mixing matrix for one generation case with one left- and one right-handed neutrinos is expressed as

$$U_{LR} = \begin{pmatrix} \cos\theta & e^{i\beta}\sin\theta \\ e^{i\delta}\sin\theta & -e^{i(\beta+\delta)}\cos\theta \end{pmatrix}. \tag{2.3.7}$$

The phenomenological implication to the $(\beta\beta)_{0\nu}$ decay is the same as Eq.(2.3.5). Some more complicated cases were discussed by Schechter and Valle.[4]

§2.3.2 The CP conserving case

The Majorana type mass matrix becomes real symmetric if CP is conserved. Then it is diagonalized by the orthogonal matrix as*)

$$\begin{pmatrix} \nu_L \\ (\nu_R)^c \end{pmatrix} = O N_L' = \begin{pmatrix} O_1 \\ O_2 \end{pmatrix} N_L', \tag{2.3.8}$$

$$O^T m O = \begin{pmatrix} \ddots & & \\ & S_k m_k & \\ & & \ddots \end{pmatrix}, \tag{2.3.9}$$

*) Hereafter, we assume that the charged lepton mass matrices is already diagonal for simplicity; that is, the transformation matrices U_ℓ and V_ℓ in Eq.(2.3.6) are unit matrices.

where $m_k > 0$ and S_k is a sign factor taking ± 1. Now the mass term is written as

$$\mathcal{L}_M = -\frac{1}{2}\sum_k S_k m_k \bar{N}_k' N_k', \tag{2.3.10}$$

where

$$N_k' = N_{kL}' + (N_{kL}')^c. \tag{2.3.11}$$

This minus sign can not be absorbed by the phase transformation in contrast to the Dirac case.

There are two ways to absorb sign factors S_k. Wolfenstein proposed that Majorana neutrinos should be defined as[44]

$$N_k = N_{kL}' + S_k (N_{kL}')^c, \tag{2.3.12}$$

and he defined the CP property of N_k as

$$\mathcal{C}\mathcal{P} N_k \mathcal{P}^{-1}\mathcal{C}^{-1} = S_k\, i\gamma^0 N_k^c(-\vec{x}, t). \tag{2.3.13}$$

Then he called N_k to be CP even for $S_k = 1$ and CP odd for $S_k = -1$.

Another way by Doi et al.[5),26] and Schechter and Valle[4),60] is that sign factors are absorbed in Majorana fields and the mixing matrix is

$$N_k = N_{kL} + (N_{kL})^c, \tag{2.3.14}$$

$$N_{kL} = \exp(i\pi(1-S_k)/4)\, N_{kL}' \tag{2.3.15}$$

$$U_{LR} = O\begin{pmatrix} \ddots & & \\ & \exp(-i\pi(1-S_k)/4) & \\ & & \ddots \end{pmatrix} = \begin{pmatrix} U_1 \\ V_1^* \end{pmatrix}. \tag{2.3.16}$$

That is, (the factor $(-i)$ is multiplied for all elements in the k-th column of O when $S_k = -1$. By comparing Eqs.(2.3.12) and (2.3.14), one may think that all N_k are CP even, but this is false. The CP property of N_k should be determined to guarantee the CP invariance of weak interaction Lagrangian,

$$\mathcal{L}_W = \frac{g_L}{2\sqrt{2}}\sum_j \bar{l}\gamma^\rho(1-\gamma_5)(U_1)_{lj} N_{jL} W_{L\rho}^- + \frac{g_R}{2\sqrt{2}}\sum_j \bar{l}\gamma^\rho(1+\gamma_5)(V_1)_{lj} N_{jR} W_{R\rho}^- + \text{h.c.}. \tag{2.3.17}$$

From the appearance of i in the mixing matrix, it is concluded that N_k is CP even for $S_k = 1$ and CP odd for $S_k = -1$ by taking all charged leptons are CP even.

Note that the i factor in the mixing matrix for CP odd Majorana neutrinos ($S_k = -1$) corresponds to the $\beta = \pi/2 \pmod{\pi}$ case for the two generation mixing matrix in Eq.(2.3.3). That is, $\beta = \pi/2$ is realized in the CP conserving case, if CP signs of N_1 and N_2 are opposite.

Also it is worthwhile to note that the neutrino mixing matrix in the CP conserving case is expressed as an orthogonal matrix in the prescription by Wolfenstein,[44] but the treatment of the quantized field is complicated, e.g., Eq.(2.4.46) with $\rho_0 = \pm 1$. On the other hand, in the choice of Eq.(2.3.16) proposed by Doi et al.[5),26)] and by Schechter and Valle,[4)] the neutrino mass is $m \geq 0$, although the neutrino mixing matrix is unitary even for the CP conserving case.

§2.4 Quantization of Majorana neutrino

§2.4.1 Two component Majorana neutrino

Let us consider the Lagrangian of a left-handed Majorana neutrino N_L given in Eq.(2.1.14a);

$$\mathcal{L}_L = \bar{N}_L\, i\gamma^\mu \partial_\mu N_L - \frac{m}{2}\left(\overline{(N_L)^c}\, N_L + \bar{N}_L (N_L)^c\right), \tag{2.4.1}$$

where $m > 0$. Hereafter, we call the mass term in Eq.(2.4.1) the positive mass case. In the two component notation,

$$N_L = \begin{pmatrix} 0 \\ \eta \end{pmatrix}, \tag{2.4.2}$$

the Lagrangian becomes Eq.(2.1.8);

$$\mathcal{L}_L = \eta^\dagger i(\partial_t - \vec{\sigma}\cdot\vec{\nabla})\eta - \frac{m}{2}(\eta^T i\sigma_2 \eta - \eta^\dagger i\sigma_2 \eta^*), \tag{2.4.3}$$

which is also called the positive mass Majorana neutrino.[5)]

By using that the canonical quantity of η_α is $i\eta_\alpha^*$, the quantization is performed by requiring the canonical commutation relations (CCR's),

$$\{\eta_\alpha(\vec{x},t),\ \eta_\beta^*(\vec{y},t)\} = \delta_{\alpha\beta}\,\delta(\vec{x}-\vec{y}),$$
$$\{\eta_\alpha(\vec{x},t),\ \eta_\beta(\vec{y},t)\} = \{\eta_\alpha^*(\vec{x},t),\ \eta_\beta^*(\vec{y},t)\} = 0. \tag{2.4.4}$$

The equation of motion is given by

$$(\partial_t - \vec{\sigma}\cdot\vec{\nabla})\eta + m\sigma_2\eta^* = 0. \tag{2.4.5}$$

In the following, wave functions are obtained for the eigenstates of J_z or the helicity. We shall treat them separately.

(i) Wave functions as eigenstates of J_z: Since the mass term relates η and η^* in the equation of motion, the positive and negative frequency parts are not independent each other. Thus the expansion of η should be expressed as follows:[5)]

$$\eta(\vec{x},t) = \int d\Omega_q \sum_{\pm s} \left\{ a^{(s)}(\vec{q})\, w_1^{(s)}(\vec{q})\, e^{-iqx} + a^{(s)\dagger}(\vec{q})\, w_2^{(s)}(\vec{q})\, e^{iqx} \right\}, \tag{2.4.6}$$

where $d\Omega_q = d^3q(2\pi)^{-3/2}\sqrt{m/\omega}$, $\omega = \sqrt{q^2+m^2}$,

$$w_1^{(s)}(\vec{q}) = D(\vec{q})\,\chi_s/\sqrt{2}, \quad w_2^{(s)}(\vec{q}) = D(\vec{q})\, i\sigma_2\chi_s/\sqrt{2}, \tag{2.4.7}$$

$$D(\vec{q}) = \exp(-\hat{q}\cdot\vec{\sigma}\,\zeta/2) = \sqrt{(\omega+m)/2m}\ \left(1 - \frac{\vec{\sigma}\cdot\vec{q}}{\omega+m}\right), \tag{2.4.8}$$

and $\sinh\zeta = q/m$.*) Here χ_s is the two component spinor, $\chi_{1/2} = \begin{pmatrix}1\\0\end{pmatrix}$ and $\chi_{-1/2} = \begin{pmatrix}0\\1\end{pmatrix}$. The creation and annihilation operators satisfy commutation relations as

*) $D(\vec{q})$ is the 2×2 matrix representing a Lorentz boost $L(\vec{q})$ for $(0, 1/2)$ representation; $D(\vec{q}) = D^{(1/2)}(L(\vec{q}))$.

$$\{ a^{(s)}(\vec{q}),\ a^{(s')\dagger}(\vec{q}') \} = \delta_{ss'}\,\delta(\vec{q}-\vec{q}'),$$

$$\{ a^{(s)}(\vec{q}),\ a^{(s')}(\vec{q}') \} = \{ a^{(s)\dagger}(\vec{q}),\ a^{(s')\dagger}(\vec{q}') \} = 0. \qquad (2.4.9)$$

There are useful relations for $D(\vec{q})$,

$$D^{T}(\vec{q}) = D^{*}(\vec{q}) = \sigma_2\, D(-\vec{q})\, \sigma_2 , \qquad (2.4.10)$$

$$D(\vec{q})^2 = \exp(-\hat{q}\cdot\vec{\sigma}\, s) = (\omega - \vec{q}\cdot\vec{\sigma})/m. \qquad (2.4.11)$$

By using the relation

$$(\omega + \vec{q}\cdot\vec{\sigma})\, D(\vec{q}) = m\, D(-\vec{q})^2\, D(\vec{q}) = m\, D(-\vec{q})$$

$$= m\,\sigma_2\, D^{*}(\vec{q})\,\sigma_2 , \qquad (2.4.12)$$

we can easily prove that η satisfies the equation of motion. Also by using Eq.(2.4.11) and

$$D(\vec{q})\, i\sigma_2\, D^{T}(\vec{q}) = D(\vec{q})\, D(-\vec{q})\, i\sigma_2 = i\sigma_2 , \qquad (2.4.13)$$

it can be proved that the CCR's for η are satisfied by using Eq.(2.4.9). The Hamiltonian H_0 is given by

$$H_0 = \frac{i}{2}\int d^3x \left[\eta^{\dagger}\partial_t \eta - (\partial_t \eta^{\dagger})\,\eta \right] . \qquad (2.4.14)$$

In terms of $a^{(s)}$ and $a^{(s)\dagger}$, H_0 is expressed as

$$H_0 = \int d^3q \sum_{s=\pm\frac{1}{2}} \varepsilon\, a^{(s)\dagger}(\vec{q})\, a^{(s)}(\vec{q}), \qquad (2.4.15)$$

so that the positivity of H_0 is assured.

The effect of space-inversion ($\mathcal{P}$), charge-conjugation ($\mathcal{C}$) and time-reversal ($\mathcal{T}$) on the free particle states is well known.[45),46),5)] It can be summarized by specifying the transformation properties of the annihilation operators:

$$\begin{aligned} \mathcal{P}\, a^{(s)}(\vec{q})\, \mathcal{P}^{-1} &= i\varepsilon_{\mathcal{P}}\, a^{(s)}(-\vec{q}), \\ \mathcal{C}\, a^{(s)}(\vec{q})\, \mathcal{C}^{-1} &= \varepsilon_{\mathcal{C}}\, a^{(s)}(\vec{q}), \\ \mathcal{T}\, a^{(s)}(\vec{q})\, \mathcal{T}^{-1} &= \varepsilon_{\mathcal{T}} \sum_{s'} (i\sigma_2)_{ss'}\, a^{(s')}(-\vec{q}). \end{aligned} \qquad (2.4.16)$$

The effect of $\mathcal{P}$, $\mathcal{C}$ and $\mathcal{T}$ on η is derived by using Eq.(2.4.10) and the antiunitary nature of $\mathcal{T}$:

$$\begin{aligned} \mathcal{P}\,\eta(\vec{x},t)\,\mathcal{P}^{-1} &= i\varepsilon_{\mathcal{P}}(-i\sigma_2)\,\eta^{*}(-\vec{x},t), \\ \mathcal{C}\,\eta(\vec{x},t)\,\mathcal{C}^{-1} &= \varepsilon_{\mathcal{C}}\,\eta(\vec{x},t), \\ \mathcal{T}\,\eta(\vec{x},t)\,\mathcal{T}^{-1} &= \varepsilon_{\mathcal{T}}(i\sigma_2)\,\eta(\vec{x},-t), \end{aligned} \qquad (2.4.17)$$

under the constraints

$$\varepsilon_{\mathcal{P}} = \pm 1, \qquad \varepsilon_{\mathcal{C}} = \pm 1, \qquad \varepsilon_{\mathcal{T}} = \pm 1. \qquad (2.4.18)$$

These constraints are sufficient to assure the invariance of Lagrangian in Eq.(2.4.3) under $\mathcal{P}$, $\mathcal{C}$ and $\mathcal{T}$.

It should be noted that the phase i for the $\mathcal{P}$ transformation is necessary for a Majorana neutrino, because η consists of $a^{(s)}$ and $a^{(s)\dagger}$ in contrast with $A^{(s)}$ and $B^{(s)\dagger}$ for a Dirac neutrino where there is a freedom for the relative phase between $A^{(s)}$ and $B^{(s)}$.

(ii)Wave functions as helicity eigenstates:The wave functions in the helicity bases are obtained by applying the rotation $D(R(\vec{q}))$ which carries the z axis into the direction $\vec{q}$,[45)]

$$W_1^{(h)}(\vec{p}) = \sum_s \left[D(R(\hat{p}))\right]_{sh} w_1^{(s)}(\vec{p}),$$

$$W_2^{(h)}(\vec{p}) = \sum_s \left[D(R(\hat{p}))^*\right]_{sh} w_2^{(s)}(\vec{p}), \qquad (2.4.19)$$

where h represents helicity $h = \pm 1/2$ and $D(R(\hat{q}))$ is expressed as*)

$$D(R(\hat{p})) = \begin{pmatrix} \cos\frac{\theta}{2} & -e^{i\phi}\sin\frac{\theta}{2} \\ e^{i\phi}\sin\frac{\theta}{2} & \cos\frac{\theta}{2} \end{pmatrix}. \qquad (2.4.20)$$

With this modification of wave functions, the creation and annihilation operators are defined as

$$a^{(h)}(\vec{p}) = \sum_s \left[D(R(\hat{p}))^*\right]_{sh} a^{(s)}(\vec{p}),$$

$$a^{(h)\dagger}(\vec{p}) = \sum_s \left[D(R(\hat{p}))\right]_{sh} a^{(s)\dagger}(\vec{p}), \qquad (2.4.21)$$

and η is expressed in the form of Eq.(2.4.6) by replacing $a^{(s)}$, $a^{(s)\dagger}$, $W_1^{(s)}$ and $W_2^{(s)}$ with $a^{(h)}$, $a^{(h)\dagger}$, $W_1^{(h)}$ and $W_2^{(h)}$, respectively. The wave functions $W_1^{(h)}$ and $W_2^{(h)}$ are explicitly written as

$$W_1^{(h)}(\vec{p}) = \sqrt{\frac{\omega+m}{4m}}\left(1 - \frac{2h\xi}{\omega+m}\right)\alpha^{(h)}(\vec{p}),$$

$$W_2^{(h)}(\vec{p}) = -\sqrt{\frac{\omega+m}{4m}}\left(1 + \frac{2h\xi}{\omega+m}\right)2h\,\alpha^{(-h)}(\vec{p}), \qquad (2.4.22)$$

where $\alpha^{(h)}(\hat{q})$ is a helicity eigenstates, $\vec{\sigma}\cdot\hat{q}\,\alpha^{(h)}(\hat{q}) = 2h\,\alpha^{(h)}(\hat{q})$ and is given by

$$\alpha^{(1/2)}(\hat{p}) = \begin{pmatrix} \cos\frac{\theta}{2} \\ e^{i\phi}\sin\frac{\theta}{2} \end{pmatrix}, \quad \alpha^{(-1/2)}(\hat{p}) = \begin{pmatrix} -e^{i\phi}\sin\frac{\theta}{2} \\ \cos\frac{\theta}{2} \end{pmatrix}, \qquad (2.4.23)$$

*) To avoid the ambiguity of double-valuedness, the Jacob-Wick form of representation $D(R(\hat{q}))$ is used.

The effects of $\mathcal{P}$, $\mathcal{C}$ and $\mathcal{T}$ on the creation and annihilation operators are obtained from Eqs.(3.4.16) and (3.4.21),

$$\mathcal{P}\,a^{(h)}(\vec{p})\,\mathcal{P}^{-1} = i\eta_f\, 2h\, e^{-2i\phi h}\, a^{(-h)}(-\vec{p}),$$

$$\mathcal{C}\,a^{(h)}(\vec{p})\,\mathcal{C}^{-1} = \eta_c\, a^{(h)}(\vec{p}), \qquad (2.4.24)$$

$$\mathcal{T}\,a^{(h)}(\vec{p})\,\mathcal{T}^{-1} = -\eta_T\, e^{2i\phi h}\, a^{(h)}(-\vec{p}).$$

Here we have used the relation

$$\left[D(R(\hat{p}))\right]_{sh} = 2h\, e^{2i\phi h}\left[D(R(-\hat{p}))\right]_{s-h}. \qquad (2.4.25)$$

The transformations of η are the same as those in Eq.(2.4.17) by construction.

It should be noted from Eq.(2.4.22) that in the limit $p \to \infty$, $W_1^{(h)}$ has only $h = -1/2$ state, while $W_2^{(h)}$ has $h = 1/2$ state. For finite q, $h = 1/2$ state in addition to $h = -1/2$ state appears for $W_1^{(h)}$. The limit $q \to \infty$ in turn is interpreted as the $m \to 0$ limit. For $p \gg m$, the main component of $W_1^{(h)}$ is $h = -1/2$ state and $h = 1/2$ state is suppressed by $1 - q/(\omega+m) \propto m/\omega$ in comparison with $h = -1/2$ state as seen from Eq.(2.4.22).

For the right-handed neutrino N_R or ξ, the quantization can be done similarly to η case. A simple way is to quantize $\tilde{\xi}$ at first and then to transform $\tilde{\xi}$ to ξ by using the relation in Eq.(2.1.9). For $\tilde{\xi}$, the result for η is used because the Lagrangian for $\tilde{\xi}$ is exactly the same as that for η as seen from Eq.(2.1.7)

§2.4.2 Majorana neutrinos in four component form

Majorana neutrino (η or ξ) is expressed in a four component form as given in Eq.(2.1.13);[5]

$$N = \begin{pmatrix} -i\sigma_2 \eta^* \\ \eta \end{pmatrix} = N_L + (N_L)^C$$

$$= \int d\Omega_q \sum_{\pm s} \left\{ a^{(s)}(\vec{q})\, u^{(s)}(\vec{q})\, e^{-iqx} + a^{(s)\dagger}(\vec{q})\, v^{(s)}(\vec{q})\, e^{iqx} \right\}, \quad (2.4.26)$$

where

$$u^{(s)}(\vec{q}) = \begin{pmatrix} -i\sigma_2 w_2^{(s)*}(\vec{q}) \\ w_1^{(s)}(\vec{q}) \end{pmatrix}, \quad v^{(s)}(\vec{q}) = C\, \overline{u^{(s)}(\vec{q})}^T. \quad (2.4.27)$$

The four component spinor $u^{(s)}(\vec{q})$ is nothing but a Dirac spinor in the Weyl basis of γ matrix. The $\mathcal{P}$, $\mathcal{C}$ and $\mathcal{T}$ transformations of N are readily obtained from Eq.(2.4.17),

$$\mathcal{P}\, N(\vec{x}, t)\, \mathcal{P}^{-1} = i\eta_P \gamma^0 N(-\vec{x}, t),$$

$$\mathcal{C}\, N(\vec{x}, t)\, \mathcal{C}^{-1} = \eta_C N(\vec{x}, t) = \eta_C N^C(\vec{x}, t), \quad (2.4.28)$$

$$\mathcal{T}\, N(\vec{x}, t)\, \mathcal{T}^{-1} = \eta_T \gamma^1\gamma^3 N(\vec{x}, -t).$$

§2.4.3 Propagators for Majorana neutrino

The propagators of Majorana neutrinos are obtained from Eq.(2.4.6) for $\eta(x)$ in the two component form,

$$\langle T(\eta_\alpha(x)\, \eta_\beta^*(y)) \rangle = i(\partial_t + \vec{\sigma}\cdot\vec{\nabla})\, \Delta_F(x-y),$$

$$\langle T(\eta_\alpha(x)\, \eta_\beta(y)) \rangle = m(-i\sigma_2)_{\alpha\beta}\, i\Delta_F(x-y), \quad (2.4.29)$$

$$\langle T(\eta_\alpha^*(x)\, \eta_\beta^*(y)) \rangle = -m(-i\sigma_2)_{\alpha\beta}\, i\Delta_F(x-y),$$

where

$$\Delta_F(x-y) = \int \frac{d^4q}{(2\pi)^4} \frac{e^{-iq(x-y)}}{q^2 - m^2 + i\varepsilon}. \quad (2.4.30)$$

For the four component form of Majorana neutrino N(x) we find from Eq.(2.4.26),

$$\langle T(N(x)\, \bar{N}(y)) \rangle = i S_F(x-y),$$

$$\langle T(N(x)\, N^T(y)) \rangle = i S_F(x-y) C^T,$$

$$\langle T(\bar{N}^T(x)\, \bar{N}^T(y)) \rangle = C^{-1} i S_F(x-y) C^T, \quad (2.4.31)$$

$$\langle T(\bar{N}^T(x)\, \bar{N}(y)) \rangle = C^{-1} i S_F(x-y),$$

where $S_F(x-y) = (i\gamma^\mu\partial_\mu + m)\Delta_F(x-y)$ and T means the transpose. Note that in the case of the Dirac neutrino, $\langle T(\Psi(x), \bar{\Psi}(y)) \rangle = iS_F(x-y)$ is remained, as it is easily confirmed by using Eq.(2.5.1).

§2.4.4 Dirac method of quantization of Majorana neutrino

Let us consider the quantization in the four component form with constraint $N = N^C$. The starting Lagrangian is

$$\mathcal{L} = \bar{N}(i\gamma^\mu\partial_\mu - m) N. \quad (2.4.32)$$

The canonical quantity of N is $\pi = iN^*$, but that of N^* is $\pi^* = 0$. Therefore, there are three primary constraints $\phi_i \approx 0$, where

$$\phi_1 = N - N^C, \quad \phi_2 = \pi - iN^*, \quad \phi_3 = \pi^*. \quad (2.4.33)$$

By using the Poisson bracket such as

$$\{ N_\alpha(\vec{x}, t), \pi_\beta(\vec{y}, t) \} = i\delta_{\alpha\beta}\delta(\vec{x}-\vec{y}),$$

$$\{ N_\alpha^*(\vec{x}, t), \pi_\beta^*(\vec{y}, t) \} = i\delta_{\alpha\beta}\delta(\vec{x}-\vec{y}), \quad \text{etc.}, \quad (2.4.34)$$

we evaluate the matrix $\Phi(x, y)$ defined by the Poisson brackets among ϕ_i,

$$\mathfrak{C}(\vec{x},\vec{y}) = \{\phi^T(\vec{x}),\phi(\vec{y})\} = \begin{pmatrix} 0 & 1 & -C\gamma^{0T} \\ -1 & 0 & -i1 \\ C\gamma^{0T} & i1 & 0 \end{pmatrix} \delta(\vec{x}-\vec{y}), \tag{2.4.35}$$

where $\phi^T(\vec{x}) = (\phi_1(\vec{x}), \phi_2(\vec{x}), \phi_3(\vec{x}))$. The matrix $\mathfrak{C}(\vec{x}, \vec{y})$ is non-singular and thus the constraints are the second class. Let us define the inverse of $\mathfrak{C}(\vec{x}, \vec{y})$ by

$$\int \mathfrak{C}(x,y)\,\mathfrak{C}^{-1}(y,z)\,dy = \delta(x-z). \tag{2.4.36}$$

Then we find

$$\mathfrak{C}^{-1}(\vec{x},\vec{y}) = -\frac{1}{2}\begin{pmatrix} -iC\gamma^{0T} & -1 & C\gamma^{0T} \\ 1 & -iC\gamma^{0T} & -i1 \\ -C\gamma^{0T} & i1 & -iC\gamma^{0T} \end{pmatrix}\delta(\vec{x}-\vec{y}). \tag{2.4.37}$$

Now the Dirac bracket $\{A, B\}^*$ is defined as

$$\{A(\vec{x}), B(\vec{y})\}^* = \{A(\vec{x}), B(\vec{y})\} - \int d\vec{z}\,d\vec{z}'\{A(\vec{x}),\phi(\vec{z})\}\mathfrak{C}^{-1}(\vec{z},\vec{z}')\{\phi(\vec{z}'), B(\vec{y})\}. \tag{2.4.38}$$

Then by the explicit evaluation, we find

$$\{N(\vec{x}), \pi(\vec{y})\}^* = \frac{i}{2}\delta(\vec{x}-\vec{y}), \tag{2.4.39a}$$

$$\{N^*(\vec{x}), \pi(\vec{y})\}^* = \frac{i}{2}C\gamma^{0T}\delta(\vec{x}-\vec{y}), \tag{2.4.39b}$$

$$\{N(\vec{x}), \pi^*(\vec{y})\}^* = \{N^*(\vec{x}), \pi^*(\vec{y})\} = 0, \tag{2.4.39c}$$

$$\{N(\vec{x}), N^*(\vec{y})\}^* = \frac{1}{2}\delta(\vec{x}-\vec{y}), \tag{2.4.39d}$$

$$\{N(\vec{x}), N(\vec{y})\}^* = \frac{1}{2}C\gamma^{0T}\delta(\vec{x}-\vec{y}), \tag{2.4.39e}$$

$$\{N^*(\vec{x}), N^*(\vec{y})\}^* = \frac{1}{2}C\gamma^{0T}\delta(\vec{x}-\vec{y}). \tag{2.4.39f}$$

These Dirac brackets are consistent even when the constraints $\phi_1 = \phi_2 = \phi_3 = 0$ are imposed strongly. There we obtained Dirac brackets among N and N^* in Eqs.(2.4.39d)-(2.4.39f), which are exactly those derived from Eqs.(2.4.26) and (2.4.4).

§2.4.5 Ambiguity in the description of Majorana neutrino

Kayser[46] and Bernabeu and Pascual[47] considered some different expressions of Majorana neutrinos. Here we shall explain the relation between our definition of η in Eq.(2.4.6) and theirs.

At first, we shall show that η in Eq.(2.4.6) is the most general form if the positive mass Lagrangian is used. Let us parametrize η as

$$\eta(\vec{x},t) = \int d\Omega_q \sum_{\pm s}\{\rho_1 a^{(s)}(\vec{q})\,w_1^{(s)}(\vec{q})\,e^{-iqx} + \rho_2\, a^{(s)\dagger}(\vec{q})\,w_2^{(s)}(\vec{q})\,e^{iqx}\}, \tag{2.4.40}$$

where ρ_1 and ρ_2 are some complex numbers. By substituting it into Eqs.(2.4.4) and (2.4.5), we find the constraints,

$$|\rho_1| = |\rho_2| = 1 \qquad \text{from CCR's,} \tag{2.4.41}$$

$$\rho_1 = \rho_2^* \qquad \text{from equation of motion.} \tag{2.4.42}$$

Then these phase factors ρ_1 and ρ_2 can be absorbed in the definition of $a^{(s)}(\vec{q})$ and $a^{(s)\dagger}(\vec{q})$. Thus, we obtain Eq.(2.4.6). Note that the positivity of Hamiltonian is guaranteed by the constraints in Eq.(2.4.41).

In order to relax the constraint in Eq.(2.4.42), the complex mass has to be considered,

$$\mathcal{L}_L = \eta_\rho^\dagger O_- \eta_\rho - \frac{m}{2}(\rho_0\,\eta_\rho^T i\sigma_2\,\eta_\rho - \rho_0^*\,\eta_\rho^\dagger i\sigma_2\,\eta_\rho^*), \tag{2.4.43}$$

where ρ_0 is a phase factor and $m > 0$. Here we attached the suffix ρ for η to indicate the complex mass. The relation between the real mass case η and the complex mass case η_ρ is given by

$$\eta_\rho(x,t) = \sqrt{\rho_0^*}\,\eta(x,t), \tag{2.4.44}$$

which corresponds to the Majorana field considered by Bernabeu and Pascual.[47] By absorbing $\sqrt{\rho_0^*}$ in the annihilation operator

$$a^{(s)}(\vec{q})' = \sqrt{\rho_0^*}\; a^{(s)}(\vec{q}), \tag{2.4.45}$$

we obtain

$$\eta_\rho' = \int d\Omega_q \sum_{\pm s} \{ a^{(s)'}(\vec{q})\, w_1^{(s)}(\vec{q})\, e^{-iqx} + \rho_0\, a^{(s)'\dagger}(\vec{q})\, w_2^{(s)}(\vec{q})\, e^{iqx} \}, \tag{2.4.46}$$

which is the field discussed by Kayser.[46] For this Majorana field with complex mass, the four component form should be expressed as

$$N_\rho(x) = \begin{pmatrix} -\rho_0 i\sigma_2\, \eta_\rho'^*(x) \\ \eta_\rho'(x) \end{pmatrix} = N_L(x) + \rho_0 (N_L(x))^c, \text{ and } [N_\rho(x)]^c = \rho_0 N_\rho(x). \tag{2.4.47}$$

Now the Majorana type propagators depend on ρ_0, for example, as

$$\langle T(N(x)\, N^T(y)) \rangle = \rho_0\, i S_F(x-y)\, C^T. \tag{2.4.48}$$

It is clear that the use of the complex masses for neutrino is inconvenient for the practical calculation in comparison with the use of the simple real masses.

§2.5 Possible types of neutrinos

§2.5.1 Dirac neutrino

Let us construct a Dirac neutrino out of a pair of Majorana neutrinos with degenerate mass in the following manner:[5]

$$\begin{aligned} \psi_L &= (N_{1L} + i\, N_{2L})/\sqrt{2}, \\ \psi_R &= ((N_{1L})^c + i\,(N_{2L})^c)/\sqrt{2}, \end{aligned} \tag{2.5.1}$$

where

$$N_j = \begin{pmatrix} -i\sigma_2\, \eta_j^* \\ \eta_j \end{pmatrix} \quad \text{or} \quad \begin{pmatrix} \xi_j \\ i\sigma_2\, \xi_j^* \end{pmatrix}. \tag{2.5.2}$$

Then, $\psi = \psi_L + \psi_R$ is written as

$$\psi(x,t) = \int d\Omega_q \sum_{\pm s} \{ A^{(s)}(\vec{q})\, u^{(s)}(\vec{q})\, e^{-iqx} + B^{(s)\dagger}(\vec{q})\, v^{(s)}(\vec{q})\, e^{iqx} \}, \tag{2.5.3}$$

where $u^{(s)}(\vec{q})$ and $v^{(s)}(\vec{q})$ are defined in Eq.(2.4.27) and

$$\begin{aligned} A^{(s)}(\vec{q}) &= (a_1^{(s)}(\vec{q}) + i\, a_2^{(s)}(\vec{q}))/\sqrt{2}, \\ B^{(s)}(\vec{q}) &= (a_1^{(s)}(\vec{q}) - i\, a_2^{(s)}(\vec{q}))/\sqrt{2}. \end{aligned} \tag{2.5.4}$$

The annihilation operator $A^{(s)}(\vec{q})$ and $B^{(s)}(\vec{q})$ should behave as those of a Dirac particle under $\mathcal{P}$, $\mathcal{C}$ and $\mathcal{T}$,

$$\begin{aligned} &\mathcal{P}\, A^{(s)}(\vec{q})\, \mathcal{P}^{-1} = i\,\varepsilon_P\, A^{(s)}(-\vec{q}), \quad \mathcal{P}\, B^{(s)}(\vec{q})\, \mathcal{P}^{-1} = i\,\varepsilon_P\, B^{(s)}(-\vec{q}), \\ &\mathcal{C}\, A^{(s)}(\vec{q})\, \mathcal{C}^{-1} = \varepsilon_C\, B^{(s)}(\vec{q}), \quad \mathcal{C}\, B^{(s)}(\vec{q})\, \mathcal{C}^{-1} = \varepsilon_C\, A^{(s)}(\vec{q}), \\ &\mathcal{T}\, A^{(s)}(\vec{q})\, \mathcal{T}^{-1} = \varepsilon_T \sum_{s'} (i\sigma_2)_{ss'}\, A^{(s')}(-\vec{q}), \\ &\mathcal{T}\, B^{(s)}(\vec{q})\, \mathcal{T}^{-1} = \varepsilon_T \sum_{s'} (i\sigma_2)_{ss'}\, B^{(s')}(-\vec{q}). \end{aligned} \tag{2.5.5}$$

In order to satisfy Eq.(2.5.5), $a_1^{(s)}$ and $a_2^{(s)}$ in Eq.(2.5.4) should have the same parity, but the opposite signs for the charge conjugation and the time reversal, i.e.,

$$\varepsilon_{P_1} = \varepsilon_{P_2} = \varepsilon_P, \quad \varepsilon_{C_1} = -\varepsilon_{C_2} = \varepsilon_C, \quad \varepsilon_{T_1} = -\varepsilon_{T_2} = \varepsilon_T. \tag{2.5.6}$$

For the Dirac field ψ, we find

$$\begin{aligned} &\mathcal{P}\, \psi(x,t)\, \mathcal{P}^{-1} = i\,\varepsilon_P\, \gamma^0\, \psi(-x,t), \\ &\mathcal{C}\, \psi(x,t)\, \mathcal{C}^{-1} = \varepsilon_C\, C\, \bar{\psi}^T(x,t), \\ &\mathcal{T}\, \psi(x,t)\, \mathcal{T}^{-1} = \varepsilon_T\, \gamma^1\gamma^3\, \psi(x,-t). \end{aligned} \tag{2.5.7}$$

Since we have started from massive Majorana neutrinos, the parity phase is $\pm i$ rather than ± 1. Also, ε_P, ε_C and ε_T are restricted to be ± 1. It is possible to construct a Dirac field as $\psi_- = (N_1 - iN_2)/\sqrt{2}$, but there is no physical difference between ψ and ψ_-.

A Dirac field can also be constructed from two Majorana fields related to N_1 and N_2 by the orthogonal transformation[5]

$$\begin{pmatrix} N_1(\alpha) \\ N_2(\alpha) \end{pmatrix} = \begin{pmatrix} \cos\alpha & -\sin\alpha \\ \sin\alpha & \cos\alpha \end{pmatrix} \begin{pmatrix} N_1 \\ N_2 \end{pmatrix}. \tag{2.5.8}$$

Then a Dirac field $\psi_\alpha = (N_1(\alpha) + i N_2(\alpha))/\sqrt{2}$ is related to ψ by $\psi_\theta = e^{i\alpha}\psi$. This is the origin of the phase freedom for Dirac field. If the unitary transformation is used in Eq.(2.5.8), a Jauch field is obtained, instead of a Dirac field, because particle and anti-particle are mixed in this case.[48]

In the above, we have explained how to construct a Dirac neutrino from a pair of mass degenerate neutrinos. There are two types of Dirac neutrino. If a pair of neutrinos are in the same flavor, the composed Dirac neutrino is an <u>ordinary Dirac neutrino</u> with the definite lepton number which is conserved. The other is the case where two or more flavors of neutrinos are involved. Then, the combination of lepton numbers is conserved for this type of Dirac neutrinon which is called the <u>Konopinski-Mahmoud (KM) Dirac neutrino</u>, proposed by Konopinski and Mahmoud in 1953.[13),50),168)]

For definiteness, let us consider the following mass term,

$$\mathcal{L}_M = -\frac{1}{2}\left(\overline{(\nu_{eL})^c}, \overline{(\nu_{\mu L})^c}\right)\begin{pmatrix} 0 & m \\ m & 0 \end{pmatrix}\begin{pmatrix} \nu_{eL} \\ \nu_{\mu L} \end{pmatrix} + \text{h.c.}. \tag{2.5.9}$$

In this case, a KM Dirac neutrino is formed as

$$\psi = \nu_{eL} + (\nu_{\mu L})^c \text{ and } \mathcal{L}_M = -m\,\bar{\psi}\psi, \tag{2.5.10}$$

which is characterized by the conserved lepton number

$$L_e - L_\mu . \tag{2.5.11}$$

This is because the mass term is invariant under the phase transformation,

$$\nu_{eL} \to e^{i\alpha}\nu_{eL}, \quad \nu_{\mu L} \to e^{-i\alpha}\nu_{\mu L}. \tag{2.5.12}$$

Let us examine this case from the viewpoint of Majorana neutrino. Define

$$\nu_{eL} = \begin{pmatrix} 0 \\ \chi_e \end{pmatrix}, \quad \nu_{\mu L} = \begin{pmatrix} 0 \\ \chi_\mu \end{pmatrix}. \tag{2.5.13}$$

Then the mass term becomes

$$\mathcal{L}_M = -\frac{m}{2}\left(\chi_e^T i\sigma_2 \chi_\mu + \chi_\mu^T i\sigma_2 \chi_e - \chi_e^\dagger i\sigma_2 \chi_\mu^\dagger - \chi_\mu^\dagger i\sigma_2 \chi_e^*\right). \tag{2.5.14}$$

By the transformation,

$$\begin{aligned} \chi_e &= (\eta_1 + i\eta_2)/\sqrt{2}, \\ \chi_\mu &= (\eta_1 - i\eta_2)/\sqrt{2}, \end{aligned} \tag{2.5.15}$$

we obtain

$$\mathcal{L}_M = -\frac{m}{2}\left(\eta_1^T i\sigma_2 \eta_1 + \eta_2^T i\sigma_2 \eta_2 - \eta_1^\dagger i\sigma_2 \eta_1^* - \eta_2^\dagger i\sigma_2 \eta_2^*\right). \tag{2.5.16}$$

Now from Eq.(2.1.8), η_1 and η_2 are the left-handed Majorana neutrinos with degenerate mass and have even and odd CP signs, respectively, due to the i factor. A KM Dirac neutrino is constructed from these Majorana neutrinos as

$$\psi = \frac{1}{\sqrt{2}}\left\{\begin{pmatrix} -i\sigma_2\eta_1^* \\ \eta_1 \end{pmatrix} + i\begin{pmatrix} -i\sigma_2\eta_2^* \\ \eta_2 \end{pmatrix}\right\} = \begin{pmatrix} -i\sigma_2\chi_\mu^* \\ \chi_e \end{pmatrix}, \tag{2.5.17}$$

which corresponds to Eq.(2.5.10).

§2.5.2 The pseudo Dirac (PD) neutrino

Suppose that the mass degeneracy of neutrinos arises as a consequence of the special symmetry in the mass matrix. Then a pair of degenerate Majorana neutrinos forms a Dirac neutrino, as we saw in the example of the Konopinski-Mahmoud Dirac neutrino. If the symmetry of mass matrix is not the symmetry of the weak interaction, the mass degeneracy is solved by the higher order perturbations of weak interaction and thus neutrinos which form a Dirac neutrino at tree level split into two Majorana neutrinos with different masses. If the mass splitting is finite, then it must be very small in comparison with their masses so that almost degenerate neutrinos come out. These neutrinos are called the pseudo-Dirac (PD) neutrino.[49),50),5)]

By the detailed analysis, it was argued that there needs some underlying global or discrete symmetry which is broken spontaneously in order to obtain the finite mass splitting of a PD neutrino.[168)]

The PD neutrino gives an attractive mechanism to suppress the contribution from the neutrino mass part of the $(\beta\beta)_{0\nu}$ mode $\langle m_\nu \rangle$, although their masses may not be small. This is because $\langle m_\nu \rangle$ vanishes in the limit of zero mass splitting due to the Dirac character of it. Explicitly, in the two generation mixing in Eq.(2.3.3) with $\beta = \pi/2$, the weak eigenstate neutrinos are expressed in the tree level as

$$\begin{aligned} \nu_{eL} &= \cos\xi\ \psi_L + \sin\xi\ (\psi^c)_L, \\ \nu_{\mu L} &= -\sin\xi\ \psi_L + \cos\xi\ (\psi^c)_L, \end{aligned} \tag{2.5.18}$$

where $\sin\xi = (\cos\theta - \sin\theta)/\sqrt{2}$ and $\cos\xi = (\cos\theta + \sin\theta)/\sqrt{2}$. The KM Dirac neutrino in Eq.(2.5.10) is the special case with $\theta = \pi/4$ $(\xi = 0)$, where the weak interaction becomes

$$\mathcal{L}_W = (g_L/\sqrt{2})\left[\bar{e}\,\gamma_\rho\,\psi_L + \bar{\mu}\,\gamma_\rho\,(\psi^c)_L\right] W_L^\rho + h.c. \tag{2.5.19}$$

corresponding to Eq.(2.3.17). But if $\theta \neq \pi/4$ $(\xi \neq 0)$, the small mass splitting due to the coexistence of ψ_L and $(\psi^c)_L$ arises as $\Delta m = |m_1 - m_2| \ll |m_1 + m_2|$ and $\theta = \pi/4 + O(\Delta m/|m_1 + m_2|)$. Thus $\langle m_\nu \rangle$ in Eq.(2.3.5) is suppressed considerably. There are two left-handed Majorana neutrinos with the tiny mass difference, instead of a Konopinski-Mahmoud Dirac neutrino.

§2.6 Models of neutrino mass matrix

§2.6.1 The see-saw mechanism and the effective mass of neutrino

Let us briefly discuss a mechanism to explain the small masses of the observed left-handed neutrinos, the so-called see-saw mechanism which was discovered by Yanagida,[6] Gell-Mann, Ramond and Slanski.[6]

For simplicity, we shall consider a case where there are one left-handed and one right-handed neutrinos. The mass matrix of them in the CP conservation case is written in the form Eq.(2.2.10) as

$$\mathcal{M} = \begin{pmatrix} \mu & m \\ m & M \end{pmatrix}, \tag{2.6.1}$$

where μ, m and M are real. As an example, let us assume that $\mu \geq 0$, $M > 0$ and $(m^2/M) > \mu$. In general the right-handed Majorana mass M is assumed to be produced when the left-right symmetry is broken, the Dirac mass m is induced when the $SU(2)_L \times U(1)$ symmetry is broken so that it is the same order of the charged lepton or quark masses, and finally the left-handed Majorana mass μ is assumed to be zero or small, i.e., $\mu \ll |m| \ll M$. By diagonalizing the mass matrix, neutrinos ν_L and ν_R are related to the mass eigenstate Majorana neutrinos:

$$\begin{pmatrix} \nu_L \\ (\nu_R)^c \end{pmatrix} = \begin{pmatrix} i\cos\theta & \sin\theta \\ -i\sin\theta & \cos\theta \end{pmatrix} \begin{pmatrix} N_{1L} \\ N_{2L} \end{pmatrix}, \tag{2.6.2}$$

where N_1 and N_2 are Majorana neutrinos with masses

$$m_1 \simeq m^2/M - \mu, \qquad m_2 \simeq M + m^2/M, \tag{2.6.3}$$

$$\tan\theta \simeq +m/M, \tag{2.6.4}$$

Here the i factor is introduced in the mixing matrix to make m_1 positive as discussed in Eq.(2.3.16).

From Eq.(2.6.3), we observe an interesting mass relation,

$$m_1 \ll |m| \ll m_2. \tag{2.6.5}$$

That is, the small mass of the left-handed neutrino (m_1), say, electron neutrino in comparison with the charged lepton mass (m), electron, is naturally explained. The size of its mass depends on models in consideration. For example, if $\mu = 0$, $m = m_e$ and $M \sim 1$ TeV which may be realized in some models based on $SU(2)_L \times SU(2)_R \times U(1)$, $m_{\nu_e} \sim 0$ (1 eV) is expected.

Another interesting aspect is that N_1 and N_2 have opposite CP signs because of the i factor, so that they contribute to the m_ν part of the $(\beta\beta)_{0\nu}$ mode destructively (the cancellation between the light left-handed and heavy right-handed Majorana neutrinos). This possibility of suppressing $\langle m_\nu \rangle$ was discussed by Halprin, Petcov and Rosen. (See §9.2.)[52]

Let us consider the system of two light left-handed neutrinos where mass matrix has the similar mass hierarchy $\mu \ll |m| \ll M \sim 0$ (1 MeV) in Eq.(2.6.1). We assume that there is no charged lepton mixing so that the transformation matrix in Eq.(2.6.2) becomes the neutrino mixing matrix U. Assuming that both Majorana neutrinos are not heavy, we find that the effective neutrino mass $\langle m_\nu \rangle$ is rewritten by using Eq.(2.6.2) as

$$\langle m_\nu \rangle = \left| \sum_{j=1}^{2} m_j U_{ej}^2 \right| = \left| \sum_{j=1}^{2} U_{ej}\, m_j\, (U^T)_{je} \right|$$
$$= |m_{ee}| = \mu. \tag{2.6.6}$$

In particular, if $\mu = 0$, the effective mass vanishes and the m_ν part does not contribute to the $(\beta\beta)_{0\nu}$ mode. This case was discussed by Fukugita and Yanagida.[53] One drawback of this scenario is that in the actual situation, there is a charged lepton mixing which changes the neutrino mixing slightly from the transformation matrix in Eq.(2.6.2). Then the delicate balance of cancellation is destroyed. Explicitly we have

$$\langle m_\nu \rangle = (O_\ell^T m O_\ell)_{ee} = \mu \cos^2\theta_\ell - 2m \sin\theta_\ell \cos\theta_\ell + M \sin^2\theta_\ell,$$
$$O_\ell = \begin{pmatrix} \cos\theta_\ell & \sin\theta_\ell \\ -\sin\theta_\ell & \cos\theta_\ell \end{pmatrix}, \qquad (2.6.7)$$

where O_ℓ is the orthogonal matrix with the rotation angle θ_ℓ and represents the mixing matrix for charged leptons. Since $M \sim 0$ (1 MeV), even the small mixing θ_ℓ may produce the large contribution $M \sin^2\theta_\ell$ from N_2.

§2.6.2 Models of mass matrix with an approximate global symmetry

In the previous subsection, we saw that in the light neutrino system, it is delicate to suppress the neutrino mass contribution to the $(\beta\beta)_{0\nu}$ mode, $\langle m_\nu \rangle$. Here we shall consider a possibility that the cancellation among contributions from light neutrinos is assured by an approximate global symmetry. One simple example is the situation of the PD neutrino where the combination of lepton numbers is approximately conserved. This kind of possibility was first considered by Wolfenstein[49] and later by many authors.[5),50),51] Here we shall explore this possibility in two, three and four generation cases. Although the symmetry is violated by a small amount so that a small $(\beta\beta)_{0\nu}$ decay rate is expected, we pretend here that the symmetry is exact.

(i) Two generation case

In order to provide the neutrino mass to forbid the $(\beta\beta)_{0\nu}$ mode, only possible conserved lepton number out of individual lepton numbers $L_{e,\mu,\tau}$ is $L_e - L_\mu$ or $L_e - L_\tau$. The conservation of this kind of lepton number is realized by the Konopinski-Mahmoud Dirac neutrino consisting of two mass degenerate neutrinos ν_{eL} and $\nu_{\mu L}$ or ν_{eL} and $\nu_{\tau L}$ as shown in Eq.(2.5.10). In addition, the neutrino oscillations between ν_{eL} and $\nu_{\mu L}$ or ν_{eL} and $\nu_{\tau L}$ are forbidden if $L_e - L_\mu$ or $L_e - L_\tau$ is conserved. If the symmetry is broken by a small amount, we have almost degenerate two Majorana neutrinos (the PD neutrino).

(ii) Three generation case

There are three possibilities to forbid the $(\beta\beta)_{0\nu}$ mode as discussed by Dugan, Gelmini, Georgi and Hall;[54] the conserved $L_e + L_\mu - L_\tau$, $L_e + L_\tau - L_\mu$ or $L_e - L_\mu - L_\tau$ number. In the basis where the first (second, third) row and column refer to the weak eigenstate neutrino ν_{eL} ($\nu_{\mu L}$, $\nu_{\tau L}$) and where the charged lepton mass matrix is diagonal, the most general mass matrix is written as follows:

$$m_1 = m \begin{pmatrix} 0 & \sin\theta & 0 \\ \sin\theta & 0 & \cos\theta \\ 0 & \cos\theta & 0 \end{pmatrix} \quad \text{for } L_e + L_\tau - L_\mu \text{ conservation,} \qquad (2.6.8)$$

$$m_2 = m \begin{pmatrix} 0 & 0 & \sin\theta \\ 0 & 0 & \cos\theta \\ \sin\theta & \cos\theta & 0 \end{pmatrix} \quad \text{for } L_e + L_\mu - L_\tau \text{ conservation,} \qquad (2.6.9)$$

$$m_3 = m \begin{pmatrix} 0 & \sin\theta & \cos\theta \\ \sin\theta & 0 & 0 \\ \cos\theta & 0 & 0 \end{pmatrix} \quad \text{for } L_e - L_\mu - L_\tau \text{ conservation.} \qquad (2.6.10$$

The mass matrix $\mathcal{M}_1$ is readily diagonalized by the unitary transformation of neutrinos (the $L_e + L_\tau - L_\mu$ case),

$$\begin{aligned}
\nu_{eL} &= \cos\theta\, N_{1L} + \frac{1}{\sqrt{2}} \sin\theta\, (N_{2L} - i N_{3L}), \\
\nu_{\mu L} &= \frac{1}{\sqrt{2}} (N_{2L} + i N_{3L}), \\
\nu_{\tau L} &= -\sin\theta\, N_{1L} + \frac{1}{\sqrt{2}} \cos\theta\, (N_{2L} - i N_{3L}),
\end{aligned} \tag{2.6.11}$$

where N_1 is massless Majorana neutrino, while N_2 and N_3 are Majorana neutrinos with the degenerate mass m. From Eq.(2.5.1), a pair of mass degenerate Majorana neutrinos N_2 and N_3 can form a Konopinski-Mahmoud Dirac neutrino ψ with the mass m. Thus, we find

$$\begin{aligned}
\nu_{eL} &= \cos\theta\, N_{1L} + \sin\theta\, (\psi^c)_L, \\
\nu_{\mu L} &= \psi_L, \\
\nu_{\tau L} &= -\sin\theta\, N_{1L} + \cos\theta\, (\psi^c)_L.
\end{aligned} \tag{2.6.12}$$

For the $L_e + L_\mu - L_\tau$ conservation case, the above relations are used by the exchange of ν_{μ_L} and ν_{τ_L}. Similarly for $L_e - L_\mu - L_\tau$, the exchange of ν_{eL} and ν_{μ_L} is sufficient.

The interesting point of these models is that there are one mass zero Majorana neutrino and a Konopinski-Mahmoud Dirac neutrino. The neutrino oscillation between ν_{eL} and ν_{μ_L} is forbidden for the $L_e + L_\tau - L_\mu$ and $L_e - L_\mu - L_\tau$ cases, but is allowed for the $L_e + L_\mu - L_\tau$ case where the mixing angle is restricted severely by the $\nu_{eL} - \nu_{\mu_L}$ oscillation experiment (the small mixing case). The electron neutrino ν_{eL} does not mix with other neutrinos for the $L_e - L_\mu - L_\tau$ case. Therefore, if large mixing between the massless

and massive neutrinos is considered, only the $L_e + L_\tau - L_\mu$ conservation is compatible

If the above symmetry is broken spontaneously by a small amount, then the Dirac neutrino ψ splits into two Majorana neutrinos with different masses by the higher order perturbation. Since the mass splitting is finite,[168] two neutrinos with almost degenerate mass come out (the PD neutrino).

The approximate $L_e + L_\mu - L_\tau$ conservation may be naturally realized in the Zee model.[55] In this model, neutrinos are massless in the tree level and acquire masses in the one loop order by the singlet Higgs coupling to neutrinos. According to Zee, the mass matrix is expressed as

$$\begin{pmatrix}
0 & f_{e\mu}(m_\mu^2 - m_e^2) & f_{e\tau}(m_\tau^2 - m_e^2) \\
f_{e\mu}(m_\mu^2 - m_e^2) & 0 & f_{\mu\tau}(m_\tau^2 - m_\mu^2) \\
f_{e\tau}(m_\tau^2 - m_e^2) & f_{\mu\tau}(m_\tau^2 - m_\mu^2) & 0
\end{pmatrix}. \tag{2.6.13}$$

It is expected that $f_{e\mu}$, $f_{e\tau}$ and $f_{\mu\tau}$ are the quantities of the same order of magnitude. Since $f_{e\mu} m_\mu^2 \ll f_{e\tau} m_\tau^2$, we arrive at the mass matrix $\mathcal{M}_2$ in Eq.(2.6.9). The property of this case was discussed in Ref. 41.

(iii) Four generation case

Three generation case predicted a massless Majorana neutrino and a massive Dirac neutrino. If one wants to have all massive neutrinos, one simple way is to consider the four generation case where two massive Dirac neutrino appear. For definiteness, we shall consider

the $L_e + L_\tau - L_\mu - L_{\tau'}$ conservation, where τ' is the fourth generation of lepton. In the basis of $(\nu_{eL}, \nu_{\tau L}, \nu_{\mu L}, \nu_{\tau' L})$ and the diagonal mass of charged leptons, the neutrino mass matrix is given by

$$\mathcal{M} = \begin{pmatrix} 0 & A \\ A^T & 0 \end{pmatrix}, \tag{2.6.14}$$

where A is the 2×2 matrix. The matrix A is diagonalized by the unitary transformation as

$$\alpha^+ A \beta = D_\nu, \tag{2.6.15}$$

where D_ν is the diagonal matrix with positive eigenvalues. With the aid of the 2×2 unitary matrix α and β, $\mathcal{M}$ is diagonalized as

$$\frac{1}{\sqrt{2}}\begin{pmatrix} 1 & 1 \\ -i1 & i1 \end{pmatrix}\begin{pmatrix} \alpha^+ & 0 \\ 0 & \beta^T \end{pmatrix}\begin{pmatrix} 0 & A \\ A^T & 0 \end{pmatrix}\begin{pmatrix} \alpha^* & 0 \\ 0 & \beta \end{pmatrix}\frac{1}{\sqrt{2}}\begin{pmatrix} 1 & -i1 \\ 1 & i1 \end{pmatrix}$$

$$= \frac{1}{\sqrt{2}}\begin{pmatrix} 1 & 1 \\ -i1 & i1 \end{pmatrix}\begin{pmatrix} 0 & D_\nu \\ D_\nu & 0 \end{pmatrix}\frac{1}{\sqrt{2}}\begin{pmatrix} 1 & -i1 \\ 1 & i1 \end{pmatrix} = \begin{pmatrix} D_\nu & 0 \\ 0 & D_\nu \end{pmatrix}. \tag{2.6.16}$$

Therefore we have two pairs of degenerate Majorana neutrinos. The weak eigenstate neutrinos are related to the mass eigenstate Majorana neutrinos as

$$\begin{pmatrix} \nu_{eL} \\ \nu_{\tau L} \\ \nu_{\mu L} \\ \nu_{\tau' L} \end{pmatrix} = \begin{pmatrix} \alpha^* & 0 \\ 0 & \beta \end{pmatrix}\frac{1}{\sqrt{2}}\begin{pmatrix} 1 & -i1 \\ 1 & i1 \end{pmatrix}\begin{pmatrix} N_{1L} \\ N_{2L} \\ N_{3L} \\ N_{4L} \end{pmatrix}$$

$$= \begin{pmatrix} \alpha^* & 0 \\ 0 & \beta \end{pmatrix}\begin{pmatrix} (\psi_1^c)_L \\ (\psi_2^c)_L \\ \psi_{1L} \\ \psi_{2L} \end{pmatrix}, \tag{2.6.17}$$

where the degenerate pair N_1 and N_3 form a Dirac neutrino ψ_1, and N_2 and N_4 do ψ_2 as seen in Eq.(2.5.1). Again the neutrino oscillation between ν_{eL} and $\nu_{\mu L}$ is forbidden.

The physical implication of these schemes will be discussed in §9.

§2.7 Electromagnetic property of neutrinos

In this section, we shall discuss how neutrinos interact with electromagnetic fields. Since neutrino is neutral, there is, of course, no coupling to photon in the Lagrangian and two static moments (the magnetic and electric dipole moments) come from the loop effect.

A massless chiral (Weyl) neutrino cannot have a nonzero electric and magnetic moments. The same is true for a Majorana neutrino, independently of whether massless or massive: This is due to a relation characteristic to Majorana neutrinos from $N_j^C = N_j$,[59),60)]

$$\int d^4x\, \overline{N_1}\, i\sigma_{\mu\nu}(a + b\gamma_5)\, \partial^\nu N_2 = -\int d^4x\, \overline{N_2}\, i\sigma_{\mu\nu}(a + b\gamma_5)\, \partial^\nu N_1 . \tag{2.7.1}$$

Only the transition moments between different Majorana neutrinos are allowed.

On the other hand, a massive Dirac neutrino can have a magnetic (and electric if T is violated) moment. We denote the magnetic moment of neutrino by $\vec{\mu}_{\nu_i} = \mu_{\nu_i}\vec{\sigma}$, where the index i labels the mass eigenstate neutrino. The μ_ν arises at one loop level in the weak interaction and its value in the standard $SU(2)_L \times U(1)$ theory is[56),57)]

$$\mu_\nu^{(stand)} = \frac{3e G_F m_\nu}{8\pi^2\sqrt{2}} = 1.85 \cdot 10^{-27} (m_\nu/1eV)\ e\mathrm{V}\ G^{-1}. \tag{2.7.2}$$

The μ_ν is very sensitive to the right-handed currents. If it presents (at a phenomenologically allowed level), these could lead to $\mu_\nu \gg \mu_\nu^{(stand)}$.[58]

As we saw, massive Majorana neutrinos have only the transition moments which were derived and discussed by various authors.[56),59),60)] The transition moments give the weak correction to the neutral current and the decay of the heavy neutrino ν_H to the lighter one ν_L electromagnetically, $\nu_H \to \nu_L + \gamma$ which is important in the connection with cosmology.

The fact that the magnetic moment exists for a massive Dirac neutrino, but not for a massive Majorana neutrino may give another possibility to discriminate Dirac and Majorana neutrinos. Although the magnetic dipole moment of a Dirac neutrino is extremely small, it may have significant astrophysical consequences. Fujikawa and Shrock[57] considered a possibility that the magnetic moment $\vec{\mu}_\nu$ causes the neutrino spin to rotate by a cosmological constant magnetic field. In the $SU(2)_L \times U(1)$ theories with massive neutrinos, a neutrino is produced as a mixture of helicity states $\psi_\nu(\pm 1/2)$, but the relativistic cosmic ν is predominantly in the $h = -1/2$ state. A spin rotation from $\psi_\nu(-1/2)$ toward $\psi_\nu(+1/2)$ will reduce the resultant effective weak neutral and charged current scattering cross sections for ν which arise, predominantly, from the helicity state h (-1/2) in the relativistic case. By assuming the magnetic field $B \sim 10^{13}$ G which may be realized in the region of space near a supernova or neutron star, they found that the half-rotation length with $\hat{p} \perp \vec{B}$ (magnetic field perpendicular to neutrino direction, the most effective case) is 17 Km.

Since Majorana neutrinos have transition moments, the spin rotation also occurs for Majorana neutrinos if they pass through a (gigantic) magnetic field with some space-time inhomogeneity, which is needed to make the transition between different massive neutrinos possible. According to Schechter and Valle,[60] we have the spin-flavor rotation. In this case, the spin rotation changes neutrino to antineutrino.

Finally, we would like to mention how a Dirac neutrino gets the magnetic moment when it is constructed from two Majorana neutrinos. By using $\psi = (N_1 + i N_2)/\sqrt{2}$, we find

$$\int d^4x\, \bar{\psi}\, i\sigma_{\mu\nu}\, \partial^\nu \psi = \frac{i}{2}\int d^4x\, (\bar{N}_1\, i\sigma_{\mu\nu}\, \partial^\nu N_2 - \bar{N}_2\, i\sigma_{\mu\nu}\, \partial^\nu N_1)$$
$$= i\int d^4x\, \bar{N}_1\, i\sigma_{\mu\nu}\, \partial^\nu N_2 \,. \qquad (2.7.3)$$

That is, the transition moment between N_1 and N_2 gives rise to the magnetic moment of a Dirac neutrino.

Part II The $\beta\beta$ Decay

In this part II, we shall discuss the $0^+ \to 0^+$ and $0^+ \to 2^+$ transitions of the $(\beta\beta)_{2\nu}$ and $(\beta\beta)_{0\nu}$ modes both in the two nucleon (2n) and N* mechanisms. We shall also discuss the $\beta\beta$ decay with the other mechanisms such as due to the Higgs exchange and, the emission of a Majoron. [§5].

§3 The $\beta\beta$ decay in the two neucleon (2n-) mechanism

The purpose of this section is to derive the decay rate formulae for the $\beta\beta$ decay in the 2n-mechanism.

§3.1 Basic machinery

§3.1.1 Effective charged current weak interaction

The $(\beta\beta)_{2\nu}$ mode takes place in the second order perturbation of the standard V-A current-current form of the weak interaction. Possible deviation from the V-A theory such as the Majorana property of neutrinos, neutrino masses and the V+A interaction is the object to examine the $(\beta\beta)_{0\nu}$ mode. In this section, we neglect the possibility of the scalar and pseudoscalar currents via Higgs boson exchange, because these contributions are expected to be small due to either the small couplings to leptons or the heavy masses of Higgs bosons.

Historically, in the pioneering work of 1959, Primakoff and Rosen[24] adopted a most general form of weak interaction consisting of S, V, T, A and P currents in the case of massless neutrino. Massive neutrino was first considered by Greuling and Whitten[25] in the V-δA interaction. A simple parametrization incorporating the

V+A interaction was introduced by Primakoff and Rosen[27] in their paper of the first exploration of the N* mechanism:

$$H_W = \frac{G}{\sqrt{2}} \bar{e} \gamma^\rho [(1-\gamma_5) + \eta (1+\gamma_5)] \nu_e \; J_{L\rho}^+ + h.c., \tag{3.1.1}$$

where ν_e is a Majorana neutrino and $J_{L\rho}$ is the V-A hadronic current. Since then, various authors have adopted this form of the effective interaction to analyze the $(\beta\beta)_{0\nu}$ mode. A rather general form of interaction was considered by Doi, Kotani, Nishiura and Takasugi,[21),26),35)]

$$H_W = \frac{G}{\sqrt{2}} \left[j_L^\rho (J_{L\rho}^+ + \kappa J_{R\rho}^+) + j_R^\rho (\eta J_{L\rho}^+ + \lambda J_{R\rho}^+) \right] + h.c., \tag{3.1.2}$$

where $j_{L(R)}^\rho$ and $J_{L(R)}^\rho$ are leptonic and hadronic V-A (V+A) currents, respectively.

In this article, we shall adopt the most general form of effective interaction consisting of V and A currents which also take the mirror leptons into account,*)

$$H_W = \frac{G}{\sqrt{2}} \left[j_L^\rho J_{L\rho}^+ + \kappa j_L^{\rho\prime} J_{R\rho}^+ + \eta j_R^{\rho\prime} J_{L\rho}^+ + \lambda j_R^\rho J_{R\rho}^+ \right] + h.c., \tag{3.1.3}$$

where λ, η and κ are chosen to be real, and the leptic currents are

$$\begin{aligned} j_L^\rho &= \bar{e} \gamma^\rho (1-\gamma_5) \nu_{eL}, \quad j_L^{\rho\prime} = \bar{e} \gamma^\rho (1-\gamma_5) \tilde{\nu}_{eL}, \\ j_R^\rho &= \bar{e} \gamma^\rho (1+\gamma_5) \nu_{eR}', \quad j_R^{\rho\prime} = \bar{e} \gamma^\rho (1+\gamma_5) \tilde{\nu}_{eR}'. \end{aligned} \tag{3.1.4}$$

---

*) It is possible to take into account the mirror quarks for hadronic current. However, we do not consider them to avoid the confusion.

Here ν_{eL}, $\tilde{\nu}_{eL}$, ν'_{eL} and $\tilde{\nu}'_{eR}$ are the weak eigenstate electron neutrinos which are expressed as superpositions of mass eigenstate Majorana neutrinos N_j with the mass m_j;

$$\nu_{eL} = \Sigma_j U_{ej} N_{jL} , \quad \tilde{\nu}_{eL} = \Sigma_j U'_{ej} N_{jL} ,$$
$$\nu'_{eR} = \Sigma_j V_{ej} N_{jR} , \quad \tilde{\nu}'_{eR} = \Sigma_j V'_{ej} N_{jR} . \tag{3.1.5}$$

As we have explained in §2.5.1, a Dirac neutrino can be composed of a pair of mass degenerate neutrinos. Therefore, the above expressions involving Majorana neutrinos are the most general forms.

In models based on gauge theories, there are constraints on mixing parameters; the normalization conditions,

$$\Sigma_j |U_{ej}|^2 = \Sigma_j |U'_{ej}|^2 = \Sigma_j |V_{ej}|^2 = \Sigma_j |V'_{ej}|^2 = 1 , \tag{3.1.6a}$$

and the orthogonality conditions,

$$\Sigma_j U_{ej} V_{ej} = \Sigma_j U_{ej} V'_{ej} = \Sigma_j U'_{ej} V_{ej} = \Sigma_j U'_{ej} V'_{ej} = 0 . \tag{3.1.6b}$$

The latter are for four following pairs; ν_{eL} and $(\nu'_{eR})^C$, ν_{eL} and $(\tilde{\nu}'_{eR})^C$, $\tilde{\nu}_{eL}$ and $(\nu'_{eR})^C$, and $\tilde{\nu}_{eL}$ and $(\tilde{\nu}'_{eR})^C$. This is because, for example, ν_{eL} and ν'_{eR} transform differently due to their opposite helicities and thus they must represent the independent degree of freedom. On the other hand, two different situations arise for ν_{eL} and $\tilde{\nu}_{eL}$. If they are independent due to the existence of mirror leptons [see § A.2.1(iii)], the constraint $\Sigma_j U_{ej} U'_{ej} = 0$ is required. If $\nu_{eL} = \tilde{\nu}_{eL}$, then $U_{ej} = U'_{ej}$. The similar situation occurs for ν'_{eR} and $\tilde{\nu}'_{eR}$. If there is no mirror lepton, then $U_{ej} = U'_{ej}$ and $V_{ej} = V'_{ej}$ so that the interaction in Eq.(3.1.3) reduces to that in Eq.(3.1.2). The phenomenological interaction in Eq.(3.1.1) is not supported in

gauge theories from the following reasons: Formally it is derived from Eq.(3.1.3) by restricting $\chi = \lambda = 0$, $U_{ej} = \delta_{j1}$ and $V'_{ej} = \delta_{j1}$ which do not satisfy the constraints in Eq.(3.1.6b). That is, with this choice, ν_{eL} equals to $(\tilde{\nu}'_{eR})^C$ and thus the degree of freedom is reduced by half so that ν_{eL} and $\tilde{\nu}'_{eR}$ are no more independent. The interaction in Eq.(3.1.1) is valid if ν_e is a Dirac particle, which is realized with the choice that $U_{ej} = \delta_{j1}$, $V'_{ej} = \delta_{j\,n+1}$ and $m_1 = m_{n+1}$, n being the number of generations. That is, a pair of mass degenerate Majorana neutrinos N_{1L} and $N_{n+1\,R}$ compose a Dirac particle.

The interaction in Eq.(3.1.3) is general and can incorporate the theories with the right-handed gauge bosons as well as mirror leptons. The order of magnitudes of parameters κ, η and λ and the mixing parameters U_{ej}, U'_{ej}, V_{ej} and V'_{ej} in various models are discussed in Appendix A.

As typical examples with the right-handed interactions, we shall consider the $SU(2)_L \times SU(2)_R \times U(1)$ models (no mirror leptons) and the $SU(2)_L \times U(1)$ models with mirror leptons here.

For $SU(2)_L \times SU(2)_R \times U(1)$ models, we obtain

$$U_{ej} = U'_{ej} , \quad V_{ej} = V'_{ej} ,$$
$$\kappa = \eta = \eta_0 , \quad \lambda = \lambda_0 > 0 , \tag{3.1.7}$$

where η_0 and λ_0 are defined in Eqs.(A.1.7) and (A.1.8) and, if $M_{WR} \gg M_{WL}$ they are written approximately as

$$\eta_0 \simeq -\tan\zeta , \quad \lambda_0 \simeq \left(M_{W_L}/M_{W_R}\right)^2 . \tag{3.1.8}$$

Here ζ is the mixing angle between the left gauge boson W_L with the mass M_{W_L} ($\sim M_1$) and the right gauge boson W_R with M_{W_R} ($\sim M_2$).

For $SU(2)_L \times U(1)$ models with mirror leptons, we have from Eq.(A.1.15)

$$\eta = 1 \quad , \quad \kappa = \lambda = 0 \tag{3.1.9}$$

so that only the relevant mixing parameters for H_W in Eq.(3.1.3) are U_{ej} and V'_{ej} in this type of models.

§3.1.2 Hadronic Currents

In the effective weak interaction in Eq.(3.1.3), there are V±A hadronic currents ($\Delta S = \Delta C = 0$) which are expressed in terms of quarks in the lowest order of perturbation,

$$J^+_{L\rho} = g_V \bar{u} \gamma_\rho (1-\gamma_5) d \ ,$$
$$J^+_{R\rho} = g_V' \bar{u} \gamma_\rho (1+\gamma_5) d \ , \tag{3.1.10}$$

where

$$g_V = \cos\theta_C \ , \quad g_V' = e^{i\alpha} \cos\theta_C' \ . \tag{3.1.11}$$

Here θ_C and θ_C' are the Cabibbo-Kobayashi-Maskawa mixing angles for the left- and right-handed d and s quarks, and α is the CP violating phase due to both the mixing of right-handed quarks and the mixing of the left- and right-gauge bosons, W_L and W_R (see Eq.(A.2.4) in Appendix A).[51]

By the higher order perturbation of strong and electromagnetic interactions, the axial vector part $\gamma_\rho\gamma_5$ is renormalized and the

weak magnetism $i\sigma_{\rho\nu}Q^\nu$ and the pseudoscalar term $Q_\rho\gamma_5$ are induced, where Q_ρ is the four momentum transfer. Then we convert quark currents into the ones involving nucleons by assuming the impulse approximation. We find,

$$J^+_{L\rho} = \bar{\Psi}\tau^+ [\, g_V\gamma_\rho - g_A\gamma_\rho\gamma_5 + g_W\, i\sigma_{\rho\nu}Q^\nu + g_P Q_\rho\gamma_5 \,]\Psi \ ,$$
$$J^+_{R\rho} = \bar{\Psi}\tau^+ [\, g_V'\gamma_\rho + g_A'\gamma_\rho\gamma_5 + g_W'\, i\sigma_{\rho\nu}Q^\nu - g_P' Q_\rho\gamma_5 \,]\Psi \ , \tag{3.1.12}$$

where Ψ represents the nucleon doublet, Q_ρ is the nucleon recoil momentum, and the second class currents are neglected. The conserved vector form factors g_V and g_V' are assumed not to be renormalized so that the relations in Eq.(3.1.11) are used for currents in Eq.(3.1.12)

There are some relations among form factors in $J^+_{L\rho}$ and $J^+_{R\rho}$, because the strong and electromagnetic interactions conserve parity;

$$\frac{g_A}{g_V} = \frac{g_A'}{g_V'} = 1.25 \ , \quad \frac{g_W}{g_V} = \frac{g_W'}{g_V'} \ , \quad \frac{g_P}{g_V} = \frac{g_P'}{g_V'} \tag{3.1.13}$$

which are discussed in § A.2.2 of Appendix A. The strength of the induced weak magnetism is obtained by the CVC hypothesis,[61]

$$g_W/g_V = -(\mu_p - \mu_n)/2M \simeq -3.7/2M \ , \tag{3.1.14}$$

where $\mu_{p(n)}$ and M are the magnetic moment of proton(neutron) and nucleon mass, respectively. The induced pseudoscalar form factor is given

by the Goldberger-Treiman relation as [61]

$$g_P/g_A = 2M/m_\pi^2 , \tag{3.1.15}$$

with m_π being the pion mass.

Within the non-relativistic impulse approximation, the hadronic currents for the nuclear β decay are written as

$$J_L^{\rho\dagger}(\vec{x}) = \sum_n \tau_n^+ \left[(g_V - g_A C_n) g^{\rho 0} + (g_A \sigma_n^k - g_V D_n^k) g^{\rho k} \right] \delta(\vec{x} - \vec{r}_n), \tag{3.1.16a}$$

$$J_R^{\rho\dagger}(\vec{x}) = \sum_n \tau_n^+ \left[(g_V' + g_A' C_n) g^{\rho 0} + (-g_A' \sigma_n^k - g_V' D_n^k) g^{\rho k} \right] \delta(\vec{x} - \vec{r}_n), \tag{3.1.16b}$$

where τ_n^+, $\vec{\sigma}_n$ amd $\vec{r}_n$ are the isospin raising, the spin and the position operators acting on the n-th neutron, respectively. The operators C_n and $\vec{D}_n$ are nucleon recoil terms defined by

$$C_n = \left[(\vec{P}_n + \vec{P}_n') \cdot \vec{\sigma}_n - (g_P/g_A)(E_n - E_n') \vec{Q}_n \cdot \vec{\sigma}_n \right] / 2M, \tag{3.1.17a}$$

$$\vec{D}_n = \left[(\vec{P}_n + \vec{P}_n') - (1 - 2M(g_W/g_V)) i \vec{\sigma}_n \times \vec{Q}_n \right] / 2M, \tag{3.1.17b}$$

where

$$\vec{Q}_n = \vec{P}_n - \vec{P}_n' \tag{3.1.18}$$

and $(E_n, \vec{P}_n)$ and $(E_n', \vec{P}_n')$ are the initial and final four momenta of the n-th nucleon.

§3.1.3 Distorted electron wave function

In the $\beta\beta$ decay, the emitted two electrons are attracted by the Coulomb force of nucleus. This attraction is substantial for the medium-heavy nuclei and enhances the overlap of wave functions of electrons and nucleus. Here we shall explain the essence of the Coulomb correction necessary for understanding the $\beta\beta$ decay. The detailed explanation is given in Appendix D.

The electron wave function is expanded in terms of spherical waves as

$$\psi(\varepsilon, \vec{r}) = \psi^{(S)}(\varepsilon, r) + \psi^{(P)}(\varepsilon, \vec{r}) + \cdots\cdots, \tag{3.1.19}$$

where ε is the energy of electron. Here S and P represent the S- and P-waves;

$$\psi^{(S)}(\varepsilon, r) = \begin{pmatrix} \tilde{g}_{-1} \chi_s \\ (\vec{\sigma}\cdot\hat{r}) \tilde{f}_1 \chi_s \end{pmatrix}, \tag{3.1.20a}$$

$$\psi^{(P)}(\varepsilon, \vec{r}) = i \begin{pmatrix} \left(\tilde{g}_1 (\vec{\sigma}\cdot\hat{r})(\vec{\sigma}\cdot\hat{p}) + \tilde{g}_{-2} \left[3(\hat{r}\cdot\hat{p}) - (\vec{\sigma}\cdot\hat{r})(\vec{\sigma}\cdot\hat{p}) \right] \right) \chi_s \\ \left(-\tilde{f}_{-1} (\vec{\sigma}\cdot\hat{r}) + \tilde{f}_2 \left[3(\hat{r}\cdot\hat{p})(\vec{\sigma}\cdot\hat{p}) - (\vec{\sigma}\cdot\hat{r}) \right] \right) \chi_s \end{pmatrix}, \tag{3.1.20b}$$

where $\hat{r}$ and $\hat{p}$ are unit vectors of position and direction of electron, respectively, and χ_s is a two component spinor. The radial wave functions $g_{-1}(\varepsilon, r)$ and $f_1(\varepsilon, r)$ are S-wave with the total angular momentum $j = 1/2$, and g_1 and f_{-1} are P-wave with $j = 1/2$, while g_{-2} and f_2 are P-wave with $j = 3/2$.

We shall adopt the relativistic electron wave function in a uniform charge distribution of nucleus. By keeping the lowest power in the expansion of r (no finite de Broglie wave length correction), the radial wave functions are given by

$$\begin{pmatrix} \tilde{g}_{-1} \\ \tilde{f}_{1} \end{pmatrix} = \tilde{A}_{\mp 1}\,, \tag{3.1.21}$$

$$\begin{pmatrix} \tilde{g}_{1} \\ \tilde{f}_{-1} \end{pmatrix} = \pm \tilde{A}_{\pm 1}\left[\alpha Z/2 + (\mathcal{E} \pm m_e)R/3\right](r/R), \tag{3.1.22}$$

$$\begin{pmatrix} \tilde{g}_{-2} \\ \tilde{f}_{2} \end{pmatrix} = \tilde{A}_{\mp 2}\,(pr/3)\,, \tag{3.1.23}$$

where α is the fine structure constant, Z is the atomic number of daughter nucleus and R is the nuclear radius. The normalization constants $\tilde{A}_{\pm k}$ are explicitly shown in Eq.(D.18) of Appendix D, but their good approximations up to $(\alpha Z)^2$ are given by

$$\tilde{A}_{\pm k} \cong \sqrt{(\mathcal{E} \mp m_e)/2\mathcal{E}}\;\sqrt{F_{k-1}(Z,\mathcal{E})}\,, \tag{3.1.24}$$

where

$$F_{k-1}(Z,\mathcal{E}) = \left[\frac{\Gamma(2k+1)}{\Gamma(k)\,\Gamma(2\gamma_k+1)}\right]^2 (2pR)^{2(\gamma_k-k)}\,|\Gamma(\gamma_k+iy)|^2\, e^{\pi y}, \tag{3.1.25}$$

$$\gamma_k = \sqrt{k^2-(\alpha Z)^2}\,, \qquad y = \alpha Z\mathcal{E}/p. \tag{3.1.26}$$

The wave function ψ in Eq.(3.1.19) is reduced to the plane wave in the limit $\alpha Z \to 0$, where $F_{k-1} \to 1$. At first we notice that the substantial enhancement is expected due to the factor $(2pR)^{2(\gamma_k-k)}$ because $pR \lesssim 1/20$ for the $\beta\beta$ decaying nuclei. This was pointed out

by Haxton, Stephenson and Strottman,[34] and Nishiura.[35] Next it should be noted that the αZ correction for the P-wave function with $j = 1/2$ is important for the medium heavy nuclei because $\alpha Z/2 \sim 1/6$ and $(\mathcal{E} \pm m_e)R/3 \sim 1/60$ so that $\alpha Z/2 \gg (\mathcal{E} \pm m_e)R/3$. Note that the $(\mathcal{E} \pm m_e)R/3$ term corresponds to the $pR/3$ term of P-wave in the plane wave approximation. This αZ effect was introduced by Doi, Kotani, Nishiura and Takasugi and called the P-wave effect.[21),31] They found that this effect appears in the $0^+ \to 0^+$ transition of the $(\beta\beta)_{0\nu}$ mode in association with the η term of the V+A currents. Finally for the P-wave with $j = 3/2$, the Coulomb correction appears as $\sqrt{F_1}$ rather than $\sqrt{F_0}$, and becomes necessary for the analysis of the $0^+ \to 2^+$ transition of the $(\beta\beta)_{0\nu}$ mode. With these respects, the correct treatment of the nuclear Coulomb effect is quite important for the $\beta\beta$ decay.

In the $\beta\beta$ decay, there is an additional Coulomb repulsive interaction between two emitted electrons. This effect is of order of the fine structure constant $\alpha \sim 1\%$. We shall not consider this final state interaction in this paper. Furthermore, the electron emitted first is influenced by the Coulomb field of the intermediate nucleus with (Z-1) protons before the second neutron decay occurs, but finally both electrons in the $\beta\beta$ decay are attracted by the daughter nucleus with Z protons. This correction is less than a few percent and will not be taken into consideration, also. The estimation of this effect will be discussed at the last paragraph of Appendix D.

§3.2 The $(\beta\beta)_{2\nu}$ mode: $(A, Z-2) \to (A, Z) + 2e^- + 2\overline{\nu}_e$

The $(\beta\beta)_{2\nu}$ mode can take place within the standard electroweak interaction, so that both the right-handed parts and the nucleon recoil terms of the hadronic currents are neglected. Similarly to the allowed transition of the single β decay, all emitted electrons and neutrinos are taken to be in the S-wave. The diagram of the $\beta\beta$ transition is shown in Fig. 1.2.

Many theoretical works have been done on the double β decay. The $(\beta\beta)_{2\nu}$ mode was first discussed by Mayer[11] and after 1957, the $0^+ \to 0^+$ transition is considered by Primakoff and Rosen,[24] Konopinski,[62] Doi, Kotani, Nishiura, Okuda and Takasugi,[26] Haxton, Stephenson and Strottman[34] and Grotz, Klapdor and Metzinger.[83] As for the $0^+ \to 2^+$ transition, Molina and Pascual,[63] and Doi et al.[26),21] have shown that it is suppressed in comparison with the $0^+ \to 0^+$ transition, because of the cancellation among terms involving energy denominators.

The contributions from the pion exchange current, as shown in Fig. 3.1, have never been estimated and will not be included in this paper.

§3.2.1 The $0^+ \to 0^+$ transition

The half-life of the $0^+ \to 0^+$ transition is expressed as

$$\left[T_{2\nu}(0^+ \to 0^+)\right]^{-1} = \frac{a_{2\nu}}{\ln 2} \int d\Omega_{2\nu}\, a(\varepsilon_1, \varepsilon_2) \cdot \left| \sum_a \left[M_{GTa}^{(2\nu)} - \left(\frac{g_V}{g_A}\right)^2 M_{Fa}^{(2\nu)} \right] \frac{1}{2} (K_a + L_a) \right|^2, \qquad (3.2.1)$$

where the constant term $a_{2\nu}$ is

$$a_{2\nu} = \left[(G g_A)^4 m_e^9 / 64\pi^7 \right] \xi_P . \qquad (3.2.2a)$$

Here ξ_P represents the effect of the neutrino mixing defined by Eq.(B.3.3) in Appendix B and shall be taken to be $\xi_P = 1$ in practice. The phase space factor $d\Omega_{2\nu}$ is

$$d\Omega_{2\nu} = m_e^{-11} p_1 p_2 \omega_1 \omega_2 p_1 p_2 \varepsilon_1 \varepsilon_2 \, \delta(\varepsilon_1 + \varepsilon_2 + \omega_1 + \omega_2 + M_f - M_i) \, d\omega_1 \, d\omega_2 \, d\varepsilon_1 \, d\varepsilon_2 \, d(\hat{p}_1 \cdot \hat{p}_2), \qquad (3.2.2b)$$

where ε_k and ω_k are the energies of the k-th electron and neutrino, respectively, and M_i and M_f are the masses of the parent and daughter nuclei. The Coulomb correction $a(\varepsilon_1, \varepsilon_2)$ is defined in Eq.(B.3.6), but can be estimated within the approximation in Eq.(3.1.24) by

$$a(\varepsilon_1, \varepsilon_2) \simeq F_0(Z, \varepsilon_1)\, F_0(Z, \varepsilon_2), \qquad (3.2.2c)$$

where $F_0(Z,\varepsilon)$ defined in Eq.(3.1.25) is the square of the Dirac S-wave scattering solution for a point charge Z to a plane wave evaluated at the nuclear surface. The combinations of energy denominators appeared in the second order perturbation are

$$K_a = \left\{ \left[\mu_a + (\varepsilon_1 + \omega_1 - \varepsilon_2 - \omega_2)/2m_e \right]^{-1} + \left[\mu_a - (\varepsilon_1 + \omega_1 - \varepsilon_2 - \omega_2)/2m_e \right]^{-1} \right\},$$

$$L_a = K_a(\omega_1 \gtrless \omega_2), \qquad (3.2.2d)$$

where

$$\mu_a m_e = E_a - (M_i + M_f)/2, \qquad (3.2.3)$$

E_a being the energy of the intermediate nuclens (N_a). In Eq.(3.2.1),

we neglected the small terms proportional to the difference, $|K_a - L_a| \leq 10^{-2}(K_a + L_a)$, Cf.Eqs.(B.3.5) and (B.3.10) in Appendix B.

The reduced nuclear matrix element due to the successive Fermi transitions is

$$M_{Fa}^{(2\nu)} = \langle 0_f^+ \| \sum_n \tau_n^+ \| N_a(0^+) \rangle \langle N_a(0^+) \| \sum_m \tau_m^+ \| 0_i^+ \rangle, \qquad (3.2.4a)$$

and the other for the double Gamow-Teller transitions is

$$M_{GTa}^{(2\nu)} \equiv -\langle 0_f^+ \| \sum_n \tau_n^+ \sigma_n \| N_a(1^+) \rangle \langle N_a(1^+) \| \sum_m \tau_m^+ \sigma_m \| 0_i^+ \rangle. \qquad (3.2.4b)$$

The definition of the reduced matrix element is written in Eq.(B.1.5) of Appendix B to avoid the confusion: The minus sign in the definition $M_{GTa}^{(2\nu)}$ is introduced so that by the closure property, we have

$$[M_{GT}^{(2\nu)}]_C \equiv \sum_a M_{GTa}^{(2\nu)} = \langle 0_f^+ \| \sum_{n,m} \tau_n^+ \tau_m^+ (\vec{\sigma}_n \cdot \vec{\sigma}_m) \| 0_i^+ \rangle. \qquad (3.2.5)$$

The derivation of the decay rate and the angular correlation between two electrons are given in Eq.(B.3.1) of Appendix B.

Since the energy denominators K_a and L_a depend on the energies of electrons and neutrinos, it is difficult to take the sum of all allowed intermediate nuclear states before the phase space integration is performed: That is, the phase space integration is made for each intermediate states, which is rather time

consuming procedure. However, there is a good approximation to bypass it.[41),64)] At first, we observe that due to the phase space factor, the energy spectrum has a peak at $(\varepsilon_1 - m_e) \sim (\varepsilon_2 - m_e) \sim \omega_1 \sim \omega_2 \sim (Tm_e)/4$, where $T m_e$ is the maximum kinetic energy release,

$$T m_e = M_i - M_f - 2m_e. \qquad (3.2.6)$$

Then we can take $(\varepsilon_k + \omega_\ell - \varepsilon_{k'} - \omega_{\ell'}) \approx 0$ as a good approximation and thus we find

$$K_a \cong L_a \simeq 2/\mu_a. \qquad (3.2.7)$$

Now K_a and L_a are independent of energies of electrons and neutrinos, and the sum of a can be taken without conflicting with the phase space integration. The error of the above approximation is the order of $[(\varepsilon_k + \omega_\ell - \varepsilon_{k'} - \omega_{\ell'})/\mu_a m_e]^2$. With these considerations, we find the following formula,

$$[T_{2\nu}(0^+ \to 0^+)]^{-1} = \left| \left(\frac{M_{GT}^{(2\nu)}}{\mu_0} \right) - \left(\frac{g_\nu}{g_A} \right)^2 \left(\frac{M_F^{(2\nu)}}{\mu_{0F}} \right) \right|^2 G_{GT}(\langle \mu_a \rangle), \qquad (3.2.8)$$

where

$$\left(M_{GT}^{(2\nu)}/\mu_0 \right) \equiv \Sigma_a \mu_a^{-1} M_{GTa}^{(2\nu)}, \qquad (3.2.9)$$

$$\left(M_F^{(2\nu)}/\mu_{0F} \right) \equiv \Sigma_a \mu_a^{-1} M_{Fa}^{(2\nu)}, \qquad (3.2.10)$$

and

$$G_{GT}(\langle\mu_a\rangle) = \frac{a_{2\nu}}{\ln 2}\int d\Omega_{2\nu}\, A(\varepsilon_1,\varepsilon_2)\langle\mu_a\rangle^2\left(\frac{\langle K_a\rangle+\langle L_a\rangle}{2}\right)^2. \quad (3.2.11)$$

Here $\langle\mu_a\rangle$ is some average value of μ_a, and $\langle K_a\rangle$ and $\langle L_a\rangle$ are the quantities obtained from K_a and L_a by replacing μ_a with $\langle\mu_a\rangle$. To derive the above formula, first we replace K_a and L_a by $2/\mu_a$ and the sum of a is taken. Next in order to take into account the energy dependence of leptons in K_a and L_a, the factor $\langle\mu_a\rangle^2[(\langle K_a\rangle+\langle L_a\rangle)/2]^2$ is introduced for the phase space integration. If the $\langle\mu_a\rangle$ dependence of the integrated kinematical factor $G_{GT}(\langle\mu_a\rangle)$ is minor, the above approximation is valid.

The μ_a dependence of $G_{GT}(\mu_a)$ is examined and is plotted in Fig. 3.2 for various nuclei. Since the double Gamow-Teller matrix element $M^{(2\nu)}_{GT\,a}$ gives the dominant contribution, the energy levels of 1^+ intermediate states are crucial. The vertical lines in the figure show the value of μ_a corresponding to the first 1^+ excited state. The arrow means that the 1^+ states are not yet confirmed so that the minimum value of μ_a must be above it. In all cases, the μ_a dependence of $G_{GT}(\mu_a)$ is quite weak above the μ_a values indicated by the vertical lines.

There remains a problem how to determine $\langle\mu_a\rangle$, although its dependence is weak. The reasonable value will be obtained from the equality,

$$\left|\sum_a M^{(2\nu)}_{GT\,a}\right| / \langle\mu_a\rangle = \sum_a \mu_a^{-1}\left|M^{(2\nu)}_{GT\,a}\right|, \quad (3.2.12)$$

which will predict the value of $\langle\mu_a\rangle$ around the peak of the energy spectrum of the intermediate 1^+ states.

The half-life formula is further simplified if we use the fact that $\left|M^{(2\nu)}_{GT}/\mu_0\right| \gg \left|M^{(2\nu)}_{F}/\mu_0\right|$ as explained in § 7.1. We find

$$\left[T_{2\nu}(0^+\to 0^+)\right]^{-1} = \left|\frac{M^{(2\nu)}_{GT}}{\mu_0}\right|^2 G_{GT}(\langle\mu_a\rangle). \quad (3.2.13)$$

Only the quantity $\left|M^{(2\nu)}_{GT}/\mu_0\right|$ depends on the nuclear models, because the integrated kinematical factor G_{GT} is calculable with good accuracy. Its theoretical prediction can be compared with the one obtained from the experimental data on the $0^+\to 0^+$ transition of the $(\beta\beta)_{2\nu}$ mode.

So far we have not used the so-called closure approximation, where the sum of the intermediate states are taken by closure, after replacing E_a by some average $\langle E_a\rangle_{av}$:

$$\left(M^{(2\nu)}_{GT}/\mu_0\right) = \sum_a \mu_a^{-1} M^{(2\nu)}_{GT\,a} \longrightarrow [M^{(2\nu)}_{GT}]_C / \langle\mu_a\rangle_{av}, \quad (3.2.14)$$

Here $\langle\mu_a\rangle_{av} = (\langle E_a\rangle_{av} - (M_i + M_f)/2)/m_e$ and $[M^{(2\nu)}_{GT}]_C$ is defined in Eq. (3.2.5). If we take $\langle\mu_a\rangle = \langle\mu_a\rangle_{av}$ in Eqs. (3.2.9) and (3.2.11), the half-life formula in Eq. (3.2.8) is reduced to the one used in previous articles.[34),21)] Although the thoeretical evaluation of the nuclear matrix element is simplified because $[M^{(2\nu)}_{GT}]_C$ depends on only the initial and final nuclei, a new parameter $\langle E_a\rangle_{av}$ is introduced.

The validity of the closure approximation is simply a question of the choice of the average excitation energy $\langle E_a\rangle_{av}$. Haxton and Stephenson have pointed out that if the signs of $M^{(2\nu)}_{GT\,a}$ were

predominantly one value for some E_a and the opposite value for larger E_a, the closure approximation could fail badly.[17] For the case where there is no such cancellation, they have proposed the equation from which the approximate value of $\langle E_a \rangle_{av}$ is determined,

$$\left(\langle \mu_a \rangle_{av}\right)^{-1} \sum_a \left| \langle N_a(1^+) \| \Sigma_n \tau_n^+ \sigma_n \| 0_i^+ \rangle \right|^2 = \sum_a \mu_a^{-1} \left| \Sigma_a \langle N_a(1^+) \| \Sigma_n \tau_n^+ \sigma_n \| 0_i^+ \rangle \right|^2 . \quad (3.2.15)$$

It is an important question to investigate whether such cancellations occur or not. There are some estimates of $(M_{GT}^{(2\nu)}/\mu_0)$ without using the closure approximation which will be discussed in §7.1.

In Table 3.1 , the values of the integrated kinematical factor G_{GT} $(\langle \mu_a \rangle)$ are given for various nuclei. For some of $\langle \mu_a \rangle$, we adopted the values by Haxton et al. through Eq. (3.2.15), because these values are good enough to evaluate $G_{GT}(\langle \mu_a \rangle)$ due to the weak dependence on $\langle \mu_a \rangle$.

§3.2.2 The $0^+ \to 2^+$ transition

The $0^+ \to 2^+$ transition of the $(\beta\beta)_{2\nu}$ mode is given by

$$\left[T_{2\nu}(0^+ \to 2^+) \right]^{-1} = G_{2n}(\langle \mu_a \rangle) \left| M_2^{(2\nu)}/\mu_2^3 \right|^2 , \quad (3.2.16)$$

where

$$\left(M_2^{(2\nu)}/\mu_2^3 \right) = \frac{1}{\sqrt{3}} \sum_a \mu_a^{-3} \langle 2_f^+ \| \Sigma_n \tau_n^+ \sigma_n \| N_a(1^+) \rangle \langle N_a(1^+) \| \Sigma_m \tau_m^+ \sigma_m \| 0_i^+ \rangle , \quad (3.2.17)$$

and

$$G_{2n}(\langle \mu_a \rangle) = \frac{G_{2\nu} \langle \mu_a \rangle^6}{\ln 2} \int d\Omega_{2\nu} A(\varepsilon_1, \varepsilon_2) \left(\langle K_a \rangle - \langle L_a \rangle \right)^2 . \quad (3.2.18)$$

The detailed derivation of this formula is given in Appendix B. The transition is suppressed due to the cancellation,[26),21)]

$$\langle K_a \rangle - \langle L_a \rangle \cong 2(\varepsilon_1 - \varepsilon_2)(\omega_1 - \omega_2) / (m_e^2 \langle \mu_a \rangle^3) . \quad (3.2.19)$$

The factor $\langle \mu_a \rangle^6$ is introduced in $G_{2n}(\langle \mu_a \rangle)$ to compensate the $\langle \mu_a \rangle$ dependence of $\langle K_a \rangle - \langle L_a \rangle$. Therefore, $G_{2n}(\langle \mu_a \rangle)$ is expected to have weak dependence on $\langle \mu_a \rangle$ and has the same order of magnitude as $G_{GT}(\langle \mu_a \rangle)$, because $\left| (\varepsilon_1 - \varepsilon_2)(\omega_1 - \omega_2)/m_e^2 \right| \sim 1$. On the other hand, the nuclear matrix element $(M_2^{(2\nu)}/\mu_2^3)$ is expected to be much smaller than $(M_{GT}^{(2\nu)}/\mu_0)$, because of μ_2^3 factor instead of μ_0. However, there needs some caution to compare them because the μ_a^{-3} factor in Eq. (3.2.17) will enhance the low lying states, so that μ_2 may well be smaller than μ_0. Although we have found the suppression of the $0^+ \to 2^+$ transition, the degree of it depends on the size of $(M_2^{(2\nu)}/\mu_2^3)$. Naively speaking, $T_{2\nu}(0^+ \to 2^+)$ is at least about 10^4 times longer than $T_{2\nu}(0^+ \to 0^+)$, provided $\mu_2 \sim 10$.

Within the closure approximation, Eq. (3.2.17) becomes

$$\left(M_2^{(2\nu)}/\mu_2^3 \right) \Longrightarrow \left[M_2^{(2\nu)} \right]_c / \langle \mu_a \rangle_{av}^3 , \quad (3.2.20)$$

where, by using Eq. (B.1.3),

$$\left[M_2^{(2\nu)} \right]_c = \langle 2_f^+ \| \Sigma_{n,m} \tau_n^+ \tau_m^+ \left[\sigma_n \otimes \sigma_m \right]^{(2)} \| 0_i^+ \rangle . \quad (3.2.21)$$

In Table 3.2, the values of the integrated kinematical factor $G_{2n}(\langle \mu_a \rangle)$ with the choice of $\langle \mu_a \rangle = 10$ are presented. The μ_a

dependence of G_{2n} is very weak and the variation is less than a few %, when $\langle \mu_a \rangle$ is changed from 20 to 10.

Since the main terms are canceled and this process is included in the geochemical data, we may wonder the contributions from the higher spherical waves of electrons and neutrinos and also the nucleon recoil terms. The estimates of these terms are performed in Appendix B, and it turns out that these contributions are at most the order of the S-wave case as shown in Table B.2 in Appendix B.

§3.3 The $(\beta\beta)_{0\nu}$ mode: $(A, Z-2) \to (A, Z) + 2e^-$

The $(\beta\beta)_{0\nu}$ mode in the 2n-mechanism shown in Fig.1.3 was proposed first by Furry [12], and later discussed in detail by Primakoff and Rosen for massless neutrinos.[24] Greuling and Whitten have derived the formula by using the $V-\delta A$ leptonic current for a massive neutrino.[25] Assuming massless neutrinos, Molina and Pascual[63] investigated the $0^+ \to 0^+$, 1^+ and 2^+ transitions in the framework of the $V-\delta A$ interaction without nuclear Coulomb corrections. Primakoff and Rosen proposed in 1969 the V+A parameter, η, in the form of Eq.(3.1.1),[27] and in 1976, Halprin, Minkowski, Primakoff and Rosen analyzed the contribution from the finite neutrino mass and also discussed the character of the neutrino propagation.[65] In 1981, Vergados proposed to introduce the nucleon form factor to take account of the recoil effect due to the heavy neutrino,[66] while Doi, Kotani, Nishiura, Okuda and Takasugi proposed to treat both the m_ν and V+A parts simultaneously within the framework of the gauge theory including the neutrino mixing.[26] Furthermore, Doi et al. take into account the relativistic Coulomb wave functions for electrons by using the rather general weak interaction

Hamiltonian in Eq.(3.1.2).[21),31] Their results are consistent with ones by Haxton and Stephenson,[17] except the P-wave effect and the nucleon recoil effect.[64] Thus, the fundamental formalism in the 2n-mechanism has been established. However, from the view point of nuclear physics, we need to take into account some modifications. For example, Vergados considered the $(\beta\beta)_{0\nu}$ mode based on the pion exchange between two nucleons,[67] i.e. the fundamental process like $\pi^- + \pi^+ + 2e^-$ as proposed by Pontecorvo as shown in Fig. 3.3a.[14] This contribution can be taken into consideration as a modification of the form factor in Eq.(3.1.16). Also there are other possibilities in Figs. 3.3b and 3.3c. This should be considered as the modifications of the nuclear matrix elements for the $(\beta\beta)_{0\nu}$. These modifications are not considered in this review.

In this section, the $0^+ \to J^+$ transitions are discussed within the following approximations: (a) Among various spherical waves of electrons, the lowest waves which give the non-vanishing contributions are kept. (b) The terms which vanish in the closure approximation are not included in the decay rate formulae. (c) The finite de Broglie wave length corrections are neglected. In Appendix C, the detailed derivation of the decay rate formulae is given. There, we include the terms vanishing in the closure approximation and discuss the order of magnitudes of various other contributions.

The $(\beta\beta)_{0\nu}$ mode takes place in the second order perturbation of the effective weak Hamiltonian in Eq.(3.1.3), as shown in Fig.1.3. The decay amplitude is divided into two parts by the structure of lepton vertices due to the helicity matching of the propagating neutrino. If both vertices are V-A or V+A, the neutrino mass m_j of the propagating neutrino contributes (the m_ν-part). If one vertex is V-A and the other is V+A, the four momentum of neutrino q^μ

contributes (the V+A part). This situation is explicitly seen as follows: The lepton part of the amplitude is written as

$$\bar{e}(x)\gamma_\rho(L\text{ or }R)\,\overbrace{N_j(x)\;\bar{e}(y)\gamma_\sigma(L\text{ or }R)N_k(y)}$$
$$= -\bar{e}(x)\gamma_\rho(L\text{ or }R)\,\overbrace{N_j(x)\,N_k^T(y)}\,(L^T\text{ or }R^T)\gamma_\sigma^T\,\bar{e}^T(y)$$
$$= -i\,\delta_{jk}\int\frac{d^4q}{(2\pi)^4}\frac{e^{-iq(x-y)}}{q^2-m_j^2}\;\bar{e}(x)\gamma_\rho(L\text{ or }R)(q^\mu\gamma_\mu+m_j)(L\text{ or }R)\gamma_\sigma\,e^c(y), \tag{3.3.1}$$

where $L=(1-\gamma_5)/2$, $R=(1+\gamma_5)/2$, the line connecting N_j and N_k^T means the contraction. The contraction between N_j and N_k^T is allowed, if N_j is a Majorana neutrino, and the propagator in Eq.(2.4.31) has been used to derive the final expression. The characteristic features stated above are immediately derived from Eq.(3.3.1) by noticing $L(q^\mu\gamma_\mu+m_j)L=m_jL$ and $L(q^\mu\gamma_\mu+m_j)R=q^\mu\gamma_\mu R$. In the following, we shall discuss the m_ν and the V+A parts separately.[64]

§3.3.1 The m_ν part

Let us consider the general properties of the m_ν part. We shall discuss here only the L-L part in Eq.(3.3.1), because the V+A coupling is much smaller than the V-A coupling. The L-L part of the R matrix is given by (see Eq.(C.2.2) in Appendix C),

$$(R_{0\nu})_{m_\nu}\propto\sum_j m_j\int d^3x\,d^3y\int\frac{d^3\xi}{\omega}\,e^{i\vec{\xi}(\vec{x}-\vec{y})}\sum_a J_{LL}^{\rho\sigma}(\vec{x},\vec{y},a)S_{L\rho\sigma}(\vec{x},\vec{y},a), \tag{3.3.2}$$

where the virtual neutrino energy is $\omega=\sqrt{q^2+m_j^2}$ and the integration

over $\vec{q}$ means to take into account the virtual neutrino propagation and will be expressed as the neutrino potential later in §3.4. The nuclear transition due to the hadronic current part is expressed by

$$J_{LL}^{\rho\sigma}(\vec{x},\vec{y};a)=\langle N_f|\,\tilde{J}_L^{\rho\dagger}(\vec{x})\,|N_a\rangle\langle N_a|\,\tilde{J}_L^{\sigma\dagger}(\vec{y})\,|N_i\rangle, \tag{3.3.3}$$

where $|N_a\rangle$ stands for the intermediate nuclear states. It is convenient to classify the nuclear operators $J_{L(R)}^{\rho\dagger}(\vec{x})$ in Eq.(3.1.16) by the leptonic currents, as seen from Eq.(3.3.1). Therefore, a combination $\tilde{J}_L^{\rho\dagger}(\vec{x})$, instead of $J_{L(R)}^{\rho\dagger}(\vec{x})$ itself, has been used, as its details will be given by Eq.(C.1.4) in Appendix C. The suffix L of $\tilde{J}_L^\rho$ means that the left-handed (V-A) leptonic current is taken into consideration at the β-decaying vertex. The leptonic part in Eq.(3.3.2) is

$$S_{L\rho\sigma}(\vec{x},\vec{y};a)=\frac{t_{\rho\sigma}^L(\varepsilon_1\vec{x},\varepsilon_2\vec{y})}{\omega+A_2}-\frac{t_{\rho\sigma}^L(\varepsilon_2\vec{x},\varepsilon_1\vec{y})}{\omega+A_1} \tag{3.3.4}$$

where the m_j part of the electron current in Eq.(3.3.1) is

$$t_{\rho\sigma}^L(\varepsilon_1\vec{x},\varepsilon_2\vec{y})=\bar{\psi}(\varepsilon_1,\vec{x})\gamma_\rho(1-\gamma_5)\gamma_\sigma\psi^c(\varepsilon_2,\vec{y}), \tag{3.3.5}$$

and the energy denominator due to the second order perturbation is expressed by $\omega+A_k$,

$$\begin{pmatrix}A_1\\A_2\end{pmatrix}=\mu_a m_e\pm\frac{1}{2}(\varepsilon_1-\varepsilon_2). \tag{3.3.6}$$

Here $\psi(\varepsilon,\vec{x})$ is the wave function of electron with the energy ε

in Eq.(3.1.19), and $\mu_a m_e = E_a - (M_i + M_f)/2$ in Eq.(3.2.3). This $S_{L\rho\sigma}(\vec{x}, \vec{y}, a)$ is antisymmetric under the exchange of two electrons $(\varepsilon_1 \leftrightarrows \varepsilon_2)$, because of the Pauli exclusion principle. Note that the position vectors $\vec{x}$ and $\vec{y}$ in $S_{L\rho\sigma}$ work also as the nuclear tensor operators, if both electrons are not in the S-wave state. The exact definitions of the decay rate and the R matrix are presented in Eqs.(C.2.1) and (C.2.4) of Appendix C.

Let us examine the nuclear tensor operators which make the nuclear transitions possible. Due to the identity $\gamma_\rho \gamma_\sigma = g_{\rho\sigma} + [\gamma_\rho, \gamma_\sigma]/2$ in Eq.(3.3.5), the hadronic current part is divided into the rank 0 tensor $\tilde{J}_L^{\rho\dagger}\, \tilde{J}_{L\rho}^{\dagger}$ and the rank 1 tensor $\left(\tilde{J}_L^{\rho\dagger}\, \tilde{J}_L^{\sigma\dagger} - \tilde{J}_L^{\sigma\dagger}\, \tilde{J}_L^{\rho\dagger}\right)$. Notice that $J_L^{0\dagger}$ is of rank 0 and $J_L^{k\dagger}$ is of rank 1. Only other source of nuclear tensor operators is electron wave functions ψ, because the neutrino propagator gives only the rank 0 tensor through $|\vec{x} - \vec{y}|^{-1}$. If both electrons are in the S-wave, the lepton part is of rank 0 so that only the transitions with $\Delta J = 0$ or 1 are allowed. This can also be understood by using the angular momentum conservation and by noticing that the total angular momentum of two S-wave electrons are 0 or 1, as mentioned in §1.3(ii), cf. Table C.1 in Appendix C.

From the above considerations, we conclude that the $0^+ \to 0^+$ and $0^+ \to 1^+$ transitions are allowed, but the $0^+ \to 2^+$ transition is forbidden for the m_ν part in the case of two S-wave electrons.

Let us examine the decay amplitude more closely. We shall parametrize the hadronic current part as

$$J_{\alpha\beta}^{\rho\sigma}(\vec{x}, \vec{y}; a) = J_{\alpha\beta+}^{\rho\sigma}(\vec{x}, \vec{y}; a) + J_{\alpha\beta-}^{\rho\sigma}(\vec{x}, \vec{y}; a), \tag{3.3.7}$$

where suffices α and β stand for L or R, and

$$J_{\alpha\beta\pm}^{\rho\sigma}(\vec{x}, \vec{y}; a) = \left[J_{\alpha\beta}^{\rho\sigma}(\vec{x}, \vec{y}; a) \pm J_{\beta\alpha}^{\sigma\rho}(\vec{y}, \vec{x}; a) \right]/2. \tag{3.3.8}$$

They have the properties,

$$J_{\alpha\beta\pm}^{\rho\sigma}(\vec{x}, \vec{y}; a) = \pm J_{\beta\alpha\pm}^{\sigma\rho}(\vec{y}, \vec{x}; a). \tag{3.3.9}$$

This parametrization is introduced because the term $J_{\alpha\beta-}^{\rho\sigma}$ vanishes in the closure approximation. This is derived from the facts that the hadronic currents act on two different neutrons and $[\tilde{J}_\alpha^{\rho\dagger}(\vec{x}), \tilde{J}_\beta^{\sigma\dagger}(\vec{y})] = 0$ for $\vec{x} \neq \vec{y}$. By using the identity

$$t_{\rho\sigma}^{L}(\varepsilon_2 \vec{x}, \varepsilon_1 \vec{y}) = - t_{\sigma\rho}^{L}(\varepsilon_1 \vec{y}, \varepsilon_2 \vec{x}), \tag{3.3.10}$$

we find that

$$J_{LL\pm}^{\rho\sigma}(\vec{x}, \vec{y}; a)\, t_{\rho\sigma}^{L}(\varepsilon_2 \vec{x}, \varepsilon_1 \vec{y}) = \mp J_{LL\pm}^{\sigma\rho}(\vec{y}, \vec{x}; a)\, t_{\sigma\rho}^{L}(\varepsilon_1 \vec{y}, \varepsilon_2 \vec{x}). \tag{3.3.11}$$

Applying this relation to the decay amplitude, we find that the non-vanishing term in the closure approximation is always proportional to

$$\frac{1}{\omega+A_2} + \frac{1}{\omega+A_1} \quad , \tag{3.3.12}$$

while the vanishing term is proportional to

$$\frac{1}{\omega+A_2} - \frac{1}{\omega+A_1} = \frac{\varepsilon_{12}}{(\omega+A_1)(\omega+A_2)} \quad , \tag{3.3.13}$$

where

$$\varepsilon_{12} = \varepsilon_1 - \varepsilon_2 \quad . \tag{3.3.14}$$

The cancellation of the energy denominators in Eq.(3.3.13) gives the suppression by $|\varepsilon_{12}|/(\omega+A_1) \sim 0(1/40)$ with $|\varepsilon_{12}| \sim 1$ MeV and $\omega \sim 1/R \sim 40$ MeV, in comparison with Eq.(3.3.12). This result is general and independent of the choice of electron spherical waves.

The systematic study of the $0^+ \to J^+$ transition including the contributions from higher spherical waves and the finite de Broglie wave length corrections are given in Appendix C.

§3.3.2 The V+A part

The V+A part is proportional to $q^\mu = (\omega, \vec{q})$ and is conveniently divided into two terms, the ω-term and the $\vec{q}$-term. For the ω-term, the dominant contribution is expected from two S-wave electrons.

On the other hand, for the $\vec{q}$-term, either one of the following cases should happen because $\vec{q}$ acts as a parity odd operator for nucleus: One of electrons is in P-wave while the other is in S-wave, or the nucleon recoil terms take part in with both electrons in S-wave. Therefore, it is generally expected that the $\vec{q}$-term is suppressed in comparison with the ω-term. However, it is not so, because there is a large cancellation for the ω-term which makes it comparable or minor to the $\vec{q}$-term.

Let us examine the R matrix

$$(R_{\sigma\nu})_{V+A} \propto \sum_j \int d^3x\, d^3y \int \frac{d^3q}{\omega} e^{i\vec{q}\cdot(\vec{x}-\vec{y})} \sum_\alpha \left(J^{\rho\sigma}_{LR} V_{L\rho\sigma} + J^{\rho\sigma}_{RL} V_{R\rho\sigma} \right), \tag{3.3.15}$$

where the nuclear transition due to the hadronic current part is expressed as

$$J^{\rho\sigma}_{\alpha\beta}(\vec{x}, \vec{y}; a) = \langle N_f | \tilde{J}^\rho_\alpha(\vec{x}) | N_a \rangle \langle N_a | \tilde{J}^\sigma_\beta(\vec{y}) | N_i \rangle . \tag{3.3.16}$$

which corresponds to Eq. (3.3.3) in the m_ν part. The leptonic part is

$$V_{L(R)\rho\sigma} = \frac{u^{L(R)}_{\rho\sigma}(\varepsilon_1, \vec{x}, \varepsilon_2, \vec{y})}{\omega + A_2} - \frac{u^{L(R)}_{\rho\sigma}(\varepsilon_2, \vec{x}, \varepsilon_1, \vec{y})}{\omega + A_1} , \tag{3.3.17}$$

where the V+A part of the electron current in Eq.(3.3.1) is

$$u^{L(R)}_{\rho\sigma}(\varepsilon_1, \vec{x}, \varepsilon_2, \vec{y}) = g^\mu \bar{\psi}(\varepsilon_1, \vec{x}) \gamma_\rho (1 \mp \gamma_5) \gamma_\mu \gamma_\sigma \psi^c(\varepsilon_2, \vec{y}) . \tag{3.3.18}$$

The derivation of the R matrix will be given in Eq.(C.2.7) of Appendix C.

We observe that only the nuclear tensor operators of rank 0 and 1 are derived from the combination of $\tilde{J}^{\rho+}_\alpha$, $\tilde{J}^{\sigma+}_\beta$ and q^μ. This is because $\gamma_\rho \gamma_\mu \gamma_\sigma$ in Eq.(3.3.18) satisfies the identity $\gamma_\rho \gamma_\mu \gamma_\sigma = g_{\mu\rho}\gamma_\sigma + g_{\mu\sigma}\gamma_\rho - g_{\rho\sigma}\gamma_\mu + i\varepsilon_{\rho\mu\sigma\kappa}\gamma_5\gamma^\kappa$. Note that $q^\mu \tilde{J}^+_{\alpha\mu}$ and $\tilde{J}^{\mu+}_\alpha \tilde{J}^+_{\beta\mu}$ are rank 0 tensor operators, cf. Table C.2 in Appendix C.

If two electrons are taken to be in the S-wave, only the transitions with $\Delta J \simeq 0$ and 1 are allowed. This situation occurs for the ω-term and for the $\vec{q}$-term with nucleon recoil terms. In other words, these terms do not contribute to the $0^+ \to 2^+$ transition. The dominant contribution to the $0^+ \to 2^+$ transition is from the $\vec{q}$-term with one P wave electron. Generally these results are also derived by using the argument based on the angular momentum and parity conservations, as shown in Table 1.2.

Let us closely examine the structure of the decay amplitude. We rewrite the hadronic current parts $J_{LR}^{\rho\sigma}$ and $J_{RL}^{\rho\sigma}$ in terms of $J_{LR\pm}^{\rho\sigma}$ and $J_{RL\pm}^{\rho\sigma}$ in Eq.(3.3.7). Similarly to the m_ν part, the terms involving $J_{\alpha\beta}^{\rho\sigma}$ vanish in the closure approximation and thus they are omitted in the following discussions. In contrast with Eq.(3.3.10), we find

$$u_{\rho\sigma}^{L(R)}(\varepsilon_2\vec{x},\varepsilon_1\vec{y}) = u_{\sigma\rho}^{R(L)}(\varepsilon_1\vec{y},\varepsilon_2\vec{x}) \qquad (3.3.19)$$

By applying the relations in Eqs.(3.3.9) and (3.3.19), the transition amplitude is written as follows:

$$(R_{0\nu})_{V+A} \propto \sum_j \int d^3x\, d^3y \int \frac{d^3q}{\omega}\, J_{LR+}^{\rho\sigma}(\vec{x},\vec{y};a) \cdot \left\{ \left[\frac{u_{\rho\sigma}^{L}(\varepsilon_1\vec{x},\varepsilon_2\vec{y})}{\omega+A_2} - \frac{u_{\sigma\rho}^{R}(\varepsilon_1\vec{y},\varepsilon_2\vec{x})}{\omega+A_1} \right] e^{i\vec{q}\cdot(\vec{x}-\vec{y})} - \left[\frac{u_{\rho\sigma}^{L}(\varepsilon_1\vec{x},\varepsilon_2\vec{y})}{\omega+A_1} - \frac{u_{\sigma\rho}^{R}(\varepsilon_1\vec{y},\varepsilon_2\vec{x})}{\omega+A_2} \right] e^{-i\vec{q}\cdot(\vec{x}-\vec{y})} \right\}. \qquad (3.3.20)$$

Since $u_{\rho\sigma}^{L(R)}$ is proportional to q^μ, we conclude from Eq.(3.3.20) that the non-vanishing terms in the closure approximation have the

following structure;

$$\text{the } \omega\text{-term} \;:\; \omega\left(\frac{1}{\omega+A_2} - \frac{1}{\omega+A_1}\right) = \frac{\varepsilon_{12}\,\omega}{(\omega+A_1)(\omega+A_2)}, \qquad (3.3.21)$$

$$\text{the } \vec{q}\text{-term} \;:\; \vec{q}\left(\frac{1}{\omega+A_2} + \frac{1}{\omega+A_1}\right), \qquad (3.3.22)$$

where the integration variables $\vec{q}$ in the second line in Eq.(3.3.20) have been replaced by $-\vec{q}$. It is clear that there is a large cancellation between energy denominators for the ω-term and its contribution is suppressed by the order of $|\varepsilon_{12}|/\omega \sim 1/40$, cf. Eq.(3.3.13). Resultantly, the ω-term becomes comparable to the ordinary P wave contribution $(1/3)pR \sim 1/60$ in the $\vec{q}$-term.

Let us examine the contribution from the $\vec{q}$-term to the $0^+ \to 0^+$ transition. At first, we shall consider the P-wave electron whose wave functions are $\tilde{g}_1$ and $\tilde{f}_{-1}$ with $j = 1/2$ due to the angular momentum conservation. There are two terms, as seen from Eq.(3.1.22), the Coulomb correction $\propto Z/2$ and the ordinary P-wave factors $(\varepsilon \pm m_e)R/3$ which is reduced to $pR/3$ after multiplying $A_{\pm 1}$ in Eq.(3.1.24). For typical $\beta\beta$ decaying nuclei, $\alpha Z/2 \sim 1/6$ and $pR/3 \sim 1/60$ so that the αZ correction may well give much larger contribution than the $pR/3$ and ω-terms. We found that this αZ correction appears only in coefficients of a right-handed current parameter η. (See Appendix C for the detailed discussions.) This Coulomb enhancement has been called the P wave effect.[21),31)]

It turns out that nucleon recoil terms also appear in coefficients of η as discussed in Appendix C, and its magnitude is about $\vec{D}/M \sim 4.7\,\vec{Q}/M$ from Eqs.(3.1.17) and (3.1.14). Since $|\vec{Q}| \sim q \sim 80\ m_e$, this term gives

an important contribution, because both electrons are in the S-wave. This contribution will be referred to as the recoil effect.

The relative order of magnitudes of various contributions to the $0^+ \to 0^+$ transition are summarized in Table 3.3.. The extra $1/m_e$ factor is introduced to normalize the coefficients. For the ω- and pR/3-terms, $1/m_e$ will work as a natural scale for ε_{12} and p/3. For αZ and recoil terms, $1/m_e$ term is separated as $1/m_e R$ which is included in the phase space integration. The $qr(\sim 1)$ factor in pR/3 and $\alpha Z/2$ terms is included in the definition of the neutrino potential which arises after $\vec{q}$ integration as discussed in § 3.4. Similarly, for the recoil term, q^2R/M ($\sim 1/25$) is included in the potential also.

The rough evaluation is given by taking $|\varepsilon_{12}| \sim 2m_e$, $p \sim 4m_e$, $\alpha Z \sim 1/3$, $m_e R \sim 1/80$ and $q \sim 1/R \sim 80 m_e$. As for the nuclear operators, the sufficies m and n mean operators acting on the m-th and n-th nucleons which arise from the impulse approximation of hadronic currents in Eq.(3.1.16). In our notation, neutrino transmits always from the m-th nucleon to the n-th nucleon. The double Gamow-Teller operator $\vec{\sigma}_n \cdot \vec{\sigma}_m$ takes the value -3 if two neutrons are prediminantly in the spin singlet state. The value for $(1/2)\hat{r}_{+nm}\cdot[\hat{r}_{nm}\times(\vec{\sigma}_n - \vec{\sigma}_m)] \sim -2/5$ is due to the estimate by Haxton et al.[17] Naively, the recoil term is estimated by multiplying $(\vec{q}/m_e)\cdot(\vec{D}/M)$ with $\vec{\sigma}_n \cdot \vec{\sigma}_m$, but the value turns out to be the overestimate by factor 4 due to the cancellations in the integration of $\vec{q}$, as will be discussed in § 3.4.

§ 3.4 Neutrino potentials

The exchange of the virtual neutrino gives rise to neutrino potentials. The explicit forms of them are obtained by integrating the neutrino momentum $\vec{q}$ in Eqs.(3.3.2) and (3.3.15). We find the following four types of them in the nuclear matrix elements which are nonvanishing in the closure approximation.

For the m_ν part, we have from Eqs.(3.3.2), (3.3.12) and (C.2.11a),

$$h_+(r, E_a) \equiv (R/2)(H_2 + H_1) , \tag{3.4.1}$$

where we define, by using $A_{1,2} = \mu_a m_e \pm \varepsilon_{12}/2$ in Eq.(3.3.6),

$$\begin{aligned} H_k(r, E_a) &\equiv \frac{1}{2\pi^2}\int \frac{d\vec{q}}{\omega}\frac{1}{\omega + A_k} e^{i\vec{q}\cdot\vec{r}} \\ &= \frac{2}{\pi}\frac{1}{r}\int_0^\infty dq \frac{q \sin(qr)}{\omega(\omega + A_k)} , \end{aligned} \tag{3.4.2}$$

where $\vec{r} = \vec{r}_n - \vec{r}_m$ from Eq.(3.1.16). The nuclear radius R is introduced to make the potential h_+ dimensionless, because H_k behaves as the Coulomb $(1/r)$ or Yukawa potential.

For the ω-term, the energy denominator appears in the form of Eq.(3.3.21) (see also Table 3.3),

$$\frac{\omega}{\omega + A_2} - \frac{\omega}{\omega + A_1} = \frac{\varepsilon_{12}}{2}\left(\frac{1}{\omega + A_2} + \frac{1}{\omega + A_1}\right) - \mu_a m_e \varepsilon_{12}\frac{1}{(\omega + A_2)(\omega + A_1)} . \tag{3.4.3}$$

Since there is a common factor ε_{12}, the potential for the ω-term is defined as

$$\begin{aligned} h_{0\omega}(r, E_a) &\equiv \frac{R}{\varepsilon_{12}}\frac{1}{2\pi^2}\int \frac{d^3q}{\omega}\left(\frac{\omega}{\omega + A_2} - \frac{\omega}{\omega + A_1}\right) e^{i\vec{q}\cdot\vec{r}} \\ &= h_+ - \mu_a m_e R\, h_0 , \end{aligned} \tag{3.4.4}$$

where

$$h_0(r, E_a) \equiv (1/\epsilon_{12})(H_2 - H_1)$$

$$= \frac{1}{2\pi^2}\int \frac{d^3q}{\omega} \frac{1}{(\omega + A_2)(\omega + A_1)} e^{i\vec{q}\cdot\vec{r}} . \qquad (3.4.5)$$

The above potential is defined so that $h_{0\omega}$ has the same order of magnitude as h_+ in Eq.(3.4.1) because $\mu_a m_e R \sim 1/4$ ($\mu_a \sim 20$).

For the $\vec{q}$-term, we have the potential from Eq.(3.3.20) and (3.3.22),

$$\vec{H}_{q1}(\vec{r}, E_a) + \vec{H}_{q2}(\vec{r}, E_a) , \qquad (3.4.6)$$

where

$$\vec{H}_{qk}(\vec{r}, E_a) \equiv \frac{1}{2\pi^2}\int \frac{d^3q}{\omega} \frac{\vec{q}}{\omega + A_k} e^{i\vec{q}\cdot\vec{r}} . \qquad (3.4.7)$$

This potential is formally divergent, but this divergence is harmless by the following reason:[27),33)] The neutrino propagates from one neutron to the other so that the propagating range r has the upper and lower limits, $r_c < r < 2R$, r_c being the core radius of nucleon. These limits in turn provide cutoffs for q so that the $\vec{q}$ integration becomes finite. Let us formulate the above argument quantitatively.[33)] The important point is that if the $\vec{q}$ integral is formally divergent, the overlap integration of nuclear wave functions has to be made first. That is, from Eq.(3.3.20), the part of the transition amplitude including both $\vec{H}_{qk}$ and the overlap of nuclear wave functions $\rho_0(\vec{r}_n, \vec{r}_m)$ should be written in the following order;

$$\frac{1}{2\pi^2}\int \frac{d^3q}{\omega} \frac{\vec{q}}{\omega + A_k} \int d\vec{r}_n\, d\vec{r}_m\, \rho_0(\vec{r}_n, \vec{r}_m) e^{i\vec{q}\cdot\vec{r}_{nm}} \qquad (3.4.8)$$

The overlap function $\rho_0(\vec{r}_n, \vec{r}_m)$ is a rapidly decreasing function for $r_{nm} > 2R$ and vanishes at $\vec{r}_n = \vec{r}_m$ because two distinct neutrons participate in the $\Delta Q = 2$ nuclear transition. Thus, the following changes of expression are allowed:

$$\vec{q}\int d\vec{r}_n\, d\vec{r}_m\, \rho_0(\vec{r}_n, \vec{r}_m) e^{i\vec{q}\cdot\vec{r}_{nm}} = \int d\vec{r}_n d\vec{r}_m\, \rho_0(\vec{r}_n, \vec{r}_m)\left(-i\frac{\partial}{\partial \vec{r}_{nm}} e^{i\vec{q}\cdot\vec{r}_{nm}}\right)$$

$$= \int d\vec{r}_n\, d\vec{r}_m \left(i\frac{\partial}{\partial \vec{r}_{nm}} \rho_0(\vec{r}_n, \vec{r}_m)\right) e^{i\vec{q}\cdot\vec{r}_{nm}} \qquad (3.4.9)$$

Now we apply the Riemann-Lebesgue theorem to the last expression, and find that Eq.(3.4.9) vanishes as $\vec{q} \to \infty$. Therefore, the $\vec{q}$ integration in Eq.(3.4.8) is convergent. Now we would like to make the exchange of the $\vec{q}$ and $\vec{r}_n$, $\vec{r}_m$ integrations, by using the second expression in Eq.(3.4.9). Then we find the convergent expression of potential with $\hat{r} = \vec{r}/r$,

$$\vec{H}_{qk}(r, E_a) = -i\hat{r}\frac{d}{dr} H_k(r, E_a) . \qquad (3.4.10)$$

As we see in Table 3.3, pR/3 and αZ terms include the factor r from the P-wave electron. Therefore, it is convenient to define the potential appearing in the nuclear matrix elements as,

$$h_+'(r, E_a) \equiv (R/2)\left[-i\vec{r}\cdot(\vec{H}_{q2} + \vec{H}_{q1})\right]$$

$$= -r\frac{d}{dr} h_+ , \qquad (3.4.11)$$

which behaves like $h_+ \sim R/r$.

The nucleon recoil term in the $\vec{q}$-part gives rise to a new type of potential, because they contain the nuclear recoil momentum $\vec{Q}$, as seen from Eq.(3.1.17).[33] Since the emitted electron energy ($\varepsilon_j \sim$ a few MeV) is much smaller than the average neutrino momentum ($q \sim 1/R \sim 40$ MeV), Q is roughly equal to q,

$$\vec{Q}_m \simeq -\vec{Q}_n \simeq \vec{q} \quad . \tag{3.4.12}$$

Therefore, the extra $\vec{q}$ factor has to be included in the q-intagration of the potential $\vec{H}_{qk}$,

$$h_R(r, E_a) \equiv \frac{R}{M}\frac{R}{2}\left(H_{R2}+H_{R1}\right), \tag{3.4.13}$$

where

$$H_{Rk}(r, E_a) = \frac{1}{2\pi^2}\int \frac{d^3q}{\omega}\,\frac{\vec{q}\cdot\vec{q}}{\omega+A_k}\,e^{i\vec{q}\cdot\vec{r}} \quad . \tag{3.4.14}$$

The factor R/M is introduced to make h_R dimensionless and its origin is understood from Table 3.3. The divergence of h_R is treated similarly to the case of $\vec{H}_{qk}$ and its convergent form is expressed as

$$h_R(r, E_a) = -\frac{R}{M}\frac{\partial^2}{\partial r^2} h_+ \quad . \tag{3.4.15}$$

The potentials h_+, h_0, h_+' and h_R are essentially independent of electron energies because $\omega + A_k \sim \omega + \mu_a m_e \gg |\varepsilon_{12}|$ ($\sim 2m_e$). Also they are independent of m_ν in the region $m_\nu < 1$ MeV because $q \sim 1/R \sim 40$ MeV so that the replacement $\omega = \sqrt{q^2 + m_\nu^2} \sim q$ is allowed.

The m_ν dependence of them, including the heavier neutrino region will be shown in Fig. 3.4.

The analytical forms of potentials are obtained for $m_\nu = 0$;[25),26)]

$$h_+(r, E_a) = \frac{R}{r}\,\phi(\mu_a m_e r), \tag{3.4.16a}$$

$$h_{0\omega}(r, E_a) = h_+ - \mu_a m_e R\, h_0, \tag{3.4.16b}$$

$$h_+'(r, E_a) = h_+ + \mu_a m_e R\, h_0, \tag{3.4.16c}$$

$$h_R(r, E_a) = -\frac{\mu_a m_e}{M}\left\{\frac{2}{\pi}\left(\frac{R}{r}\right)^2 - \mu_a m_e R\, h_+\right\}, \tag{3.4.16d}$$

where

$$h_0(r, E_a) = -\phi'(\mu_a m_e R) \tag{3.4.17}$$

and

$$\phi(x) = \frac{2}{\pi}\left[\sin x\, Ci(x) - \cos x\, Si(x)\right], \tag{3.4.18a}$$

$$\phi'(x) = \frac{d}{dx}\phi = \frac{2}{\pi}\left[\cos x\, Ci(x) + \sin x\, Si(x)\right]. \tag{3.4.18b}$$

We now consider the μ_a dependence of potentials for light neutrinos, i.e., $\omega \approx q$. Let us consider h_+ first. The integrand of h_+ behaves as $\sin qr/(q + A_k) \sim \sin qr/(q + \mu_a m_e)$. Therefore, it is understood that h_+ is a slowly decreasing function of μ_a. In particular, if $\mu_a m_e \ll 1/r \sim 1/R \sim 80\, m_e$, the effect of $\mu_a m_e$ can be neglected and h_+ has the value 1/r. If $\mu_a m_e \gg 1/r$, the oscillation due to sin(qr) dumps the integration. The μ_a dependence of

$h_+(r, E_a)$ with $r = R$ is plotted in Fig. 3.5. The potential $h_{0\omega}$ in Eq.(3.4.4) depends on $\mu_a m_e R h_0$ which increases linearly with μ_a due to $\mu_a m_e R$ factor until $\mu_a m_e \sim 1/r$. For the larger domain of μ_a, the $\mu_a m_e$ factor is compensated by the $(\omega+\mu_a m_e)^{-2}$ factor in the integrand. Therefore, $\mu_a m_e R h_0$ behaves as the curve in Fig. 3.5. For smaller values $\mu_a \lesssim 20$, the effect of $\mu_a m_e R h_0$ to $h_{0\omega}$ is small because $\mu_a m_e R \sim 20/80 \sim 1/4$. For larger values, the cancellation between h_+ and $\mu_a m_e h_0$ becomes effective but $h_{0\omega}$ is always positive as seen from Eq.(3.4.3). The other potentials h'_+ and h_R are given by taking the derivatives of h_+ with respect to r, so that it is not easy to see their behaviour. From the analytic form of h'_+ in Eq.(3.4.16c), h'_+ is a slow decreasing function of μ_a as shown in Fig. 3.5. We expect from Eq.(3.4.16d), h_R behaves as the second derivative of ϕ, and the μ_a dependence of ϕ is readily read off from h_+ because the curve is for $r = R$. From the curve of h_+, we expect that h_R increases for smaller μ_a and decreases for larger μ_a as in the case of $\mu_a m_e R h_0$. These are shown in Fig. 3.5.

For completeness, the r dependence of potentials are shown in Fig.3.6 for ^{76}Ge with $\mu_a = 18.51$. The m_ν dependence of potentials for light neutrinos are given explicitly in Eq.(3.4.16) and for heavy neutrinos, $m_\nu \gg \mu_a m_e$, in Eq.(E.2). It is not easy to obtain the m_ν dependence of potentials for 1 MeV $\lesssim m_\nu \lesssim$ 1 GeV. The analytic forms of h_+ and h'_+ were examined in detail in Ref.26, where the m_ν dependences of h_+ and h'_+ were given numerically in Fig. 5. of Ref.26. Here we reproduce their results in Fig. 3.4.

§3.5 The half-life formulae for the $(\beta\beta)_{0\nu}$ mode

In the previous subsections, we gave the brief derivation of the decay formulae of the $(\beta\beta)_{0\nu}$ mode in the 2n-mechanism. We have used the most general effective interaction consisting of V±A currents in Eq.(3.1.3). The impulse approximation for hadronic currents is assumed, but the nucleon recoil terms are retained, as given in Eq.(3.1.16). We retain only the non-vanishing terms under the closure approximation. The lowest spherical waves of electrons which give leading contributions are only taken into account. We showed that the neutrino mass part contributes only to the $0^+ \to 0^+$ transition [§3.3.1] and the right-handed interactions are needed for the $0^+ \to 2^+$ transition [§3.3.2]. The importance of the P-wave effect and the recoil effect are stressed [§3.3.2] and it is explained visually what kinds of neutrino potentials appear in the half-life formulae [§3.4].

Within these approximations, we shall present the half-life formulae for the $0^+ \to 0^+$ and $0^+ \to 2^+$ transitions in the approximation of keeping the contribution from the light virtual neutrinos ($m_j \lesssim 10$ MeV) for simplicity. The detailed derivation will be given in Appendix C, where the contributions from the vanishing terms in the closure approximation are presented and the correction terms due to the higher spherical waves and the finite de Broglie wave length corrections are evaluated. The leading contributions from these correction terms are compiled in Eq.(C.3.7) for the $0^+ \to 0^+$ transition and in Table C.2 for both the $0^+ \to 0^+$ and $0^+ \to 2^+$ transitions.

§3.5.1 The $0^+ \to 0^+$ transition

The half-life formula includes nine nuclear parameters:[64),31)] For the m_ν-part, nuclear tensor operators come from only hadronic currents in Eq.(3.1.16) because electrons are in the S-wave state. They are the Gamow-Teller type $\tau_n^+ \vec{\sigma}_n$ and the Fermi type τ_n^+, because the neucleon recoil terms require the P-wave for one of electrons. Therefore, we have the double Gamow-Teller and double Fermi type nuclear matrix elements with the neutrino potential h_+ in Eq.(3.4.1),

$$M_{GT}^{(0\nu)} = \sum_a \langle 0_f^+ \| h_+(r_{nm}, E_a)\, \vec{\sigma}_n \cdot \vec{\sigma}_m \| 0_i^+ \rangle, \tag{3.5.1}$$

$$\chi_F = \sum_a \langle 0_f^+ \| h_+(r_{nm}, E_a) \| 0_i^+ \rangle (g_V/g_A)^2 / M_{GT}^{(0\nu)}, \tag{3.5.2}$$

where the abbreviation for the reduced nuclear matrix elements in Eq.(B.1.5) is used. These are obtained from z_1 in Eq.(C.2.16).

For the ω-term, we have the potential $h_{0\omega}$ in Eq.(3.4.4), but the nuclear tensor operators are the same as the m_ν part, as explicitly seen from Eq.(C.2.38), because of two S-wave electrons:

$$\chi_{GT\omega} = \sum_a \langle 0_f^+ \| h_{0\omega}(r_{nm}, E_a)\, \vec{\sigma}_n \cdot \vec{\sigma}_m \| 0_i^+ \rangle / M_{GT}^{(0\nu)} = 1 - \mu_0' m_e R\, \chi_{GT}^{(0)}, \tag{3.5.3a}$$

$$\chi_{F\omega} = \sum_a \langle 0_f^+ \| h_{0\omega}(r_{nm}, E_a) \| 0_i^+ \rangle (g_V/g_A)^2 / M_{GT}^{(0\nu)} = \chi_F - \mu_0' m_e R\, \chi_F^{(0)}, \tag{3.5.3b}$$

where the second expressions are derived by using the potential h_0 in Eq.(3.4.5),

$$\mu_0' \chi_{GT}^{(0)} = \sum_a \langle 0_f^+ \| \mu_a h_0(r_{nm}, E_a)\, \vec{\sigma}_n \cdot \vec{\sigma}_m \| 0_i^+ \rangle / M_{GT}^{(0\nu)}, \tag{3.5.4a}$$

$$\mu_0' \chi_F^{(0)} = \sum_a \langle 0_f^+ \| \mu_a h_0(r_{nm}, E_a) \| 0_i^+ \rangle (g_V/g_A)^2 / M_{GT}^{(0\nu)}. \tag{3.5.4b}$$

For the $\vec{q}$-term, we have the following new nuclear tensor operators in addition to the Gamow-Teller $\tau_n^+ \sigma_n^+$ and the Fermi τ_n^+ operators; the three momentum of the virtual neutrino $\vec{q} \propto \vec{r}_{nm}$ and also either the terms from P-wave electron $\vec{r}_n$ ($\vec{r}_{nm}$ and $\vec{r}_{+nm} = \vec{r}_n + \vec{r}_m$) or the nucleon recoil term D_n^+. The potential in this case is h_+' in Eq.(3.4.11). Thus, we find the variety of nuclear matrix elements,

$$\chi_{GT}' = \sum_a \langle 0_f^+ \| h_+'(r_{nm}, E_a)\, \vec{\sigma}_n \cdot \vec{\sigma}_m \| 0_i^+ \rangle / M_{GT}^{(0\nu)}, \tag{3.5.5}$$

$$\chi_F' = \sum_a \langle 0_f^+ \| h_+'(r_{nm}, E_a) \| 0_i^+ \rangle (g_V/g_A)^2 / M_{GT}^{(0\nu)}, \tag{3.5.6}$$

$$\chi_T' = \sum_a \langle 0_f^+ \| h_+'(r_{nm}, E_a) [(\vec{\sigma}_n \cdot \hat{r}_{nm})(\vec{\sigma}_m \cdot \hat{r}_{nm}) - \vec{\sigma}_n \cdot \vec{\sigma}_m/3] \| 0_i^+ \rangle / M_{GT}^{(0\nu)}, \tag{3.5.7}$$

$$\chi_P' = \sum_a \langle 0_f^+ \| i\, h_+'(r_{nm}, E_a) \left(\frac{r_{+nm}}{r_{nm}}\right) [(\vec{\sigma}_n - \vec{\sigma}_m) \cdot (\hat{r}_{nm} \times \hat{r}_{nm})] \| 0_i^+ \rangle \left(\frac{g_V}{g_A}\right) / M_{GT}^{(0\nu)}, \tag{3.5.8}$$

$$\chi_R' = \sum_a \langle 0_f^+ \| h_+'(r_{nm}, E_a) \left(\frac{R}{2 r_{nm}}\right) [\hat{r}_{nm} \cdot (\vec{\sigma}_n \times \vec{D}_n + \vec{D}_n \times \vec{\sigma}_n)] \| 0_i^+ \rangle \left(\frac{g_V}{g_A}\right) / M_{GT}^{(0\nu)}. \tag{3.5.9}$$

Here the first three, χ_{GT}', χ_F' and χ_T' which come from z_5 in Eq.(C.2.43) represent the contributions from the usual electron P-wave (no αZ term in Eq.(3.1.22)), while χ_P' which is obtained from z_6 in Eq.(C.2.43) is associated with the P-wave effect. The last nuclear parameter χ_R' stands for the nucleon recoil effect of z_{4R} in Eq.(C.2.39)*) obtained for the case of two S-wave electrons.

*) As for the relation between our χ_P' and $\mathrm{Im}(M_4'^*)$ defined by Haxton and Stephenson,[17)] there is a sign mistake in Eq.(4.14h) of Ref.64 and the corrected one is $\mathrm{Im}(M_4'^*) = -\chi_P' (\frac{1}{R})(g_A/g_V) M_{GT}^{(0\nu)}$. We indebted to Professor A. Faessler for pointing out it.

For the recoil term χ_R', $\vec{D}_n$ includes the nucleon recoil momentum $\vec{Q}_n$ which is related to the virtual neutrino momentum $\vec{q}$ by Eq.(3.4.12). Therefore, the $\vec{q}$-integration in the definition of h_+' should be extended to $\vec{D}_n$ and thus the potential h_R in Eq.(3.4.15) emerges for χ_R'.

With the nuclear parameters given above, the inverse half-life is given by

$$[T_{0\nu}(0^+\to 0^+)]^{-1} = |M_{GT}^{(0\nu)}|^2 \Big\{ C_1 \Big(\frac{\langle m_\nu\rangle}{m_e}\Big)^2 + C_2\langle\lambda\rangle \frac{\langle m_\nu\rangle}{m_e}\cos\psi_1 + C_3\langle\eta\rangle\frac{\langle m_\nu\rangle}{m_e}\cos\psi_2 + C_4(\langle\lambda\rangle)^2 + C_5(\langle\eta\rangle)^2 + C_6\langle\lambda\rangle\langle\eta\rangle\cos(\psi_1-\psi_2)\Big\}, \tag{3.5.10}$$

where C_i is the coefficient including nuclear matrix elements and will be defined later. Here the following abbreviations for the neutrino mass and right-handed parameters are used from Eqs.(1.2.2), (1.2.5) and (3.1.5),

$$\langle m_\nu\rangle = |\Sigma_j' m_j U_{ej}^2|, \tag{3.5.11}$$

$$\langle\lambda\rangle = \lambda\,|\Sigma' U_{ej} V_{ej}' (g_{AV}'/g_V)|, \tag{3.5.12}$$

$$\langle\eta\rangle = \eta\,|\Sigma' U_{ej} V_{ej}'|, \tag{3.5.13}$$

and the relative phases are defined as

$$\psi_1 = \arg[(\Sigma' m_j U_{ej}^2)(\Sigma' U_{ej} V_{ej}' (g_{AV}'/g_V))^*], \tag{3.5.14a}$$

$$\psi_2 = \arg[(\Sigma' m_j U_{ej}^2)(\Sigma' U_{ej} V_{ej}')^*]. \tag{3.5.14b}$$

If CP is conserved, ψ_1 and ψ_2 take 0 or π. The primed sum in the above expressions means that the sum extends over only the light neutrinos ($m_j \lesssim 10$ MeV) and the contribution from heavier neutrinos are neglected. The necessary modification for the inclusion of heavier neutrinos will be discussed in §9.1.

It should be noted that $\langle m_\nu\rangle$, $\langle\lambda\rangle$ and $\langle\eta\rangle$ vanish strictly in the massless limit of weak eigenstate electron neutrinos, ν_{eL}, $\tilde{\nu}_{eL}$, ν_{eR}', and $\tilde{\nu}_{eR}'$ in Eq.(3.1.5). (If there is no mirror neutrino, we have $\nu_{eL}=\tilde{\nu}_{eL}$ and $\nu_{eR}'=\tilde{\nu}_{eR}'$; that is, there are relations $U_{ej}=U_{ej}'$ and $V_{ej}=V_{ej}'$ for neutrino mixing matrices.) This is because these neutrinos are independent each other and have no mixing among them. Therefore, we find that $\langle m_\nu\rangle = \langle\lambda\rangle = \langle\eta\rangle = 0$. Furthermore, if all neutrinos are light, then $\langle\lambda\rangle = \langle\eta\rangle = 0$ because of the condition $\Sigma_j U_{ej}V_{ej} = \Sigma_j U_{ej}V_{ej}' = 0$ in Eq.(3.1.6) which represent the independence among ν_{eL}, ν_{eR}' and $\tilde{\nu}_{eR}'$.

In Eq.(3.5.10), we have neglected the m_ν part for the case where only the V + A weak interaction acts at both vertices, corresponding to z_2 in Eq.(C.2.18), because the effective neutrino mass in this case is, for example, $\langle m_\nu\rangle_R = |\Sigma_j' m_j \lambda^2 V_{ej}^2| \ll \langle m_\nu\rangle$ in Eq.(3.5.11).

The coeffieients C_i are expressed as combinations of 8 nuclear parameters and 9 integrated kinematical factors:[31),64)]

$$C_1 = (1-\chi_F)^2 G_{01}, \tag{3.5.15a}$$

$$C_2 = -(1-\chi_F)[\chi_{2-} G_{03} - \chi_{1+} G_{04}], \tag{3.5.15b}$$

$$C_3 = (1-\chi_F)[\chi_{2+} G_{03} - \chi_{1-} G_{04} - \chi_P' G_{05} + \chi_R' G_{06}], \tag{3.5.15c}$$

$$C_4 = [\chi_{2-}^2 G_{02} + \tfrac{1}{9}\chi_{1+}^2 G_{04} - \tfrac{2}{9}\chi_{1+}\chi_{2-} G_{03}], \tag{3.5.15d}$$

$$C_5 = [\chi_{2+}^2 G_{02} + \tfrac{1}{9}\chi_{1-}^2 G_{04} - \tfrac{2}{9}\chi_{1-}\chi_{2+} G_{03} + \chi_P'^2 G_{08} - \chi_P'\chi_R' G_{07} + \chi_R'^2 G_{09}] \tag{3.5.15e}$$

$$C_6 = -2[\chi_{2-}\chi_{2+} G_{02} - (\chi_{1+}\chi_{2+} + \chi_{2-}\chi_{1-}) G_{03}/9 + \tfrac{1}{9}\chi_{1+}\chi_{1-} G_{04}], \tag{3.5.15f}$$

where all nuclear parameters in Eqs.(3.5.1)-(3.5.9) are assumed to be real and some combinations of nuclear parameters are introduced,

$$\chi_{1\pm} = \chi'_{GT} - 6\chi'_{T} \pm 3\chi'_{F} \tag{3.5.16a}$$

$$\chi_{2\pm} = \chi_{GTw} \pm \chi_{Fw} - \frac{1}{9}\chi_{1\pm}. \tag{3.5.16b}$$

The nine integrated kinematical factors are defined by

$$G_{0k} = \frac{a_{0\nu}}{\ell n 2 (m_e R)^2} \int d\Omega_{0\nu}\, b_{0k}, \qquad \text{for } k = 1 \sim 9, \tag{3.5.17a}$$

where the constant term $a_{0\nu}$ and the phase space factor $d\Omega_{0\nu}$ are,

$$a_{0\nu} = (G g_A)^4 m_e^9 / (64\pi^5), \tag{3.5.17b}$$

$$d\Omega_{0\nu} = m_e^{-5} p_1 p_2 \varepsilon_1 \varepsilon_2 \delta(\varepsilon_1 + \varepsilon_2 + M_f - M_i)\, d\varepsilon_1 d\varepsilon_2 d(\hat{p}_1 \cdot \hat{p}_2). \tag{3.5.17c}$$

The kinematical factors b_{0k} are defined as

$$b_{01} = \alpha_+ + \beta_+, \qquad b_{02} = \left(\frac{\varepsilon_{12}}{m_e}\right)^2 \beta_+,$$

$$b_{03} = 2\left(\frac{\varepsilon_{12}}{m_e}\right)\beta_-, \qquad b_{04} = \left(\frac{4}{9}\right)\beta_+,$$

$$b_{05} = \frac{4}{3}\,\frac{(\zeta\alpha_- - 2m_e R\alpha_+)}{m_e R}, \qquad b_{06} = \frac{8}{m_e R}\alpha_-,$$

$$b_{07} = \frac{16}{3}\,\frac{(\zeta\alpha_+ - 2m_e R\alpha_-)}{(m_e R)^2}$$

$$b_{08} = \frac{4}{9}\,\frac{[\zeta^2\alpha_+ + 4m_e R(m_e R\alpha_+ - \zeta\alpha_-)]}{(m_e R)^2},$$

$$b_{09} = \left(\frac{4}{m_e R}\right)^2 \alpha_+, \tag{3.5.18}$$

where the characteristic features of the $P_{1/2}$-wave in Eq.(3.1.22) are expressed as

$$\zeta = 3\alpha Z + (T+2) m_e R. \tag{3.5.19}$$

In the approximation Eq.(3.1.24), we find from the definitions of $\alpha_\pm$ and $\beta_\pm$ in Eq.(C.3.12),

$$\begin{pmatrix}\alpha_+ \\ \beta_+\end{pmatrix} \Rightarrow \frac{1}{2}(\varepsilon_1\varepsilon_2 \pm m_e^2)\, C_{00}, \tag{3.5.20a}$$

$$\begin{pmatrix}\alpha_- \\ \beta_-\end{pmatrix} \Rightarrow \frac{1}{2}(\varepsilon_1 \pm \varepsilon_2)\, C_{00}, \tag{3.5.20b}$$

where

$$C_{k\ell} = \sqrt{F_k(Z,\varepsilon_1)\, F_\ell(Z,\varepsilon_2)}\,/\,\varepsilon_1\varepsilon_2. \tag{3.5.21}$$

The large enhancement factor $(m_e R)^{-2} \approx (80)^2$ in the denominator of G_{0k} in Eq.(3.5.17a) appears in comparison with G_{GT} in Eq.(3.2.11) for the $(\beta\beta)_{2\nu}$ mode. The origin of it is the Coulomb type potential due to the neutrino propagation; that is, the nuclear radius R is introduced to normalize this potential as (R/γ), as it was discussed from the view point of the virtual neutrino momentum at the end of §1.3.(ii). Other enhancement factor $(m_e R)^{-2}$ in b_{07}, b_{08} and b_{09} in Eq.(3.5.18) represents the $\vec{q}$ term of the neutrino propagator, but there is no such factor in b_{02} from the ω term, because of the cancellation between two energy denominator terms.

The P-wave effect appears in $b_{05} \sim 2(2\alpha Z/m_e R)\alpha_-$ associated with χ'_P and $b_{08} \sim (2\alpha Z/m_e R)^2 \alpha_+$ with χ'^2_P. The origin of this large enhancement factor $2\alpha Z/m_e R \sim 50$ is explained in Table 3.3. The recoil effect is expected to produce $4/m_e R \sim 320$ factor which appears in

$b_{06} \sim 2(4/m_e R)\alpha_-$ with χ_R' and $b_{09} \sim (4/m_e R)^2 \alpha_+$ with $\chi_R'^2$. The important features of the P-wave and recoil effects are that they appear only in the coefficients of $\langle m_\nu \rangle \langle \eta \rangle$ and $\langle \eta \rangle^2$ terms, i.e., C_3 and C_5. Therefore, the accurate knowledge on nuclear parameters χ_p' and χ_R' is important for determining the magnitude of $\langle \eta \rangle$.

The numerical values of the integrated kinematical factors G_{0k} are given in Table 3.4, from which the above discussions can be confirmed numerically.

§3.5.2 The $0^+ \to 2^+$ transition

The dominant contribution to the $0^+ \to 2^+$ transition comes from the case where one electron is in the S-wave and the other is in the P-wave with $j = 3/2$ due to the angular momentum conservation. The Coulomb correction for these electrons enter only through the normalization factor F_0 and F_1 as it is seen from Eqs. (3.1.21) and (3.1.23) and thus there is no extra αZ correction like the P-wave effect for the $0^+ \to 0^+$ transition.

The inverse half-life is expressed as, from Eq. (C.4.9)

$$[T_{0\nu}(0^+ \to 2^+)]^{-1} = |\Xi_{21}|^2 G_{21} + |\Xi_{22}|^2 G_{22}, \tag{3.5.22}$$

$$\Xi_{21} = \begin{cases} \langle \lambda \rangle [M_{2a} - 2M_{2b} + M_{2c} + 2M_{2d}] e^{i(\Psi_0 - \Psi_1)} \\ -\langle \eta \rangle [M_{2a} - 2M_{2b} - M_{2c}] e^{i(\Psi_0 - \Psi_1)} \end{cases},$$

$$\Xi_{22} = 2\langle \eta \rangle M_{2e} e^{i(\Psi_0 - \Psi_1)}, \tag{3.5.23}$$

where*

$$M_{2a} = \sum_a \langle 2_f^+ \| h_+'(r_{nm}, E_a) \vec{\sigma}_n \cdot \vec{\sigma}_m [\hat{r}_{nm} \otimes \hat{r}_{nm}]^{(2)} \| 0_i^+ \rangle, \tag{3.5.24a}$$

$$M_{2b} = \frac{1}{2} \sum_a \langle 2_f^+ \| h_+'(r_{nm}, E_a) \{ (\vec{\sigma}_n \cdot \hat{r}_{nm}) [\hat{r}_{nm} \otimes \vec{\sigma}_m]^{(2)} + [\hat{r}_{nm} \otimes \vec{\sigma}_n]^{(2)} (\vec{\sigma}_m \cdot \hat{r}_{nm}) \} \| 0_i^+ \rangle, \tag{3.5.24b}$$

$$M_{2c} = \sum_a \langle 2_f^+ \| h_+'(r_{nm}, E_a) [\hat{r}_{nm} \otimes \hat{r}_{nm}]^{(2)} \| 0_i^+ \rangle (g_V/g_A)^2, \tag{3.5.24c}$$

$$M_{2d} = \frac{i}{2} \sum_a \langle 2_f^+ \| h_+'(r_{nm}, E_a) [\hat{r}_{nm} \otimes (\hat{r}_{nm} \times (\vec{\sigma}_n + \vec{\sigma}_m))]^{(2)} \| 0_i^+ \rangle (g_V/g_A), \tag{3.5.24d}$$

$$M_{2e} = \frac{i}{2} \sum_a \langle 2_f^+ \| h_+'(r_{nm}, E_a) \frac{\vec{r}_{nm}}{r_{nm}} [\hat{r}_{nm} \otimes [\hat{r}_{nm} \times (\vec{\sigma}_n - \vec{\sigma}_m)]]^{(2)} \| 0_i^+ \rangle (g_V/g_A). \tag{3.5.24d}$$

The integrated kinematical factors G_{21} and G_{22} are defined by Eq. (3.5.17a) with b_{21} and b_{22} in Eqs. (C.4.12) which have the approximate forms as

$$b_{21} \Rightarrow \frac{1}{6}(\varepsilon_1 \varepsilon_2 + m_e^2) \left[(p_1/m_e)^2 C_{10} + (p_2/m_e)^2 C_{01} \right], \tag{3.5.25a}$$

$$b_{22} \Rightarrow \frac{1}{6}(\varepsilon_1 \varepsilon_2 - m_e^2) \left[(p_1/m_e)^2 C_{10} + (p_2/m_e)^2 C_{01} \right], \tag{3.5.25b}$$

where C_{01} and C_{10} are defined in Eq. (3.5.21). The numerical values of G_{21} and G_{22} are given in Table 3.5.

---

*) Note that M_{2b} can be reexpressed as

$$M_{2b} = \begin{cases} (1/3) M_{2a} + (1/3) \sum_a \langle 2_f^+ \| h_+'(r_{nm}, E_a) [\vec{\sigma}_n \otimes \vec{\sigma}_m]^{(2)} \| 0_i^+ \rangle \\ -\sqrt{7/12} \sum_a \langle 2_f^+ \| h_+'(r_{nm}, E_a) [[\hat{r}_{nm} \otimes \hat{r}_{nm}]^{(2)} \otimes [\vec{\sigma}_n \otimes \vec{\sigma}_m]^{(2)}] \| 0_i^+ \rangle \end{cases} \tag{3.5.26}$$

§4. The N* mechanism

Let us consider a possibility that the $\beta\beta$ decay takes place through the transitions between nucleon ($J^P I = 1/2^+ 1/2$) and $\Delta(1232)(3/2^+ 3/2)$, as an example is shown in Fig. 1.4,

$$\begin{aligned} \Delta^- &\longrightarrow p + 2e^- \ (+2\bar{\nu}_e) \ , \\ n &\longrightarrow \Delta^{++} + 2e^- \ (+2\bar{\nu}_e) \ . \end{aligned} \tag{4.1}$$

This mechanism becomes important especially for the $(\beta\beta)_{0\nu}$ mode, because the transitions occur inside (the single) hadron and thus the range of neutrino propagation $r \lesssim 2/m_\pi$ becomes much shorter than that in the 2n-mechanism. Since the neutrino potential behaves like 1/r, this short range propagation will give the enhancement which may overcome the small admixture of Δ ($\sim 1\%$) inside nucleus.

The N^* mechanism was introduced by Primakoff and Rosen for the $(\beta\beta)_{0\nu}$ mode within the effective interaction in Eq.(3.1.1).[27] Smith, Picciotto and Brymann applied it to the $(\beta\beta)_{2\nu}$ mode.[69] Later, Halprin, Minkowski, Primakoff and Rosen considered the $(\beta\beta)_{0\nu}$ mode mediated by a heavy neutrino.[65]

Recently, Doi, Kotani, Nishiura, Okuda and Takasugi[26),21] and later Haxton, Stephenson and Strottman[34] gave the arguments that the $0^+ \to 0^+$ transition is forbidden in the static approximation of the hadronic currents in this N* mechanism. In the following, we shall derive this selection rule first.

In order for the N^* mechanism to work, the tensor operators should make the following transitions allowed; (i) the transition between the parent and daughter nuclei, and (ii) the $\Delta J = 1$ transitions between hadrons in Eq.(4.1). It is important to notice that the tensor

operators for two transitions (i) and (ii) are in general different, because the relevant operators for (ii) are those measured from the center of the hadron.

Let us consider the $\Delta^- \to p + 2e^- (+2\bar{\nu}_e)$ transition inside nucleus. The parent and daughter nuclei are expressed as

$$\begin{aligned} |N_i\rangle &= \sqrt{P(\Delta)}\,|\Delta^-\rangle|\Phi_i\rangle + \sqrt{1-P(\Delta)}\,|N_i'\rangle \ , \\ |N_f\rangle &= |p\rangle|\Phi_f\rangle \end{aligned} \tag{4.2}$$

where $|\Delta^-\rangle$ and $|p\rangle$ represent the intrinsic parts of Δ and p, and the orbital angular momenta of them around the center of nucleus are included in the residual part Φ_i and Φ_f. The factor $P(\Delta)$ is the probability of Δ (inside a nucleus, and is expected to be around 1%.

Now we shall classify the nuclear tensor operators. In the static approximation of the hadronic currents $\tilde{J}^\beta_\lambda$ (in Eq.(4.3) where the recoil terms are neglected, the currents act only on the intrinsic part of $|\Delta^-\rangle$ (in other words, quarks in Δ^-). On the other hand, the position operator of leptons $\vec{r}_n$ should be divided into $\vec{r}_n = \vec{r}_G + \vec{r}_n'$, where $\vec{r}_G$ is the position vector of the center of Δ^- and $\vec{r}_n'$ is the position of the decaying quark from this center. Then, $\vec{r}_n'$ operates on Δ^-, but $\vec{r}_G$ acts on Φ_i. The position vectors of leptons come in the amplitude when the higher spherical waves ($l \geq 1$) are taken into account. Finally, the momentum of virtual neutrino $\hat{q} \sim \hat{r}_{nm}$ acts only on Δ^- because $\vec{r}_{nm} = \vec{r}_n - \vec{r}_m = \vec{r}_{nm}'$.

Now we shall show that if the $0^+ \to 0^+$ nuclear transition (i) is allowed, then the hadronic transitions (ii) are forbidden. If all leptons are taken to be in the S-wave, the relevant tensor operators are of

rank 0 consisting of $\widetilde{J}^{\rho+}_{\alpha}$ and $\widetilde{J}^{\sigma+}_{\beta}$. Since these $\Delta J \neq 0$ operators act also on Δ^-, the $\Delta J = 1$ transitions (ii) are forbidden. If one of electrons is in P-wave, two cases occur: One is that the rank 0 nuclear tensor operators are formed from $\widetilde{J}^{\rho+}_{\alpha}$, $\widetilde{J}^{\sigma+}_{\beta}$, $\vec{q}$ and $\vec{r}'_n$ (or $\vec{r}'_m$), then the transition (ii) are forbidden because all operators act on Δ^-. The other is the case where $\widetilde{J}^{\rho+}_{\alpha}$, $\widetilde{J}^{\sigma+}_{\beta}$, $\vec{q}$ and $\vec{r}_G$ participate in. Then, the tensor operators acting on Δ^- are of rank 1, but the parity odd operators. The parity conserving transitions (ii) are forbidden. In any case, the $0^+ \to 0^+$ transition is forbidden. As it is clear from the above argument, the $0^+ \to 0^+$ transition occurs if higher spherical waves are taken into account, but is highly suppressed.

Now we shall derive the half-life of the $0^+ \to 2^+$ transition in the N^* mechanism. At first, we notice that the half-life formulae of the $(\beta\beta)_{2\nu}$ and $(\beta\beta)_{0\nu}$ modes in the 2n-mechanism can be used for the N^* mechanism also, because in any case the nuclear transition (i) has to occur. As a corollary, the $0^+ \to 2^+$ transition of the $(\beta\beta)_{0\nu}$ mode occurs only from the right handed current (V+A) part, similarly to the 2n-mechanism. Only a particular care should be payed to evaluate the nuclear matrix elements, because they should allow the hadronic transition (ii).

In order to evaluate the nuclear matrix elements, we use the SU(6) quark model and the static approximation of hadronic currents,[26),21)]

$$J^{\rho+}_{L}(\vec{x}) = g_V \sum_n \tau_n^+ \left(g^{\rho 0} + g^{\rho j} \sigma_n^j \right) \delta(\vec{x} - \vec{r}_n), \tag{4.3a}$$

$$J^{\rho+}_{R}(\vec{x}) = g_V' \sum_n \tau_n^+ \left(g^{\rho 0} - g^{\rho j} \sigma_n^j \right) \delta(\vec{x} - \vec{r}_n), \tag{4.3b}$$

where the relations $g_V = g_A$ and $g'_V = g'_A$ are used because the SU(6) quark model evaluation is considered to include the strong interaction corrections automatically.

Within the closure approximation and the assumption that the transitions in Eq.(4.1) take place independently of the residual nucleus, the following results are obtained:

For the $(\beta\beta)_{2\nu}$ mode, we have from Eqs. (3.2.20) and (3.2.21) that

$$\begin{aligned}
\left(M_2^{(2\nu)}/\mu_2^3\right) &= \langle \mu_a \rangle_{av}^{-3} \langle 2_f^+ \| \textstyle\sum_{n,m} \tau_n^+ \tau_m^+ \left[\sigma_n \otimes \sigma_m\right]^{(2)} \| 0_i^+ \rangle \\
&= \langle \mu_a \rangle_{av}^{-3} \left[\langle p \| \textstyle\sum_{n,m} \tau_n^+ \tau_m^+ \left[\sigma_n \otimes \sigma_m\right]^{(2)} \| \Delta^- \rangle \sqrt{P(\Delta)} \langle \Phi_f | \Phi_i \rangle \right. \\
&\quad \left. + \langle \Delta^{++} \| \textstyle\sum_{n,m} \tau_n^+ \tau_m^+ \left[\sigma_n \otimes \sigma_m\right]^{(2)} \| n \rangle \sqrt{P(\Delta)} \langle \Phi_f' | \Phi_i \rangle \right] \\
&= \langle \mu_a \rangle_{av}^{-3} 4\sqrt{5} \sqrt{P(\Delta)} \langle \Phi_f | \Phi_i \rangle ,
\end{aligned} \tag{4.4}$$

where we have assumed that $\langle \Phi'_f | \Phi'_i \rangle = \langle \Phi_f | \Phi_i \rangle$. By substituting the above evaluation of the nuclear matrix element into Eq.(3.2.16), the half-life formula is obtained,

$$\begin{aligned}
\left[T_{2\nu}^{N^*}(0^+ \to 2^+)\right]^{-1} &= g_0 \left(1/1.25\right)^4 G_{2n} P(\Delta) \left| \langle \Phi_f | \Phi_i \rangle \right|^2 / \langle \mu_a \rangle_{av}^6 , \\
&= G_{N^*2\nu} P(\Delta) \left| \langle \Phi_f | \Phi_i \rangle \right|^2 / \langle \mu_a \rangle_{av}^6 ,
\end{aligned} \tag{4.5}$$

where G_{2n} is defined in Eq.(3.2.18) and the factor $(g_V/g_A)^4 = (1/1.25)^4$ is introduced to make correction to the choice $g_V = g_A$ and $g'_V = g'_A$.

The values of $G_{N^*2\nu}$ for the typical nuclei are listed in Table 3.2

In order to evaluate the nuclear matrix elements for the $(\beta\beta)_{0\nu}$ mode, the following facts should be taken into account: In the SU(6) quark model, both Δ and nucleon are in ℓ (orbital angular momentum) = 0 state, so that the hadronic transitions (ii) take place only by the spin operators of rank 1 or 2. Also the position operators which act on quarks should form rank 0 tensors. This means that the rank 2

tensors should arise from the spin part, i.e., two spin operators $\vec{\sigma}_n$ and $\vec{\sigma}_m$ are needed. We find that $M_{2a}=M_{2c}=M_{2d}=M_{2e}=0$ in Eq.(3.5.24), becuase they contain only the rank 0 or 1 combination of $\vec{\sigma}_n$ and $\vec{\sigma}_m$. Note that for M_{2e}, the operator $\vec{r}_{+nm}$ is derived as $\vec{r}_{+nm}=2\vec{r}_G+\vec{r}'_{+nm}$. The above argument applies to the $\vec{r}'_{+nm}$ part. For the $\vec{r}_G$ part, the parity conserving hadronic transitions (ii) do not occur because $\vec{r}_G$ is a parity odd operator and thus the residual operators acting on Δ are also parity odd.

The nuclear matrix element M_{2b} can be evaluated similarly to Eq.(4.4) by using Eq.(3.5.26) and is given by

$$M_{2b}=(4\sqrt{5}/3)(R/a)\,X_\Delta\sqrt{P(\Delta)}\,\langle\Phi_f|\Phi_i\rangle\,, \tag{4.6}$$

where

$$\begin{aligned} X_\Delta &= \left[\langle p|\frac{1}{6}\left(\frac{a}{R}\right)\sum_{n\neq m}h'_+(r_{nm},\langle E_a\rangle)|\Delta^-\rangle\right]_R \\ &= \left[\langle\Delta^{++}|\frac{1}{6}\left(\frac{a}{R}\right)\sum_{n\neq m}h'_+(r_{nm},\langle E_a\rangle)|n\rangle\right]_R \simeq 1\,. \end{aligned} \tag{4.7}$$

Here the subscript R means that X_Δ is the overlap integration of radial wave functions of hadrons, and the parameter a is the mean distance between quarks inside the hadron ($a\sim 0.7$ fm) and is introduced becuase $h'_+\sim R/r\sim R/a$. The half-life is obtained by substituting the above evaluation into Eqs.(3.5.22) and (3.5.23),

$$\left[T^{N^*}_{0\nu}(0^+\to 2^+)\right]^{-1}=\left[\langle\lambda\rangle^2-2\langle\lambda\rangle\langle\eta\rangle\cos(\psi_1-\psi_2)+\langle\eta\rangle^2\right]G_{N^*0\nu}|X_\Delta|^2P(\Delta)\left|\langle\Phi_f|\Phi_i\rangle\right|^2, \tag{4.8}$$

where

$$G_{N^*0\nu}=\left(\frac{320}{9}\right)\left(\frac{1}{1.25}\right)^4\left(\frac{R}{a}\right)^2 G_{21}\,. \tag{4.9}$$

Primakoff and Rosen suggested that $P(\Delta)\sim 10^{-2}$ and $\left|\langle\Phi_f|\Phi_i\rangle\right|^2\sim 0.1$ With these values and the integrated kinematical factor $G_{N^*0\nu}$ in Table 3.5, we can evaluate the half-lives of the $0^+\to 2^+$ transition. In the above derivation, we used the SU(6) quark model and neglected the recoils of quarks which are not small in the bag model.[70]

In the N* mechanism, the $0^+\to 0^+$ transition is forbidden, as discussed before. However, Haxton and Stephenson pointed out that it is allowed, if the $\Delta\to\Delta$ transition in Fig. 1.5 is taken into account.[17),14)] As they argued, the $0^+\to 0^+$ transition by this mechanism is allowed through both the m_ν and V+A parts, but its rate is smaller than the one in the 2n or N*-mechanism, because of the suppression by an additional factor of the probability of Δ, $P(\Delta)\sim 10^{-3}$. Another modification to avoid the $0^+\to 0^+$ relection rule has been proposed by Halprin.[70] The $\Delta J=0$ transition can occur if various higher resonance states of Δ with $J=1/2$ are taken into account, instead of $\Delta(1232)$, the so-called 3-3 resonance state. However, it is reasonable to consider that the probability of finding such a resonance state in the nuclens is reduced relative to $\Delta(1232)$. In this review, these processes are not taken into consideration. Further investigations including the original N*-mechanism will be necessary, especially by the relativistic quark model like the bag model.

§5. Mechanisms beyond the standard model

In this section, we will consider the possibility that the decay occurs through Higgs(scalar) bosons. There are two types of processes, (i) the process where Higgs bosons appear in the intermediate states as shown in Fig. 1.6 and (ii) the process accompanying a Goldstone boson, say, Majoron in the final states as shown in Fig. 1.7. In general, the process (i) is suppressed due to the small couplings of them to neutrinos, while the process (ii) should be examined carefully, because the Goldstone boson couplings to neutrinos are not small.

---

§5.1 The $\beta\beta$ decay mediated by Higgs bosons

The simplest extension of the standard $SU(2)_L \times U(1)$ model to allow a Majorana type mass term for neutrinos is to add a triplet Higgs boson $\vec{H}$,

$$-\frac{1}{\sqrt{2}} \Sigma_{\ell,\ell'} h_{\ell\ell'} \overline{(\psi_{\ell L})^c} H^\dagger \psi_{\ell' L} + h.c., \qquad (5.1.1)$$

where

$$\psi_{\ell L} = \begin{pmatrix} \nu \\ \ell \end{pmatrix}, \quad H = \begin{pmatrix} H^0 & H^-/\sqrt{2} \\ H^-/\sqrt{2} & H^{--} \end{pmatrix}. \qquad (5.1.2)$$

By the spontaneous breakdown of the symmetry $\langle H^0 \rangle = v_H/\sqrt{2}$, we obtain the Majorana type mass term $-(1/2) \Sigma h_{\ell\ell'} v_H \overline{(\nu_{\ell L})^c} \nu_{\ell' L} + h.c.$. Mohapatra and Vergados[37] considered the possibility in Fig. 1.6, by adding the interaction between a triplet $\vec{H}$ and doublet Higgs bosons ϕ as

$$m_H \phi^\dagger H \phi + h.c., \qquad (5.1.3)$$

where m_H is a coupling constant with the dimension of mass and $\phi^T = (\phi^0, \phi^-)$. However, as discussed by Schechter and Valle,[22] and Wolfenstein,[38] this process is suppressed by the following reasons: Since the doublet Higgs boson is mainly responsible to generate the masses of gauge bosons, quarks and charged leptons, $m_W \sim g v_\phi$ with $\langle \phi^0 \rangle = v_\phi/\sqrt{2}$, it is expected that $v_H/v_\phi \sim (m_\mu/h_{ee})/(m_W/g) \sim (m_\mu/m_W) \sim 10^{-10}$. Next, we consider the couplings of H_p^- to quarks. The Goldston boson is written as $G^- = (v_\phi \phi^- + \sqrt{2} v_H H^-)/\sqrt{v_\phi^2 + 2v_H^2}$ and becomes the longitudinal part of W^- and thus the physical Higgs boson is expressed as $H_p^- = (-\sqrt{2} v_H \phi^- + v_\phi H^-)/\sqrt{v_\phi^2 + 2v_H^2}$. Therefore, the couplings of H_p^- to quarks are suppressed by the factor $-\sqrt{2}\, v_H/v_\phi$. Also the triplet coupling in Eq. (5.1.3) is suppressed by $(v_H/v_\phi)^2$. Thus, the contribution from the diagram in Fig. 1.6 is proportional to $(v_H/v_\phi)^4 \sim 10^{-40}$. Furthermore, Haxton, Rosen and Stephenson[38] argued that the nuclear matrix element in this case is suppressed. From these reasons, this contribution seems to be unimportant, although the above suppression may be avoided by considering the complicated Higgs sector with fine tuning of parameters.[22),71]

§5.2 The process with a Majoron emission: $(A,Z-2)\to(A,Z)+2e^-+M^0$

The Majoron is the Goldstone boson arising from the spontaneous symmetry breaking of global B-L (baryon number - lepton number) symmetry. The Majoron (Higgs singlet) was first considered by Chikashige, Mohapatra and Peccei[40], but its coupling to neutrino was very small. Later Gelmini and Roncadelli[40] proposed a model with a Majoron arising from H^0 of triplet Higgs boson in Eq.(5.1.2). They showed that the coupling to neutrinos $h_{ee}\sim m_\nu/v_H$ may not be very small because the vacuum expectation value of triplet Higgs v_H can be taken to be small.

Then the evaluation of the Majoron emitting process in Fig. 5.2 becomes important because it mimics the $(\beta\beta)_{2\nu}$ mode and thus may become its important beckground.

Let us assume the effective interaction Hamiltonian as

$$H_{int}=(G/\sqrt{2})\,j_{L\rho}\,J_L^{\rho\dagger}+(i/2)\sum g_{jk}\,\overline{N_j}\,\gamma_5\,N_k\,\varphi_M\,, \qquad (5.2.1)$$

where φ_M is a Majoron field. In a single triplet model by Gelmini and Roncadelli,[40] $g_{ij}=\delta_{ij}\,m_j\,v_\phi/(v_\phi\sqrt{v_\phi^2+2v_\Delta^2})\sim\delta_{ij}\,m_j/v_\Delta$.

Here we shall present only the half-life formula obtained from Eq.(F.1.5) in Appendix F and the detailed derivation will be given there:[39),44),72]

$$[T_{0\nu\beta}(0^+\to 0^+)]^{-1}=|\langle g_\beta\rangle|^2\,|M_{GT}^{(0\nu)}|^2\,|1-\chi_F|^2\,G_\beta\,, \qquad (5.2.2)$$

where

$$\langle g_\beta\rangle=\Sigma_{j,k}\,g_{jk}\,U_{ej}\,U_{ek}\,, \qquad (5.2.3)$$

$$G_\beta=\frac{a_{0\nu}\,m_e^{-7}}{4\pi^2\ell n2\,(m_eR)^2}\int b_{01}\,\delta(\varepsilon_1+\varepsilon_2+k+E_f-M_i)\,\varepsilon_1\varepsilon_2 p_1p_2\,k\,d\varepsilon_1\,d\varepsilon_2\,dk \qquad (5.2.4)$$

Here k is the momentum of the emitted Majoron and $M_{GT}^{(0\nu)}$, χ_F, b_{01}, and $a_{0\nu}$ are defined in Eqs.(3.5.1), (3.5.2), (3.5.18) and (C.3.2), respectively. The numerical values of G_β for various nuclei are given in Table 3.1. The magnitude of $\langle g_\beta\rangle$ and thus the expected half-life will be discussed in §7. The similar results are also obtained for familons, the Nambu-Goldstone boson associated with the spontaneous breaking of the horizontal (family) symmetry.[73]

§5.3 Superweak interaction

Pontecorvo[14] proposed the $\Delta L=2$ superweak interaction analogous to the $\Delta S=2$ superweak interaction postulated by Wolfenstein.[74] He considered both $\Delta^0\leftrightarrow\Delta^{++}$ and $\pi^+\leftrightarrow\pi^-$ transitions inside nucleus and estimated that a superweak coupling $\sim 10^{-9}$ G could give the $(\beta\beta)_{0\nu}$ decay rate comparable to the $(\beta\beta)_{2\nu}$ decay.

§6. Electron kinetic energy spectra and angular correlations

In this section, all nuclear matrix elements are assumed to be real. The detailed discussions were given in Refs.31 and 28.

§6.1 The $(\beta\beta)_{2\nu}$ mode

Let us discuss the $0^+ \to 0^+$ transition first. The single electron kinetic energy spectrum and the sum energy spectrum of two electrons are obtained from Eqs.(B.3.1), (B.3.5) and (B.3.8). Since $A_{GT}^{(+)}$ is almost constant with respect to electron energies, and $a(\varepsilon_1, \varepsilon_2)$ behaves like $(\varepsilon_1\varepsilon_2/p_1p_2)$ in the smaller region of p_k from Eqs.(B.3.13) and (D.32), the spectra are determined essentially from the phase space factor, except the finite value at the small p region. They are shown in Figs. 6.1 and 6.2 for typical nucleus, ^{76}Ge.

The angular correlation is obtained by comparing the spectrum part $A_0^{(2\nu)}$ in Eq.(B.3.9) and the angular correlation part $B_0^{(2\nu)}$ in Eq.(B.3.11). The angular dependence is expressed as

$$\frac{d\Gamma}{d\varepsilon_1\, d\varepsilon_2\, d\cos\theta} \propto \left(1 + \alpha(\varepsilon_1, \varepsilon_2)\cos\theta\right), \qquad (6.1.1)$$

with $\cos\theta = \hat{p}_1 \cdot \hat{p}_2$. Within the approximation that $\left|A_{GT}^{(+)}\right| \gg \left|A_{GT}^{(-)}\right|$ in Eq.(B.3.9), we find

$$\alpha(\varepsilon_1, \varepsilon_2) = -2\, b(\varepsilon_1, \varepsilon_2)/a(\varepsilon_1, \varepsilon_2) \cong -p_1p_2/\varepsilon_1\varepsilon_2, \qquad (6.1.2)$$

where the final approximate equality is derived by using Eqs.(B.3.13) and (B.3.14).

The kinetic energy spectra of the $0^+ \to 2^+$ transition in the 2n-mechanism are quite different from the $0^+ \to 0^+$ transition due to the factor $(K-L)^2$ in Eq.(3.2.18) and are shown in Figs. 6.3 and 6.4. The angular correlation is expressed as

$$\alpha(\varepsilon_1, \varepsilon_2) = +(1/3)\; b(\varepsilon_1, \varepsilon_2)/a(\varepsilon_1, \varepsilon_2) \cong +(1/3)\, p_1p_2/\varepsilon_1\varepsilon_2, \qquad (6.1.3)$$

from Eqs.(B.3.16) and (B.3.17).

The above features are valid also for the $0^+ \to 2^+$ transition in the N^* mechanism, because the decay formula has the same structure as that in the 2n-mechanism, as seen from Eq.(4.5).

§ 6.2 The $(\beta\beta)_{0\nu}$ mode

This mode contains various contributions from the m_ν and V+A parts, and thus the single electron kinetic energy spectrum and the angular correlation are rather complicated. The sum energy spectrum of two electrons peaks at the maximum kinetic energy release due to the energy conservation as shown in Fig.6.2.[24]

Let us first concentrate on the $0^+ \to 0^+$ transition. As explained in § 3.3, the energy denominators appear as the sum for the m_ν part and the $\vec{q}$-term in the V+A part, as seen from Eqs.(3.3.12) and (3.3.22), while they appear as the difference for the ω-term in the V+A part, as seen from Eq.(3.3.21). Due to this kinematical reason, the spectrum is divided into two types; the mountain type for the m_ν part and the $\vec{q}$-term due to the phase space factor as shown in Fig.6.5a, and the valley type for the ω-term due to the factor $(\varepsilon_1 - \varepsilon_2)^2$ in Eq.(3.3.21), as shown in Fig.6.6a. In terms of the kinematical factors (Eqs.(3.5.18) and (3.5.20)), b_{01}, b_{04} and $b_{05} - b_{09}$ give the mountain type spectrum, while the others b_{02} and b_{03} belong to the valley type.

The fact that the single electron kinetic energy spectrum of the $\langle m_\nu \rangle^2$ term is mountain type is also seen from its coefficient C_1 in Eq.(3.5.15a). The spectra of $\langle \eta \rangle^2$ and $\langle \lambda \rangle^2$ terms are in general the mixture of both mountain and valley types because they contains both the ω- and $\vec{q}$-terms. However, the coefficient C_4 of the $\langle \lambda \rangle^2$ term in Eq.(3.5.15d) is essentially determined (by) b_{02}, so that the spectrum of the $\langle \lambda \rangle^2$ term is valley type. On the other hand, the coefficient C_5 of $\langle \eta \rangle^2$ term in Eq.(3.5.15e) includes b_{07}, b_{08} and b_{09} which come from the P-wave and recoil effects for the $\vec{q}$-term. According to the recent theoretical estimates by Haxton et al.[17] for χ'_P and by Doi, Kotani and Takasugi[33] for χ'_R, these terms give the dominant contribution to C_5. Thus the spectrum of the $\langle \eta \rangle^2$ term is mountain type. If there were complete cancellation between χ'_P and χ'_R as Tomoda et al. reported,[32] then the spectra would give the similar behavior to the $\langle \lambda \rangle^2$ term.

The angular correlation of the m_ν part is expected to be 1-cosθ type in the following reason: Both electrons are emitted from the V-A vertex, so that their main helicities are the same. Due to the angular momentum conservation in the plane made of two electrons, two S-wave electrons should be emitted predominantly in the back to back configuration for the $0^+ \to 0^+$ transition. For the V+A part (η and λ terms), one electron is emitted from the V-A vertex and the other is from V+A, and thus their main helicities are opposite. Therefore, two electrons with $j = 1/2$ (S-and/or $P_{1/2}$-waves) are emitted mostly in the same direction, i.e., the 1+cosθ type.

These features can be seen explicitly by examining the spectrum part $A_0^{(0\nu)}$ in Eq.(C.3.4) and the angular correlation part $B_0^{(0\nu)}$ in Eq.(C.3.14) in Appendix C. We consider only the CP conserving case, i.e., $\psi_i = 0$ or π in Eq.(3.5.14). The kinematical factor $b_{0k}^{(B)}$ in Eq.(C.3.17) for the angular correlation part corresponding to b_{0i} for the spectrum part in Eq.(3.5.18) have the following properties: There are no terms in the angular correlation part corresponding to b_{03} and b_{06} so that the terms involving them are independent of θ. The terms involving b_{01} and b_{04} behave as the $1 - \cos\theta$ type because $b_{01}^{(B)}$ and $b_{04}^{(B)}$ have negative sign factor in their coefficients as seen from Eqs. (C.3.15a) and (C.3.15b), while the terms involving b_{02}, b_{05}, b_{07}, b_{08} and b_{09} behave as the $1 + \cos\theta$ type because the corresponding terms in the angular correlation part are positive.

In Fig. 6.5, 6.6 and 6.7 we plotted the single electron kinetic energy spectrum and the angular correlation factor which is defined by

$$\frac{d\Gamma}{d\varepsilon_1 \, d\cos\theta} \propto \left(1 + \alpha(\varepsilon_1, \varepsilon_2) \cos\theta \right) , \qquad (6.2.1)$$

with $\varepsilon_2 = (T+2)m_e - \varepsilon_1$. The calculated shapes of them are those expected from the above arguments. The sharp dumping of $\alpha(\varepsilon_1, \varepsilon_2)$ at $(\varepsilon_1 - m_e)/m_e = T/2$ is due to the fact that the main terms b_{02} and b_{03} vanish at that point and the minor term b_{04} plays a role instead. The degree of this dumping depends on the nuclear matrix elements. The spectrum and the angular correlation for the $\langle \eta \rangle^2$ term are valid as far as the terms involving χ'_P and χ'_R do not cancell each other completely. For calculating the above figures, we use the values of nuclear matrix elements in Table 7.5, i.e., Haxton's plus "pot" values.

For the $0^+ \to 2^+$ transition in the 2n-mechanism, the electron spectrum is essentially the mountain type as seen from Eq.(3.5.25). The angular correlation is rather complicated and its form is expressed as

$$\frac{d\Gamma}{d\varepsilon_1 \, d\cos\theta} \propto \left[1 + \alpha \cos\theta + \beta \left(\cos^2\theta - \tfrac{1}{3} \right) \right] . \qquad (6.2.2)$$

As seen from Eqs.(C.4.9), (C.4.10) and (C.4.11), the spectrum and the angular correlation for the $\langle\lambda\rangle^2$ term are independent of the nuclear matrix elements, because Z_{22} is independent of $\langle\lambda\rangle$, c.f. Eq.(3.5.23). On the other hand, the angular correlation for the $\langle\eta\rangle^2$ term is different from the $\langle\lambda\rangle^2$ term, because the nuclear parameter $\Sigma_{22}=2\langle\eta\rangle M_{2e}$ enters in $B_2^{(0\nu)}$ and $C_2^{(0\nu)}$ differently from $A_2^{(0\nu)}$ as seen in Eqs.(C.4.9~11) and thus depend explicitly on the values of nuclear matrix elements for which we use the estimates by Haxton et al.[17] in Table 7.6 . In Figs. 6.8 and 6.9 , the spectrum and the angular correlations are shown for $\langle\eta\rangle^2$ and $\langle\lambda\rangle^2$ terms. The case of the N^* mechanism gives the same result as the $\langle\lambda\rangle^2$ term because $M_{2e}=0$.

§6.3 The Majoron emitting process

The spectrum part of this process has a simple form, $b_{01}\cong\varepsilon_1\varepsilon_2 C_{00}$ as seen from Eqs.(5.2.4),(3.5.18) and (3.5.20a). Therefore, the electron kinetic energy spectra are essentially determined by the phase space factor. In contrast to the $(\beta\beta)_{2\nu}$ mode, this process is the four body decay so that the peaks of both the single elctron kinetic energy spectrum and the sum energy spectrum of two electrons are shifted to the higher energy domain than the $(\beta\beta)_{2\nu}$ case, as seen from Fig. 6.10 and 6.11. The spectra are compared with those for the $(\beta\beta)_{2\nu}$ decay. As for the relative magnitude of them, we have used the limit, $|g_B|<2.2\cdot10^{-4}$, which will be derived in Eq.(8.2.11).

§7 Theoretical estimation of nuclear matrix elements

The nuclear matrix elements appeared in the $(\beta\beta)_{2\nu}$ mode and the $(\beta\beta)_{0\nu}$ mode are quite different because the energies of the intermediate nuclei E_a play the different roles. Therefore, we shall treat them separately.

§7.1 Nuclear matrix elements for the $(\beta\beta)_{2\nu}$ mode

The nuclear matrix elements for the $0^+\to0^+$ transition in Eqs.(3.2.9) and (3.2.10) are

$$\left(M_{GT}^{(2\nu)}/\mu_0\right)\equiv-\sum_a\mu_a^{-1}\langle0_f^+\|\textstyle\sum_n\tau_n^+\sigma_n\|N_a(1^+)\rangle\langle N_a(1^+)\|\sum_m\tau_m^+\sigma_m\|0_i^+\rangle, \quad (7.1.1a)$$

$$\left(M_F^{(2\nu)}/\mu_0\right)\equiv\sum_a\mu_a^{-1}\langle0_f^+\|\textstyle\sum_n\tau_n^+\|N_a(0^+)\rangle\langle N_a(0^+)\|\sum_m\tau_m^+\|0_i^+\rangle. \quad (7.1.1b)$$

Here $T_+=\sum_n\tau_n^+$ is the total isospin raising operator so that it connects states in the same isospin multiplets. The double Fermi term $(M_F^{(2\nu)}/\mu_0)$ is suppressed because of the isospin missmatching between either the intermediate isobaric states and the initial or the final nuclei. This qualitative feature is confirmed numerically by Haxton et al.[34),17] Hereafter only the double Gamow-Teller term $\left(M_{GT}^{(2\nu)}/\mu_0\right)$ will be discussed.

As we have emphasized below Eq.(3.2.13), the experimentally observed quantity is $\left(M_{GT}^{(2\nu)}/\mu_0\right)$. However, theoretically the nuclear matrix element $[M_{GT}^{(2\nu)}]_C$ in Eq.(3.2.5) and the average excitation energy $\langle\mu_a\rangle_{av}\equiv(\langle E_a\rangle_{av}-(M_i+M_f)/2)/m_e$ were estimated by many authors, because they used the closure approximation. (See Eq.(3.2.14).) The most elaborate shell model calculation in this approximation was performed by Haxton, Stephenson and Strottman for various nuclei.[17] They used (i) the modified Kuo interaction with the full f_p-shell

for ^{48}Ca decay, (ii) the modified Kuo interaction in the weak coupling approximation with the canonical shell model space $2p_{1/2} - 2p_{3/2} - 1f_{5/2} - 1g_{9/2}$ omitting the spin-orbit pairing states (partners) $1f_{7/2}$ and $1g_{f/2}$ for ^{76}Ge and ^{82}Se decays, (iii) the Baldridge-Vary interaction with the model space $2d_{5/2} - 1g_{7/2} - 3s_{1/2} - 2d_{3/2} - 1h_{11/2}$ omitting the spin-orbit pairing states $1g_{9/2}$ and $1h_{9/2}$ for ^{128}Te and ^{130}Te. The average excitation energy $\langle E_a \rangle_{av}$ was determined by using Eq.(3.2.15). Their theoretical values are given in Table 7.1, where the estimates by other authors are included also. Vergados[75] used the Kuo-Brown interaction with the $(f_{7/2})^8$ shell model space for ^{48}Ca decay and with the $h_{11/2}$ shell model space for ^{128}Te and ^{130}Te, and Skouras and Vergados made the similar calculation for ^{48}Ca with f-shell neutrons and f_p-shell protons.[76] The nuclear matrix elements $[M_{GT}^{(2\nu)}]_C$ were also estimated by Zamic and Auerback[77] by using the Nilsson-pairing model for ^{48}Ca and ^{76}Ge, and later by Haxton and Stephenson[17),78] for ^{76}Ge and ^{238}U. Bogdan, Faessler and Petrovici[79] evaluated it by using the extended decoupling model with Davydov-Filippov wave functions for ^{76}Ge, Scholten and Yu[80] took into account the nuclear deformation by using the interacting boson approximation for ^{128}Te and ^{130}Te, and Wu, Song, Kuo, Cheng and Strottman[81] adopted the effective operator approach with the ground state closure neutron $f_{7/2}$ shell.

The above estimates depend on the closure approximation. The validity of it lies in the accurate determination of $\langle E_a \rangle_{av}$, because Eq.(3.2.14) can be viewed as a definition of $\langle E_a \rangle_{av}$ also. As Haxton and Stephenson stated,[17] the approximation could fail badly if the sign of $M_{GTa}^{(2\nu)}$ were predominantly one value for small E_a and the opposite value for large E_a. In order to test this sign change,

they completed a sum over approximately 500 1^+ states lying below 5 MeV in ^{82}Br, the intermediate nucleus for ^{82}Se$\rightarrow^{82}$Kr and discussed the validity of the closure approximation.

Let us see the theoretical situation of the evaluation of $(M_{GT}^{(2\nu)}/\mu_0)$ by summing the intermediate 1^+ state without recourse to the closure approximation. Huffman[82] was the first to evaluate it for ^{130}Te in RPA (random-phase-approximation) with pairing and Gamow-Teller interactions. Recently, Grotz, Klapdor and Metzinger[83),36] performed similar calculation with somewhat modified treatment by including the four quasiparticle admixture and the mixing of intermediate states for ^{76}Ge, ^{82}Se, ^{128}Te, ^{130}Te, ^{134}Xe, ^{136}Xe and ^{142}Ce. They also included the effect from the admixture of the Δ-h excitation and found about 30% reduction of the nuclear matrix element. Very recently, Vogel and Fisher[84] made the estimates for ^{76}Ge, ^{82}Se, ^{100}Mo, ^{128}Te, ^{130}Te, ^{136}Xe, ^{150}Nd by including the effects of pairing, static quadrupole deformation, spin-isospin polarization, and the Δ isobar admixture. Their results are given in Table 7.2, where we list the experimental half-lives or upper limits of $T_{2\nu}$ and also the values of $|M_{GT}^{(2\nu)}/\mu_0|$ evaluated by using Eq.(3.2.13) and Table 3.1. They will be explained in the next section.

The important observation was made recently by Tsuboi, Muto and Horie[85] who performed the similar shell model calculation for ^{48}Ca to by Haxton et al.[17] Tsuboi et al. found that signs of $M_{GTa}^{(2\nu)}$ are one value for the lowlying intermediate 1^+ states and the opposite value for the highlying states, and there is a large cancellation between these two groups of states. Their value for $(M_{GT}^{(2\nu)}/\mu_0)$ is twice larger than experimental limit, as seen from Table 7.2. Also they evaluated $[M_{GT}^{(2\nu)}]_C$ in Eq.(3.2.5), and

obtained the value of $\langle \mu_a \rangle_{av}$ by requiring the equality in Eq.(3.2.14). This value is given in Table 7.1 with the asterisk. Their value $\langle \mu_a \rangle_{av} = 7.66$ is much smaller than that of Haxton et al. $\langle \mu_a \rangle_{av} = 15.10$. Klapdor et al.[36] derived the values of $\langle \mu_a \rangle_{av}$ by using the same procedure and found that their values are about half of those by Haxton et al., as seen in Table 7.1. As for the cancellation between the lowlying and highlying states for ^{48}Ca, Tsuboi et al. showed that the spin orbit pairing states play the important role. It is suggested that the inclusion of them could produce the similar cancellation. If this situation did happen, the closure approximation would be no more a good approximation for evaluating $(M_{GT}^{(2\nu)}/\mu_0)$.

For the $0^+ \to 2^+$ transition, the nuclear matrix element $[M_2^{(2\nu)}]_C$ in Eq.(3.2.21) was evaluated by Haxton et al.[17] for ^{48}Ca and ^{76}Ge and they are listed in Table 7.3. Muto and Horie[85] made the direct evaluation of $(M_2^{(2\nu)}/\mu_2^3)$ for ^{48}Ca by summing the intermediate 1^+ states. They evaluated $[M_2^{(2\nu)}]_C$ also and derived $\langle \mu_a \rangle_{av}$ by requiring the equality in Eq.(3.2.20). Their value $\langle \mu_a \rangle_{av} = \left\{ [M_2^{(2\nu)}]_C / (M_2^{(2\nu)}/\mu_2^3) \right\}^{1/3} = 6.48$ is much smaller than the one found by Haxton et al. for the $0^+ \to 0^+$ transition, $\langle \mu_a \rangle_{av} = 15.10$.[17] This is expected that the contributions from the lowlying states are enhanced due to the factor μ_a^{-3}.

At present, there seems to be some discrepancies between the theoretical estimates and experimental results on $\left| M_{GT}^{(2\nu)}/\mu_0 \right|$, as shown in Table 7.2. The complementary information on nuclear matrix elements may be obtained from the double charge exchange reaction of pions by nucleus,

$$\pi^{\pm} + N_i(Z) \longrightarrow N_f(Z \pm 2) + \pi^{\mp}. \qquad (7.1.2)$$

Since the $\beta\beta$ decay is the low momentum transfer phenomena, the data on the above reaction should be extrapolated to obtain the necessary values for the nuclear matrix elements. Ching and Ho have analyzed the data on ^{40}Ca on this direction.[68] Another interesting phenomenon is a double γ ray emission in the $0^+ \to 0^+$ transition which occurs through the virtual 1^+ nuclear states, although the initial and final states are the same nuclei in contrast to the different nuclei for the $\beta\beta$ decay.[87] The (n,p) and (p,n) reactions are also interesting, because they offer the information on the Gamow-Teller states of the intermediate nucleus.[155]

§7.2 Nuclear matrix elements for the $(\beta\beta)_{0\nu}$ mode

In the evaluation of nuclear matrix elements of the $(\beta\beta)_{0\nu}$ mode, the closure approximation is commonly used. The merit of this approximation is as follows: The neutrino potentials depend on $r_{nm} = |\vec{r}_n - \vec{r}_m|$ and thus the expansion of them in terms of $\vec{r}_n$ and $\vec{r}_m$ consists of all partial waves.*) Therefore, the sum of the intermediate states extends over all angular momentum states, if the nuclear matrix elements are evaluated faithfully. If the closure approximation is assumed, this complicated situation can be avoided.

Now, let us discuss the validity of the closure approximation. In contrast to the $(\beta\beta)_{2\nu}$ mode, the dependence on the energy of intermediate nuclear state E_a enters through $\mu_a m_e = E_a - (M_i + M_f)/2$ in A_k of the neutrino potentials, h_+, $h_{0\omega}$, h_+' and h_R in Eqs.(3.4.1), (3.4.4),

*) $$\frac{1}{|\vec{r}_n - \vec{r}_m|} = \sum_{l=0}^{\infty} \sum_{m} \frac{4\pi}{(2l+1)} \frac{r_<^l}{r_>^{l+1}} Y_l^{m*}(\hat{r}_n) Y_l^m(\hat{r}_m). \qquad (7.2.1)$$

(3.4.11) and (3.4.15). If these potentials are slowly varying functions of μ_a, the closure approximation is well founded. The μ_a dependences of potentials for light neutrinos are given in Fig. 3.5. We see that h_+, $h_{0\omega}$ and h'_+ are slowly decreasing functions of μ_a, but h_R shows the different behavior. The origins of these behaviors were discussed in §3.4. From these dependences, we conclude that the closure approximation may be used for all potentials if $\langle \mu_a \rangle_{av} \sim 20$ is taken, but there needs some caution. For nuclear matrix elements with h_+, $h_{0\omega}$ and h'_+, the use of the closure approximation with $\langle \mu_a \rangle \sim 20$ gives some overestimation of high lying states ($\mu_a \gg 20$). In contrast, for nuclear matrix elements with $\mu_a m_e R h_0$ and h_R, the highlying states are underestimated. Therefore, the degree of accuracy of the closure approximation may be different for nuclear matrix elements with h_+, $h_{0\omega}$ and h'_+ and for those with $\mu_a m_e R h_0$ and h_R.

For heavy neutrinos, the closure approximation is valid because $\omega + \mu_a m_e = \sqrt{q^2 + m_\nu^2} + \mu_a m_e \sim \sqrt{q^2 + m_\nu^2}$ due to $m_\nu \gg \mu_a m_e$.

By using the similar methods explained for the $(\beta\beta)_{2\nu}$ mode, the estimations of $M_{GT}^{(0\nu)}$ in Eq. (3.5.1) and χ_F in Eq. (3.5.2) were made by Haxton et al.[17] and by Klapdor et al[36] in the closure approximation. Their results are given in Table 7.4, where the values of $[[M_{GT}^{(2\nu)}]_C]$ for the $(\beta\beta)_{2\nu}$ mode within the closure approximation are listed for comparion. In addition, Haxton et al. estimated the other four nuclear parameters χ'_{GT}, χ'_F, χ'_T and χ'_P which are given in Table 7.5. Very recently, Faessler[32] gave us the values of $\chi_{GT}^{(0)}$ and $\chi_F^{(0)}$ for ^{76}Ge. Bogdan et al.[79] made the estimate of $M_{GT}^{(0\nu)}$ without using the closure approximation, but restricting the orbital angular momentum of the intermediate states to be less than one. Tomoda et al.[32] evaluated χ'_R.

These values are not listed in Table 7.4, because it is hard to find their values from their papers.

Since there is no systematic research on $\mu'_0 m_e R \chi_{GT}^{(0)}$, $\mu'_0 m_e R \chi_F^{(0)}$ and the nucleon recoil term χ'_R, we shall give a semiquantative method to evaluate them. Before going into detail, we shall first consider the structure of the recoil term in Eq. (3.5.9), which is written by using the explicit form of $\vec{D}_n$ in Eq. (3.1.17b) given first by Tomoda et al.[32]

$$\begin{aligned}
&\frac{1}{2}\hat{r}_{nm}\cdot\left(\vec{\sigma}_n\times\vec{D}_m+\vec{D}_n\times\vec{\sigma}_m\right)\\
&=\frac{1}{M}\Big\{-\frac{1}{4}\vec{\sigma}_n\cdot\left(\hat{r}_{nm}\times(\vec{p}_m+\vec{p}'_m)\right)+\frac{1}{4}\vec{\sigma}_m\cdot\left(\hat{r}_{nm}\times(\vec{p}_n+\vec{p}'_n)\right)\\
&\quad+f_W(\sqrt{15}/2)\,i\left[\left[\vec{\sigma}_n\otimes\vec{\sigma}_m\right]^{(2)}\otimes\left[\hat{r}_{nm}\otimes\vec{Q}_{nm}\right]^{(2)}\right]^{(0)}\\
&\quad+f_W(\sqrt{3}/2)\,i\left[\left[\vec{\sigma}_n\otimes\vec{\sigma}_m\right]^{(1)}\otimes\left[\hat{r}_{nm}\otimes\vec{p}_{nm}\right]^{(1)}\right]^{(0)}\\
&\quad-f_W(1/3)\,i\,(\vec{\sigma}_n\cdot\vec{\sigma}_m)(\hat{r}_{nm}\cdot\vec{p}_{nm})\Big\},
\end{aligned}\tag{7.2.1}$$

where $\vec{p}_{nm} = [(\vec{p}_n - \vec{p}'_n) + (\vec{p}_m - \vec{p}'_m)]/2$ + (electron momentum), and

$$\vec{Q}_{nm} = \left[(\vec{p}_n - \vec{p}'_n) - (\vec{p}_m - \vec{p}'_m)\right]/2. \tag{7.2.2}$$

We assume that

$$\vec{Q}_{nm} = -\vec{q}, \tag{7.2.3}$$

where $\vec{q}$ is the momentum of the virtual neutrino. This may be reasonable because each momentum of emitted electrons is a few MeV, while the momentum of virtual neutrino is about 80 m_e. Tomoda et al.[32] have argued that among five terms in Eq. (7.2.1), the last term with the operator $\vec{\sigma}_n\cdot\vec{\sigma}_m$ will be dominant because the main contribution is expected to come from a spin singlet state ($S = 0$) of two nucleons and it has a large coefficient $f_W = 4.7$. We shall follow

their argument. Then by substituting Eqs.(3.4.11), (7.2.1), (7.2.3) into Eq.(3.5.9), we obtain

$$\chi'_R \simeq (f_W/3)(g_V/g_A)\langle 0_f^+ \| h_R(r_{nm}, E_a)\,\vec{\sigma}_n\cdot\vec{\sigma}_n \| 0_i^+\rangle / M_{GT}^{(0\nu)}, \tag{7.2.4}$$

where h_R is defined in Eq.(3.4.13).

Hereafter we shall evaluate nuclear matrix elements in the closure approximation. For the $(\beta\beta)_{0\nu}$ mode, we shall omit the notation $[\ ]_C$ which indicates this approximation.

At first, let us observe the interesting similarity among $M_{GT}^{(2\nu)}$, $M_{GT}^{(0\nu)}$, χ'_{GT}, $\chi^{(0)}_{GT}$ and χ'_R: They contain the double Gamow-Teller type tensor operator $\vec{\sigma}_n\cdot\vec{\sigma}_m$ and only the differences come from the potentials which they contain. Therefore, the ratios of them may be evaluated by comparing some average of potentials which we call here the semiqualitative method. That is, we expect that

$$M_{GT}^{(0\nu)}/M_{GT}^{(2\nu)} \sim \langle h_+\rangle, \tag{7.2.5a}$$

$$\chi'_{GT} \sim \langle h'_+\rangle/\langle h_+\rangle, \tag{7.2.5b}$$

$$\chi^{(0)}_{GT} \sim \langle h_0\rangle/\langle h_+\rangle, \tag{7.2.5c}$$

$$\chi'_R \sim (f_W/3)(g_V/g_A)\langle h_R\rangle/\langle h_+\rangle. \tag{7.2.5d}$$

The similar situation occurs for χ_F, χ'_F and $\chi^{(0)}_F$, i.e., $\chi'_F/\chi_F \sim \langle h'_+\rangle_F/\langle h_+\rangle_F$ etc..

As an approximation, the average potentials are evaluated with the weight of the uniform distribution of nucleons. The detailed calculations are given in Appendix E. The values obtained in the semiquantitative method for χ'_{GT}, $\chi^{(0)}_{GT}$, χ'_R, χ'_F and $\chi^{(0)}_F$ are

given in the column named "pot." in Table 7.5 for light neutrinos. The values in this method agree very well with the elaborate estimates by Haxton et al.[17] for χ'_{GT} and χ'_F. Also the values of $\chi^{(0)}_{GT}$ and $\chi^{(0)}_F$ for ^{76}Ge agree reasonably well with the estimates by Faessler.[87],*) These agreements show the rather unexpected reliability of this naive computation.

The nuclear matrix elements for the $0^+\to 2^+$ transition in Eq.(3.5.24) were estimated by Haxton et al.[17] for ^{48}Ca and ^{76}Ge, which are listed in Table 7.6. For ^{48}Ca, Vergados[88] evaluated the nuclear matrix elements for the $0^+\to 2^+$ transition**) and also the $0^+\to 1^+_2$ transition.

---

*) The values of $\chi^{(0)}_{GT}$ and $\chi^{(0)}_F$ may be obtained from the identities, $\chi'_{GT} = 1 + \mu'_0 m_e R\chi^{(0)}_{GT}$ and $\chi'_F = \chi_F + \mu'_0 m_e R\chi^{(0)}_F$ by assuming the appropriate values for μ'_0, cf. Eq.(3.4.16).

**) The relations between nuclear matrix elements by Vergados[88] and ours in Eq.(3.5.24) are $\langle 2^+\|\Omega_5\|0^+\rangle = 9M_{2c}$ and $\langle 2^+\|\Omega_6\|0^+\rangle = (3\sqrt{2})M_{2e}$, but his $\langle 2^+\|\Omega_4\|0^+\rangle$ is not proportional to our $(M_{2a} - 2M_{2b} - M_{2c})$. He did not calculate M_{2d}. His results are as follows:

	$\langle 2^+\|\Omega_4\|0^+\rangle$	$\langle 2^+\|\Omega_5\|0^+\rangle$	$\langle 2^+\|\Omega_6\|0^+\rangle$
$0^+\to 2^+_1$(0.98 MeV)	0.132	0.354	1.106
$0^+\to 2^+_2$(2.42 MeV)	0.507	1.18	0.738

The estimations by Vergados[88] for M_{2c} and M_{2e} are larger than those by Haxton and Stephenson,[17] e.g. $(M_{2e})_{\text{Vergados}} \sim (-2)(M_{2e})_{\text{Haxton}}$ for the $0^+\to 2^+_1$ transition.

§8. The data analysis

In this section, the experimental data on the $(\beta\beta)_{2\nu}$ and $(\beta\beta)_{0\nu}$ modes are analyzed. The experimental values of $\left|M_{GT}^{(2\nu)}/\mu_0\right|$ for the $0^+ \to 0^+$ transition of the $(\beta\beta)_{2\nu}$ mode are obtained and are compared with the theoretical predictions discussed in the previous section. The bounds on the neutrino mass and the right-handed parameters η and λ are derived from the experimental data on the $0^+ \to 0^+$ transition of the $(\beta\beta)_{0\nu}$ mode.

§8.1 The data analysis of the $(\beta\beta)_{2\nu}$ mode

At present, there are two types of experimental methods to measure the $(\beta\beta)_{2\nu}$ mode, and to obtain the information on the $0^+ \to 0^+$ transition. One is due to the geochemical method where the abundance of the isotopic composition in the old ore is measured and the excess from the composition essentially in the air is attributed to the $\beta\beta$ decay. The measured half-life includes all contributions to the $\beta\beta$ decay; the $0^+ \to 0^+$ and $0^+ \to 2^+$ transitions of the $(\beta\beta)_{2\nu}$ mode and other transitions such as the $(\beta\beta)_{0\nu}$ mode and the process with a Majoron emission, if they exist.

The other is the direct counting measurement. For the measurement of ^{48}Ca, ^{82}Se, ^{150}Nd, the chamber (counter) experiments were performed, where the flight trucks and energies of two electrons are observed. On the other hand, for the ^{76}Ge experiment, only the sum energy of two electrons was measured because ^{76}Ge works as a source and the energy detector itself. However, the ^{76}Ge detector has a good energy resolution and can detect the sum energy precisely. In the former visible methods, the loss of energies at the surface

of source gives the broadning of energy resolution. The energy spectra and the angular correlation of two electrons will be needed to confirm the $(\beta\beta)_{2\nu}$ mode (see Fig.6.2 and Eq.(6.1.2)). In this measurement the $(\beta\beta)_{2\nu}$ mode can be separated in principle from the $(\beta\beta)_{0\nu}$ mode by measuring the sum energy of two electrons as shown in Fig.6.2. Then the background may arise from the four body final states as the Majoron emission process. In both measurements, the estimation of these other contributions becomes important to discuss the $0^+ \to 0^+$ transition of the $(\beta\beta)_{2\nu}$ mode.

Let us examine the order of magnitudes of contributions from the three body decays such as the $(\beta\beta)_{0\nu}$ mode and from the four body decays like the Majoron emitting process. The important experimental information is that these contributions are at most comparable order to the $(\beta\beta)_{2\nu}$ mode for ^{128}Te, (will be) as discussed in §8.2. The reason why the information of ^{128}Te is interesting and important lies in the fact that the maximum kinetic energy release $T m_e$ for ^{128}Te ($T \sim 1.7$) is much smaller than ordinary $\beta\beta$ decaying nuclei ($T \sim 5$). Note that the transition probability of the $(\beta\beta)_{0\nu}$ behaves like T^5 due to the three body phase space, and that of the Majoron emission process (the four body decay) does like T^8, while the $(\beta\beta)_{2\nu}$ mode is the five body decay behaving like T^{11}. Suppose the contributions from the $(\beta\beta)_{0\nu}$ mode and the Majoron emitting process are comparable to the $(\beta\beta)_{2\nu}$ decay for ^{128}Te, then the yields from them for ordinary nuclei ($T \sim 5$) are suppressed by the factor $(1.7/5)^{11-5} \sim 1.5 \cdot 10^{-3}$ or $(1.7/5)^{11-8} \sim 4 \cdot 10^{-2}$. Therefore, their contributions to the ^{48}Ca, ^{82}Se and ^{150}Nd decays are less than a few % and can be neglected. The detailed discussions of these contributions will be given in §8.2.

Now we know that the $(\beta\beta)_{2\nu}$ mode is the dominant mode in the $\beta\beta$ decay. Furthermore, we showed in §3.2.2 that the $0^+ \to 2^+$ transition is suppressed in comparison with the $0^+ \to 0^+$ transition. Thus, the $0^+ \to 0^+$ transition is the dominant mode in the $\beta\beta$ decay and its information is obtained equally well from the half-lives by the geochemical method and the direct measurement. Since the half-life formula in Eq.(3.2.13) includes only one nuclear parameter $\left(M_{GT}^{(2\nu)}/\mu_0\right)$ because $\left|M_F^{(2\nu)}/\mu_0\right| \ll \left|M_{GT}^{(2\nu)}/\mu_0\right|$, the value of $\left|M_{GT}^{(2\nu)}/\mu_0\right|$ is determined from the experiments and can be compared with the theoretical predictions.

In Table 7.2, the experimental data on the half-lives of the decay are presented. The underlined data are due to the geochemical method. The latest Missouri data[89] for ^{130}Te is in sharp conflict with the world average by Kirsten.[16] Although the persistent effort by the Irvine group has been made to measure the ^{82}Se decay, no clear event for the $(\beta\beta)_{2\nu}$ mode has been reported.[90] Also recent results are listed for ^{48}Ca by the Columbia group,[91] for ^{76}Ge by the Santa Barbara-LBL,[92] Battelle-South Carolina,[93] Milano Groups,[94] and ^{150}Nd by the Moscow group.[95] These results from the direct counting methods are not inconsistent with the geochemical ones. Concerning the older data, we do not repeat them, because Haxton and Stephenson[17] and Kirsten[16] made a laborious review.

In Table 7.2, the predictions in the closure approximation are tabulated in the row "$[M_{GT}^{(2\nu)}]_C/\langle\mu_a\rangle_{av}$" and the direct calculations of $(M_{GT}^{(2\nu)}/\mu_0)$ by summing the intermediate 1^+ states are listed in the row "$M_{GT}^{(2\nu)}/\mu_0$" as we explained in §7.1. The theoretical values for ^{82}Se are about factor 2 larger than the experimental values. The factor 10 discrepancy between the prediction by Haxton et al.[17] for ^{130}Te and the geochemical data is serious, while the prediction

by Klapdor et al.[83] differs by factor 5. Variety of values of predictions for ^{130}Te show the difficulty of the theoretical computation. In the situation like ^{82}Se and ^{130}Te, the experimental values of $\left|M_{GT}^{(2\nu)}/\mu_0\right|$ may be used to normalize the absolute magnitudes of nuclear matrix elements for the $(\beta\beta)_{0\nu}$ mode with the hope that their ratios may be calculable with better reliability.

The experimental data of the $0^+ \to 2^+$ transition of the $(\beta\beta)_{2\nu}$ mode are not reported so far. Here we shall give the theoretical predictions in Table 8.1. For the 2n-mechanism, the nuclear matrix elements in Table 7.3. are used, together with $\langle\mu_a\rangle_{av} = 10$ for the case of Haxton et al.[17] As explained in §7, the average value of μ_a should be smaller than that in the $0^+ \to 0^+$ transition due to the μ_a^{-3} factor. For the N^* mechanism, $P(\Delta)\left|\langle\Psi_f|\Psi_i\rangle\right|^2 \sim 10^{-3}$ is assumed with $\langle\mu_a\rangle_{av} = 10$. The predicted half-lives are pretty long and it seems difficult to observe them.

§8.2 The data analysis of the $(\beta\beta)_{0\nu}$ mode

The half-life formula of the $0^+ \to 0^+$ transition of the $(\beta\beta)_{0\nu}$ mode is given in Eq.(3.5.10). Here we shall evaluate the coefficients C_i by using the values of ratios of nuclear matrix elements in Table 7.5 and the integrated kinematical factors in Table 3.4. In order to see the P-wave (χ_p') and recoil (χ_R') effects clearly, we parametrize the coefficients of $\langle m_\nu\rangle\langle\eta\rangle$ and $\langle\eta\rangle^2$ terms as follows;

$$\langle m_\nu\rangle\langle\eta\rangle \text{ term}: \quad C_3/C_1 = C_{31} + C_{32}\left(\chi_p' - C_{33}\chi_R'\right), \tag{8.2.1a}$$

$$\langle\eta\rangle^2 \text{ term}: \quad C_5/C_1 = C_{51} + C_{52}\left(\chi_p' - C_{53}\chi_R'\right)^2. \tag{8.2.1b}$$

The numerical results are given in Table 8.2. To evaluate them, the estimates by Haxton et al.[17] are used for χ_F, χ'_{GT}, χ'_F, χ'_T and χ'_P. For $\chi^{(0)}_{GT}$, $\chi^{(0)}_F$ and χ'_R, the estimates obtained in a semiquantative method (pot.) in § 7 are adopted, which are listed in Table 7.5.

Here the following comments are in order: (i) The large values of coefficients of χ'_P and χ'^2_P, i.e., C_{32} and C_{52} are due to the P-wave (αZ) effect, and the much larger values of coefficients of recoil terms χ'_R and χ'^2_R, i.e., $C_{32}C_{33}$ and $C_{52}C^2_{53}$ are due to the fact that both electrons are emitted in the S-wave. (ii) By observing the values of χ'_P and χ'_R in Table 7.5 and the values of C_{32}, C_{33}, C_{52} and C_{53}, we find that the P-wave (χ'_P) and recoil (χ'_R) effects have the same order of magnitudes and give the main contributions to the coefficients of $\langle m_\nu\rangle\langle\eta\rangle$ and $\langle\eta\rangle^2$ terms, i.e., C_3 and C_5. From the relative signs of χ'_P and χ'_R in Table 7.5, we observe that both effects appear destructively for ^{48}Ca and constructively for ^{76}Ge, ^{82}Se, ^{128}Te and ^{130}Te. Very recently, Tomoda et al.[32] *) stated that they found the opposite sign of χ'_P to the one by Haxton et al.[17] for ^{76}Ge. If this were true, both effects would appear destructively for ^{76}Ge. The further investigation are necessary for χ'_P and χ'_R. (iii) Even though the terms $\mu'_0 m_e R\chi^{(0)}_{GT}$ and $\mu'_0 m_e R\chi^{(0)}_F$ in $\chi_{GT\omega}$ and $\chi_{F\omega}$ are small due to $\mu'_0 m_e R \sim 1/4$ (see Eq.(3.5.3)), they give the sizable contributions to the coefficients of $\langle m_\nu\rangle\langle\lambda\rangle$, $\langle\lambda\rangle^2$ and $\langle\lambda\rangle\langle\eta\rangle$ terms, i.e., C_2/C_1, C_4/C_1 and C_6/C_1. *) Thus, their effects are important for obtaining the information on $\langle\lambda\rangle$ and the further investigation of $\chi^{(0)}_{GT}$ and $\chi^{(0)}_F$ is necessary. We shall adopt the coefficients including $\chi^{(0)}_{GT}$ and $\chi^{(0)}_F$ for the analysis of the $(\beta\beta)_{0\nu}$ mode. Note that for light neutrinos, χ'_{GT} and χ'_F in Eqs.(3.5.5) and (3.5.6) are rewritten by using Eq.(3.4.16c) as $\chi'_{GT} = 1 + \mu'_0 m_e R\chi^{(0)}_{GT}$ and $\chi'_F = \chi_F + \mu'_0 m_e R\chi^{(0)}_F$. Therefore, the terms $\mu'_0 m_e R\chi^{(0)}_{GT}$ and $\mu'_0 m_e R\chi^{(0)}_F$ should be included in $\chi_{GT\omega}$ and $\chi_{F\omega}$ for consistency. The values of $\chi^{(0)}_{GT}$ and $\chi^{(0)}_F$ are obtained by using the estimates by Haxton et al. for χ'_{GT}, χ'_F and assuming $\mu'_0 = \langle\mu_a\rangle_{av}$ (the values by Haxton et al.[17]). Thus obtained values are in good agreement with the semiquantative estimates (pot.) in Table 7.5.

Now we are in a position to analyze experimental data. There are two different sources: One is the ratio of half-lives of ^{128}Te to ^{130}Te measured in geochemical method. The other is the lower bounds on half-lives of the $0^+ \to 0^+$ transition of the $(\beta\beta)_{0\nu}$ mode for ^{48}Ca, ^{76}Ge, ^{82}Se, ^{130}Te and ^{150}Nd measured by the direct observation of two electron energies. Let us discuss them separately in below.

---

*) The theoretical formula given by Tomoda et al.[32] for ^{76}Ge can be expressed in our notation of Eq.(3.5.10) as

$\lvert M^{(0\nu)}_{GT}\rvert^2 C_1$	C_2/C_1	C_3/C_1	C_4/C_1	C_5/C_1	C_6/C_1
$3.2\cdot10^{-13}$(1/y)	-0.44	-0.36	1.46	0.34	-1.25

*) In the approximation $\chi_{GT\omega} = 1$ and $\chi_{F\omega} = \chi_F$, i.e., $\chi^{(0)}_{GT} = \chi^{(0)}_F = 0$ which was used by Haxton et al.[17] and Tomoda et al.,[32] we find

	C_2/C_1	C_3/C_1	C_{31}	C_4/C_1	C_5/C_1	C_{51}	C_6/C_1
^{76}Ge	-0.4371	-10.50	-0.0445	1.456	117.8	0.3556	-1.360
^{130}Te	-0.5109	-10.31	-0.0856	2.372	157.1	0.4713	-1.994

§8.2.1 The analysis of $R_T = T_{1/2}(^{128}\mathrm{Te})/T_{1/2}(^{130}\mathrm{Te})$

The interest in the ratio (R_T) of half-lives of ^{128}Te to ^{130}Te lies in the following facts: (i) The maximum kinetic energy release of ^{128}Te (T = 1.700) is much smaller than that of ^{130}Te (T = 4.957). Thus, the yield from the $(\beta\beta)_{0\nu}$ mode to the ^{128}Te decay must be much larger than that to the ^{130}Te decay if the $(\beta\beta)_{0\nu}$ mode exists, as it will be discussed later. (ii) Since ^{128}Te and ^{130}Te are nearby isotopes, the nuclear matrix elements for them are expected to be similar as pointed out by Pontecorvo.[14] Moreover, the analysis on R_T depends on the ratios of nuclear matrix elements and thus is free from the ambiguity of the absolute magnitude of nuclear matrix elements.

Pontecorvo[14] was the first to recognize the importance of this ratio and analyzed the data by Takaoka and Ogata[15] by using the $\Delta L = 2$ superweak interaction. In 1975, the Missouri group[96] reported the data

$$R_T = (1.59 \pm 0.05) \cdot 10^3 , \qquad (8.2.2a)$$

and obtained the bound $|\eta| \lesssim 0.8 \cdot 10^{-4}$ by using the half-life formulae by Primakoff and Rosen[24] based on the interaction in Eq.(3.1.1). In 1980, Doi, Nishiura, Okuda, Kotani and Takasugi[26] interpreted this Missouri data in terms of neutrino mass and found that the electron neutrino has the mass around 34 eV, by using the estimates of $M_{GT}^{(2\nu)}$ by Vergados[75] and by taking $\xi = 0.55$, where

$$\xi = M_{GT}^{(0\nu)} / M_{GT}^{(2\nu)} . \qquad (8.2.3)$$

Minkowski[97] pointed out that ξ should be much larger than the above value due to the short range spin-spin correlation and he chose $\xi = (4.8 \sim 7.3) \cdot 10^2$. Later Haxton, Stephenson and Strottman[34] obtained the mass around 10·2 eV by using their new values of nuclear matrix elements.[21]

In 1983, the new data were reported by the Heidelberg (Max-Planck) group,[98]

$$(R_T)^{-1} = (1.03 \pm 1.13) \cdot 10^{-4} . \qquad (8.2.2b)$$

We will take this data seriously and try to draw the information of the neutrino mass and the right-handed parameters.

At first, we shall derive an interesting relation by assuming that the contributions to the $\beta\beta$ decay aside from the $(\beta\beta)_{2\nu}$ mode are the three body decays such as the $(\beta\beta)_{0\nu}$ mode and the four body decays as the Majoron emitting process,

$$(R_T)^{-1} \equiv \frac{T_{1/2}(^{130}\mathrm{Te})}{T_{1/2}(^{128}\mathrm{Te})} \geq \frac{T_{2\nu}(^{130}\mathrm{Te})}{T_{2\nu}(^{128}\mathrm{Te})} , \qquad (8.2.4)$$

where $T_{1/2}$ and $T_{2\nu}$ are the total half-life and the half-life of the $(\beta\beta)_{2\nu}$ mode, respectively. Since the transition rates Γ of the three body decay (the $(\beta\beta)_{0\nu}$ mode) Γ_{three}, the four body decay (the Majoron emitting process) Γ_{four} and the five body decay (the $(\beta\beta)_{2\nu}$ mode) depend roughly on the maximum kinetic energy release T as T^5, T^8 and T^{11}, the relative yields of them to the ^{128}Te and ^{130}Te decays are as follows:

$[(\Gamma_{\mathrm{three}}/\Gamma_{2\nu})(^{128}\mathrm{Te})/(\Gamma_{\mathrm{three}}/\Gamma_{2\nu})(^{130}\mathrm{Te})] \sim (1.7)^{-6}/(4.957)^{-6} \sim 600$ and

$[(\Gamma_{\mathrm{four}}/\Gamma_{2\nu})(^{128}\mathrm{Te})/(\Gamma_{\mathrm{four}}/\Gamma_{2\nu})(^{130}\mathrm{Te})] \sim (1.7)^{-3}/(4.957)^{-3} \sim 25$,

where the nuclear matrix elements are assumed to be roughly equal for ^{128}Te and ^{130}Te. Now we notice that the ratio of half-lives

is parametrized as

$$(R_T)^{-1} = \frac{T_{2\nu}(^{130}Te)}{T_{2\nu}(^{128}Te)} \left[\frac{1+\{(\Gamma_{three}/\Gamma_{2\nu})+(\Gamma_{four}/\Gamma_{2\nu})\}(^{128}Te)}{1+\{(\Gamma_{three}/\Gamma_{2\nu})+(\Gamma_{four}/\Gamma_{2\nu})\}(^{130}Te)} \right]. \tag{8.2.5}$$

By combining the above argument with Eq.(8.2.5), we can derive the relation in Eq.(8.2.4), where the equality holds only when $\Gamma_{three} = \Gamma_{four} \approx 0$.

Let us examine the experimental information for the relation in Eq.(8.2.4). For convenience, we define

$$(R_{2\nu})^{-1} \equiv \frac{T_{2\nu}(^{130}Te)}{T_{2\nu}(^{128}Te)} = \rho_{2\nu}^{-1} \gamma_{2\nu}^{-1} \tag{8.2.6}$$

where; by neglecting the contributions from the $0^+ \to 2^+$ transitions in the $(\beta\beta)_{2\nu}$ mode given in Table 8.1, we have

$$\rho_{2\nu}^{-1} = \left[(M_{GT}^{(2\nu)}/M_0)(^{128}Te) / (M_{GT}^{(2\nu)}/M_0)(^{130}Te) \right] \tag{8.2.7}$$

and

$$\gamma_{2\nu}^{-1} = \frac{G_{GT}(^{128}Te)}{G_{GT}(^{130}Te)} = (1.78 \pm 0.08) \cdot 10^{-4}. \tag{8.2.8}$$

The uncertainty in $r_{2\nu}$ is due to the experimental errors of T in Table 1.1. The ratio of nuclear matrix elements $\rho_{2\nu}$ is expected to be around one as suggested by Pontecorvo.[14] In Table 8.3, we listed the theoretical values of $\rho_{2\nu}^{-1}$ by Vergados,[75] Haxton et al.[17] within the closure approximation and Klapdor et al.[83),36] without the closure approximation. Certainly, their values are close to one. By inserting these values and $r_{2\nu}^{-1}$ into Eq.(8.2.6) and the ratio $(R_{2\nu})^{-1}$ is evaluated for each $\rho_{2\nu}^{-1}$. The result is shown in Table 8.3 . Note that the central value of $(R_T)^{-1}$ by Heidelberg group does not satisfy the

relation in Eq.(8.2.4) for all three values of $\rho_{2\nu}^{-1}$. Hereafter we shall allow the uncertainty of 2σ

$$(R_T)^{-1} \leq 3.29 \cdot 10^{-4}, \tag{8.2.9}$$

and derive the constraints on the $(\beta\beta)_{0\nu}$ mode and the Majoron emitting process. It should be noted that even with the 2σ constraint, the deviation from the $(\beta\beta)_{2\nu}$ mode is not large.

Now we shall attribute the deviation from the $(\beta\beta)_{2\nu}$ mode in Eq.(8.2.9) to the $(\beta\beta)_{0\nu}$ mode. As discussed before, the deviation should mainly due to the ^{128}Te decay. We keep only the contribution from the $0^+ \to 0^+$ transition and neglect the $0^+ \to 2^+$ transition. Anyway the omission of other contributions gives the looser bound on the $0^+ \to 0^+$ transition, i.e. the effective neutrino mass, $\langle m_\nu \rangle$, and the right-handed parameters, $\langle \lambda \rangle$ and $\langle \eta \rangle$. In the analysis, the CP conservation ($\psi_1, \psi_2 = 0$ or π) is assumed. By using the half-life formula in Eq.(3.5.10) and the numerical values of coefficients in Table 8.2 , we found the upper bounds on $\langle m_\nu \rangle$, $\langle \eta \rangle$ and $\langle \lambda \rangle$, which are shown in Figs. 8.1 and 8.2 . The insides of ellipsoides in Fig. 8.1 are allowed domain. We obtain the bounds,

$$\langle m_\nu \rangle < 5.67 eV \quad (7.85 \ e\sigma) \tag{8.2.10a}$$

$$|\langle \lambda \rangle| < 2.50 \cdot 10^{-5} \quad (2.97 \cdot 10^{-5}) \tag{8.2.10b}$$

$$|\langle \eta \rangle| < 6.68 \cdot 10^{-7} \quad (9.12 \cdot 10^{-7}) \tag{8.2.10c}$$

The limits are obtained by taking the other parameters to be zero. Contrarily, the values in parenthesis correspond to the case where other parameters are kept arbitrary, cf. Fig. 8.1. The somewhat severe constraint on $\langle m_\nu \rangle$ is obtained, if the value of $\rho_{2\nu}$ by

Klapdor et al.[36] is used. These results are given in Table 8.4. With these constraints, we find that $(\Gamma_{0\nu}/\Gamma_{2\nu}) < 3\cdot10^{-3}$, $8\cdot10^{-3}$, $2\cdot10^{-3}$ and $3\cdot10^{-3}$ for ^{48}Ca, ^{76}Ge, ^{82}Se and ^{130}Te, respectively, where the nuclear matrix elements by Haxton et al.[17] are used and $\langle m_\nu \rangle = 5.67\,eV$, $\langle \lambda \rangle = \langle \eta \rangle = 0$.

Next we shall repeat the similar discussion for the Majoron emitting process. We attribute the deviation from the $(\beta\beta)_{2\nu}$ mode to the Majoron emitting process. By using Eq.(5.2.2), the values of nuclear parameters by Haxton et al.[17] and the integrated kinematical factors in Table 3.1, we find [64]

$$|g_{\sigma\beta}| = |\Sigma'_{jk} g_{jk} U_{ej} U_{ek}| < 2.2\cdot10^{-4} \quad . \tag{8.2.11}$$

For the value by Grotz and Klapdor[36] in Table 7.4, we find $|g_\beta| < 5.\cdot10^{-5}$.

§ 8.2.2 The analysis of the $0^+ \to 0^+$ transition of the $(\beta\beta)_{0\nu}$ mode

The lower bounds on the half-lives of the $0^+ \to 0^+$ transition are reported for ^{48}Ca by the Columbia group,[91] for ^{76}Ge by the Milano,[94] Santa Barbara-LBL,[92] Bartelle-South Carolina,[93] Osaka,[99] Guelph,[100] and Caltech groups,[101] for ^{82}Se by the Columbia[91] and Irvine groups,[90] for ^{96}Ze, ^{100}Mo and ^{130}Te by the Ukrainian Academy group,[102] and for ^{130}Nd by the Moscow group.[95] They are listed

in Table 8.5 . In order to obtain the limits on the neutrino mass etc., the absolute magnitudes of nuclear matrix element $M_{GT}^{(0\nu)}$ are needed. In Table 7.4. , the theoretical values by Haxton et al.[17] and Klapdor et al.[36] are given. As we have seen in Table 7.2 , there are some discrepancies between the experimental values of $|M_{GT}^{(2\nu)}/\mu_0|$ and the theoretical predictions. In view of this, we may take a rather conservative attitude to scale the theoretical values of $M_{GT}^{(0\nu)}$ by the factors which are needed for the agreement between the theoretical predictions and the experimental data of the $(\beta\beta)_{2\nu}$ mode. Explicitly, we make the scaling as[21]

$$[M_{GT}^{(0\nu)}]_{scaled} = [M_{GT}^{(0\nu)}]_{Theory} \cdot \frac{|M_{GT}^{(2\nu)}\mu_0|_{Exp.}}{|M_{GT}^{(2\nu)}/\mu_0|_{Theory}} . \tag{8.2.12}$$

By using the values by Haxton et al.[17] for $|M_{GT}^{(2\nu)}/\mu_0|$ in the closure approximation, we obtain the reduction factors 0.38 for ^{82}Se and 0.079 for ^{130}Te (from data by Ref.16). We obtain the scaled values of $M_{GT}^{(0\nu)}$ for ^{82}Se and ^{130}Te. They are shown as the values underlined in Table 7.4. Also, we assume the same reduction factor for ^{76}Ge as ^{82}Se, and ^{128}Te as ^{130}Te.

In below, we shall analyze the data by using the two set of values of $M_{GT}^{(0\nu)}$, the estimates by Haxton et al.[17] and the scaled values.[21] The experimental data is analyzed by using the half-life formula in Eq.(3.5.10) together with the values of coefficients in Table 8.2 and the values of $M_{GT}^{(0\nu)}$ in Table 7.4 . We find the constraints on $\langle m_\nu \rangle$, $\langle \lambda \rangle$ and $\langle \eta \rangle$ which are shown in Figs. 8.3, 8.4, 8.5 and 8.6. The insides of the ellipsoides are the allowed domains and we assumed the CP conservation (ψ_1, $\psi_2 = 0$ or π).

The experiments on ^{76}Ge have improved rapidly and now give the best bounds on $\langle m_\nu \rangle$, $\langle \lambda \rangle$ and $\langle \eta \rangle$, from $T_{0\nu}(0^+ \to 0^+; {}^{76}Ge) > 1.2 \cdot 10^{23}$ yr,

$$\langle m_\nu \rangle < \begin{cases} 3.67\ eV\ (4.31\ eV) & [\text{NM by Haxton et al.}] \\ 9.66\ eV\ (11.3\ eV) & [\text{Scaled NM}] \end{cases} \quad (8.2.13a)$$

$$\langle \lambda \rangle < \begin{cases} 0.714 \cdot 10^{-5}\ (0.733 \cdot 10^{-5}) & [\text{NM by Haxton et al.}] \\ 1.88 \cdot 10^{-5}\ (1.93 \cdot 10^{-5}) & [\text{Scaled NM}] \end{cases} \quad (8.2.13b)$$

$$|\langle \eta \rangle| < \begin{cases} 0.663 \cdot 10^{-6}\ (0.767 \cdot 10^{-6}) & [\text{NM by Haxton et al.}] \\ 1.74 \cdot 10^{-6}\ (2.02 \cdot 10^{-6}) & [\text{Scaled NM}], \end{cases} \quad (8.2.13c)$$

where NM means the nuclear matrix elements in Table7.4. The limits are obtained by taking the other parameters to be zero. Contrarily, the values in parenthesis correspond to the case where other parameters are kept arbitrary, cf. Fig. 8.4.

At this point, it is worthwhile to comment that the much improved bound on $\langle \eta \rangle$ in comparison with $\langle \lambda \rangle$ is due to the P-wave and recoil effects. We found that these contributions are constructive and thus improved the bound. However, according to their calculation, Tomoda et al.[32] found the opposite sign of χ'_P to that by Haxton et al.[17] and claimed that these contributions are destructive and the cancellation was complete. They found the following upper limits: $\langle m_\nu \rangle < 27.5$ eV, $|\langle \eta \rangle| < 1.9 \cdot 10^{-4}$ and $\langle \lambda \rangle < 8.9 \cdot 10^{-5}$. The relative phase of χ'_P and χ'_R and their magnitudes are the important issue to be made clear as soon as possible

The Majoron coupling g_B is constrained severely by the ^{76}Ge data, $T_{0\nu\chi}(0^+ \to 0^+) > 1.10^{21}$yr by the Santa Barbara-LBL group.[92]

By substituting various estimations for nuclear matrix elements given in Table 7.4, we find

$$|g_B| < \begin{cases} 8.1 \cdot 10^{-4} & [\text{NM by Haxton et al.}] \\ 21 \cdot 10^{-4} & [\text{Scaled NM}] \\ 3.2 \cdot 10^{-4} & [\text{NM by Klapdor et al.}]. \end{cases} \quad (8.2.14)$$

The experimental data for the $0^+ \to 2^+$ transition of the $(\beta\beta)_{0\nu}$ mode are reported for ^{76}Ge by the Santa Barbara-LBL,[92] Osaka,[99] Milano,[94] Bordeaux-Zaragoza,[103] and Guelph groups,[100] for ^{100}Mo, ^{148}Nd and ^{150}Nd by the Milano group[104] and they are listed in Table 8.6 . Also the theoretical lower limits of their half-lives are given there by using the bounds on $|\langle \eta \rangle| < 7 \cdot 10^{-7}$ and $|\langle \lambda \rangle| < 2 \cdot 10^{-5}$. Here we used the nuclear matrix elements in Table 7.6 by Haxton et al. for ^{48}Ca and ^{76}Ge to evaluate the contributions from the 2n-mechanism. For the N* mechanism, $P(\Delta)|\langle f|H|i\rangle|^2 \sim 10^{-3}$ is assumed.

§9. The neutrino mass

§9.1. Experimental information of neutrino masses

From the analysis of the $\beta\beta$ decay, we have derived the upper bounds for the effective mass of neutrino $\langle m_\nu \rangle$ by neglecting the contribution from heavy neutrinos ($m_j \geq 10\,\mathrm{MeV}$). The result is summarized in Table 8.4 . If the heavy neutrino contribution is not negligible, the effective mass $\langle m_\nu \rangle$ in Eq.(3.5.11) should be modified as follows;

$$\langle m_\nu \rangle = \left| \sum_j m_j U_{ej} M_{GT}^{(0\nu)}(m_j) [1-\chi_F(m_j)] \Big/ M_{GT}^{(0\nu)}(m_j=0)[1-\chi_F(m_j=0)] \right| , \tag{9.1.1}$$

where the neutrino mass (m_j) dependence of the nuclear matrix element $M_{GT}^{(0\nu)}$ comes from the neutrino potential $h_+(r_{nm}, E_a)$. This situation can be seen from the definitions of $M_{GT}^{(0\nu)}$ in Eq.(3.5.1) and the potential in Eq.(3.4.1) with $\omega = \sqrt{q^2+m_j^2}$ for the propagation of the neutrino N_j.

Let us examine the m_j dependence of $\langle m_\nu \rangle$ in Eq.(9.1.1). We know that the potential h_+ behaves as $(R/r)\phi(\mu_a m_e r)$ for light neutrino ($m_j \ll q \sim 1/R \sim 80\, m_e$) from Eq.(3.4.16a) and as $(R/r)e^{-m_j r}$ for heavy neutrino ($m_j \gg \langle \mu_a \rangle_{av} m_e \sim 40\, m_e$) from Eq.(E.2). In the intermediate mass region $10\,\mathrm{MeV} < m_j < 16\,\mathrm{MeV}$, it is difficult to express h_+ in a compact analytical form, cf. Appendix A of Ref.26 . The m_j dependence of potential h_+ was numerically evaluated and shown in Fig. 3.4. Thus by neglecting χ_F for simplicity, the effective mass is expressed for light and heavy neutrinos approximately as

$$\langle m_\nu \rangle = \left| \sum_{j=light} m_j U_{ej}^2 + \sum_{j=heavy} m_j U_{ej}^2 \left[\left\langle \frac{R}{r} e^{-m_j r} \right\rangle \Big/ \left\langle \frac{R}{r}\phi \right\rangle \right] \right| , \tag{9.1.2}$$

where r represents r_{nm} and $\langle O_{nm} \rangle \equiv \sum_a \langle 0_f^+ \| O_{nm} \vec{\sigma}_n \cdot \vec{\sigma}_m \| 0_i^+ \rangle$ as in

Eq.(3.5.1). Note that the expression of $\langle m_\nu \rangle$ in Eq.(3.5.11) corresponds to the first part in Eq.(9.1.2). The values of nuclear matrix element $[M_{GT}^{(0\nu)}]_C$ in Table 7.4 are obtained in the small mass limit of neutrino mass, that is, for $\langle (R/r)\phi(\mu_a m_e r) \rangle$ given in Eq.(3.4.16a).We shall examine the contribution from heavy neutrinos in the next subsection.

Next, it may be worthwhile to comment that $\langle m_\nu \rangle$ vanishes for Dirac neutrinos: Suppose that two mass degenerate Majorana neutrinos N_k and $N_{k'}$ form a Dirac neutrino, then we find

$$m_k = m_{k'} , \quad U_{ek} = \pm i U_{ek'} , \tag{9.1.3}$$

as seen, for example, from Eqs.(2.6.11) and (2.6.12). As a result, the contributions from a pair N_k and $N_{k'}$ to $\langle m_\nu \rangle$ cancell each other.

In the following, we shall compare the information on neutrino masses obtained from the $\beta\beta$ decay with constraints derived from other experiments.

(i) The electron spectrum of the β decay

The energy spectrum of the β decay is expressed as

$$N(\varepsilon) \sim p\varepsilon \Delta \sum_j |U_{ej}|^2 (\Delta^2 - m_j^2)^{1/2} \theta(\Delta - m_j) , \tag{9.1.4}$$

where ε is the energy of electron and $\Delta = \varepsilon_{max} - \varepsilon$, ε_{max} being the maximum energy of electron in the zero neutrino mass limit. In contrast to the $(\beta\beta)_{0\nu}$ mode, neutrinos come out in the final states so that neutrino masses are explored directly.

According to the Particle Data Group,[105] the following bounds on neutrino masses are given

$$m_{\bar{\nu}_e} < 46\,eV \quad (60\,eV^{106)}),$$
$$m_{\nu_\mu} < 500\,KeV, \qquad (9.1.5)$$
$$m_{\nu_\tau} < 164\,MeV \quad (125\,MeV^{107)}).$$

From the analysis of the electron energy spectrum of the tritium β decay around the end point $(\varepsilon \sim \varepsilon_{max})$, ITEP group reported the finite neutrino mass under "realistic assumptions",[108]

$$20\,eV < m_{\bar{\nu}_e} < 45\,eV \qquad (9.1.6a)$$

and the model independent bound

$$m_{\bar{\nu}_e} > 9\,eV \ . \qquad (9.1.6b)$$

On these results, Bergkvist[109] made critical comments from the view point of the resolution function of electron energy. Recently, Kündig[110] reported new data on the tritium spectrum around the end point by varying the thickness of the sample. His result was consistent with zero neutrino mass.

While, Simpson[111] examined the electron energy spectrum of tritium β decay in the low energy region $(\varepsilon \sim 1\,KeV)$, and reported an anormalous deviation from the zero mass neutrino case. He attributed this anormaly to the emission of a heavier neutrino N_2 with the mass m_2 as seen from Eq.(9.1.4),

$$m_2 = 17.1\ KeV,$$
$$\tan^2\theta \simeq 0.03 \ , \qquad (9.1.7)$$

where θ is the mixing angle between a light neutrino N_1 and a heavier one N_2, i.e., $\nu_{eL} = \cos\theta\, N_{1L} + e^{i\beta}\sin\theta\, N_{2L}$ as given

in Eq.(2.3.3). Note that the CP violating phase (β) intrinsic to Majorana neutrino system never appears in the single β emitter. Since the observed anormaly is in the low electron energy region $(Q = 18.6\,KeV)$, the relatively large background is expected. To avoide it, the β decays with the Q value around 2 m_2 are advantageous, because the maximum yield is achieved there. Experiments for ^{35}S (Q = 166.84 KeV) by Caltech and Princeton groups and for ^{63}Ni (Q = 65.92 KeV) by Guelph group are now underway. The measurement of γ energy in the capture of 1s and 2p electrons in ^{125}I ($^{125}I + e^- \rightarrow {}^{125}Te^* + \nu_e + \gamma$) was performed by CERN group and their preliminary data showed no indication of the heavier neutrino N_2.[112]

(ii) The nuetrino oscillations

The neutrino produced by the weak interaction (the weak eigenstate neutrino) is in general expressed as the superposition of mass eigenstate neutrinos as in Eq.(3.1.5). Since the time evolution of mass eigenstate neutrino depends on its mass, the combination of them changes as time goes on. Thus the oscillations among weak eigenstate neutrinos occur. The transition probability for appearence of the second flavor ℓ' in a beam which is initially in the pure ℓ flavor is given by

$$P(\nu_\ell \rightarrow \nu_{\ell'}) = \sum_{j,k} U_{\ell j}\, U^*_{\ell' j}\, U^*_{\ell k}\, U_{\ell' k}\, e^{-i(E_j - E_k)} \qquad (9.1.8)$$

where $U_{\ell j}$ is the mixing matrix in Eq.(2.3.1). It should be noticed that

$$E_j - E_k = (m_j^2 - m_k^2)/(E_j + E_k) \simeq (m_j^2 - m_k^2)/2E \ , \qquad (9.1.9)$$

so that the information on the squared mass difference $\Delta m_{jk}^2 = m_j^2 - m_k^2$ is obtained from the neutrino oscillation experiment.

For the case of the two neutrino mixing in Eq.(2.3.3), $P(\nu_\ell \to \nu_{\ell'})$ $(\ell \neq \ell')$ is written by

$$P(\nu_\ell \to \nu_{\ell'}) = \sin^2 2\theta \sin^2 (1.27 \Delta m^2 R/E) \qquad (9.1.10)$$

and the probability for the disappearence experiment is

$$P(\nu_\ell \to \nu_\ell) = 1 - P(\nu_\ell \to \nu_{\ell'}) , \qquad (9.1.11)$$

where R(m) is the distance between neutrino source and detector, E and Δm^2 are measured in units of MeV and eV^2, respectively.

At present, there is essentially no indication of the neutrino oscillation. The bounds on the squared mass difference and the mixing angles are given from the various types of experiments. Among many data, some of the most stringent bounds are as follows:

$$\nu_\mu \to \nu_e : \sin^2 2\theta < 0.006 \quad \text{for } \Delta m^2 \gtrsim 20\,eV^2,\ ^{113)} \qquad (9.1.12a)$$

$$\nu_\mu \to \nu_\tau : \sin^2 2\theta < (0.05\text{-}0.06) \quad \text{for } \Delta m^2 \gtrsim 20\,eV^2,\ ^{113),114),115)} \qquad (9.1.12b)$$

$$\nu_e \to \nu_x : \sin^2 2\theta < 0.07 \quad \text{for } \Delta m^2 \gtrsim 50\,eV^2,\ ^{115)} \qquad (9.1.12c)$$

$$\bar{\nu}_e \to \bar{\nu}_x : \begin{cases} \sin^2 2\theta < 0.16 \\ \Delta m^2 < 1.6 \cdot 10^{-2}\ eV \end{cases} \quad \begin{matrix} \text{for } \Delta m^2 \gtrsim 0.1\ eV^2,\ ^{7)} \\ \text{for } \sin^2 2\theta = 1 . \end{matrix} \qquad (9.1.12d)$$

Here X in $\nu_e \to \nu_x$ oscillation means the unspecified neutrino which does not produce any e or μ charged current events. Recently a Grenoble-Annecy group working at the Bugey reactor [8] reported the affirmative conclusion of neutrino oscillation $\Delta m^2 \sim 0.2\ eV^2$ and $\sin^2 2\theta = 0.25$ from the $\bar{\nu}_e$ oscillation experiment. However their result seems to be in contradiction with the data in Eq.(9.1.12d) by the Caltech-Munich-SIN experiment at the Gosgen power reactor.[7]

(iii) Heavy neutrino search

Heavy neutrino search has been made extensively in the pseudoscalar meson $(\pi, K, D, \cdots)$ decays

$$M \longrightarrow \nu_H + \ell + X, \qquad (9.1.13a)$$

where X represents the vacuum or some system of hadrons. The other is the decay of heavy neutrinos like

$$\nu_H \longrightarrow \ell^- + \ell^+ + \bar{\nu}_\ell . \qquad (9.1.13b)$$

Various experimental results may be summarized as follows:[116]

$$m_H < 10\ MeV \quad \text{or} \quad m_H > 1.5\ GeV, \qquad (9.1.14)$$

if $|U_{eH}|^2,\ |U_{\mu H}|^2 \gtrsim 10^{-5} \sim 10^{-6}$, where $|U_{\ell H}|^2$ represents the admixture of heavy neutrino in the weak eigenstate neutrino with the flavor ℓ .

(iv) Other sources of information on neutrino masses

Various groups are continuing to measure the electron neutrino mass in the electron capture of ^{163}Ho by utilizing its small Q value. The reported neutrino mass bounds are the order of 1 KeV.[117]

The cosmology gives the bound on neutrino mass,[118]

$$\Sigma_j m_j \leq 100\ eV, \qquad (9.1.15)$$

where the sum extends over the stable neutrinos (at least in the order of age of universe). The above bound is obtained from the constraint that the mass density of neutrino should not exceed the critical mass density.

The solar neutrino has been one of the topics which suggests

massive neutrinos and neutrino mixing.[42] By detecting the solar neutrino, it will be possible to test the neutrino oscillation with the mass difference of order 10^{-6} eV.

§ 9.2 Interpretation of various data on neutrino masses

Among various data on neutrino masses, we shall take the information from the following processes in granted; the neutrino oscillation, the $\beta\beta$ decay and the bounds on masses of ν_e, ν_μ and ν_τ in Eq.(9.1.5).

The null result from the neutrino oscillation implies that two neutrinos are in the following situations; (a) the small mass squared difference case, $\Delta m^2 \simeq 0$, if the mixing is relatively large and (b) the small mixing case $\sin^2 2\theta \simeq 0$, if the mass squared difference is relatively large. If neutrinos are Majorana particles, the $\beta\beta$ decay gives a very strong constraint on the mixing scheme.

Let us discuss the Majorana neutrino system consisting of two, three or four neutrinos first, and later consider the Dirac neutrino system. Our aim is to explore the possible scheme of neutrino mixing and the nature of neutrinos by taking into account the ITEP data and/or the Simpson's data.

In the following discussions, we shall assume the CP invariance for simplicity.

(i) Two Majorana neutrino mixing

First we shall consider the ITEP result in Eq.(9.1.6) seriously, in addition to the neutrino oscillation and the $\beta\beta$ decay

experiments.

For the case (a), masses of two Majorana neutrinos N_1 and N_2 are almost degenerate and their masses should be close to the one by the ITEP experiment. Since $\langle m_\nu \rangle < m_{\bar{\nu}_e}$, N_1 and N_2 have the large mixing between them and contribute destructively to $\langle m_\nu \rangle$. The destructive interference is possible only if the CP signs of N_1 and N_2 are the opposite ($\beta = \pi/2$ in Eq.(2.1.3)) and the mixing angle θ should be close to $\pi/4$ (see Eq.(2.3.5)). Almost degenerate Majorana neutrinos with the opposite CP signs and almost maximum mixing $\theta \sim \pi/4$ are called the pseudo Dirac (PD) neutrino,[49),50),51)] as discussed in § 2.5.2. In the extreme limit, $m_1 = m_2$, $\theta = \pi/4$ and $\beta = \pi/2$, the $(\beta\beta)_{0\nu}$ mode is strictly forbidden and also $\langle m_\nu \rangle = 0$ (the Konopinski-Mahmoud Dirac neutrino case).

As realistic models which have the above characters of the PD neutrino, two examples are shown within the SU(5) GUTS,[5),168)] but no successful model has yet been reported in the simple SO(10) model.[86)] The possible constraints on the CP violting phase β have been analized from the data on the $(\beta\beta)_{0\nu}$ mode and the ^{3}H decay.[167)]

For the case (b), we have to assign the mass of the lighter neutrino to that detected by ITEP. Since the mixing is small, only way to suppress $\langle m_\nu \rangle$ use the character of the destructive interference between the light neutrino with the mass $m_{\bar{\nu}_e}$ and a heavier one, i.e., $m_1 < m_2 < 10$ keV and these neutrino should have the opposite CP signs. In addition, a delicate balance between the mixing angle θ and the masses is needed, i.e., $\tan\theta \simeq \sqrt{m_1/m_2}$ in Eq.(2.3.5). As discussed in § 2.6.1, this situation may be realized by considering the mass matrix in Eq.(2.6.1) with $\mu = 0$ for two left-handed neutrino. Note that from the constraints

in Eq.(9.1.14), if N_2 has the mass around 100 KeV, then it should decay first due to Eq.(9.1.15). The fast decay of N_2 is achieved by the Majoron or familon emission process.[53),119)]

Another possibility for the case (b) is to utilize the destructive interference between the light left-handed and the heavy right-handed neutrinos,[52)] i.e. $m_1 \sim 20$ eV and $m_2 > 10$ MeV. In this case, the effective mass is expressed from Eq.(9.1.2) as

$$\langle m_\nu \rangle = \left| m_1 \cos^2\theta - m_2 \sin^2\theta \left[\left\langle \frac{R}{r} e^{-m_2 r} \right\rangle / \left\langle \frac{R}{r} \phi \right\rangle \right] \right| . \quad (9.2.1)$$

Here we use the mixing matrix in Eq.(2.3.3) with $\beta = \pi/2$. The evaluation of the average potential for heavy neutrino $\langle (R/r) e^{-m_\nu r} \rangle$ depends sensitively on the two-nucleon correlation function because the contribution comes from the short distance region $r \lesssim O(1/m_\nu)$. Commonly, hard core at 0.5 fm[65)] or a soft core[17)] has been used. For heavy neutrinos, the effect of finite nucleon size may become important as stressed by Vergados.[66)] Since the ratio of nuclear matrix elements in the second term has the A dependence, A being the mass number, the experimental values of $\langle m_\nu \rangle$ should be different for various $\beta\beta$ decaying nuclei. In other words, even if the suppression of the $(\beta\beta)_{0\nu}$ mode occurs for one nucleus, this suppression mechanism may not work so well for other nuclei.

Next we shall consider the Simpson's result in Eq.(9.1.7) seriously, instead of ITEP data. Then the case (a) is trivially inconsistent with it and also the case (b) is excluded because

$$\langle m_\nu \rangle = \left| m_1 \cos^2\theta + m_2 e^{2i\beta} \sin^2\theta \right| \sim m_2 \sin^2\theta \sim 500 \text{eV} \quad (9.2.2)$$

Therefore, three Majorana neutrino mixing should be considered.

(ii) Three Majorana neutrino mixing

The ITEP data is already incorporated for the two neutrino mixing case so that variety of mixing schemes can be constructed for three nertrino mixing case. Therefore, we do not consider this case.

Therefore, we shall consider the mixing scheme consistent with the Simpson's result. A simple, but almost unique mixing scheme is derived by imposing the approximate $L_e + L_\tau - L_\mu$ symmetry,[54)] where L_e, L_μ, L_τ are individual lepton numbers, see Eq.(2.6.8). In the exact symmetry limit, the $(\beta\beta)_{0\nu}$ mode is forbidden and the ν_e-ν_μ oscillation does not occur, as examined in Eq.(2.6.12). In the case of this kind of symmetry in §2.6.2 there are a massless Majorana neutrino and a pair of mass degenerate Majorana neutrinos which form a KM Dirac neutrino. In this model, the $\nu_e - \nu_\tau$ oscillation is allowed and the mixing angle θ has the value $\tan\theta \sim \sqrt{0.03}$, which is in weak conflict with the $\nu_e - \nu_X$ oscillation data, $\sin^2 2\theta < 0.07$ in Eq.(9.1.12c) by assigning $X = \nu_\tau$. With the small breaking of the $L_e + L_\tau - L_\mu$ symmetry, a massless Majorana neutrino gets small mass and the KM Dirac neutrino splits into two Majorana neutrinos with almost degenerate mass (the P D neutrino). Now the $(\beta\beta)_{0\nu}$ takes place slowly and the small $\nu_e - \nu_\mu$ oscillation occurs. Now the P D neutrino with the mass around 17.1 KeV should decay fast to avoid the confliction with the cosmological bound in Eq.(9.1.15). One of most attractive story is the heavier neutrino decay in association with a Majoron(Goldsone boson).

A systematic exploration of the mixing scheme was performed

by Dugan, Manohor and Nelson.[120] Their result is as follows ; either the model with the approximate $L_e + L_\tau - L_\mu$ symmetry or the model with ν_μ heavier than 250 KeV is only allowed to incorporate Simpson's result. Note that the fine tuning of parameters is needed for the latter case.

The ITEP data seems hard to be incorporated to the model with the approximate $L_e + L_\tau - L_\mu$ symmetry, because the mass of N_1 is derived from the radiative correction. One simple proposal will be the consideration of four neutrino mixing which will be discussed next.

(iii) Four Majorana neutrino mixing

Many phenomenological mixing schemes can be constructed to explain both the ITEP and Simpson's results consistently.

Here we examine the mixing scheme by imposing the approximate $L_e + L_\tau - L_\mu - L_{\tau'}$ symmetry, where τ' represents leptons of the fourth generation. In the exact symmetry limit, the $(\beta\beta)_{0\nu}$ mode and the $\nu_e - \nu_\mu$ oscillation are forbidden, while the $\nu_e - \nu_\tau$ and $\nu_\mu - \nu_{\tau'}$ oscillations occur. As discussed in §2.6.2 (iii), there are two pairs of mass degenerate neutrinos and each pair forms a KM Dirac neutrino. Both KM Dirac neutrinos are massive and the mixing among them is determined by the unitary matrices α and β in Eq.(2.6.17). In this model, the $\nu_e - \nu_\tau$ oscillation is large and in weak conflict with the data in Eq.(9.1.12c) similarly to the model with the $L_e + L_\tau - L_\mu$ symmetry. With the small breaking of the $L_e + L_\tau - L_\mu - L_{\tau'}$ symmetry, each KM Dirac neutrino splits into two almost degenerate Majorana neutrinos.

(iv) Dirac neutrinos

Since the $(\beta\beta)_{0\nu}$ mode does not take place for Dirac neutrinos, constraints are from the ν oscillation, the ITEP result and Simpson's result.

Let us consider first the two ordinary Dirac neutrino mixing case where the ordinary Dirac neutrino means that it consists of the left- and right-handed neutrinos of the same flavor with the same mass but with opposite CP signs. Then, these three experimental results are explained by taking $m_1 \sim 20$ eV, $m_2 \sim 17.1$ KeV and $\tan\theta = \sqrt{0.03}$. However, in this case, there is one problem why these neutrinos are light in comparison with the charged lepton masses. Recently, some complicated models have been proposed to explain the light Dirac neutrinos.[121] Furthermore, it seems difficult to assure the fast decay of the heavier neutrino N_2 which is needed to respect the cosmological bound in Eq.(9.1.15).

On the other hand, more attractive case is to consider the KM Dirac neutrino. As we have already seen in Models (ii) and (iii), we have the KM Dirac neutrino(s) in the limit of the exact $L_e + L_\tau - L_\mu$ or $L_e + L_\tau - L_\mu - L_{\tau'}$ symmetry. Suppose that the above symmetry is the global symmetry which is broken spontaneously. Then there appears the Nambu-Goldstone boson (Majoron or familon) which interacts with neutrinos. This coupling constant is not weak, see Eqs.(5.2.1) and (8.2.14). Thus, in principle, the heavier neutrino (now the PD neutrino) can decay fast into the lighter ones by emitting the Majoron or familon. This mechanism gives an attractive scenario of the PD neutrinos.

§10 Constraints on the right-handed parameters

The β, μ and K decays as well as the $\beta\beta$ decay have offered some constraints on the right-handed parameters. They are compared in this section.

The analysis of the β and μ decays have been done by many authors without taking into account the neutrino mixing.[122),123),124)] Since we adopt a different parametrization for the semileptonic weak interaction Hamiltonian Eq.(3.1.3) from the previous works, we shall reexpress these constraints in terms of our parameters with neutrino mixing matrices in order to compare with the constraints from the $\beta\beta$ decay.

In these three decays, various neutrino mixing matrices appear in different forms, and depend on the relative magnitudes of contributing neutrino masses. Therefore, the following three cases will be considered for the $SU(2)_L \times SU(2)_R \times U(1)$ model (type II B in Table A.1 in Appendix A): Case (D): All neutrinos are Dirac particles with masses lighter than 0.5 MeV in Eq.(9.1.5). Case (M-I): All neutrinos are Majorana particles with light masses. Case (M-II): There exist both light ($m_{N_I} \lesssim O(\text{MeV})$) and heavy ($m_{N_{II}} \gtrsim O(\text{GeV})$) Majorana neutrinos, e.g. Eq.(2.2.11). It is possible that some of Dirac neutrinos are light and the others are heavy. But the results for this case is similar to the case M-II, if some parameters are reinterpreted, so that this case is not mentioned separately. There are some cases where both Dirac and Majorana neutrinos coexist, but they are considered as a special case of cases M-I or M-II, because a Dirac particle consists of two Majorana neutrinos with the same mass.

As another example, let us consider the $SU(2)_L \times U(1)$ model with mirror particles (type III of Table A.1).[125),126)] If masses of mirror particles are light ($\lesssim O(\text{MeV})$), then we have to get the large deviation from predictions by the minimum standard model. Therefore, we shall consider only the case with heavy mirror neutrinos and light left-handed neutrinos. This case will be referred to as case M-III.

Throughout this section, we allow two standard deviations on all input data as conservative as possible.

§10.1 Constraints from the $\beta\beta$ decay

The $\beta\beta$ decay gives constraints on the right-handed current parameters $\langle\lambda\rangle$ and $\langle\eta\rangle$, as shown in Table 8.4 and in Eqs.(8.2.10) and (8.2.13). In the $SU(2)_L \times SU(2)_R \times U(1)$ model, the mixing matrices and the right-handed parameters are given in Eq.(3.1.7), and we have

$$\begin{aligned} \langle\lambda\rangle &= \lambda_0 \left| (g_V'/g_V) \sum{}' U_{ej} V_{ej} \right|, \\ \langle\eta\rangle &= \eta_0 \left| \sum{}' U_{ej} V_{ej} \right|, \end{aligned} \tag{10.1.1}$$

where λ_0 and η_0 are defined in Eqs.(A.2.7) and (A.2.8), and the primed sum extends over only light neutrinos ($m_j \lesssim 10$ MeV). In contrast to the $\langle m_\nu \rangle$ case, the contribution from heavy neutrinos can be neglected, because there is no enhancement factor like m_j for $\langle m_\nu \rangle$ and neutrino potentials dump like the Yukawa potential.

For Dirac neutrinos (case D), $\langle\lambda\rangle$ and $\langle\eta\rangle$ become zero similarly to the effective mass $\langle m_\nu \rangle$, because a Dirac neutrino consists of two mass degenerate Majorana neutrinos N_k and N_{n+k}, and $U_{ek} = \pm i U_{e\,n+k}$, $U'_{ek} = \pm i U'_{e\,n+k}$, $V_{ek} = \pm i V_{e\,n+k}$ and $V'_{ek} = \pm i V'_{e\,n+k}$.

In the case M-I, the $(\beta\beta)_{0\nu}$ decay is effectively forbidden within the approximation that the neutrino mass dependence of the neutrino potentials are neglected. This approximation is justified

as seen from Fig.3.4. In the zero mass case of weak eigenstate electron neutrinos, ν_{e_L}, $\tilde{\nu}_{e_L}$, ν_{e_R}' and $\tilde{\nu}_{e_R}'$, we have $\langle\lambda\rangle = \langle\eta\rangle = 0$ in addition to $\langle m_\nu\rangle = 0$, as discussed in §3.5.

Let us examine the case M-II. Note that $U_{ej} \sim O(1)$ and $V_{ej} \sim O(\theta_{LR})$ for light left-handed neutrinos $(1 \le j \le n)$, and $U_{ej} \sim O(\theta_{LR})$ and $V_{ej} \sim O(1)$ for heavy right-handed neutrinos $(n+1 \le j \le 2n)$ where θ_{LR} is a mixing angle between left- and right-handed neutrinos. Since there is a small deviation from the unitarity character in Eq.(3.1.6), we define

$$\left| \sum{}' U_{ej} V_{ej} \right| = \bar{v}_e \tag{10.1.2}$$

where $\bar{v}_e$ is a small quantity of order θ_{LR}. Then we have

$$\begin{aligned} \langle\lambda\rangle &= \lambda_0' \bar{v}_e \qquad \left(\lambda_0' = \lambda_0 (g_V'/g_V)\right), \\ \langle\eta\rangle &= \eta_0 \bar{v}_e . \end{aligned} \tag{10.1.3}$$

Bounds in Eqs.(8.2.10) and (8.2.13) give constraints in Table 10.1.

For the $SU(2)_L \times U(1)$ model with mirror leptons (the case M-III), we have from Eq.(3.1.9)

$$\langle\lambda\rangle = 0 , \qquad \langle\eta\rangle = \bar{v}_{Me} , \tag{10.1.4}$$

where $\bar{v}_{Me}$ is a small quantity defined similarly to Eq.(10.1.2) and is of order of the mixing angle θ_M between ordinary and mirror leptons. Similarly to the case M-II, we obtain the constraints shown in Table 10.1.

§10.2 Constraints from the single β decay

The longitudinal polarization of the β ray and the β ray asymmetry with respect to the initial nuclear spin will be analyzed by using the weak interaction Hamiltonian in Eq.(3.1.3).

(i) The longitudinal polarization

The longitudinal polarization P of an emitted electron (positron) is defined by

$$P = \mp \frac{d\Gamma(\uparrow) - d\Gamma(\downarrow)}{d\Gamma(\uparrow) + d\Gamma(\downarrow)} , \tag{10.2.1}$$

where $d\Gamma(\uparrow)$ and $d\Gamma(\downarrow)$ are decay rates for the β ray spin polarization pararell and anti-pararell to its momentum direction, respectively. The longitudinal polarizations P_{GT} and P_F for the pure allowed Gamow-Teller and superallowed Fermi β transitions are expressed in units of v/c as

$$P_{GT} = 1 - 2 \frac{\sum_j' |\varepsilon_{Aj}|^2}{\sum_j' (|C_{Aj}|^2 + |\varepsilon_{Aj}|^2)} , \tag{10.2.2}$$

$$P_F = 1 - 2 \frac{\sum_j' |\varepsilon_{Vj}|^2}{\sum_j' (|C_{Vj}|^2 + |\varepsilon_{Vj}|^2)} , \tag{10.2.3}$$

where C_{Vj}, C_{Aj}, ε_{Vj} and ε_{Aj} are combinations of the right-handed current parameters and the mixing matrices, and defined in Eq.(C.1.5). Here primed sum extends over only neutrinos which are allowed energetically in the β decay.*) In the minimum standard model, P_{GT} and P_F are unity.

Klinken et al.[127] reported the ratio

$$\frac{P_F(^{26m}\mathrm{Al})}{P_{GT}(^{30}\mathrm{P})} = 0.986 \pm 0.038, \tag{10.2.4}$$

*) For simplicity, we have neglected the neutrino mass in comparison with its momentum and omitted also terms like m_j/m_e.

which is advantageous because various systematic errors are reduced. From Eqs.(10.2.2)-(10.2.4), we obtain the constraint

$$-9.0\cdot10^{-2} < 2\delta < 6.2\cdot10^{-2} \tag{10.2.5}$$

where

$$\delta = \frac{\sum_j' |\varepsilon_{Aj}|^2}{\sum_j'(|G_{Aj}|^2+|\varepsilon_{Aj}|^2)} - \frac{\sum_j' |\varepsilon_{vj}|^2}{\sum'(|G_{vj}|^2+|\varepsilon_{vj}|^2)} . \tag{10.2.6}$$

In the $SU(2)_L \times SU(2)_R \times U(1)$ model, we have from Eqs.(3.1.7) and (C.1.5)

$$\begin{aligned} G_{vj} &= (1+\eta_0')(g_v/g_A)\,U_{ej}, \quad G_{Aj} = (1-\eta_0')\,U_{ej}, \\ \varepsilon_{vj} &= (\lambda_0'+\eta_0)(g_v/g_A)\,V_{ej}, \quad \varepsilon_{Aj} = (\lambda_0'-\eta_0)V_{ej}, \\ \lambda_0' &= \lambda_0\,(g_v'/g_v) \quad \text{and} \quad \eta_0' = \eta_0\,(g_v'/g_v). \end{aligned} \tag{10.2.7}$$

In the cases of Dirac neutrino (case D) and all light Majorana neutrinos (case M-I), primed sum runs over all neutrinos. Then the normalization condition in Eq.(3.1.6a) can be used, and these constraints in Table 10.1 are obtained from Eq.(10.2.5) by keeping only the leading terms with respect to small quantities.

In the case M-II, we have deviations from the normalization and orthogonality conditions in Eq.(3.1.6) due to heavy neutrinos and express as

$$\sum' |U_{ej}|^2 = 1 - \bar{u}_e^2 , \tag{10.2.8}$$

$$\sum' |V_{ej}|^2 = \bar{v}_e^2 , \tag{10.2.9}$$

where $\bar{u}_e$ is a small quantity like $\bar{v}_e$ and of order θ_{LR}. The constraint is given in Table 10.1.

In the case M-III, we have

$$\begin{aligned} G_{vj} &= (g_v/g_A)\,U_{ej}, \quad G_{Aj} = U_{ej}, \\ \varepsilon_{vj} &= (g_v/g_A)\,V_{ej}, \quad \varepsilon_{Aj} = -V_{ej}, \end{aligned} \tag{10.2.10}$$

and

$$\sum' |U_{ej}|^2 = 1 - \bar{u}_{Me}^2 \tag{10.2.11}$$

$$\sum' |V_{ej}|^2 = \bar{v}_{Me}^2 \tag{10.2.12}$$

where $\bar{u}_{Me}$ is of order θ_M. In this case, P_F/P_{GT} is equal to unity, independent of the mixing parameters, as seen from Eqs.(10.2.2), (10.2.3) and (10.2.10).

Measurements of P_{GT} itself were made by many authors. Among them we will take the value by Klinken[128]

$$P_{GT} = 1.001 \pm 0.008. \tag{10.2.13}$$

This is an average value of data from ^{32}P, ^{60}Co, ^{114}In, ^{147}Pm, ^{147}Nd, ^{153}Sm and ^{198}Au isotopes. From Eqs.(10.2.2) and (10.2.13), we have

$$\frac{\sum_j' |\varepsilon_{Aj}|^2}{\sum_j'(|G_{Aj}|^2+|\varepsilon_{Aj}|^2)} < 7.5\cdot10^{-3}. \tag{10.2.14}$$

After similar arguments, we obtain the results in Table 10.1.

(ii) The asymmetry parameter

The asymmetry A(p) is defined as

$$d\Gamma \propto [\,1 + (p/\varepsilon)\,A(p)\,P\cos\theta\,]\,dp\,d\cos\theta \tag{10.2.15}$$

where p and ε are momentum and energy of the β ray, respectively, and θ is an angle of the β ray direction relative to the polarization P

of a parent nucleus. For the $^{19}Ne(\frac{1^+}{2} \to \frac{1^+}{2})$ decay, the reported value by Calaprice et al.[129] is

$$A(0) = -0.0391 \pm 0.0014. \tag{10.2.16}$$

The theoretical expression of A(0) for the $\frac{1^+}{2} \to \frac{1^+}{2}$ nuclear decay is given by

$$A(0) = 2\,\frac{\sum_j' \{(|G_{Aj}|^2 - |\varepsilon_{Aj}|^2)|\mathcal{M}_{GT}|^2/3 - \mathrm{Re}[(G_{Aj}^* G_{Vj} - \varepsilon_{Aj}^* \varepsilon_{Vj})\mathcal{M}_{GT}^* \mathcal{M}_F]/\sqrt{3}\}}{\sum_j' \{(|G_{Aj}|^2 + |\varepsilon_{Aj}|^2)|\mathcal{M}_{GT}|^2 + (|G_{Vj}|^2 + |\varepsilon_{Vj}|^2)|\mathcal{M}_F|^2\}}, \tag{10.2.17}$$

where $\mathcal{M}_F$ and $\mathcal{M}_{GT}$ are Fermi and Gamow-Teller type reduced matrix elements, respectively. For the ^{19}Ne decay, A(0) is sensitive to the right-handed current contributions, because of accidental cancellation between the V-A terms G_A and G_V.

According to Holstein and Treiman,[130] the ratio of nuclear matrix elements is obtained experimentally by comparing the ft value $(ft)_{Ne}$ for the ^{19}Ne decay with the ft value $(ft)_{0^+ \to 0^+}$ for the $0^+ \to 0^+$ analog β transitions.

$$\frac{(ft)_{0^+ \to 0^+}}{(ft)_{Ne}} \approx \frac{\sum_j' \{(|G_{Vj}|^2 + |\varepsilon_{Vj}|^2)|\mathcal{M}_F|^2 + (|G_{Aj}|^2 + |\varepsilon_{Aj}|^2)|\mathcal{M}_{GT}|^2\}}{2\sum_j' (|G_{Vj}|^2 + |\varepsilon_{Vj}|^2)|\mathcal{M}_F(0^+ \to 0^+)|^2} \tag{10.2.18}$$

Hereafter we will assume that all reduced matrix elements are real and that $\mathcal{M}_F$ in the Ne decay is equal to $\mathcal{M}_F(0^+ \to 0^+)$ in the $0^+ \to 0^+$ analog β transitions. By using experimental values on the ft values,

$$(ft)_{Ne} = 1716.8 \pm 2.0 \quad \text{sec},^{131} \tag{10.2.19a}$$

$$(ft)_{0 \to 0} = 3085.4 \pm 1.3 \quad \text{sec},^{132} \tag{10.2.19b}$$

we obtain the ratio $|\mathcal{M}_{GT}/\mathcal{M}_F|$ from Eq.(10.2.18). Then the following constraint is derived from Eqs.(10.2.16) and (10.2.17),

$$-1.0 \cdot 10^{-4} < \sum_j' \{0.73\,|\varepsilon_{Aj}|^2 - 0.27\,|\varepsilon_{Vj}|^2 - 0.54\,\varepsilon_{Aj}^* \varepsilon_{Vj}\} < 1.0 \cdot 10^{-2}, \tag{10.2.20}$$

where we have kept only the leading terms. The results are given in Table 10.1.

§10.3 Constraints from the μ decay

Similarly to the parametrization of the semileptonic weak interaction Hamiltonian Eq.(3.1.3), the leptonic interaction Hamiltonian is expressed as follows; *)

$$\begin{aligned} H_W = \frac{G}{\sqrt{2}} \sum_{i,j} \{ & f_{LLji}\, \bar{\mu}\gamma^\rho(1-\gamma_5)N_j\, \bar{N}_i\gamma_\rho(1-\gamma_5)e \\ & + f_{RRji}\, \bar{\mu}\gamma^\rho(1+\gamma_5)N_j\, \bar{N}_i\gamma_\rho(1+\gamma_5)e \\ & + f_{LRji}\, \bar{\mu}\gamma^\rho(1-\gamma_5)N_j\, \bar{N}_i\gamma_\rho(1+\gamma_5)e \\ & + f_{RLji}\, \bar{\mu}\gamma^\rho(1+\gamma_5)N_j\, \bar{N}_i\gamma_\rho(1-\gamma_5)e \}, \end{aligned} \tag{10.3.1}$$

*) In the charge retention form

$$H_W = \frac{G}{\sqrt{2}} \sum_k \sum_{i,j} \bar{\mu}\Gamma_k e \cdot \bar{N}_i \Gamma_k (C_k + C_k'\gamma_5) N_j + \text{h.c.}, \tag{10.3.1a}$$

where $\Gamma_S = 1$, $\Gamma_V = \gamma^\rho$, $\Gamma_A = \gamma^\rho\gamma_5$, $\Gamma_P = i\gamma_5$ and $\Gamma_T = \sigma^{\rho\sigma}/\sqrt{2}$, we have

$$\begin{aligned} C_S &= C_P = 2(f_{LLRji} + f_{RLji}), \\ C_S' &= C_P' = -2(f_{LRji} - f_{RLji}), \\ C_V &= C_A = -(f_{LLji} + f_{RRji}), \\ C_V' &= C_A' = (f_{LLji} - f_{RRji}), \\ C_T &= C_T' = 0 \end{aligned} \tag{10.3.1b}$$

where N_i and N_j are mass-eigenstate neutrinos with masses m_i and m_j, and explicit forms of $f_{\alpha\beta ji}$ ($\alpha,\beta = L$ or R) are model dependent. This is the most general effective interaction including the V±A charged currents, and is applicable to all pure leptonic processes by replacing e and μ with other appropriate charged leptons.

In the $SU(2)_L \times SU(2)_R \times U(1)$ model,*) $f_{\alpha\beta ji}$ are given by

$$f_{LLji} = U_{\mu j} U_{ei}^{*}, \qquad f_{RRji} = \lambda_0 V_{\mu j} V_{ei}^{*},$$
$$f_{LRji} = \eta_0 U_{\mu j} V_{ei}^{*}, \qquad f_{RLji} = \eta_0 V_{\mu j} U_{ei}^{*}, \tag{10.3.2}$$

while in the $SU(2)_L \times U(1)$ model with mirror leptons, they are

$$f_{LLji} = U_{\mu j} U_{ei}^{*}, \qquad f_{RRji} = V'_{\mu j} V'^{*}_{ei},$$
$$f_{LRji} = U_{\mu j} V'^{*}_{ei}, \qquad f_{RLji} = V'_{\mu j} U_{ei}^{*}. \tag{10.3.3}$$

Mixing parameters in Eqs.(10.3.2) and (10.3.3) are defined similarly to those for the $\beta\beta$ decay in Eq.(3.15) except the suffix μ.

The μ^+ decay proceeds through the fundamental process,

$$\mu^+ \to e^+ + \bar{N}_j + N_i, \tag{10.3.4}$$

where N_i and N_j are mass-eigenstate neutrinos. The total decay rate $d\Gamma$ is obtained by the sum of the individual fundamental decay rates,

*) In the $SU(2)_L \times SU(2)_R \times U(1)$ model with mirror leptons, $f_{\alpha\beta ji}$ are given by

$$f_{LLji} = U_{\mu j} U_{ei}^{*} + \lambda_0 U'_{\mu j} U'^{*}_{ei} + \eta_0 U'_{\mu j} U_{ei}^{*} + \eta_0 U_{\mu j} U'^{*}_{ei},$$
$$f_{RRji} = \lambda_0 V_{\mu j} V_{ei}^{*} + V'_{\mu j} V'^{*}_{ei} + \eta_0 V'_{\mu j} V_{ei}^{*} + \eta_0 V_{\mu j} V'^{*}_{ei},$$
$$f_{RLji} = \eta_0 V_{\mu j} U_{ei}^{*} + \eta_0 V'_{\mu j} U'^{*}_{ei} + V'_{\mu j} U_{ei}^{*} + \lambda_0 V_{\mu j} U'^{*}_{ei}, \tag{10.3.2a}$$
$$f_{LRji} = \eta_0 U_{\mu j} V_{ei}^{*} + \eta_0 U'_{\mu j} V'^{*}_{ei} + \lambda_0 U'_{\mu j} V_{ei}^{*} + U_{\mu j} V'^{*}_{ei}.$$

and is expressed in the rest frame of the muon as[133),134)]

$$\frac{d\Gamma}{d\vec{p}} = \frac{m_\mu G^2}{3(2\pi)^4}\left\{ N(\varepsilon) - \frac{(\vec{p}\cdot\vec{n}_\mu)}{\varepsilon} P(\varepsilon) + \frac{(\vec{p}\cdot\vec{n}_e)}{\varepsilon} Q(\varepsilon) \right.$$
$$\left. - \frac{(\vec{p}\times\vec{n}_\mu)\cdot(\vec{p}\times\vec{n}_e)}{p^2} R(\varepsilon) - \frac{(\vec{p}\cdot\vec{n}_\mu)(\vec{p}\cdot\vec{n}_e)}{p^2} S(\varepsilon) + \frac{\vec{n}_\mu\cdot(\vec{p}\times\vec{n}_e)}{\varepsilon} T(\varepsilon) \right\}, \tag{10.3.5}$$

where $(\varepsilon, \vec{p})$ is a positron four momentum, and $\vec{n}_e$ and $\vec{n}_\mu$ are spin polarization vectors of positron and muon in their rest frames, respectively. Explicit expressions of N, P, Q, R, S and T for the massive Dirac and Majorana neutrino cases are given by Doi, Kotani, Nishiura, Okuda and Takasugi[134)] and by Shrock.[135)]

(i) The Michel ρ parameter

The Michel ρ parameter which characterizes the end point of the spectrum part $N(\varepsilon)$ in Eq.(10.3.5) is expressed as

$$\rho = \frac{3}{4}\left\{ 1 + \frac{\sum'_{i,j}(|f_{LRji}|^2 + |f_{RLji}|^2)}{\sum'_{i,j}(|f_{LLji}|^2 + |f_{RRji}|^2)} \right\}^{-1}, \tag{10.3.8}$$

where primed sum extends over energetically allowed neutrino pairs.

According to the Particle Data group,[105)] we have

$$\rho = 0.752 \pm 0.003, \tag{10.3.9}$$

and the constraint

$$\frac{\sum'_{i,j}(|f_{LRji}|^2 + |f_{RLji}|^2)}{\sum'_{i,j}(|f_{LLji}|^2 + |f_{RRji}|^2)} < 5.4 \cdot 10^{-3}. \tag{10.3.10}$$

Let us consider the $SU(2)_L \times SU(2)_R \times U(1)$ model. For cases of Dirac neutrinos (case D) and light Majorana neutrinos (case M-I), the sum extends over all neutrinos so that the normalization condition

in Eq.(3.1.6a) can be used;

$$\sum_{i,j} |f_{LLji}|^2 = 1 , \qquad \sum_{i,j} |f_{RRji}|^2 = \lambda_0^2 ,$$
$$\sum_{i,j} |f_{LRji}|^2 = \sum_{i,j} |f_{RLji}|^2 = \eta_0^2 . \tag{10.3.11}$$

From Eqs.(10.3.10) and (10.3.11), constraints in Table 10.1 are derived by assuming that $\lambda_0^2 < 1$.

For the case M-II, we have

$$\begin{aligned}
&\sum_{i,j}{}' |f_{LLji}|^2 = \sum_{i,j}{}' |U_{\mu j}|^2 |U_{ei}|^2 = (1-\bar{u}_\mu^2)(1-\bar{u}_e^2),\\
&\sum_{i,j}{}' |f_{RRji}|^2 = \lambda_0^2 \bar{v}_\mu^2 \bar{v}_e^2 ,\\
&\sum_{i,j}{}' |f_{LRji}|^2 = \eta_0^2 (1-\bar{u}_\mu^2)\bar{v}_e^2 ,\\
&\sum_{i,j}{}' |f_{RLji}|^2 = \eta_0^2 \bar{v}_\mu^2 (1-\bar{u}_e^2),
\end{aligned} \tag{10.3.12}$$

where we have used Eqs.(10.2.8) and (10.2.9) and similar definitions of $\bar{u}_\mu$ and $\bar{v}_\mu$ to $\bar{u}_e$ and $\bar{v}_e$.

In the $SU(2)_L \times U(1)$ model with mirror leptons (case M-III), we obtain the following results by using Eqs.(10.2.11) and (10.2.12)

$$\begin{aligned}
&\sum_{i,j}{}' |f_{LLji}|^2 = (1-\bar{u}_{M\mu}^2)(1-\bar{u}_{Me}^2)\\
&\sum_{i,j}{}' |f_{RRji}|^2 = \bar{v}_{M\mu}^2 \bar{v}_{Me}^2 ,\\
&\sum_{i,j}{}' |f_{LRji}|^2 = (1-\bar{u}_{M\mu}^2)\bar{v}_{Me}^2 ,\\
&\sum_{i,j}{}' |f_{RLji}|^2 = \bar{v}_{M\mu}^2 (1-\bar{u}_{Me}^2).
\end{aligned} \tag{10.3.13}$$

By keeping leading terms, we obtain constraints in Table 10.1.

(ii) The positron spectrum in polarized μ^+ decay

Berkley group[123] reported a precise measurement of the high momentum region of the e^+ spectrum in polarized μ^+ decay. Their measured quantity is

$$R(\varepsilon, \theta) = [N(\varepsilon) - P(\varepsilon) P_\mu \cos\theta]/N(\varepsilon) , \tag{10.3.14}$$

where P_μ is the muon polarization, and $\pi-\theta$ is the angle between $\vec{p}$ and $\vec{n}_\mu$. After subtracting the radiative corrections and terms proportional to m_e, they obtained the limiting value

$$R(\varepsilon \to \varepsilon_{max}, \theta \to 0) \simeq 1 - C_\mu , \tag{10.3.15}$$

where ε_{max} is the maximum positron energy and*)

$$C_\mu = \frac{P(\varepsilon_{max})}{N(\varepsilon_{max})} P_\mu > 0.9966. \tag{10.3.16}$$

The muon polarization P_μ in the π^+ decay is obtained by using the Hamiltonian in Eq.(3.1.3). Matrix elements of the hadronic currents $J_{L\rho}(x)$ and $J_{R\rho}(x)$ are expressed as

$$\begin{aligned}
&\langle 0|J_{L\rho}(x)|\pi^+(k)\rangle = -i f_\pi \cos\theta_c k_\rho e^{-ikx},\\
&\langle 0|J_{R\rho}(x)|\pi^+(k)\rangle = +i f_\pi \cos\theta_c' k_\rho e^{-ikx},
\end{aligned} \tag{10.3.17}$$

where f_π is the pion form factor, and θ_c and θ_c' are generalized Cabbibo mixing angles defined in Eq.(3.1.11). Then the muon

*) In terms of Michel parameters,[133] we have $P(\varepsilon_{max})/N(\varepsilon_{max}) = \delta\xi/\rho$.

polarization is expressed as

$$P_\mu = 1 - 2\,\frac{\sum_j' |\varepsilon_{Aj}^{(\pi)}|^2}{\sum_j' \left(|G_{Aj}^{(\pi)}|^2 + |\varepsilon_{Aj}^{(\pi)}|^2 \right)}, \tag{10.3.18}$$

where

$$G_{Aj}^{(\pi)} = U_{\mu j} - \kappa' U'_{\mu j} \qquad \kappa' = \kappa\,(\cos\theta_c'/\cos\theta_c),$$
$$\varepsilon_{Aj}^{(\pi)} = \lambda' V_{\mu j} - \eta V'_{\mu j} \qquad \lambda' = \lambda\,(\cos\theta_c'/\cos\theta_c), \tag{10.3.19}$$

and the primed sum extends over all energetically allowed neutrinos in the π decay. The ratio of spectrum end point is given by

$$\frac{P(\varepsilon_{max})}{N(\varepsilon_{max})} = 1 - 2\,\frac{\sum_{ij}' |f_{RRji}|^2}{\sum_{ij}' (|f_{LLji}|^2 + |f_{RRji}|^2)}. \tag{10.3.20}$$

By substituting Eqs.(10.3.18) and (10.3.20) into Eq.(10.3.16), we have

$$\frac{\sum_j' |\varepsilon_{Aj}^{(\pi)}|^2}{\sum_j' (|G_{Aj}^{(\pi)}|^2 + |\varepsilon_{Aj}^{(\pi)}|^2)} + \frac{\sum_{ij}' |f_{RRji}|^2}{\sum_{ij}' (|f_{LLji}|^2 + |f_{RRji}|^2)} < 1.7 \cdot 10^{-3}. \tag{10.3.21}$$

By using Eqs.(10.3.11)-(10.3.13) and

$$\sum_j' |G_{Aj}^{(\pi)}|^2 = \begin{cases} (1-\eta_0')^2 & \text{for cases D and M-I,} \\ (1-\eta_0')^2 (1-\bar{U}_\mu^2) & \text{for case M-II,} \\ (1-\bar{U}_{M\mu}^2) & \text{for case M-III,} \end{cases} \tag{10.3.22}$$

$$\sum_j' |\varepsilon_{Aj}^{(\pi)}|^2 = \begin{cases} (\lambda_0' - \eta_0)^2 & \text{for cases D and M-I,} \\ (\lambda_0' - \eta_0)\,\bar{U}_\mu^2 & \text{for case M-II,} \\ \bar{U}_{M\mu}^2 & \text{for case M-III,} \end{cases} \tag{10.3.23}$$

we obtain constraints which are summarized in Table 10.1.[28),29)]

(iii) The longitudinal polarization — ξ' parameter

The ξ' parameter is a coefficient factor of the longitudinal polarization $Q(\varepsilon)$ in Eq.(10.3.5),[133)] and is expressed as

$$\xi' = 1 - 2\,\frac{\sum_{ij}' (|f_{RRji}|^2 + |f_{RLji}|^2)}{\sum_{ij}' (|f_{LLji}|^2 + |f_{RRji}|^2 + |f_{LRji}|^2 + |f_{RLji}|^2)}, \tag{10.3.24}$$

Recent experiment by SIN group[136)] gave the result

$$\xi' = 0.998 \pm 0.045, \tag{10.3.25}$$

from which we have

$$\frac{\sum_{ij}' (|f_{RRji}|^2 + |f_{RLji}|^2)}{\sum_{ij}' (|f_{LLji}|^2 + |f_{RRji}|^2 + |f_{LRji}|^2 + |f_{RLji}|^2)} < 4.6 \cdot 10^{-2}. \tag{10.3.26}$$

By using Eqs.(10.3.11)-(10.3.13), constrains in Table 10.1 are obtained.

§10.4 Constraints from the K decay

The longitudinal polarization P_μ of the muon emitted in the $K^+ \to \mu^+ + \nu_\mu$ decay was measured by the Tokyo-KEK group to search for the right-handed currents in the strangeness-changing process.[137)] Their result is

$$P_\mu = 0.970 \pm 0.047. \tag{10.4.1}$$

The theoretical expression for P_μ is obtained similarly to the $\pi^+ \to \mu^+ + \nu_\mu$ decay. Matrix elements for the hadronic currents

are given by

$$\langle 0|J_{L\rho}(x)|K^+(k)\rangle = -if_K \sin\theta_c\, k_\rho e^{-ikx},$$
$$\langle 0|J_{R\rho}(x)|K^+(k)\rangle = +if_K \sin\theta_c'\, k_\rho e^{-ikx}, \qquad (10.4.2)$$

where f_K is the kaon form factor, cf. Eq.(10.3.17). Then we have the constraint

$$\frac{\Sigma_j' |\xi_{Aj}^{(K)}|^2}{\Sigma_j' (|G_{Aj}^{(K)}|^2 + |\xi_{Aj}^{(K)}|^2)} < 6.2\cdot 10^{-2}, \qquad (10.4.3)$$

where

$$G_{Aj}^{(K)} = U_{\mu j} - \kappa'' U_{\mu j}', \quad \kappa'' = \kappa \frac{\sin\theta_c'}{\sin\theta_c},$$
$$\xi_{Aj}^{(K)} = \lambda'' V_{\mu j} - \eta V_{\mu j}', \quad \lambda'' = \lambda \frac{\sin\theta_c'}{\sin\theta_c}. \qquad (10.4.4)$$

By using parametrizations similar to Eqs.(10.3.22) and(10.3.23), the constraint for the leading term is given in Table 10.1.

§10.5 Comparison of constraints from the $\beta\beta$, β, μ and K decays

Experimentally known constraints on the right-handed current parameters and the mixing matrices are summarized in Table 10.1.

For all Dirac neutrinos (case D) and all light Majorana neutrinos (case M-I), *the constraints are the same and no information is* derived from the $\beta\beta$ decay. The positron spectrum in polarized μ^+ decay gives the most stringent constraint, if we assume $\theta_C = \theta_C'$,

$$|\eta_0| \simeq |\tan\zeta| < 5.8\cdot 10^{-2},$$
$$\lambda_0 \simeq (M_1/M_2)^2 < 4.1\cdot 10^{-2}. \qquad (10.5.1)$$

For the case (M-II) where there coexist the light left-handed and heavy right-handed Majorana neutrinos in the $SU(2)_L \times SU(2)_R \times U(1)$ model, the $\beta\beta$ decay gives the bounds, for example,

$$|\lambda_0' \bar{v}_e| < 7.1\cdot 10^{-6}, \qquad (10.5.2)$$
$$|\eta_0 \bar{v}_e| < 6.7\cdot 10^{-7}, \qquad (10.5.3)$$

while the bound from the μ decay is

$$|\lambda_0' - \eta_0|\cdot|\bar{v}_\mu| < 4.1\cdot 10^{-2}. \qquad (10.5.4)$$

In view of the fact that $\bar{\nu}_e$ and $\bar{\nu}_\mu$ are roughly the same order of magnitude and have the value about θ_{LR}, we conclude that the $\beta\beta$ decay gives the most stringent bound in this case.

For the case (M-III) where light left-handed neutrinos and heavy mirror Majorana neutrinos coexist, we obtain the bound on the mixing parameters $\bar{\nu}_{Me}$ and $\bar{\nu}_{M\mu}$. The most severe bound on $\bar{\nu}_{Me}$ come from the $\beta\beta$ decay, while the bound on $\bar{\nu}_{M\mu}$ is obtained from the μ decay;

$$|\bar{v}_{Me}| < 6.6\cdot 10^{-7}, \qquad (10.5.5)$$
$$|\bar{v}_{M\mu}| < 4.1\cdot 10^{-2}. \qquad (10.5.6)$$

Since it is expected that $\bar{\nu}_{Me} \sim \bar{\nu}_{M\mu} \sim O(\theta_M)$, the $\beta\beta$ decay gives the tighter bound again.

§11 Other possible test for the Majorana character of neutrino

We have investigated the neutrinoless $\beta\beta$ decay as one of most promissing processes to examine the Majorana character of neutrinos. We will discuss in this section other possibilities. One is the processes which are allowed only if neutrinos are Majorana particles [§11.1]. Next we consider the processes which occur independently of the nature of neutrinos (Dirac or Majorana), but we can still learn the Majorana character of neutrinos [§11.2]. Here we do not discuss the magnetic moments of neutrinos, because they are already discussed in §2.7.

§11.1 Total lepton number violating processes

§11.1.1 The $\beta^+\beta^+$, β^+/EC and EC/EC decays

Corresponding to the ordinary $\beta^-\beta^-$ decay, the following nuclear decays take place;

$$\beta^+\beta^+ : \quad (A, Z+2) \rightarrow (A, Z) + 2e^+ \quad (+2\nu_e), \tag{11.1.1}$$

$$\beta^+/\mathrm{EC} : \quad e^- + (A, Z+2) \rightarrow (A, Z) + e^+ \quad (+2\nu_e), \tag{11.1.2}$$

$$\mathrm{EC/EC} : \quad 2e^- + (A, Z+2) \rightarrow (A, Z) + \gamma^* \quad (\text{or } 2\nu_e), \tag{11.1.3}$$

where γ^* is the de-excitation γ ray from the final nucleus. The β^+/EC and EC/EC decays always accompany the $\beta^+\beta^+$ decay, but may occur even in cases where the $\beta^+\beta^+$ decay is energetically forbidden. In Table 11.1, natural isotopes for these decays are listed. Note that their maximum available kinetic energies are relatively small in comparison with the $\beta^-\beta^-$ decaying nuclei listed in Table 1.1. The experimental data are summarized in Table 11.2.

The decays accompanying two neutrinos take place in the minimum standard model. Hereafter, we shall concentrate only on the neutrinoless decay modes which occur only for massive Majorana neutrinos.

The $\beta^+\beta^+$ decay formula is obtained from that of the $\beta^-\beta^-$ decay by changing the sign of Z. The decay rate is suppressed considerably in comparison with the $\beta^-\beta^-$ dacay, because of the nuclear Coulomb repulsion on positrons. Explicitly, this suppression factor is given by the square of the Fermi factor F_{k-1} in Eq. (3.1.25) and of order of $\exp(-4\pi\alpha Z) \sim 10^{-2}$ as seen from the non-relativistic form given in Eq. (D.34). However, the exchange of Z and -Z gives us some interesting interplay in the relation between the P-wave and recoil effects discussed in § 3.3.2. Since the main term of the $P_{1/2}$ wave is proportional to αZ as shown in Eq. (3.1.22), the relative sign between the P-wave and recoil effects are opposite for the $\beta^-\beta^-$ and $\beta^+\beta^+$ decays. If the contributions from the P-wave (χ'_p) and recoil (χ'_R) effects in the $\beta^-\beta^-$ decay are destructive, then they are constructive in the $\beta^+\beta^+$ decay, and vice versa, as seen from Eq. (8.2.1). If they work constructively, the $\beta^+\beta^+$ decay is favorable to examine the right-handed parameter $\langle\eta\rangle$.

The kinetic energy releases of natural isotopes are in general small in the $\beta^+\beta^+$ decay, so that the $(\beta^+\beta^+)_{0\nu}$ mode is relatively enhanced in comparison with the $\beta^-\beta^-$ decay as in the case of ^{128}Te (see § 8.2.1). Therefore, it may be interesting to make the measurement of the $(\beta^+\beta^+)_{0\nu}$ mode. However, by considering the unfavorable phase space and the Coulomb suppression, we expect $T_{1/2} \gtrsim 10^{26}$ year for the $(\beta^+\beta^+)_{0\nu}$ mode because the half-life

is expected to be about 10^2 times larger by the Coulomb repulsion than the limit of the $(\beta^-\beta^-)_{0\nu}$ mode for ^{128}Te, $T_{1/2}(^{128}Te) \gtrsim 8\cdot10^{24}$ year by Kirsten.[16] Rough estimates of half-lives for the $\beta^+\beta^+$ decays for various nuclei were given by Haxton et al.[17] Vergados,[144] and Kim and Kuboderá[145] made the theoretical investigation of these decays including the neutrino emitting mode.

§11.1.2 The neutrinoless decay between pairs of single β emitters

Let us consider a pair of the single β decays without emitting neutrinos;

$$\begin{aligned}(A,Z-1) &\to (A,Z) + \bar{\nu}_e + e^- \\ &\vdots \\ \bar{\nu}_e + (A,Z-1) &\to (A,Z) + e^- .\end{aligned} \tag{11.1.4}$$

This process may occur if neutrinos are (massive) Majorana particles. It will be referred to as the β-β decay. In contrast to the ordinary $\beta\beta$ decay, the energy conservation is

$$\varepsilon_1 + \varepsilon_2 = 2(Q + m_e), \tag{11.1.5}$$

where Q is the maximum available kinetic energy of the single β ray. Therefore, one of emitted electrons can get the kinetic energy larger than the Q value, and this is a unique signal of this event. This possibility was first considered seriously by Pacheco.[146]

Let us restrict our consideration to the allowed β transition where electrons are taken to be in the S-wave. The non-relativistic impulse approximation for hadronic currents in Eq. (3.1.16) is

used. Note that the $\vec{q}$-term of the neutrino propagator in Eq. (3.3.1) does not contribute to the allowed transition, because $\vec{q}$ acts as parity odd nuclear operator.

The decay probability $\Gamma_{\beta-\beta}$ is given as follows:

$$\begin{aligned}\Gamma_{\beta-\beta} = a_{0\nu} \left(\frac{1}{m_e d}\right)^2 \left(\frac{1}{2J_i+1}\right)^2 \int d\Omega_{\beta-\beta} \\ \Big\{ \Big|\sum_j \frac{m_j}{m_e} Z_1\Big|^2 (\alpha_+ + \beta_+) \\ + \frac{a}{m_e^2}\left[\varepsilon_1^2 + \varepsilon_2^2 - 2(Q+m_e)^2\right]\left[\Big|\sum_j Z_2\Big|^2 \beta_+ + \Big|\sum_j Z_3\Big|^2 \alpha_+\right]\Big\},\end{aligned} \tag{11.1.6}$$

where d is a distance between a pair of β emitters, J_i is a nuclear spin,

$$d\Omega_{\beta-\beta} = m_e^{-5} p_1 p_2 \varepsilon_1 \varepsilon_2 \, \delta(\varepsilon_1 + \varepsilon_2 - 2(Q+m_e))\, d\varepsilon_1 d\varepsilon_2, \tag{11.1.7}$$

constant factor $a_{0\nu}$ and Coulomb corrections α_+, .. β_+ are defined in Eqs. (C.3.2) and (C.3.12), respectively. Combinations of nuclear matrix elements are defined as follows,

$$Z_1 = G_{Vj}^2 (\mathcal{M}_F)^2 - G_{Aj}^2 (\mathcal{M}_{GT})^2, \tag{11.1.8a}$$

$$Z_2 = \varepsilon_{Vj} G_{Vj} (\mathcal{M}_F)^2 - \varepsilon_{Aj} G_{Aj} (\mathcal{M}_{GT})^2, \tag{11.1.8b}$$

$$Z_3 = 2 G_{-j} \mathcal{M}_F \mathcal{M}_{GT}, \tag{11.1.8c}$$

where $\mathcal{M}_F$ and $\mathcal{M}_{GT}$ are the Fermi and Gamow-Teller reduced matrix elements, respectively, and definitions of G_{Vj}, G_{Aj}, ε_{Vj} and ε_{Aj} are in Eq. (C.1.5) and G_{-j} in Eq. (C.2.21). Derivation of $\Gamma_{\beta-\beta}$ is very similar to the usual $(\beta\beta)_{0\nu}$ decay, and given in Appendix F.

Let us discuss feasibility of this decay, and consider for

simplicity only the contribution from virtual neutrino mass part, the first term in Eq. (11.1.6). Since $d \sim 10^5$ fm and $R \sim 5$ fm, the decay rate $\Gamma_{\beta-\beta}$ is highly suppressed in comparison with $\Gamma_{0\nu}$, $\Gamma_{\beta-\beta}/\Gamma_{0\nu} = C(R/d)^2 \sim C\cdot 10^{-9}$ where C depends on ratios of nuclear matrix elements and phase space factors. However, there is some advantage for the β-β decay where the number of event per unit time $N_{\beta-\beta}$ is proportional to the product of the numbers of the first β emitters and the second ones, in contrast to the double β decay. In other words, the number of events per unit time in the $\beta\beta$ decay is $N_{\beta\beta} = N\Gamma_{0\nu}$, while in the β-β decay $N_{\beta-\beta} = (N/2)\int \Gamma_{\beta-\beta}\, n dV$, where N is the number of the β decaying nuclei (the first β emitters) and n stands for the number density of the second β emitters $n = (N_A/A)\rho$. Here N_A and ρ are the Avogadro number and the mass density, respectively. For the spherical sample with radius D, we have

$$N_{\beta-\beta}/N_{\beta\beta} = 2\pi C N_A \rho R^2 D/A \sim 2\pi C R^2(\text{fm}) D(\text{m})\cdot 10^{-2}, \quad (11.1.9)$$

where $\rho = (A/N_A)(10^{-8}\ \text{cm})^{-3}$ is used. In order that $N_{\beta-\beta}$ becomes of comparable order of $N_{\beta\beta}$, we need $D \sim 1$ cm provided $C \sim 1$. Thus we need a large amount of radioactive source. Note that the disk-like sample with the width b is not favorable, because $N_{\beta-\beta}/N_{\beta\beta} = \pi C N_A \rho R^2 b \ln(D/10^{-8}\text{cm})/A$.

§ 11.1.3 The $e^- + e^- \to W^- + W^-$ reaction

As a test of Majorana neutrinos, Rizzo proposed the reaction[147]

$$e^-(p_1) + e^-(p_2) \to W^-(k_1) + W^-(k_2). \quad (11.1.10)$$

This process is theoretically clean because hadrons do not take part in, but it requires very high energy due to large masses of gauge boson W.

Let us consider the $W_L - W_L$ or $W_R - W_R$ production in the $SU(2)_L \times SU(2)_R \times U(1)$ model with a Higgs triplet H. Due to the requirement of the helicity matching as in the case of the $(\beta\beta)_{0\nu}$ mode (see § 1.3 (i)), only the mass part of the propagating neutrino contributes. Thus the reaction amplitude for the $W_L - W_L$ or $W_R - W_R$ production is proportional to

$$\sum_j m_j (U_{ej}^2 \text{ or } V_{ej}^2)\left\{\frac{1}{(p_1-k_1)^2 - m_j^2} + \frac{1}{(p_1-k_2)^2 - m_j^2}\right\}. \quad (11.1.11)$$

The cross section for this process is considerably small because W_L couples mainly to light left-handed neutrinos. On the other hand, the large cross section is expected for the W_R-W_R production, if the right-handed neutrinos are heavy. Rizzo estimated the differential cross section at 90° and found it to be around 10^{-36} cm^2 at the energy 350 GeV, provided $m_{\nu_R} \sim$ 100 GeV and $M_{W_R} \sim 150$ GeV.

We can also consider the W_L-W_R production where the momentum part of the neutrino propagator contributes, as in the case of the $(\beta\beta)_{0\nu}$ mode. The reaction amplitude is proportional to

$$\sum_j U_{ej} V_{ej}\left\{\frac{(p_1-k_1)^\lambda}{(p_1-k_1)^2 - m_j^2} + \frac{(p_1-k_2)^\lambda}{(p_1-k_2)^2 - m_j^2}\right\}, \quad (11.1.12)$$

where $(p_1 - k_1)^\lambda$ and $(p_1 - k_2)^\lambda$ work as enhancement factors, while $U_{ej}\ V_{ej}$ gives the suppression. This reaction is interesting because less energy is needed than the W_R-W_R production. However, it is allowed even in a special model for the Dirac neutrino proposed by Enqvist, Maalampi and Mursula,[148] as discussed by Takasugi.[23] In this model, the factor $U_{ej}\ V_{ej}$ does not work as a suppression factor so that much larger cross section is expected in comparison with the Majorana neutrino case.

§ 11.1.4 The lepton number violating modes in the K decay

We consider the lepton number violating K-decays such as

$$K^- \to \pi^+ + \mu^- + \mu^- , \qquad (11.1.13)$$

$$K^- \to \pi^+ + e^- + e^- \quad (B.R. < 1\cdot 10^{-8}), \qquad (11.1.14)$$

$$K^- \to \pi^+ + e^- + \mu^- \quad (B.R. < 7\cdot 10^{-9}). \qquad (11.1.15)$$

The first two decays occur only for the Majorana neutrino, while the last process is allowed even for the Konopinski-Mahmoud Dirac neutrino (L_e-L_μ conservation). The upper limits on the branching ratio are due to the Particle Data group.[105]

Ng and Kamal,[149] and Abad, Esteve and Pacheco[150] studied the $K^- \to \pi^+ + \mu^- + \mu^-$ process within the $SU(2)_L \times U(1)$ model. Quark diagrams are given in Fig. 11.1. The decay rate is proportional to $|\langle m_\nu \rangle_\mu|^2 = |\sum_j m_j U_{\mu j}^2|^2$ because the mass part of the neutrino propagator contributes similarly to the $(\beta\beta)_{0\nu}$ mode. Abad et al. gave the branching ratio for the relatively light neutrino mass

cases;

$$\frac{\Gamma(K^- \to \pi^+ \mu^- \mu^-)}{\Gamma(K^- \to \text{all})} = \begin{cases} 1.9 \cdot 10^{-30} & (\langle m_\nu \rangle_\mu = 15\ \text{eV}), \\ 8.5 \cdot 10^{-29} & (\langle m_\nu \rangle_\mu = 100\ \text{eV}), \\ 2.1 \cdot 10^{-23} & (\langle m_\nu \rangle_\mu = 50\ \text{keV}), \\ 1.9 \cdot 10^{-16} & (\langle m_\nu \rangle_\mu = 130\ \text{MeV}). \end{cases} \qquad (11.1.16)$$

§ 11.2 Search for the Majorana character of neutrino in the total lepton number conserving processes

§ 11.2.1 The $\mu^- - e^+$ conversion

We will consider the $\mu^- - e^+$ conversion process by the muonic atom,

$$\mu^- + (A, Z+2) \to e^+ + (A, Z). \qquad (11.2.1)$$

For the ordinary Dirac neutrino case where the indivisual lepton numbers are conserved, the $\mu^- - e^+$ conversion is forbidden.

This process is of special interest in connection with the $\beta\beta$ decay: Let us consider the ν_e and ν_μ mixing where the mixing matrix is given by Eq.(2.3.3). The effective mass in the $\mu^- - e^+$ conversion is

$$\langle m_\nu \rangle_{\mu e} = \left| \sum_j m_j U_{ej} U_{\mu j} \right| = \sin\theta \cos\theta \left| m_1 - m_2 e^{2i\beta} \right|, \qquad (11.2.2)$$

in contrust to Eq.(2.3.5) for the $(\beta\beta)_{0\nu}$ mode, $\langle m_\nu \rangle = |m_1 \cos^2\theta + m_2 e^{2i\beta} \sin^2\theta|$. Let us consider the CP conserving cases; $\beta = 0$ (the same CP signs for N_1 and N_2) or $\beta = \pm\pi/2$ (the opposite CP signs for them). For $\beta = 0$, the $(\beta\beta)_{0\nu}$ mode is enhanced while the $\mu^- - e^+$ conversion is suppressed. On the other hand, the opposite situation occurs for $\beta = \pm\pi/2$ as shown in Table

11.3. In the special limit where $\beta = \pm \pi/2$ $\theta = \pi/4$ and $m_1 = m_2$, we have a Konopinski- Mahmoud Dirac neutrino (L_e -L_μ conservation). In the pseudo Dirac neutrino case ($\beta = \pi/2$, $\theta \approx \pi/4$ and $|m_1 - m_2| \ll m_1 + m_2$), the $(\beta\beta)_{0\nu}$ mode is suppressed considerably, but the $\mu^- - e^+$ conversion is allowed.

Experimental data have been reported for the branching ratio of the $\mu^- - e^+$ conversion,

$$\frac{\Gamma(\mu^- + {}^{32}S \to e^+ + {}^{32}S_i)}{\Gamma(\mu^- A - \text{capture})} < 9 \cdot 10^{-10}, \quad ^{151)} \qquad (11.2.3)$$

$$\frac{\Gamma(\mu^- + {}^{127}I \to e^+ + {}^{127}Sb)}{\Gamma(\mu^- I - \text{capture})} < 3 \cdot 10^{-10}, \quad ^{152)} \qquad (11.2.4)$$

where the last limit was obtained by assuming that the daughter nucleus is always ^{127}Sb.

Kamal and Ng,[153] and Vergados et al.[154] examined this process. We also worked out, but found somewhat different result so that we present here only our result. The difference will be discussed in Appendix F.

The essential ingredient of the $\mu^- - e^+$ conversion is that since the muon brings huge energy into the parent nucleus, the positron is emitted in the various spherical waves and the final nucleus can be in one of various excited levels. For simplicity, we present here the conversion rate due to the mass part of the neutrino propagator (see the complete formula in Appendix F),

$$\Gamma_{\mu e} = \frac{\alpha^3}{2\pi} (g_A G)^4 m_\mu^5 Z_{\text{eff}}^4 (Z-1) \cdot 2\pi\alpha Z \left|1 - \exp(2\pi\alpha Z)\right|^{-1}$$
$$\cdot \left|\sum m_j U_{ej} U_{\mu j}\right|^2 \langle N_i | \sum |\tilde{R}(r_{nn})|^2 | N_i \rangle \left(Z(Z-1)\right)^{-1}$$
$$\cdot \left\{ \left((\mathcal{A}/g_A)^2 - S\right)^2 + 2\left(3(\mathcal{A}/g_A) - S\right) + (9 - S^2) \right\}, \qquad (11.2.5)$$

where Z_{eff} is an effective nuclear charge for muon, and $\tilde{R}(r_{nn}) = (2/r_{nn}) \exp(i m_\mu r_{nn})$ is a neutrino potential. The factor S takes the value S =-3 if all pairs of protons are in the spin singlet state and S = 1 if they are in the spin triplet

state. The factor $\sum_j m_j U_{ej} U_{\mu j}$ in Eq.(11.2.5) means that the $\mu^- - e^+$ conversion takes place only when there is mixing between ν_e and ν_μ.

We obtain

$$\frac{\Gamma(\mu^- + {}^{32}S \to e^+ + {}^{32}S_i)}{\Gamma(\mu^- + {}^{32}S \to \nu_\mu + {}^{32}P)} < \begin{cases} 2 \cdot 10^{-25} & (S = -3), \\ 8 \cdot 10^{-27} & (S = 1), \end{cases} \qquad (11.2.6)$$

where the ordinary capture rate in the denominator is taken from Morita's book.[61] Here we used $\langle N_i | \sum_{nn} (Y_{nn})^2 | N_i \rangle \left(Z(Z-1)\right)^{-1} \approx (Y_{zR})^2$, R being a nuclear radius, and assumed $\Sigma_j m_j U_{ej} U_{\mu j} \approx 5.7$ eV by the analogy of the $(\beta\beta)_{0\nu}$ mode. These values are much smaller than the present experimental limits.

§ 11.2.2 The μ decay

The elementary process for the μ decay is

$$\mu^+ \to e^+ + \bar{N}_j + N_i, \qquad (11.2.7)$$

where N_i and $\bar{N}_j$ are mass-eigenstate neutrino and anti-neutrino with masses m_i and m_j, respectively.

For Dirac neutrinos, the amplitude $M_{ji}^{(a)}$ corresponding to Fig. 11.2a contributes to the decay. The decay rate $d\Gamma^{(D)}$ is given by

$$d\Gamma^{(D)} \propto \sum_{i,j}{}' |M_{ji}^{(a)}|^2, \qquad (11.2.8)$$

where primed sum is taken over only energetically allowed neutrino pairs in the μ decay and $\sum' |M_{ji}^{(a)}|^2$ is called the Dirac term.

If neutrinos are Majorana particles and there is a mixing

between ν_e and ν_μ, an additional amplitude $M_{ji}^{(b)}$ from Fig. 11.2b contributes because $N_i = \overline{N_i}$ and $\overline{N_j} = N_j$. The decay rate $d\Gamma^{(M)}$ for Majorana neutrinos is given by

$$d\Gamma^{(M)} \propto \sum_{i\geq j}{}' \varepsilon_{ij}^2 \left| M_{ji}^{(a)} + M_{ji}^{(b)} \right|^2$$

$$= \sum_{i,j}{}' \left| M_{ji}^{(a)} \right|^2 + \frac{1}{2} \sum_{i,j}{}' \mathrm{Re}\left(M_{ji}^{(a)*} M_{ji}^{(b)} \right), \qquad (11.2.9)$$

where $\varepsilon_{ij} = 1/\sqrt{2}$ for $i = j$ and 1 for $i \neq j$ and we have used the relation $\sum_{i\geq j}{}' \varepsilon_{ij}^2 \left(|M_{ji}^{(a)}|^2 + |M_{ji}^{(b)}|^2 \right) = \sum_{i,j}{}' |M_{ji}^{(a)}|^2$.

Difference between $d\Gamma^{(D)}$ and $d\Gamma^{(M)}$ comes from the interference term (Majorana term) $\sum' M_{ji}^{(a)*} M_{ji}^{(b)}$. The Majorana term can be used to discriminate Dirac or Majorana neutrinos, as pointed out by Doi, Kotani, Nishiura, Okuda and Takasugi,[134] and by Shrock.[135]

The Majorana term is suppressed in comparison with the Dirac term by the small factors m_j/m_μ, λ and η (right-handed current parameters), and its effect is in general small. However there is a term which shows the Majorana character clearly, the time reversal non-invariant term $\vec{n}_\mu \times (\vec{n}_e \times \vec{p})/\varepsilon$ in Eq.(10.3.5). The coefficeint $T(\varepsilon)$ is expressed within the Hamiltonian in Eq. (10.3.1) as

$$T(\varepsilon) = -\varepsilon_M \sum{}' \left(m_\mu \, \mathrm{Im}\, f_{Lji}^{*} f_{RRij} + 3 m_j \, \mathrm{Im}\, f_{Lji}^{*} f_{LRij} \right)$$

$$+ 3 \sum{}' m_j \, \mathrm{Im}\, f_{Lji}^{*} f_{LRji}, \qquad (11.2.10)$$

where $\varepsilon_M = 1$ for Majorana neutrinos and 0 for Dirac neutrinos and thus the first term shows the Majorana character. Note that if all neutrinos are massless, $T(\varepsilon) = 0$ due to the orthogonality condition Eq.(3.1.6b). In the $SU(2)_L \times SU(2)_R \times U(1)$ model where light and heavy neutrinos coexist, the relative order of

the first term in Eq.(10.2.10) to the second term is about $m_\mu f_{RRji}/m_j f_{LRji} \sim (\lambda_0/\eta_0)(m_\mu/m_j)\, \bar{v}_\mu$ where Eq.(10.3.2) has been used and $\bar{v}_\mu \sim V_{ji}/U_{ji} \sim \theta_{LR}, \theta_{LR}$ being defined in Eq.(A.2.9). Provided that $\lambda_0 \sim \eta_0$ and $m_\mu/m_j \sim 10^7$ with some mixing θ_{LR}, the Majorana term dominates over the Dirac term, so that the Majorana property of neutrinos can be observed in $T(\varepsilon)$ if time reversal is violated.

§11.2.3 The $\mu^+ + e^- \to \mu^- + e^+$ reaction

This reaction does not conserve the individual lepton numbers L_e and L_μ separately, but conserves the total lepton number $L_e + L_\mu$, so that the reaction occurs even for Dirac neutrinos if there is a mixing between ν_e and ν_μ.

Experimental results for the muonium-antimuonium transition have been analyzed by using the effective four Fermi interaction,

$$H_W = C \left(\frac{G}{\sqrt{2}} \right) \bar{\mu} \gamma^\rho (1-\gamma_5) e \cdot \bar{\mu} \gamma_\rho (1-\gamma_5) e + \mathrm{h.c.}, \qquad (11.2.12)$$

and the experimental upper limits on C are

$$C < \begin{cases} 5.8 \cdot 10^3 \,, & [156] \\ 6.1 \cdot 10^2 \quad (\text{from } e^- + e^- \to \mu^- + \mu^-), & [157] \\ 4.2 \cdot 10 \,, & [158] \end{cases} \qquad (11.2.13)$$

For Dirac neutrinos, only the Feynman diagram in Fig. 11.3a contributes to the transition, while for Majorana neutrinos an additional diagram in Figs. 11.3b appears.

Halprin[159] estimated the effective coupling constant*) in the

*) Halprin defined the coupling constant C as

$$H_W = C \left(\frac{G}{\sqrt{2}} \right) \left[\bar{\mu} \gamma^\rho (1-\gamma_5) e \cdot \bar{\mu} \gamma_\rho (1+\gamma_5) e + (\gamma_5 \to -\gamma_5) \right] + \mathrm{h.c.}.$$

$SU(2)_L \times SU(2)_R \times U(1)$ model by assuming no ν_e-ν_μ mixing (no contribution from Fig. 11.3a) and by using the value of the right-handed current parameters, $\lambda_0 \sim 10^{-4}$ and $\lambda_0 \gg \zeta_0$, λ_0 and ζ_0 being defined in Eqs.(A.2.7) and (A.2.8). His result is $C \simeq 3 \times 10^{-6}$ which is much smaller than the present upper limits. But if there is a Higgs triplet H with a large effective coupling to leptons, the diagram in Fig. 11.3c may become important as pointed out by Halprin.

§11.2.4 The ν_e e scattering

In gauge theory, there is no distinction between Majorana and Dirac neutrino cases in the ν_e e scattering in the massless limit of the left-handed neutrino ν_{eL}, and thus the difference between these cases is at most m_ν/ω, ω being the neutrino energy. The case where the difference appears clearly is only for heavy neutrinos. Since the admixture of heavy neutrinos in ν_{eL} is very small, it is essentially impossible to observe this effect in the ν_{eL} e scattering.

Kayser and Shrock,[160] and later Garavaglia[161] studied the $\nu_\ell \ell'$ and $\bar{\nu}_\ell \ell'$ scattering cross sections, and showed that significant difference between Majorana and Dirac neutrinos appears if incident neutrino ν_ℓ (anti-neutrino $\bar{\nu}_\ell$) is heavy.

On the other hand, Rosen[162] showed that the ratio of forward to backward cross sections of ν_e e and $\bar{\nu}_e$ e scatterings plays a role of discriminator between Dirac and Majorana neutrinos if the tensor interaction is present in the charge retention form of the effective interaction. However as far as the weak interaction

consisting of V and A currents is concerned, no difference between Dirac and Majorana neutrinos arises in the observation. The tensor interaction in the charge retention form is generated by the scalar and/or pseudoscalar interactions due to the Higgs boson exchange.

§12. Summary and remarks

A Dirac neutrino is composed of a pair of Majorana neutrinos with the same mass but with the opposite CP signs, as shown in Eq.(2.5.1). This review has been written from this standpoint, as discussed in §2. If these two Majorana neutrinos belong to the same generation, we have an ordinary Dirac neutrino, which has a conserved lepton number characterized by that generation. On the other hand, there is a case where the Dirac neutrino consists of two Majorana neutrinos of different generations. Then the difference of two lepton numbers for these generations is conserved. This type of Dirac neutrino is called the Konopinski-Mahmoud (KM) Dirac neutrino, as shown in Eq.(2.5.17) as an example.

In the gauge theory, the conservation of lepton numbers as well as the electric charge is assured by the phase transformation of fields. The Dirac field has such a phase freedom, but the Majorana field does not, because of the constraint $N^C = N$ in Eq. (2.4.33). Therefore, the Majorana neutrino makes the total lepton number non-conserving processes possible. Where is the origin of the phase freedom for the Dirac neutrino from, if it consists of two Majorana neutrinos? Let us express the Dirac neutrino as $\psi = (N_1 + iN_2)/\sqrt{2}$ in Eq.(2.5.1). Since two Majorana neutrinos N_1 and N_2 have the same mass, there is a freedom for mixing N_1 and N_2 by some arbitrary orthogonal transformation, as shown in Eq.(2.5.8). A mixing angle (α) of this transformation appears as the angle of the phase transformation for ψ, i.e.$\psi \to e^{i\alpha}\psi$, in spite of no phase freedom for each N_1 or N_2. This is the reason for the difference between the Dirac and Majorana neutrinos for the lepton number conservation.

The mass degeneracy of two Majorana neutrinos which constitute a Dirac neutrino is achieved as a consequence of the special symmetry of the neutrino mass matrix. If this symmetry of mass matrix is not the symmetry of the weak interaction, the mass degeneracy of these neutrinos is broken by the higher order perturbation of weak interaction. Thus, these mass degenerate neutrinos at the tree level split into two Majorana neutrinos with different masses, although this mass difference should be small because it comes from the loop effect due to the weak interaction. These two Majorana neutrinos with almost degenerate masses are called the pseudo Dirac (P. D.) neutrinos. An example has been presented in Eq.(2.5.18) and the relations among two Majorana, pseudo Dirac and KM Dirac neutrinos are shown in Table. 11.3.

In this review, we have taken the viewpoint that the fundamental description of the quantized neutrino field is the Majorana type. Two prescriptions for it have been used until now. One[3),4),5)] is to quantize the neutral particle field under the constraint $N^C = N$, and the other[46),47)] under the constraint $N^C = \rho_0 N$ with $|\rho_0| = 1$. It was shown in §§2.4.2 and 2.4.4 that the former prescription describes the Majorana neutrino with the positive mass. While, as shown in §2.4.5, the latter corresponds to the complex mass case, including $\rho_0 = \pm 1$ (positive and negative masses) as a special case given in Eq.(2.3.12)[44)]. The treatment of the quantized Majorana field is rather cumbersome in the latter $N^C = \rho_0 N$ case, because each neutrino propagator has to be specified by ρ_0, as shown in Eq.(2.4.48) and two Majorana neutrinos which constitute a Dirac neutrino have different masses, e.g., positive and negative masses. In general, the mass matrix is complex even for the CP

conserving case with $\rho_0 = \pm 1$, although the neutrino mixing matrix U_{ej} is an orthogonal matrix. Therefore, we have used the former prescription with the constraint $N^C = N$ in this paper: The quantized Majorana neutrino field is described in the simpler form similar to the ordinary Dirac neutrino, except no antiparticle, as shown in Eq.(2.4.26). However, even for the CP conserving case, the neutrino mixing matrix U_ν becomes a unitary matrix, an orthogonal matrix multiplied by a diagonal matrix, whose element is either 1 or (-i), depending on the even or odd CP sign of the mass eigenstate Majorana neutrino, as shown in Eq.(2.3.16) and discussed below Eq.(2.3.17).

In order to decide whether neutrinos are Majorana or Dirac, the $(\beta\beta)_{0\nu}$ mode has been shown to be the most attractive and promising experiment among many other possible processes discussed in §11. The interesting observation is that if the $(\beta\beta)_{0\nu}$ mode takes place, then the electron neutrino ν_{eL} is the massive Majorana particle. It is stated as the theorem 1 in §1.3 (iii). As its negation, if ν_{eL} is massless in all order of perturbation, then the $(\beta\beta)_{0\nu}$ decay does not take place within the framework of the gauge theory. These statements have been proved in Appendix A.1.

Experimentally, the $(\beta\beta)_{0\nu}$ mode has not yet been observed. However, the present experimental limits give the severe bounds on both the effective neutrino mass and the effective right-handed parameters by using Eq.(3.5.10) and Table 8.2. We have found from Table 8.4 and Eq.(8.2.13), $T_{0\nu}(0^+ \to 0^+;\ ^{76}\mathrm{Ge}) > 1.2 \cdot 10^{23}$yr, that

$$\langle m_\nu \rangle < (1.5 \sim 11)\mathrm{eV}, \tag{12.1}$$

$$|\langle \lambda \rangle| < (0.71 \sim 1.9)\cdot 10^{-5}, \tag{12.2}$$

$$|\langle \eta \rangle| < (0.67 \sim 2.0)\cdot 10^{-6}, \tag{12.3}$$

where main ambiguities come from the theoretical estimates of nuclear matrix elements, although there are minor uncertainties from the coexistence of three unknown parameters, as seen from an ellipsoide in Fig. 8.4 for ^{76}Ge. Concerning the latter problem, it is useful to obtain the experimental information on the $0^+ \to 2^+$ transition in the $(\beta\beta)_{0\nu}$ mode, which depends on only $\langle\lambda\rangle$ and $\langle\eta\rangle$, as shown in Table 1.2 and Eq.(3.5.23).

The accuracy of the theoretical estimate of nuclear matrix elements can be tested by the data on the $(\beta\beta)_{2\nu}$ mode. Experimental results on the $(\beta\beta)_{2\nu}$ mode gives us the unambiguous information on the ratio of the double Gamow-Teller nuclear matrix element to the energy denominator of the intermediate state, $|M_{GT}^{(2\nu)}/\mu_0|$, as shown in Eq.(3.2.13). The present theoretical estimates are larger than those from the data on ^{82}Se, ^{130}Te and ^{150}Nd, as seen from Table 7.2. Therefore, we have investigated the next correction terms due to higher spherical waves of leptons in Appendix B and it is confirmed that our formula in Eq.(3.2.13) is accurate within 1% error. Thus, it can be concluded that it is necessary to refine the theoretical treatment of $|M_{GT}^{(0\nu)}/\mu_0|$ to reproduce data on the $(\beta\beta)_{2\nu}$ mode.

In the case of the $(\beta\beta)_{0\nu}$ mode, an additional complication appears from the Coulomb type potential due to the neutrino propagation, which gives the enhancement of the short range correlation.

In order to determine the constraints on $\langle m_\nu \rangle$, the estimations

of two nuclear matrix elements $M_{GT}^{(0\nu)}$ and χ_F in Eqs.(3.5.1) and (3.5.2) are required, as shown in Table 1.1. In all previous theoretical calculations, the closure approximation has been assumed. In practice, the μ_a dependence of the neutrino potentials in Fig. 3.5 is ignored by assuming μ_a to be some average value, say 20, where $\mu_a m_e = E_a - (M_i+M_f)/2$ in Eq.(3.2.3). In order to obtain the precise value of $\langle m_\nu \rangle$, it will be necessary to estimate the effect due to this μ_a dependence. In addition, there are some correction terms which come from the vanishing terms in the closure approximation and also the higher spherical waves of electrons. These corrections have been shown to be small in §C.2.1.

Concerning the determination of the effective right-handed parameters, $\langle\lambda\rangle$ and $\langle\eta\rangle$, from the $0^+ \to 0^+$ transition, there is a large cancellation between two energy denominators for the ω term, and the nucleon recoil term (χ_R') becomes the leading one for the $\vec{q}$ term, as discussed in §3.3.2 and shown in Table 3.3. The neutrino potential appeared in this recoil term, h_R in Eq.(3.4.15), is more singular in comparison with other h_+ and h_+', as shown in Fig. 3.6. The μ_a dependence becomes stronger, as shown in Fig. 3.5. The validity of the closure approximation to evaluate χ_R' should be carefully examined. The next leading term is χ_P' (the P-wave effect $\cdots$ $\alpha Z/2$) from the $\vec{q}$ term, as seen from Table 3.3. These χ_R' and χ_P' appear only in the coefficient of $\langle\eta\rangle$. Therefore, the constraint on $\langle\eta\rangle$ depends on the relative magnitude of them, as shown in Eq.(8.2.1) and by C_3 and C_5 in Table 8.2. If there were a large cancellation between χ_R' and χ_P' as Tomoda et al.[32] argued, then the next correction terms given in Eq.(C.3.7a) should be examined carefully, which include the vanishing term in the

closure approximation.

Concerning the constraint on $\langle\lambda\rangle$, there is no large numerical coefficient in comparison with the $\langle\eta\rangle$ case, as seen from Table 8.2. The numerical values of C_2 and C_4 in Table 8.2 are sensitive to the relative magnitudes of many nuclear matrix elements in Eq. (3.5.15). When the precise value of $\langle\lambda\rangle$ is discussed, it will be desirable as the next correction term to estimate the order of magnitude of $\{z_5\}_C$ appeared in Eqs.(C.3.7b) and (C.2.45), although it is a vanishing term in the closure approximation.

As for the $0^+ \to 2^+$ transition of the $(\beta\beta)_{0\nu}$ mode, which gives another information on $\langle\lambda\rangle$ and $\langle\eta\rangle$, the nuclear matrix elements in the 2n-mechanism have been estimated by Haxton and Stephenson[17] and by Vergados[88], as given in the last paragraph of §7.2. Their values in Table 7.6 are much smaller than $M_{GT}^{(0\nu)}$ in Table 7.4. If their values are taken, then the observation of this transition due to the 2n-mechanism is hopeless by the present experimental method, as shown in Table 8.6. However, there may be still some possibility to observe this transition through the N*-mechanism, as shown in the last row of Table 8.6. In order to confirm this possibility, the further theoretical investigation will be necessary for the probability of $\Delta(1232)$ inside a nucleus [$P(\Delta)$] and the overlapping integral of the residual nuclear wave functions [$\langle\Phi_f|\Phi_i\rangle$] in Eq.(4.5). In addition, although the static SU(6) quark model has been used in this review, the recoil effect of quarks should be taken into account by using the relativistic quark model like the bag model.

In §9, the experimental constraints on $\langle m_\nu \rangle$ from the $(\beta\beta)_{0\nu}$ experiments have been compared with those on the neutrino masses

from other processes. If the mass of the left-handed electron neutrino ν_{eL} were around 20eV, as the ITEP group reported,[108] and if the neutrino were the Majorana particle, then the $(\beta\beta)_{0\nu}$ mode would really require some mechanism to suppress $\langle m_\nu \rangle$, because $\langle m_\nu \rangle$ in Eq.(12.1) is smaller than 20eV. One of candidates is the PD neutrinos mentioned above. Various other suppression mechanisms have been proposed, as summarized in §9.2. All of them utilize the destructive interference among contributions from massive Majorana neutrinos. This situation occurs, if some of neutrinos have the opposite CP sign to the rest, as shown in Eq.(2.3.5) with $\beta = \pi/2$. Therefore, when we construct some realistic gauge model to explain the masses of quarks and leptons, we have to take into account this CP character for the Majorana neutrino system. In the extreme case where all pairs of Majorana neutrinos form the Dirac or KM Dirac neutrinos, we have $\langle m_\nu \rangle = 0$ exactly, as shown in Eq.(9.1.3).

As for the effective right-handed parameters $\langle \lambda \rangle$ and $\langle \eta \rangle$, the $(\beta\beta)_{0\nu}$ mode gives the most stringent bounds, if the left-handed neutrinos are light ($m_j \lesssim 10$ MeV) and the right-handed ones are heavy, as shown in Table 10.1. However, if all neutrinos are the Dirac particles or light Majorana ones, then we have $\langle \lambda \rangle = \langle \eta \rangle = 0$. Thus the bounds from the μ decay by the Berkeley group are the severest, as shown in Eq.(10.5.1).

Let us comment on the Majoron emitting process, the $(\beta\beta)_{0\nu,B}$ mode, which is shown in Fig.7.7. It has been shown from the data on $^{128}Te/^{130}Te$ by the Heidelberg group[98] that this decay rate is much smaller than the $0^+ \to 0^+$ transition in the $(\beta\beta)_{2\nu}$ mode for the typical nuclei, as shown in Fig. 6.11.[64] The direct measurement

on ^{76}Ge by the Santa Barbara-LBL group[92] gives the contraint on the Majoron coupling constant with the light Majorana neutrino ($m_j \lesssim 10$ MeV), as given in Eq.(8.2.14).

$$|g_B| < (3.2 \sim 21) \cdot 10^{-4} . \qquad (12.4)$$

Again, the uncertainly is due to the ambiguity of the nuclear matrix element $M_{GT}^{(0\nu)}$.

We stress again the need for the definite measurements of the half-life of the $(\beta\beta)_{2\nu}$ mode, which takes place within the minimum standard model. Such experiments will give us an information on the experimental possibility to observe the $(\beta\beta)_{0\nu}$ mode as well as revealing the reliability of the theoretical treatment. Of course, the most desirable one is to observe the $(\beta\beta)_{0\nu}$ mode directly.

Acknowledgements

We would like to express our sincere thanks to Professors H. Ejiri, H. Horie, M. Kenmoku, M. Morita and K. Muto for their valuable discussions.

Also we are indebted to Professors S. M. Austin, F. T. Avignone, F. Boehm, D. O. Caldwell, A. Faessler, E. Fiorini, W. C. Haxton, B. Kayser, T. Kirsten, H. V. Klapdor, W. Kündig, O. K. Manuel, G. A. Miller, M. K. Moe, A. Morales, E. B. Norman, A. A. Pomansky, S. P. Rosen, D. Strottman, P. Vogel and L. Zamich for kindly giving us many valuable information.

Appendix A

- Majorana neutrino and the effective charged current interaction -

In §A.1, we shall give the proof of the theorems given in §1.3 (iii) on the relation between the massive Majorana neutrino and the $(\beta\beta)_{0\nu}$ mode. In §A.2.1,the structure of the effective charged current interaction is discussed for various gauge models and the effect of renormalization to hadronic currents is examined in §A.2.2.

§A.1 Proof of the theorems on Majorana neutrino and the $(\beta\beta)_{0\nu}$ mode.

The theorems 1 and 2 state that the necessary and sufficient condition for the $(\beta\beta)_{0\nu}$ mode to take place is that the electron neutrino ν_{eL} is massive Majorana particle. Here, following the argument by Takasugi,[23] we shall give the proof by using the facts mentioned in §1.3(iii), the u and d quarks and electron (e) are massive and (b) there is at least the standard V-A interaction in Eq. (1.3.1).

We first notice that the fundamental process for the $(\beta\beta)_{0\nu}$ mode is

$$d + d \rightarrow u + u + 2e^{-}, \tag{A.1.1}$$

where u and d quarks are constituents of nucleon and have charges 2/3 and -1/3, respectively. At first, we shall show that there is a non-trivial and non-vanishing contribution to the Majorana type mass term for ν_{eL}, namely $\overline{(\nu_{eL})^{c}}\nu_{eL} = -\nu_{eL}^{T}C^{-1}\nu_{eL}$.

Let us consider the diagram in Fig. A.1. The inside of broken lines corresponds to the fundamental process for the

$(\beta\beta)_{0\nu}$ mode. The black dot works as a filter which makes all quarks and electrons to have left-handed components. This is always possible thanks to the assumption (a) by mass insertion if necessary. By applying the left-handed interaction [assumption (b)] to create ν_{eL} at both vertices, we can obtain the Majorana type mass term for ν_{eL}. This is one diagram contributing to the Majorana type mass term for ν_{eL}. The problem is that there may be other diagrams which could produce the net effect of vanishing Majorana type mass term. However, such a cancellation is unlikely because it requires the fine tuning of masses and mixing angles which are unstable under the perturbation. In order to guarantee the cancellation in all orders,there needs some unbroken discrete symmetry to protect the Majorana type mass term. Such a discrete symmetry is expressed as

$$\begin{aligned} &\nu_{eL} \rightarrow \eta_{\nu}\,\nu_{eL}\,, \qquad e_{L} \rightarrow \eta_{e}\,e_{L}\,, \\ &q_{L} \rightarrow \eta_{q}\,q_{L}\ (q=u,d),\ W_{L}^{+} \rightarrow \eta_{W}\,W_{L}^{+}\,, \end{aligned} \tag{A.1.2}$$

where η is a phase factor. Let us examine whether this symmetry is compatible with the $(\beta\beta)_{0\nu}$ mode. The protection of Majorana type mass term $\nu_{eL}^{T}C^{-1}\nu_{eL}$ and the invariance of Lagrangian in Eq. (1.3.1) require the following constraints,

$$\eta_{\nu}^{2} \neq 1\,, \tag{A.1.3a}$$

$$\eta_{\nu}^{*}\eta_{e}\eta_{W} = \eta_{u}^{*}\eta_{d}\eta_{W} \tag{A.1.3b}$$

On the other hand, as discussed before (see Fig. A.1), the $(\beta\beta)_{0\nu}$ mode implies the existence of process $d_{L} + d_{L} + u_{L} + u_{L} + e_{L} + e_{L}$

which requires that

$$\eta_u^2 \eta_d^{*2} \eta_e^2 = 1 . \qquad \text{(A.1.3c)}$$

The condition in Eq. (A.1.3b) leads to $\eta_\nu = \eta_u \eta_d^* \eta_e$ which contradicts with Eqs. (A.1.3a) and (A.1.3c). This means that if the Majorana type mass term of ν_{eL} is forbidden, the $(\beta\beta)_{0\nu}$ mode does not take place (the proof of corollary). Conversely, if the $(\beta\beta)_{0\nu}$ mode is allowed, there is no protection of the Majorana type mass term for ν_{eL} by the symmetry and the cencellation between the diagram in Fig. A.1 and the other diagrams does not happen in all orders. That is, the electron neutrino ν_{eL} is the massive Majorana particle, if the $(\beta\beta)_{0\nu}$ mode takes place (the proof of the theorem 1). Also, it is clear that the existence of the Majorana type mass term for ν_{eL} ($\eta_\nu^2 = 1$) is in contradiction with forbidding the $(\beta\beta)_{0\nu}$ mode ($\eta_u^2 \eta_d^{*2} \eta_e^2 \neq 1$). Therefore if the electron neutrino ν_{eL} is a massive Majorana particle, then the $(\beta\beta)_{0\nu}$ mode should occur in some order of perturbation (the proof of the theorem 2).

So far, we have discussed the general theorems which are valid in all order of perturbation. From now on, we shall discuss the case where the electron neutrino ν_{eL} is massless at the tree level, but it becomes massive in the higher order perturbation. The question whether the $(\beta\beta)_{0\nu}$ mode occurs in this case is different from the corollary given in §1.3(iii). This situation is interesting because the neutrino mass matrix at the tree level is usually discussed when we construct the models of neutrinos.

In order to confine our argument, we shall consider a simple

example where the electron interacts with two Majorana neutrinos as

$$(g/2\sqrt{2})\,\bar{e}\gamma^\rho[\cos\theta_M(1-\gamma_5)\nu_{eL} + \sin\theta_M(1+\gamma_5)\tilde{\nu}'_{eR}]W^-_{L\rho} + h.c., \qquad \text{(A.1.4)}$$

where the right-handed neutrino $\tilde{\nu}'_{eR}$ is commonly called the mirror neutrino of the electron neutrino ν_{eL} and θ_M is introduced to represent the mixing between the electron and its mirror electron. In order to forbid the $(\beta\beta)_{0\nu}$ mode, $\tilde{\nu}'_{eR}$ is also required to be massless at the tree level because otherwise the $(\beta\beta)_{0\nu}$ mode takes place through the 2n-mechanism by the propagation of $\tilde{\nu}'_{eR}$. Next, if ν_{eL} and $\tilde{\nu}'_{eR}$ are the left- and right-handed projection of one massless Majorana neutrino N, i.e., $\nu_{eL} = N_L$ and $\tilde{\nu}'_{eR} = N_R$, then the $(\beta\beta)_{0\nu}$ mode also takes place through the 2n-mechanism because ν_{eL} and $\tilde{\nu}'_{eR}$ can be connected. However, this situation is not allowed in the gauge theories because fermions are introduced as the states with the definite chirality, and thus ν_{eL} and $\tilde{\nu}'_{eR}$ are independent each other, as shown in Eq.(3.1.6). Therefore, the $(\beta\beta)_{0\nu}$ mode does not take place. Note that the neutrino mass term is induced for ν_{eL} and $\tilde{\nu}'_{eR}$ from the one loop diagram, but it is only the Dirac type mass term. Therefore, ν_{eL} and $\tilde{\nu}'_{eR}$ form a Dirac neutrino.

In order to see this simple example from the different side, we shall consider the mixing between ν_{eL} and $\tilde{\nu}'_{eR}$ as

$$\begin{pmatrix} \nu_{eL} \\ (\tilde{\nu}'_{eR})^c \end{pmatrix} = \begin{pmatrix} \cos\alpha & -\sin\alpha \\ \sin\alpha & \cos\alpha \end{pmatrix} \begin{pmatrix} N_{1L} \\ N_{2L} \end{pmatrix}, \qquad \text{(A.1.5)}$$

where N_1 and N_2 are massless Majorana neutrinos. Now the interaction

becomes

$$(g/2\sqrt{2})\,\bar{e}\gamma^{\rho}\left[\left(\cos\theta_H\cos\alpha(1-\gamma_5)+\sin\theta_H\sin\alpha(1+\gamma_5)\right)N_1 + \left(-\cos\theta_H\sin\alpha(1-\gamma_5)+\sin\theta_H\cos\alpha(1+\gamma_5)\right)N_2\right]W_{L\rho}^{-}+h.c. \tag{A.1.6}$$

In this parametrization, $N_1(N_2)$ appears in both the left- and right-handed interactions. If $N_2(N_1)$ term were absent, the $(\beta\beta)_{0\nu}$ mode would take place even for the massless Majorana neutrino $N_1(N_2)$ at the tree level. However, in reality, the contribution from N_1 to the $(\beta\beta)_{0\nu}$ mode is compensated by that from N_2, and the $(\beta\beta)_{0\nu}$ mode is forbidden as a net effect. As we have stressed, the argument relies on the fact that in gauge theories, fermions are introduced in the chiral states as independent degrees of freedom.

§A.2 The structure of the effective charged current interaction

In §A.2.1, the magnitudes of right-handed parameters $\varkappa$, λ, η and the mixing parameters, U_{ej}, U'_{ej}, V_{ej} and V'_{ej} in the effective Hamiltonian in Eq. (3.1.3) are discussed for various gauge models. The effect from the strong and electromagnetic interactions to the left- and right-handed hadronic charged currents is also discussed in §A.2.2.

§ A.2.1 Parameters in various gauge models

(i) $SU(2)_L\times U(1)$ models

In this kind of models, neutrino masses are derived from Yukawa couplings of two left-handed doublet leptons ($\psi_{\ell L}$) and a triplet (H) or a singlet (h^-) Higgs boson. The triplet coupling is already shown in Eq. (5.1.1) and the singlet coupling is

$$f_{\ell\ell'}\,\overline{(\psi_{\ell L})^c}\,i\tau_2\,\psi_{\ell' L}\,h^- + h.c., \tag{A.2.1}$$

where $f_{\ell\ell'}=-f_{\ell'\ell}$. These are only gauge invariant couplings because $2\otimes 2 = 3\oplus 1$. After the spontaneous breaking, the triplet Higgs boson acquires a vacuum expectation value and the triplet coupling induces a Majorana type mass term for left-handed neutrinos defined in Eq. (2.2.1). The typical example is the Majoron model[40] discussed in § 5. A Majorana type mass term is also derived from the singlet coupling through the one loop diagram, as in the case of Zee model.[55] In these models, neutrinos are in

general Majorana particles. These kinds of models with only n left-handed neutrinos are called the type I in Table A.1.

If m singlet right-handed neutrinos $\nu_{\ell' R}$ are introduced in addition, then a Majorana type mass term of right-handed neutrinos defined in Eq.(2.2.7) is derived. Also a Dirac mass term in Eq.(2.2.8) is obtained from the coupling among $\psi_{\ell L}$, $\nu_{\ell' R}$ and a doublet Higgs boson ϕ. Since right-handed neutrinos appear only in the mass term, there is no right-handed gauge coupling in this case. This kind of models is called type IIA.

The Majorana type mass in Eq.(2.2.1) or (2.2.10) is diagonalized by the unitary transformation as in Eq.(2.2.2) for type I or as in Eq.(2.2.12) for type IIA. The neutrino mixing among n or n+m Majorana neutrinos is obtained by multiplying the charged-lepton transformation matrix U_ℓ as in Eq.(2.3.1). Thus these models are incorporated in the general effective interaction Hamiltonian Eq.(3.1.3) with the choice

$$U_{ej} = \begin{cases} (U_\ell^\dagger U_\nu)_{ej} & \text{for type I,} \\ (U_\ell^\dagger U_1)_{ej} & \text{for type IIA,} \end{cases} \qquad \text{(A.2.2)}$$

where j runs from 1 to n for type I, while from 1 to n+m for type IIA.

(ii) $SU(2)_L \times SU(2)_R \times U(1)$ models

Let us assume the case where n left-handed and n right-handed doublet leptons are present. In addition to Majorana type mass terms by couplings with triplet or singlet Higgs bosons, a Dirac type mass term is derived by a coupling among left- and right-handed lepton doublets and $\phi(1/2, 1/2)$ as in the case for the charged-lepton masses. Thus the mass matrix is in general a Majorana type in Eq.(2.2.10) and is diagonalized as in Eq.(2.2.12).

The neutrino mixing is obtained by multiplying the charged lepton transformation matrix as in Eq.(2.3.6).

The right-handed coupling arises due to $SU(2)_R$ and the charged current interaction is expressed as in Eq.(2.3.17). The W_L and W_R are in general not mass eigenstates and are related to the mass eigenstates W_1 and W_2 with masses M_1 and M_2 $(M_1 < M_2)$ as

$$\begin{pmatrix} W_L^- \\ W_R^- \end{pmatrix} = \begin{pmatrix} \cos\zeta & e^{i\varphi}\sin\zeta \\ -e^{-i\varphi}\sin\zeta & \cos\zeta \end{pmatrix} \begin{pmatrix} W_1^- \\ W_2^- \end{pmatrix}. \qquad \text{(A.2.3)}$$

The effective current-current interaction is obtained in the second order perturbation. This case is incorporated in a general interaction in Eq.(3.1.3) with the choice of parameters[134]

$$U_{ej} = U'_{ej} = (U_\ell^\dagger U_1)_{ej}, \quad V_{ej} = V'_{ej} = e^{-i\varphi}(V_\ell^\dagger V_1)_{ej}, \qquad \text{(A.2.4)}$$

$$\chi = \eta = \eta_0, \quad \lambda = \lambda_0, \qquad \text{(A.2.5)}$$

$$g/\sqrt{2} = (g_L^2/8M_1^2)\cos^2\zeta\,[1 + \tan^2\zeta\,(M_1/M_2)^2], \qquad \text{(A.2.6)}$$

$$\eta_0 = -(g_R/g_L)\tan\zeta\,[1-(M_1/M_2)^2]/[1+\tan^2\zeta\,(M_1/M_2)^2], \qquad \text{(A.2.7)}$$

$$\lambda_0 = (g_R/g_L)^2[(M_1/M_2)^2 + \tan^2\zeta]/[1+\tan^2\zeta\,(M_1/M_2)^2], \qquad \text{(A.2.8)}$$

where the CP violating phase φ due to the $W_L - W_R$ mixing is absorbed in the definition of the right-handed mixing matrices V's. It should be noted that the mixing parameters U_{ej} and V_{ej} satisfy the constraints in Eq.(3.1.6) due to unitarity of the matrix $\begin{pmatrix} U \\ V^* \end{pmatrix}$.

The relation between η_0 and λ_0 by eliminating Σ is shown[134] in Fig. A.2. This shows that the relative magnitude of η_0 and λ_0 is essentially arbitrary. Note that if $\lambda_0 = 0$, then η_0 should be zero.

If the mass hierarchy $O(m_L) \ll O(m_D) \ll O(m_R)$ in Eq. (2.2.1) is assumed as in the see-saw mechanism, the resultant Majorana neutrinos are separated into two groups; the light left-handed neutrinos N_I and the heavy right-handed neutrinos N_{II} where N_I and N_{II} are defined explicitly in Eq.(2.2.11). The mixing between left(light)- and right(heavy)- neutrinos is small and is expressed by θ_{LR}. Then we find

$$U_{ej} \sim O(1), \quad V_{ej} \sim O(\theta_{LR}), \quad (j \le n). \tag{A.2.9}$$

This type of models is called type IIB in Table A.1.

(iii) Mirror neutrinos[125),126)]

Mirror lepton transforms as the corresponding ordinary lepton under the gauge transformation, but has the opposite chirality (helicity) to the ordinary one. For example, the mirror doublet $\begin{pmatrix}\tilde{N}_R \\ L_R\end{pmatrix}$ transforms as doublet under $SU(2)_L$.

Let us first consider the $SU(2)_L \times U(1)$ model. Even in this case, the right-handed interaction appears,

$$\mathcal{L}_W = \frac{g}{2\sqrt{2}} \left(\bar{l} \gamma^\rho (1-\gamma_5) \nu_L + \bar{L} \gamma^\rho (1+\gamma_5) \tilde{N}_R \right) W^-_{L\rho} + \text{h.c.}, \tag{A.2.10}$$

in contrast to the $SU(2)_L \times SU(2)_R \times U(1)$ model in Eq.(2.3.17). The neutrino mass consists of Majorana type mass terms as well as a bare Dirac type mass term,

$$(\bar{\tilde{N}}_R, \bar{L}_R) m_D \begin{pmatrix}\nu_L \\ l_L\end{pmatrix} + \text{h.c.}. \tag{A.2.11}$$

Therefore, the mass matrix is expressed by the combination of Majorana and Dirac (type) mass terms and thus neutrinos are in general Majorana particles. Type III in Table A.1 corresponds to type I with mirror leptons, while type IVA to type IIA with mirror leptons. Let us define the transformation matrices for charged-leptons and neutrinos as

$$\begin{pmatrix}l_L \\ L_L\end{pmatrix} = \begin{pmatrix}U_{l1} \\ U_{l2}\end{pmatrix} \begin{pmatrix}l'_L \\ L'_L\end{pmatrix}, \quad \begin{pmatrix}l_R \\ L_R\end{pmatrix} = \begin{pmatrix}V_{l1} \\ V_{l2}\end{pmatrix} \begin{pmatrix}l'_R \\ L'_R\end{pmatrix}, \tag{A.2.12}$$

$$\begin{pmatrix}\nu_L \\ (\tilde{N}_R)^c\end{pmatrix} = \begin{pmatrix}U_1 \\ U_2^*\end{pmatrix} N_L \qquad \text{for Type III}, \tag{A.2.13}$$

$$\begin{pmatrix}\nu_L \\ (N_R)^c \\ \nu_R^c \\ \tilde{N}_L\end{pmatrix} = \begin{pmatrix}U_1 \\ U_2^* \\ V_1^* \\ V_2\end{pmatrix} N_L \qquad \text{for Type IVA}, \tag{A.2.14}$$

where $l'_{L(R)}$ and $L'_{L(R)}$ are mass eigenstate charged leptons. Now we find that these cases are incorporated in Eq.(3.1.3) with the choice

$$U_{ej} = (U_{l1}^\dagger U_1)_{ej}, \quad V'_{ej} = (V_{l1}^\dagger U_2)_{ej}, \quad \kappa = \lambda = 0, \quad \eta = 1. \tag{A.2.15}$$

It should be noted that U_{ej} and V'_{ej} satisfy the constraints in Eq.(3.1.6).

Assuming that the ordinary left-handed neutrinos (denoted by N_I) are light and the mirror neutrinos (N_{II}) are heavy, we find

$$U_{ej} \sim O(1), \quad V'_{ej} \sim O(\theta_M), \quad (j \le n), \tag{A.2.16}$$

where θ_M is the mixing between the ordinary and mirror neutrinos.

The extention to the $SU(2)_L \times SU(2)_R \times U(1)$ models with mirror leptons is straightforward. Here we present only the result:

$$
\begin{aligned}
U_{ej} &= (U_{\ell 1}^{\dagger} U_1 + \eta_0 e^{-i\phi} U_{\ell 2}^{\dagger} V_2)_{ej}, \\
\kappa U'_{ej} &= (\eta_0 U_{\ell 1}^{\dagger} U_1 + \lambda_0 e^{-i\phi} U_{\ell 2}^{\dagger} V_2)_{ej}, \\
\eta V'_{ej} &= (V_{\ell 2}^{\dagger} U_2 + \eta_0 e^{-i\phi} V_{\ell 1}^{\dagger} V_1)_{ej}, \\
\lambda V_{ej} &= (\eta_0 V_{\ell 2}^{\dagger} U_2 + \lambda_0 e^{-i\phi} V_{\ell 1}^{\dagger} V_1)_{ej}.
\end{aligned}
\qquad \text{(A.2.17)}
$$

Here U_1, U_2, V_1 and V_2 are defined similarly to Eq. (A.2.14), η_0 and λ_0 are given in Eqs. (A.2.7) and (A.2.8), and $U_{\ell 1}$, $U_{\ell 2}$, $V_{\ell 1}$ and $V_{\ell 2}$ are the transformation matrices for charged-leptons defined in Eq. (A.2.12). It is easily proved that U_{ej}, U'_{ej}, V_{ej} and V'_{ej} satisfy the constraints in Eq. (3.1.6).

By assuming that the ordinary left-handed neutrinos (N_I) are light and the others, the right-handed neutrinos and the mirror neutrinos (N_{II}) are heavy, we find the following order of estimates;

$$
U_{ej} \sim O(1), \quad \kappa U'_{ej} \sim O(\eta_0),
$$

$$
\eta V'_{ej} \sim O(\theta_H, \eta_0 \theta_{LR}), \quad \lambda V_{ej} \sim O(\eta_0 \theta_H, \lambda_0 \theta_{LR}), \quad (j \le n) \qquad \text{(A.2.18)}
$$

These results are shown in Table A.1.

§ A.2.2 The effect of renormalization to hadronic currents

In gauge theories, the left- and right-handed quark currents are expressed in the tree level as

$$
J_L^{\rho\dagger} = g_V \bar{u} \gamma^{\rho} (1-\gamma_5) d, \quad J_R^{\rho\dagger} = g'_V \bar{u} \gamma^{\rho} (1+\gamma_5) d, \qquad \text{(A.2.19)}
$$

where u and d are up and down quarks, the constituents of nucleon, and g_V and g'_V are elements of quark mixing matrix.

The strong and electromagnetic interactions are mediated

by gluons and photon through the vector coupling to quarks, respectively. Therefore, the corrections to the currents $\gamma^{\rho}(1\mp\gamma_5)$ in arbitrary order of the perturbation are expreseed as

$$
\bar{u}(p_1) \Gamma^{\mu\nu\cdots\lambda} \gamma^{\rho} (1\mp\gamma_5) \Gamma'_{\mu\nu\cdots\lambda} d(p_2), \qquad \text{(A.2.20)}
$$

where $\Gamma^{\mu\nu\cdots\lambda}$ consists of $\gamma^{\mu}, \gamma^{\nu}, \cdots, \gamma^{\lambda}, \not{p}_1, \not{p}_2$, masses of quarks and coupling constants, and similarly for $\Gamma'_{\mu\nu\cdots\lambda}$. First $\gamma^{\mu}, \gamma^{\nu}, \cdots, \gamma^{\lambda}$ in $\Gamma^{\mu\nu\cdots\lambda}$ are contracted with corresponding $\gamma_{\mu}, \gamma_{\nu}, \cdots, \gamma_{\lambda}$ in $\Gamma'_{\mu\nu\cdots\lambda}$ by shifting them to the right. Note that the chirality factors $(1\mp\gamma_5)$ flip to $(1\pm\gamma_5)$ if odd number of $\gamma^{\mu}, \gamma^{\nu}, \cdots$ pass through $(1\mp\gamma_5)$. Thus after the contraction, the form in Eq. (A.2.20) reduces to $\bar{u}(p_1)\{\tilde{\Gamma}_1 \gamma^{\rho}(1\mp\gamma_5)\tilde{\Gamma}'_1 + \tilde{\Gamma}_2 \gamma^{\rho}(1\pm\gamma_5)\tilde{\Gamma}'_2\} d(p_2)$. Now $\not{p}_1$'s in $\tilde{\Gamma}_i$ and $\tilde{\Gamma}'_i$ are gathered to the left and $\not{p}_2$'s to the right, and then equations of motion are used. Then the vertices are generally expressed as

$$
\bar{u}(p_1)\{[A\gamma^{\rho} + B p_1^{\rho} + C p_2^{\rho}](1\mp\gamma_5) + [D\gamma^{\rho} + E p_1^{\rho} + F p_2^{\rho}](1\pm\gamma_5)\} d(p_2). \qquad \text{(A.2.21)}
$$

By using $p_2 = p_1 + Q$ and the identity

$$
p_{1\mu} = -\frac{i}{2}\sigma_{\mu\nu} Q^{\nu} + \frac{1}{2}[\gamma_{\mu}\not{p}_2 + \not{p}_1\gamma_{\mu}] + Q_{\mu}, \qquad \text{(A.2.22)}
$$

we find that the corrections to $\gamma^{\rho}(1\mp\gamma_5)$ are in general parametrized as

$$
\begin{aligned}
J_L^{\rho\dagger} &= g_V \bar{u}[\gamma^{\rho} - a\gamma^{\rho}\gamma_5 + b i\sigma^{\rho\nu}Q_{\nu} + c Q^{\rho}\gamma_5] d, \\
J_R^{\rho\dagger} &= g'_V \bar{u}[\gamma^{\rho} + a\gamma^{\rho}\gamma_5 + b i\sigma^{\rho\nu}Q_{\nu} - c Q^{\rho}\gamma_5] d. \qquad \text{(A.2.23)}
\end{aligned}
$$

Here we have used the fact that g_V and g'_V are not renor-

malized due to the conservation of vector current, and the second class currents are neglected.

It is a non-trivial problem to convert the quark currents to the nucleon currents, because it involves the bound state dynamics. By the assumption that the nucleon transition is induced by the lowest order quark transition (the impulse approximation), we can obtain the form of the nucleon currents in Eq.(3.1.12).

In the above derivation, we have considered the renormalization effect due to gluons and photon which have vector couplings. Our result is valid for the wider class of interactions which respect parity conservation. For example, consider the pion exchange interaction. In this case, γ_5's appear in $\Gamma^{\mu\nu\cdots\lambda}$ and $\Gamma'^{\mu\nu\cdots\lambda}$, but always in a pair, i.e., the number of γ_5 in $\Gamma^{\mu\nu\cdots\lambda}$ is the same as in $\Gamma'^{\mu\nu\cdots\lambda}$. Then the structures $(1\mp\gamma_5)$ do not change because $\gamma_5(1\mp\gamma_5)\gamma_5=(1\mp\gamma_5)$. Therefore our argument is valid for this case. The break-down of our argument occurs, if the interaction violates parity as in the case of the weak interaction, because the interaction discriminate $(1-\gamma_5)$ and $(1+\gamma_5)$. Thus the symmetric parametrization for J_L^+ and J_R^+ in Eq.(A.2.23) is not possible.

Appendix B

- The $(\beta\beta)_{2\nu}$ mode in the 2n-mechanism -

In the text, the decay rates are presented and discussed only for the leading terms which do not vanish in the closure approximation. However, in the case where the leading terms are cancelled, we have to estimate the order of magnitude of the next correction terms in order to know the reliability of this case.

§B.1 Notation for the reduced matrix element

Before discussing the details, it is convenient to make clear the relation between our definitions of the reduced nuclear matrix elements obtained with and without using the closure approximation. Let us confine our discussion to the $0^+ \to J^+$ transition and consider the hadronic currents for the nuclear β decay within the non-relativistic impulse approximation given in Eq.(3.1.16). In the first step of the ββ decay, the m-th neutron becomes the m-th proton by the isospin raising operator τ_m^+, and its angular momentum state is changed by the irreducible nuclear tensor operator of rank k, $T^{(k)}_{m\mu}$, where the suffix m means the operator acting on the m-th nucleon and the suffix μ stands for the component of the tensor. There are four kinds of nuclear operators aside from τ_m^+; that is, $\vec{\sigma}_m$ for the spin operator, $\hat{r}_m$ for the position operator coming from higher spherical waves of leptons at the m-th β-decaying vertex, and C_m and $\vec{B}_m$ from the nucleon recoil terms in Eq.(3.1.17). The combination of them is represented by $T^{(k)}_{m\mu}$. Therefore, the operator $\Sigma_m \tau_m^+ T^{(k)}_{m\mu}$ triggess the transition from the initial nuclear state $|0_i^+\rangle$ to the intermediate nuclear state $|N_a(k)\rangle$ with the total spin k

and its μ component. Similarly, the state $|N_a(k)>$ becomes by the operator $\Sigma_n \tau_n^+ T_{n\nu}^{(\ell)}$ to the final nuclear state $|J_f^+>$ with the total spin J (parity even) and its μ+ν component ($|\ell-k| \le J \le \ell+k$). Thus, the nuclear matrix elements for the $0^+ \to J^+$ transition in the ββ decay are expressed as products of these two successive transitions.

By using the standard prescription to obtain the reduced nuclear matrix element and by defining a tensor product as usual,

$$[T_n^{(\ell)} \otimes T_m^{(k)}]^{(J)}_{\mu+\nu} = \Sigma_{\mu,\nu} C(\ell,k,J;\nu,\mu)\, T_{n\nu}^{(\ell)} T_{m\mu}^{(k)}, \quad \text{(B.1.1)}$$

we shall introduce the following abbreviation for the reduced nuclear matrix element,

$$\sum_a <J_f^+ \| [T_n^{(\ell)} \otimes T_m^{(k)}]^{(J)} f(E_a) \| 0_i^+> \equiv (-1)^{k+\ell-J} (2\ell+1)^{-1/2} \Sigma_a <J_f^+ \| \Sigma_n \tau_n^+ T_n^{(\ell)} \| N_a(k)><N_a(k)\| \Sigma_m \tau_m^+ T_m^{(k)} \| 0_i^+> f(E_a), \quad \text{(B.1.2)}$$

where $\Sigma_n \tau_n^+$ and $\Sigma_m \tau_m^+$ are not written on the left-hand side for simplicity and $f(E_a)$ is a function of the energy level (E_a) of the intermediate nuclei (N_a). Within the closure approximation, it becomes

$$[<J_f^+ \| [T_m^{(\ell)} \otimes T_m^{(k)}]^{(J)} \| 0_i^+>]_c f(<E_a>). \quad \text{(B.1.3)}$$

In the case of the scalar products

$$[T_n^{(k)} \otimes T_m^{(k)}]_0^{(0)} = (-)^k (2k+1)^{-1/2} (T_n^{(k)} \cdot T_m^{(k)}), \quad \text{(B.1.4)}$$

the following notation will be used, according to Primakoff and and Rosen,[24]

$$\begin{aligned}
&\Sigma_a <0_f^+ \| (T_n^{(k)} \cdot T_m^{(k)}) f(E_a) \| 0_i^+> \\
&\equiv -\sqrt{2k+1}\, \Sigma_a <0_f^+ \| [T_n^{(k)} \otimes T_m^{(k)}]^{(0)} f(E_a) \| 0_i^+> \\
&\equiv \sum_a (-)^k <0_f^+ \| \Sigma_n \tau_n^+ T_n^{(k)} \| N_a(k)><N_a(k)\| \Sigma_m \tau_m^+ T_m^{(k)} \| 0_i^+> f(E_a) \qquad \text{(B.1.5)} \\
&= \sum_a <0_f^+ \| \Sigma_n \tau_n^+ \| N_a(k)><N_a(k)\| \Sigma_m \tau_m^+ \| 0_i^+> (T_n^{(k)} \cdot T_m^{(k)}) f(E_a).
\end{aligned}$$

Note that there is a factor $(-1)^k$ in the third line in Eq.(B.1.5). Within the closure approximation, this is expressed as

$$[<0^+ \| (T_n^{(k)} \cdot T_m^{(k)}) \| 0^+>]_c f(<E_a>). \quad \text{(B.1.6)}$$

In the case of the $(\beta\beta)_{0\nu}$ mode, there appear the neutrino potentials depending on $r_{nm} = |\vec{r}_n - \vec{r}_m|$, so that their expansions in terms of $\vec{r}_n$ and $\vec{r}_m$ consist of all higher spherical waves, e.g., as shown in Eq.(7.2.1). In order to avoid the cumbersome expressions, these tensor operators $\hat{r}_n$ and $\hat{r}_m$ from the neutrino propagation are inculded *in* $f(E_a)$ *instead of* $T_n^{(\ell)}$ and $T_m^{(k)}$, e.g. as $f(E_a) = h_+(r_{nm}, E_a)$. Therefore, the total spin of the intermediate state can take any value, including k.

§B.2 The transition amplitude for the $0^+ \to J^+$ transition

The decay rate for the $(\beta\beta)_{2\nu}$ mode, $N_i(A,Z-2) \to N_f(A,Z)+e_1+e_2+N_j+N_{j'}$, is obtained by the use of the reaction matrix $R_{2\nu}$,

$$d\Gamma_{2\nu} = 2\pi \sum_{j\le j'} \sum_{spin} |R_{2\nu}|^2\, \delta(\varepsilon_1+\varepsilon_2+\omega_1+\omega_2+E_f-M_i) \times d\Omega_{e_1}\, d\Omega_{e_2}\, d\Omega_{N_j}\, d\Omega_{N_{j'}}, \quad \text{(B.2.1)}$$

where $\varepsilon_k = \sqrt{p_k^2+m_e^2}$ $(k=1,2)$, $\omega_\ell = \sqrt{q_\ell^2+m_j^2}$ $(\ell=1,2)$ and E_f are energies of the k-th electron, the ℓ-th neutrino with mass m_j $(j=1,\cdots n)$ and the daughter nucleus (N_f), respectively, and M_i is a mass of the parent nucleus (N_i). It is understood that the sum of j includes the suffix j of m_j appeared in the neutrino energy ω_ℓ. The phase space factors are $d\Omega_{el} = d^3p_l/(2\pi)^3$ and so on.

By applying the second order perturbation theory, $R_{2\nu}$ is given by

$$R_{2\nu} = \left(\frac{G}{\sqrt{2}}\right)^2 U_{ej} U_{ej'} \frac{\varepsilon_{jj'}}{\sqrt{2}} \sum_a \int d\vec{x}\, d\vec{y}\; J^{\rho\sigma}(\vec{x},\vec{y},a) \left[1 - P(\varepsilon_1,\varepsilon_2)\right]\left[1 - P(N_j, N_{j'})\right] \frac{L_{\rho\sigma}(\varepsilon_1\vec{x}, \omega_1\vec{x}\,;\, \varepsilon_2\vec{y}, \omega_2\vec{y})}{E_a - M_i + \varepsilon_2 + \omega_2}, \tag{B.2.2}$$

where $\varepsilon_{jj'}/\sqrt{2}$ is a statistical factor for the final electrons and neutrinos, i.e., $\varepsilon_{jj'} = 1$ for $j \neq j'$ and $= 1/\sqrt{2}$ for $j = j'$. The spin suffices of electron (ψ) and neutrino (ϕ) wave functions are omitted, E_a is a energy of the intermediate nucleus (N_a), and P(a,b) means the exchange of a and b. Here the hadronic current part is

$$J^{\rho\sigma}(\vec{x},\vec{y};a) \equiv \langle N_f | J_L^{\rho\dagger}(\vec{x}) | N_a \rangle \langle N_a | J_L^{\sigma\dagger}(\vec{y}) | N_i \rangle, \tag{B.2.3}$$

and the leptonic current part is

$$L_{\rho\sigma}(\varepsilon_1\vec{x}, \omega_1\vec{x}\,;\, \varepsilon_2\vec{y}, \omega_2\vec{y}) = \left[\bar{\psi}(\varepsilon_1\vec{x})\gamma_\rho(1-\gamma_5)\phi^c(\omega_1\vec{x})\right]\left[\bar{\psi}(\varepsilon_2\vec{y})\gamma_\sigma(1-\gamma_5)\phi^c(\omega_2\vec{y})\right]. \tag{B.2.4}$$

In the conventional analysis, the so-called closure approximation has been used frequently. However, we shall proceed by classifying terms which do or do not vanish in this approximation. For this purpose, it is convenient to parametrize the hadronic current part as

$$J^{\rho\sigma}(\vec{x},\vec{y};a) = J_+^{\rho\sigma}(\vec{x},\vec{y};a) + J_-^{\rho\sigma}(\vec{x},\vec{y};a), \tag{B.2.5}$$

where

$$J_\pm^{\rho\sigma}(\vec{x},\vec{y};a) = \frac{1}{2}\left[J^{\rho\sigma}(\vec{x},\vec{y};a) \pm J^{\sigma\rho}(\vec{y},\vec{x};a)\right] \tag{B.2.6}$$

This parametrization is the same as the one for the $(\beta\beta)_{0\nu}$ mode given in Eq.(3.3.7). As explained there, the combination $J_-^{\rho\sigma}(\vec{x},\vec{y};a)$ vanishes in the closure approximation.

By introducing $J_\pm^{\rho\sigma}$ in Eq.(B.2.6), the R matrix can be written as

$$R_{2\nu} = C_{jj'} \sum_a \left[\left\{M_{2\nu}(a)\right\}_\eta + \left\{M_{2\nu}(a)\right\}_c\right], \tag{B.2.7}$$

where

$$C_{jj'} = \frac{G^2}{2\sqrt{2}} U_{ej} U_{ej'} \varepsilon_{jj'} \left(\frac{1}{m_e}\right), \tag{B.2.8}$$

$$\left\{M_{2\nu}(a)\right\}_\eta = \int d\vec{x}\, d\vec{y}\; J_+^{\rho\sigma}(\vec{x},\vec{y};a) \begin{bmatrix} L_{\rho\sigma}(\varepsilon_1\vec{x}, \omega_1\vec{x}\,;\, \varepsilon_2\vec{y}, \omega_2\vec{y})\, K_a \\ -L_{\rho\sigma}(\varepsilon_1\vec{x}, \omega_2\vec{x}\,;\, \varepsilon_2\vec{y}, \omega_1\vec{y})\, L_a \end{bmatrix}, \tag{B.2.9a}$$

$$\left\{M_{2\nu}(a)\right\}_c = \int d\vec{x}\, d\vec{y}\; J_-^{\rho\sigma}(\vec{x},\vec{y};a) \begin{bmatrix} L_{\rho\sigma}(\varepsilon_1\vec{x}, \omega_1\vec{x}\,;\, \varepsilon_2\vec{y}, \omega_2\vec{y})\, K_{a-} \\ -L_{\rho\sigma}(\varepsilon_1\vec{x}, \omega_2\vec{x}\,;\, \varepsilon_2\vec{y}, \omega_1\vec{y})\, L_{a-} \end{bmatrix}, \tag{B.2.9b}$$

where $\{M_{2\nu}(a)\}_c$ stands for the vanishing term in the closure approximation, because it includes $J_-^{\rho\sigma}$. Here we have used

$$J_\pm^{\rho\sigma}(\vec{x},\vec{y};a) = \pm J_\pm^{\sigma\rho}(\vec{y},\vec{x};a), \tag{B.2.10}$$

$$L_{\rho\sigma}(\varepsilon_1\vec{x}, \omega_1\vec{x}\,;\, \varepsilon_2\vec{y}, \omega_2\vec{y}) = L_{\sigma\rho}(\varepsilon_2\vec{y}, \omega_2\vec{y}\,;\, \varepsilon_1\vec{x}, \omega_1\vec{x}), \tag{B.2.11}$$

and K_a and L_a are the combinations of energy denominators defined in Eq.(3.2.3) and

$$K_{a-} = m_e\left\{\left[\mu_a m_e - (\varepsilon_{12} + \omega_{12})/2\right]^{-1} - \left[\mu_a m_e + (\varepsilon_{12} + \omega_{12})\right]^{-1}\right\},$$
$$L_{a-} = m_e\left\{\left[\mu_a m_e - (\varepsilon_{12} - \omega_{12})/2\right]^{-1} - \left[\mu_a m_e + (\varepsilon_{12} - \omega_{12})\right]^{-1}\right\}, \tag{B.2.12}$$

where $\mu_a m_e$ defined in Eq.(3.2.4) is the excitation energy measured from the average value of the initial and final nuclear masses, and $\varepsilon_{12} = \varepsilon_1 - \varepsilon_2$ in Eq.(3.3.14) and $\omega_{12} = \omega_1 - \omega_2$.

As seen from Eq.(B.2.9), the coefficients of the non-vanishing term ($J_+^{\rho\sigma}$ in $\{M_{2\nu}(a)\}_\eta$) in the closure approximation have the sum of two energy denominators like K_a and L_a, while those of the vanishing term ($J_-^{\rho\sigma}$ in $\{M_{2\nu}(a)\}_C$ of Eq.(B.2.9b)) include the difference like K_{a-} and L_{a-}. Their ratios are

$$\frac{K_{a-}}{K_a} = \frac{\varepsilon_{12} + \omega_{12}}{2\mu_a m_e} \sim O\left(\frac{1}{20}\right), \quad \frac{L_{a-}}{L_a} = \frac{\varepsilon_{12} - \omega_{12}}{2\mu_a m_e} \sim O\left(\frac{1}{20}\right). \tag{B.2.13}$$

Thus, the vanishing terms in the closure approximation have the smaller coefficients by one order of magnitude in addition to the smallness due to $J_-^{\rho\sigma}$ themselves.

In order to see these situations more explicitly, it is convenient to decompose the leptonic current part $L_{\rho\sigma}$ as the product of the electron and neutrino parts by using the Fierz transformation,

$$L_{\rho\sigma}(\varepsilon_1\vec{x}, \omega_1\vec{x}; \varepsilon_2\vec{y}, \omega_2\vec{y}) = \frac{1}{2}\begin{bmatrix} t^L_{\rho\sigma}(\varepsilon_1\vec{x}, \varepsilon_2\vec{y})\, M(\omega_2\vec{y}, \omega_1\vec{x}) \\ + t^L_{\rho\sigma k}(\varepsilon_1\vec{x}, \varepsilon_2\vec{y})\, M_k(\omega_2\vec{y}, \omega_1\vec{x}) \end{bmatrix}, \tag{B.2.14}$$

where $k = 1,2,3$. The electron parts are

$$t^L_{\rho\sigma}(\varepsilon_1\vec{x}, \varepsilon_2\vec{y}) = \bar{\psi}(\varepsilon_1\vec{x})(1+\gamma_5)\gamma_\rho\gamma_\sigma\psi^c(\varepsilon_2\vec{y}) = -t^L_{\sigma\rho}(\varepsilon_2\vec{y}, \varepsilon_1\vec{x}), \tag{B.2.15a}$$

$$t^L_{\rho\sigma k}(\varepsilon_1\vec{x}, \varepsilon_2\vec{y}) = \bar{\psi}(\varepsilon_1\vec{x})(1+\gamma_5)\gamma_\rho\gamma_0\gamma_k\gamma_\sigma\psi^c(\varepsilon_2\vec{y}) = t^L_{\sigma\rho k}(\varepsilon_2\vec{y}, \varepsilon_1\vec{x}), \tag{B.2.15b}$$

and the neutrino parts are

$$M(\omega_1\vec{x}, \omega_2\vec{y}) = \bar{\phi}(\omega_1\vec{x})(1-\gamma_5)\phi^c(\omega_2\vec{y}) = -M(\omega_2\vec{y}, \omega_1\vec{x}), \tag{B.2.16a}$$

$$M_k(\omega_1\vec{x}, \omega_2\vec{y}) = \bar{\phi}(\omega_1\vec{x})(1-\gamma_5)\gamma_0\gamma_k\phi^c(\omega_2\vec{y}) = M_k(\omega_2\vec{y}, \omega_1\vec{x}). \tag{B.2.16b}$$

Thus, $\{M_{2\nu}(a)\}_\eta$ in Eq.(B.2.9a) becomes

$$\{M_{2\nu}(a)\}_\eta = -\frac{1}{2}\int d\vec{x}\, d\vec{y}\; J_+^{\rho\sigma}(\vec{x}, \vec{y}; a)\begin{Bmatrix} t^L_{\rho\sigma}[M_+(K_a+L_a) + M_-(K_a-L_a)] \\ -t^L_{\rho\sigma k}[M^k_+(K_a-L_a) + M^k_-(K_a+L_a)] \end{Bmatrix}, \tag{B.2.17}$$

where the following abbreviation has been used; $t^L_{\rho\sigma} = t^L_{\rho\sigma}(\varepsilon_1\vec{x}, \varepsilon_2\vec{y})$, $t^L_{\rho\sigma k} = t^L_{\rho\sigma k}(\varepsilon_1\vec{x}, \varepsilon_2\vec{y})$, and

$$M_\pm = [M(\omega_1\vec{x}, \omega_2\vec{y}) \pm M(\omega_1\vec{y}, \omega_2\vec{x})]/2, \qquad M^k_\pm = [M^k(\omega_1\vec{x}, \omega_2\vec{y}) \pm M^k(\omega_1\vec{y}, \omega_2\vec{x})]/2. \tag{B.2.18}$$

The hadronic current part $J_\pm^{\rho\sigma}$ consists of combinations of $J_L^{0\dagger}$ and $J_L^{k\dagger}$ which are the tensor operators of rank 0 and 1, respectively. Since the electron current part $t^L_{\rho\sigma}$ in Eq.(B.2.15a) includes $\gamma_\rho\gamma_\sigma = g_{\rho\sigma} + [\gamma_\rho, \gamma_\sigma]/2$, the nuclear operators due to the hadronic currents are of rank 0 for $J_+^{\rho\sigma}\, t^L_{\rho\sigma}$ and of rank 1 for $J_-^{\rho\sigma}\, t^L_{\rho\sigma}$, if all four leptons are in the S-wave. On the other hand, as $t^L_{\rho\sigma k}$ in Eq.(B.2.15b) includes $\gamma_\rho\gamma_0\gamma_k\gamma_\sigma$, there are three symmetric and two antisymmetric combinations of ρ and σ, so that the hadronic current part includes rank 0, 1 and 2 nuclear tensor operators. These results are summarized in Table B.1.

Let us show these characters quantitatively by contracting the suffices ρ and σ;

$$\left\{M_{2\nu}(a)\right\}_n = -\frac{1}{2}\int d\vec{x}\,d\vec{y}\; T_a \begin{Bmatrix} [X_{2\nu}E_+ + Y^{\ell}_{2\nu}E^{\ell}_-]M_+(K_a+L_a) \\ +[X_{2\nu}E_- + Y^{\ell}_{2\nu}E^{\ell}_+]M_-(K_a-L_a) \\ -[X_{-2\nu}E^{k}_+ + X^{k\ell}_{2\nu}E^{\ell}_+ + Y^{k}_{-2\nu}E_-]M^{k}_+(K_a-L_a) \\ -[X_{-2\nu}E^{k}_- + X^{k\ell}_{2\nu}E^{\ell}_- + Y^{k}_{-2\nu}E_+]M^{k}_-(K_a+L_a) \end{Bmatrix}, \quad \text{(B.2.19)}$$

where T_a is the part of the nuclear matrix element,

$$T_a = g_A^2 \langle N_f|\sum_n \tau_n^+|N_a\rangle\langle N_a|\sum_m \tau_m^+|N_i\rangle\,\delta(\vec{x}-\vec{r}_n)\,\delta(\vec{y}-\vec{r}_m), \quad \text{(B.2.20)}$$

and it is understood that the sums of n and m extend over all suffices appeared in the nuclear operators, $\vec{r}_n=\vec{x}$, $\vec{r}_m=\vec{y}$, and

$$X_{\pm 2\nu} = \pm(g_V/g_A)^2 - (\vec{\sigma}_n\cdot\vec{\sigma}_m), \quad \text{(B.2.21a)}$$

$$Y^{\ell}_{\pm 2\nu} = -i(\vec{\sigma}_n\times\vec{\sigma}_m)^{\ell} \mp (g_V/g_A)(\sigma_n-\sigma_m)^{\ell}, \quad \text{(B.2.21b)}$$

$$X^{k\ell}_{2\nu} = (\sigma_n^{\ell}\sigma_m^{k} + \sigma_n^{k}\sigma_m^{\ell}) + i(g_V/g_A)\,\varepsilon_{k\ell j}(\sigma_n+\sigma_m)^{j}. \quad \text{(B.2.21c)}$$

Here tensor operators $X_{\pm 2\nu}$ and $Y^{\ell}_{\pm 2\nu}$ are of rank 0 and 1, respectively, and $X^{k\ell}_{2\nu}$ consists of rank 0, 1 and 2 operators. Note that tensor operators which are even under the exchange of suffices n and m are denoted by X, while the odd ones by Y. The electron currents $E_{\pm}$ and $E^{\ell}_{\pm}$ in Eq. (B.2.19) are defined as

$$E_{\pm}(\varepsilon_1\vec{x};\varepsilon_2\vec{y}) = [t(\varepsilon_1\vec{x},\varepsilon_2\vec{y}) \pm t(\varepsilon_1\vec{y},\varepsilon_2\vec{x})]/2,$$
$$E^{\ell}_{\pm}(\varepsilon_1\vec{x};\varepsilon_2\vec{y}) = [t^{\ell}(\varepsilon_1\vec{x},\varepsilon_2\vec{y}) \pm t^{\ell}(\varepsilon_1\vec{y},\varepsilon_2\vec{x})]/2, \quad \text{(B.2.22)}$$

where

$$t(\varepsilon_1\vec{x},\varepsilon_2\vec{y}) = \bar{\psi}(\varepsilon_1\vec{x})(1+\gamma_5)\psi^{c}(\varepsilon_2\vec{y}),$$
$$t^{\ell}(\varepsilon_1\vec{x},\varepsilon_2\vec{y}) = \bar{\psi}(\varepsilon_1\vec{x})(1+\gamma_5)\gamma^{0}\gamma^{\ell}\psi^{c}(\varepsilon_2\vec{y}). \quad \text{(B.2.23)}$$

Similarly, the vanishing part $\{M_{2\nu}\}_c$ in the closure approximation in Eq.(B.2.9b) becomes

$$[M_{2\nu}]_c = -\frac{1}{2}\int d\vec{x}\,d\vec{y}\; T_a \begin{Bmatrix} [X_{2\nu}E_- + Y^{\ell}_{2\nu}E^{\ell}_+]M_+(K_{a-}+L_{a-}) \\ +[X_{2\nu}E_+ + Y^{\ell}_{2\nu}E^{\ell}_-]M_-(K_{a-}-L_{a-}) \\ -[X_{-2\nu}E^{k}_- + X^{k\ell}_{2\nu}E^{\ell}_- + Y^{k}_{-2\nu}E_+]M^{k}_+(K_{a-}-L_{a-}) \\ -[X_{-2\nu}E^{k}_+ + X^{k\ell}_{2\nu}E^{\ell}_+ + Y^{k}_{-2\nu}E_-]M^{k}_-(K_{a-}+L_{a-}) \end{Bmatrix}, \quad \text{(B.2.24)}$$

The so-called closure approximation can formally be expressed as the omission of the odd part under the exchange of suffices n and m, i.e. $\vec{x}\neq\vec{y}$, as seen from T_a in Eq.(B.2.20). Under the exchange $\vec{x}\neq\vec{y}$, the electron and neutrino parts are transformed as $E^{(\ell)}_{\pm}\Rightarrow\pm E^{(\ell)}_{\pm}$ and $M^{(k)}_{\pm}\Rightarrow\pm M^{(k)}_{\pm}$. By taking into account the even and odd characters of X and Y, respectively, it can be seen easily that $\{M_{2\nu}(a)\}_n$ is even for $n\neq m$, while $\{M_{2\nu}(a)\}_c$ is odd so that it vanishes in the closure approximation.

So far, we do not make any assumptions for the lepton wave functions. Let us assume that all leptons are in the S-wave state and only the leading terms of their radial wave functions are retained, i.e. $j_0(kr)\sim 1$ for neutrino and $\psi^{(S)}(\varepsilon,r)$ with $r=0$ in Eq.(3.1.20a) for electrons. The latter assumption will be referred to as no finite de Broglie wave length correction (no FBWC).

Then, the position operators of leptons can be put equal to zero, $\vec{x} = \vec{y} \approx 0$ in the neutrino current $M(\omega_1 \vec{x}, \omega_2 \vec{y})$ and the electron current $t(\varepsilon_1 \vec{x}; \varepsilon_2 \vec{y})$, so that $M_- = M_-^k = E_- = E_-^\ell = 0$. Thus, Eqs. (B.2.19) and (B.2.24) become simpler forms;

$$\left\langle M_{2\nu}(a)\right\rangle_\eta = -\frac{1}{2}\int d\vec{x}\, d\vec{y}\, T_a \begin{Bmatrix} X_{2\nu} E_+ M_+ (K_a + L_a) \\ -[X_{-2\nu} E_+^k + X_{2\nu}^{k\ell} E_+^\ell] M_+^k (K_a - L_a) \end{Bmatrix}, \quad \text{(B.2.25)}$$

and

$$\left\langle M_{2\nu}(a)\right\rangle_c = -\frac{1}{2}\int d\vec{x}\, d\vec{y}\, T_a \begin{Bmatrix} Y_{2\nu}^\ell E_+^\ell M_+ (K_{a-} + L_{a-}) \\ -Y_{-2\nu}^k E_+ M_+^k (K_{a-} - L_{a-}) \end{Bmatrix}. \quad \text{(B.2.26)}$$

There is no extra nuclear operator except $X_{\pm 2\nu}$, $Y_{\pm 2\nu}^\ell$ and $X_{2\nu}^{k\ell}$, if all leptons are in the S-wave. Selection rules for the $0^+ \to J^+$ transition are obtained from X and Y. As a result, some special combinations of the energy denominators appear, as shown in Table B.1. It is worthwhile to note from Table B.1 that the cancellation of the energy denominators such as $(K_a - L_a)$ is the origin for the suppression of the $0^+ \to 2^+$ transition, as shown in Eq. (3.2.18).

§B.3 The decay rate for the $0^+ \to J^+$ transition

In the case where all leptons are in the S-wave state, by substituting Eqs. (B.2.25) and (B.2.26) into Eqs. (B.2.7) and (B.2.1), the decay rate for the $0^+ \to J^+$ transition ($J \le 2$) is expressed as

$$d\Gamma_{2\nu}(0^+ \to J^+) = a_{2\nu}\left[A_J^{(2\nu)} + (\hat{p}_1 \cdot \hat{p}_2) B_J^{(2\nu)}\right] d\Omega_{2\nu}, \quad \text{(B.3.1)}$$

where the constant factor $a_{2\nu}$ and the phase space factor $d\Omega_{2\nu}$ are defined as

$$a_{2\nu} = \left[(G g_A)^4 m_e^9 / (64\pi^7)\right] \xi_p \quad \text{(B.3.2)}$$

$$\xi_p = 2 \sum_{i \le j}{}' \varepsilon_{ij}^2 \left| U_{ei} U_{ej} \right|^2 \quad \text{(B.3.3)}$$

$$d\Omega_{2\nu} = m_e^{-11} p_1 p_2 \varepsilon_1 \varepsilon_2 \omega_1 \omega_2 \delta(\varepsilon_1 + \varepsilon_2 + \omega_1 + \omega_2 + E_f - M_i) \, d\omega_1 \, d\omega_2 \, d\varepsilon_1 \, d\varepsilon_2 \, d(\hat{p}_1 \cdot \hat{p}_2). \quad \text{(B.3.4)}$$

Here the primed sum in ξ_p means to extend over all energetically allowed neutrino pairs in the final states. Rigorously speaking, the sum of i and j in Eq. (B.3.3) should be taken for contributions from various mass-eigenstate neutrinos in $\omega = \sqrt{q^2 + m_j^2}$. If $m_j \ll 1$ MeV, this sum is taken only for the mixing matrices U_{ej}, because $\langle q \rangle \gg m_j$. If all neutrinos are light ($m_j < 1$MeV), we find $\xi_p = 1$.
In the case of heavier neutrinos with $m_j \gtrsim T m_e$, they are not produced in the $(\beta\beta)_{2\nu}$ mode, but it is expected that $|U_{ej}| \ll 1$. In practice, we shall take $\xi_p = 1$.

§B.3.1 The $0^+ \to 0^+$ transition

In this transition, the spectrum part $A_0^{(2\nu)}$ in Eq. (B.3.1) is

$$A_0^{(2\nu)} = a(\varepsilon_1, \varepsilon_2)\left\{\left|A_{GT}^{(+)} - \left(\frac{g_\nu}{g_A}\right)^2 A_F^{(+)}\right|^2 + \frac{1}{3}\left|A_{GT}^{(-)} + 3\left(\frac{g_\nu}{g_A}\right)^2 A_F^{(-)}\right|^2\right\}, \quad \text{(B.3.5)}$$

where the Coulomb factor $a(\varepsilon_1, \varepsilon_2)$ is defined as

$$a(\varepsilon_1, \varepsilon_2) = |\alpha_{-1-1}|^2 + |\alpha_{11}|^2 + |\alpha_{-11}|^2 + |\alpha_{1-1}|^2, \quad \text{(B.3.6)}$$

$$\alpha_{\kappa\lambda} = \tilde{A}_\kappa(\varepsilon_1)\, \tilde{A}_\lambda(\varepsilon_2), \quad \text{(B.3.7)}$$

because the electron Coulomb S-wave is the normalization $\tilde{A}_\kappa(\varepsilon)$ only as given in Eq.(3.1.21), see also Eq.(B.3.13) and Eq.(D.18) in Appendix D. The combinations of the nuclear matrix elements and the energy denominators are

$$A_{GT}^{(\pm)} = \frac{1}{2}\sum_a M_{GTa}^{(2\nu)}\,(K_a \pm L_a), \tag{B.3.8a}$$

$$A_{F}^{(\pm)} = \frac{1}{2}\sum_a M_{Fa}^{(2\nu)}\,(K_a \pm L_a). \tag{B.3.8b}$$

The nuclear matrix elements $M_{GTa}^{(2\nu)}$ and $M_{Fa}^{(2\nu)}$ in Eq.(3.2.2) come from $X_{\pm 2\nu}$ and $X_{2\nu}^{kk}$ in Eq.(B.2.21) and the combinations of (K±L) is clear from Table B.1. As it is already pointed out in Eq.(3.2.19), the factor (K-L) is smaller by μ_a^{-2} than (K+L), so that contributions from $A_{GT}^{(-)}$ and $A_F^{(-)}$ can be neglected. Thus, within the good accuracy, say less than 1% errors, we have

$$A_o^{(2\nu)} = a(\varepsilon_1,\varepsilon_2)\,\left|A_{GT}^{(+)} - (g_\nu/g_A)^2 A_F^{(+)}\right|^2. \tag{B.3.9}$$

which is used to derive Eq.(3.2.1).

It may be helpful to note that the previous result obtained in the closure approximation is, for example, for the case with $A_F^{(\pm)}=0$,

$$A_0^{(2\nu)} \simeq a(\varepsilon_1,\varepsilon_2)\left|\left[\langle 0^+\|(\sigma_n\cdot\sigma_m)\|0^+\rangle\right]_c\right|^2\left\langle\tfrac{1}{4}(K+L)^2+\tfrac{1}{12}(K-L)^2\right\rangle, \tag{B.3.10}$$

where Eq.(B.1.6) has been used.

Similarly, the angular correlation part $B_0^{(2\nu)}$ in Eq.(B.3.1) is

$$B_0^{(2\nu)} = -2\,b(\varepsilon_1,\varepsilon_2)\left\{\left|A_{GT}^{(+)}-\left(\frac{g_\nu}{g_A}\right)^2 A_F^{(+)}\right|^2-\frac{1}{9}\left|A_{GT}^{(-)}+3\left(\frac{g_\nu}{g_A}\right)^2 A_F^{(-)}\right|^2\right\}$$

$$\simeq -2\,b(\varepsilon_1,\varepsilon_2)\left|A_{GT}^{(+)}-(g_\nu/g_A)^2 A_F^{(+)}\right|^2, \tag{B.3.11}$$

where

$$b(\varepsilon_1,\varepsilon_2) = Re\left[\alpha_{-1-1}^*\,\alpha_{11}+\alpha_{-11}^*\,\alpha_{1-1}\right]. \tag{B.3.12}$$

Until now, we have used the full expression of the electron Coulomb wave function in the uniform charge distribution of the nuclear charge. If we use the approximated form in Eq.(3.1.24), then we have

$$a(\varepsilon_1,\varepsilon_2) \simeq \varepsilon_1\varepsilon_2\,C_{00}, \tag{B.3.13}$$

$$b(\varepsilon_1,\varepsilon_2) \simeq (1/2)p_1p_2\,C_{00}, \tag{B.3.14}$$

where

$$C_{k\ell} = F_k(Z,\varepsilon_1)\,F_\ell(Z,\varepsilon_2)\,/\,\varepsilon_1\varepsilon_2, \tag{B.3.15}$$

$F_k(Z,\varepsilon)$ being defined in Eq.(3.1.23). This is valid up to the order $(\alpha Z)^2$, as discussed below Eq.(D.18) in Appendix D.

Finally, let us estimate the order of magnitude of the next order correction terms, because this $0^+\to 0^+$ transition is useful to test theoretical estimates of the nuclear matrix elements. The largest correction term due to the higher spherical waves should come from the case where both electrons are emitted in the P-wave (j = 1/2) state, so that its magnitude relative to the S-wave case should be $(\alpha Z/2)^2$ kinematically, as seen from Eq.(3.1.22), in addition to the suppression due to the nuclear matrix elements which include the $(r/R)^2$ term, where r is the position of the decaying neutron. The similar corrections come from the finite de Broglie wave length correction (FBWC) for the electron S-wave function, $(\bar{p}r)^2/6$ in Eq.(D.13) in Appendix D. Thus, these corrections are less than a few percent.

§B.3.2 The $0^+\to 2^+$ transition

In the case where all leptons are emitted in the S-wave state, the spectrum part $A_2^{(2\nu)}$ and the angular correlation part $B_2^{(2\nu)}$

in Eq. (B.3.1) are

$$A_2^{(2\nu)} = a(\varepsilon_1,\varepsilon_2)\left|M_2^{(2\nu)}/\mu_2^3\right|^2(\langle K_A\rangle-\langle L_A\rangle)^2\langle\mu_A\rangle^6, \qquad (B.3.16)$$

$$B_2^{(2\nu)} = (2/3)\,b(\varepsilon_1,\varepsilon_2)\left|M_2^{(2\nu)}/\mu_2^3\right|^2(\langle K_A\rangle-\langle L_A\rangle)^2\langle\mu_A\rangle^6, \qquad (B.3.17)$$

where the reduced nuclear matrix element is defined in Eq. (3.2.17) by using Eq. (B.1.3), that is,

$$\left(M_2^{(2\nu)}/\mu_2^3\right) = \sum_a \langle 2^+\|\left[\sigma_n\otimes\sigma_k\right]^{(2)}\mu_a^{-3}\|0^+\rangle. \qquad (B.3.18)$$

This transition rate is smaller by a factor μ_a^{-4} than the $0^+\to0^+$ transition, as shown in Table B.1. Thus, we like to know contributions from the higher partial waves of leptons with the additive combination of the energy denominator like (K+L). As it is shown in case 2, 3 and 4 of Table B.2, such terms are obtained, for example, from the $D_{3/2}$ wave for one of electrons, and have the $\alpha Z(r/R)^2(pR)$ factor which is of order of 10^{-3}. The combination of two $P_{1/2}-P_{1/2}$ electron waves which gives the largest contribution from the viewpoint of lepton wave has the small energy denominator (K-L) (case 5). The nucleon recoil effect is small in the $(\beta\beta)_{2\nu}$ mode (cases 6 and 7).

In summary, we conclude that the $0^+\to2^+$ transition rate is much smaller than that of the $0^+\to0^+$ transition.

Appendix C

— The $(\beta\beta)_{0\nu}$ mode in the 2n-mechanism —

§C.1 Combinations of the right-handed parameters

The neutrino in this mode propagates as a virtual fermion between two vertices in the second order perturbation theory, as shown in Eq. (3.3.1). Therefore, it is convenient to classify the types of the weak interactions by the electron currents. The effective charged current Hamiltonian in Eq. (3.1.3) is rewritten as

$$H_w = \frac{G}{\sqrt{2}}\sum_j\left\{j_{L\rho j}\tilde{J}_{Lj}^{\rho\dagger} + j_{R\rho j}\tilde{J}_{Rj}^{\rho\dagger}\right\} + h.c., \qquad (C.1.1)$$

where the leptonic currents are, instead of Eq. (3.1.4),

$$j_{L\rho j} = \bar{e}\gamma_\rho(1-\gamma_5)N_{j\nu}, \quad j_{R\rho j} = \bar{e}\gamma_\rho(1+\gamma_5)N_{j\nu}, \qquad (C.1.2)$$

and the combinations of hadronic currents are

$$\tilde{J}_{Lj}^{\rho\dagger} = U_{ej}J_L^{\rho\dagger} + \varkappa U'_{ej}J_R^{\rho\dagger}, \qquad (C.1.3a)$$

$$\tilde{J}_{Rj}^{\rho\dagger} = \lambda V_{ej}J_R^{\rho\dagger} + \eta V'_{ej}J_L^{\rho\dagger}. \qquad (C.1.3b)$$

Within the non-relativistic impulse approximation given in Eq. (3.1.16), $\tilde{J}_L^{\rho\dagger}$ and $\tilde{J}_R^{\rho\dagger}$ are expressed as

$$\tilde{J}_{Lj}^{\rho\dagger}(\vec{x}) = g_A\sum_n\tau_n^+\left[(G_{Vj}-G_{Aj}C_n)g^{\rho0} + (G_{Aj}\sigma_n^k - G_{Vj}D_n^k)g^{\rho k}\right]\delta(\vec{x}-\vec{r}_n),$$

$$\tilde{J}_{Rj}^{\rho\dagger}(\vec{x}) = g_A\sum_n\tau_n^+\left[(\varepsilon_{Vj}+\varepsilon_{Aj}C_n)g^{\rho0} + (-\varepsilon_{Aj}\sigma_n^k - \varepsilon_{Vj}D_n^k)g^{\rho k}\right]\delta(\vec{x}-\vec{r}_n), \qquad (C.1.4)$$

where

$$G_{Vj} = (U_{ej} + \kappa' U'_{ej})(g_V/g_A), \qquad \kappa' = \kappa(g'_V/g_V),$$

$$G_{Aj} = (U_{ej} - \kappa' U'_{ej}),$$

$$\varepsilon_{Vj} = (\lambda' V_{ej} + \eta V'_{ej})(g_V/g_A), \qquad \lambda' = \lambda(g'_V/g_V),$$

$$\varepsilon_{Aj} = (\lambda' V_{ej} - \eta V'_{ej}). \tag{C.1.5}$$

Since it is generally considered that $|\kappa'|$ should be less than unity, i.e. $|\kappa' U'_{ej}| \ll |U_{ej}|$, we have $G_{Vj} \simeq (g_V/g_A)U_{ej}$ and $G_{Aj} \simeq U_{ej}$, so that the parameter κ has in effect no contribution to the $\beta\beta$ decay. Thus, the right-handed parameters (η and λ') and the neutrino mass (m_ν) are relevant to the $(\beta\beta)_{0\nu}$ mode, but in this Appendix C, the results are given by using $G_{V(A)}$ and $\varepsilon_{V(A)}$.

Hereafter, suffix j of $\tilde{J}_{L(R)j}$ and G_{Vj} and so on is suppressed to avoid the complication.

§C.2 The transition amplitudes

The decay rate $d\Gamma_{0\nu}$ for the process $N_i(A,Z-2) \to N_f(A,Z) + e_1 + e_2$ is obtained as

$$d\Gamma_{0\nu} = 2\pi \sum_{spin} |R_{0\nu}|^2 \delta(\varepsilon_1 + \varepsilon_2 + E_f - M_i)\, d\Omega_{e_1}\, d\Omega_{e_2}. \tag{C.2.1}$$

The notation is the same as for the $(\beta\beta)_{2\nu}$ case in Eq.(B.2.1)

After contracting the neutrinos as done in Eq.(3.3.1), the reaction matrix element is expressed as

$$R_{0\nu} = \frac{1}{\sqrt{2!}} \left(\frac{G}{\sqrt{2}}\right)^2 2 \sum_j \int d\vec{x}\, d\vec{y} \int \frac{d\vec{q}}{2\omega\,(2\pi)^3} e^{i\vec{q}\cdot(\vec{x}-\vec{y})}$$

$$\sum_\alpha \left[m_j (J^{\rho\sigma}_{LL} S_{L\rho\sigma} + J^{\rho\sigma}_{RR} S_{R\rho\sigma}) + (J^{\rho\sigma}_{LR} V_{L\rho\sigma} + J^{\rho\sigma}_{RL} V_{R\rho\sigma}) \right], \tag{C.2.2}$$

where the energy integration of the virtual neutrino has been performed, so that the denominator of the neutrino propagator $(q^2 - m_j^2)^{-1}$ in Eq.(3.3.1) is replaced by its residue π/ω_j. The first two terms proportional to m_j in the square bracket are the m_ν part, while the last two are the V+A part, as discussed below Eq.(3.3.1). The $J^{\rho\sigma}_{\alpha\beta}(\vec{x},\vec{y};a)$, corresponding to Eq.(B.2.3) in the $(\beta\beta)_{2\nu}$ mode, is the product of hadronic current parts, which are defined in Eqs. (3.3.3) and (3.3.16). Here, α and β stand for either L(V-A) or R(V+A) vertices. The remaining $S_{\alpha\rho\sigma}$ and $V_{\alpha\rho\sigma}$ are the electron currents divided by the energy denominator of the second order perturbation and are defined in Eqs.(3.3.4) and (3.3.17),*) respectively.

The m_ν and V+A parts include the even and odd numbers of γ's due to the numerator of neutrino propagator, respectively, as seen from Eq.(3.3.1). The corresponding electron currents $t^L_{\rho\sigma}$ in Eq.(3.3.5) and $u^L_{\rho\sigma}$ in Eq.(3.3.18) have different characters, see Eqs.(3.3.10) and (3.3.19). Therefore, it is convenient to treat these parts separately:

$$R_{0\nu} = C_{0\nu} \sum_j \sum_a \left\{ \left(\frac{m_j}{m_e}\right) \left[M_{m_\nu}(a,L) + M_{m_\nu}(a,R) \right] + M_{V+A}(a) \right\}, \tag{C.2.4}$$

where

$$C_{0\nu} = (G^2/\sqrt{2})\,(1/8\pi)\,(2m_e/R), \tag{C.2.5}$$

$$M_{m_\nu}(a,\alpha) = \frac{R}{2} \int d\vec{x}\, d\vec{y} \int \frac{d\vec{q}}{2\pi^3\omega} e^{i\vec{q}\cdot(\vec{x}-\vec{y})} J^{\rho\sigma}_{\alpha\gamma} S_{\gamma\rho\sigma}, \tag{C.2.6}$$

$$M_{V+A}(a) = \frac{R}{2m_e} \int d\vec{x}\, d\vec{y} \int \frac{d\vec{q}}{2\pi^3\omega} e^{i\vec{q}\cdot(\vec{x}-\vec{y})} (J^{\rho\sigma}_{LR} V_{L\rho\sigma} + J^{\rho\sigma}_{RL} V_{R\rho\sigma}). \tag{C.2.7}$$

---

*) The electron current $t^R_{\rho\sigma}$ in $S_{R\rho\sigma}$ corresponding to Eq.(3.3.4) is

$$t^R_{\rho\sigma}(\varepsilon_1 \vec{x};\ \varepsilon_2 \vec{y}) = \bar{\psi}(\varepsilon_1 \vec{x})\, \gamma_\rho (1+\gamma_5)\, \gamma_\sigma\, \psi^c(\varepsilon_2 \vec{y}). \tag{C.2.3}$$

§C.2.1 The m_ν part

Let us discuss the $M_{m_\nu}(a,L)$ part first,

$$M_{m_\nu}(a,L) = (R/2)\int d\vec{x}\, d\vec{y}\, \{ H_2\, t^L_{\rho\sigma}(\epsilon_1\vec{x};\epsilon_2\vec{y}) + H_1\, t^L_{\sigma\rho}(\epsilon_1\vec{y};\epsilon_2\vec{x})\}\, J^{\rho\sigma}_{LL}(\vec{x},\vec{y},a), \tag{C.2.8}$$

where $H_k(|\vec{x}-\vec{y}|, E_a)$ is defined in Eq.(3.4.2), and Eqs.(3.3.4) and (3.3.10) have been used. It is easy to rewrite Eq.(C.2.8) as

$$M_{m_\nu}(a,L) = \int d\vec{x}\, d\vec{y}\, J^{\rho\sigma}_{LL}(\vec{x},\vec{y},a)\left(\frac{R}{2}\right)\left[(H_2+H_1)E^{L(+)}_{\rho\sigma} + (H_2-H_1)E^{L(-)}_{\rho\sigma}\right], \tag{C.2.9}$$

where

$$E^{L(\pm)}_{\rho\sigma}(\epsilon_1\vec{x};\epsilon_2\vec{y}) = [t^L_{\rho\sigma}(\epsilon_1\vec{x};\epsilon_2\vec{y}) \pm t^L_{\sigma\rho}(\epsilon_1\vec{y};\epsilon_2\vec{x})]/2. \tag{C.2.10}$$

By contracting ρ and σ and replacing $(H_2 \pm H_1)$ by $h_+(r_{nm}, E_a)$ in Eq.(3.4.1) and $h_0(r_{nm}, E_a)$ in Eq.(3.4.5), we find

$$\{M_{m_\nu}(a,L)\}_n = \frac{1}{2}\int d\vec{x}\, d\vec{y}\, T_a\, h_+ [X_1 E_+ + Y^\ell_1 E^\ell_-], \tag{C.2.11a}$$

$$\{M_{m_\nu}(a,L)\}_C = \frac{\epsilon_{12} R}{4}\int d\vec{x}\, d\vec{y}\, T_a\, h_0 [X_1 E_- + Y^\ell_1 E^\ell_+], \tag{C.2.11b}$$

where $\{M_{m_\nu}(a,L)\}_n$ and $\{M_{m_\nu}(a,L)\}_C$ are the non-vanishing and vanishing parts of M_{m_ν} in the closure approximations, respectively, as explained later. The electronic currents $E_\pm$ and $E^\ell_\pm$ are defined in Eq.(B.2.22) for the $(\beta\beta)_{2\nu}$ mode. The abbreviation T_a is the part of the nuclear matrix element defined in Eq.(B.2.20). The sums of n and m in T_a extend over not only $r_{nm} = |\vec{x}-\vec{y}|$ in h_+ and h_0 but also the following nuclear operators from the hadronic currents;

$$X_1 = X_{1S} + X_{1R},$$

$$X_{1S} = G_V^2 - G_A^2(\vec{\sigma}_n\cdot\vec{\sigma}_m),$$

$$X_{1R} = -G_V G_A (C_+ - D^{kk}_{\sigma+}), \tag{C.2.12a}$$

$$Y^\ell_1 = Y^\ell_{1V} + Y^\ell_{1R},$$

$$Y^\ell_{1V} = -i G_A^2 (\vec{\sigma}_n\times\vec{\sigma}_m)^\ell - G_V G_A \sigma^\ell_-,$$

$$Y^\ell_{1R} = i G_V G_A \varepsilon_{ikl} D^{ik}_{\sigma+} + G_A^2 C^\ell_{\sigma-} + G_V^2 D^\ell_-, \tag{C.2.12b}$$

where X_1 and Y^ℓ_1 are nuclear tensor operators of rank 0 and 1, and in addition, even and odd under the exchange of n and m, respectively. Various combinations of $\sigma^\ell_{n(m)}$, $C_{n(m)}$ and $D^\ell_{n(m)}$ are defined as

$$C_\pm = C_n \pm C_m,$$

$$\sigma^\ell_\pm = \sigma^\ell_n \pm \sigma^\ell_m, \qquad C^\ell_{\sigma\pm} = \sigma^\ell_n C_m \pm C_n \sigma^\ell_m,$$

$$D^\ell_\pm = D^\ell_n \pm D^\ell_m, \qquad D^{jk}_{\sigma\pm} = \sigma^j_n D^k_m \pm D^j_n \sigma^k_m. \tag{C.2.13}$$

The suffix R in X_{1R} and Y_{1R} means to include the nucleon recoil terms C_n and $\vec{D}_n$ which have an odd parity, and the products of them like $C_n C_m$ and $(\vec{D}_n\cdot\vec{D}_m)$ are neglected.

The closure approximation means to omit the odd part of M_{m_ν} under the exchange of suffices n and m; in other words, $\vec{x}\rightleftarrows\vec{y}$, as mentioned below Eq.(B.2.24). Under this exchange, E_+, E^ℓ_+ and X_1 are transformed as even, while E_-, E^ℓ_- and Y^ℓ_1 as odd. Thus, it is clear from Eq.(C.2.11) that $\{M_{m_\nu}(a,L)\}_C$ vanishes in the closure approximation. Of course, if the closure approximation is not assumed, then it is expected that this $\{M_{m_\nu}\}_C$ part has non-vanishing small nuclear matrix elements. In addition to this smallness, this $\{M_{m_\nu}\}_C$ part includes the small kinematical coefficient like

$(\varepsilon_{12}R/2) \sim (1/80)$ in comparison with $\{M_{m_\nu}\}_n$ in Eq.(C.2.11a). Therefore, we need not consider the $\{M_{m_\nu}\}_C$ part in general.

Let us consider the case where both electrons are in the S-wave state with no FBWC, so that the electron wave has no $\vec{x}$ (or $\vec{y}$) dependence, i.e., $E_- = E_-^{\ell} = 0$. Thus, we observe from Eq.(C.2.11) that $\{M_{m_\nu}\}_n$ with X_{1S} gives the $0^+ \to 0^+$ transition of which coefficient includes h_+, while $\{M_{m_\nu}\}_C$ with Y_{1V}^{ℓ} contributes to the $0^+ \to 1^+$ transition with the suppression factor $\varepsilon_{12}Rh_0/2$, and vanishes in the closure approximation. These results are listed in Table C.1. The $0^+ \to 2^+$ transition does not occur, because the tensor operator of rank 2 can not be constructed in this S-S case. The nucleon recoil terms, X_{1R} and Y_{1R}^{ℓ}, do not contribute to the $0^+ \to J^+$ transition, because of their parity odd character.

Since the non-zero neutrino mass is an important problem, we shall list in Table C.1 various cases of the higher partial waves and the order of magnitude of their amplitudes by presenting the leading terms obtained from the leptonic currents. The corrections from them to the $0^+ \to 0^+$ transition amplitude are less than 1%, although the details depend on the nuclear matrix elements. The finite de Broglie wave length correction (FBWC) in the S-S case is the same order of magnitude as in the $P_{1/2} - P_{1/2}$ case, see Eq.(D.13) of Appendix D.

Thus, for the $0^+ \to 0^+$ transition, it is enough to consider only the combination of the S-wave and S-wave for two electron system. The $M_{m_\nu}(a,L)$ part of $R_{0\nu}$ in Eq.(C.2.4) is obtained from the X_{1S} term in Eq.(C.2.11a):

$$\sum_j \left(\frac{m_j}{m_e}\right) \sum_a M_{m_\nu}(a, L) = g_A^2 \Sigma_1 E_+(\varepsilon_1 \vec{0}\,;\, \varepsilon_2 \vec{0}\,), \tag{C.2.15}$$

where the nuclear matrix element by using the abbreviation in Eq.(B.1.5) is

$$\Sigma_1 = \sum_j \left(\frac{m_j}{m_e}\right) \sum_a \langle 0_f^+ \| [G_V^2 - G_A^2 (\vec{\sigma}_n \cdot \vec{\sigma}_m)] h_+(r_{nm}, E_a) \| 0_i^+ \rangle, \tag{C.2.16}$$

and the electron current E_+ is defined in Eq.(B.2.22) by using the electron S-wave function $\psi^{(S)}(\varepsilon, 0)$ in Eq.(3.1.17).

Similarly, if both vertices of neutron decays are the V+A type, then we find

$$\sum_j \left(\frac{m_j}{m_e}\right) \sum_a M_{m_\nu}(a, R) = g_A^2 \Sigma_2 E_{R+}(\varepsilon_1 \vec{0}\,;\, \varepsilon_2 \vec{0}\,), \tag{C.2.17}$$

where we have used $\tilde{J}_R^{f+}$ instead of $\tilde{J}_L^{f+}$ in Eq.(C.1.4) and get

$$\Sigma_2 = \sum_j \left(\frac{m_j}{m_e}\right) \sum_a \langle 0_f^+ \| [\varepsilon_V^2 - \varepsilon_A^2 (\vec{\sigma}_n \cdot \vec{\sigma}_m)] h_+(r_{nm}, E_a) \| 0_i^+ \rangle, \tag{C.2.18}$$

and the corresponding electron current is, instead of E_+,

$$E_{R+}(\varepsilon_1 \vec{x}\,;\, \varepsilon_2 \vec{y}) = \frac{1}{2}\left[\bar{\psi}(\varepsilon_1 \vec{x})(1-\gamma_5)\psi^c(\varepsilon_2 \vec{y}) + \bar{\psi}(\varepsilon_1 \vec{y})(1-\gamma_5)\psi^c(\varepsilon_2 \vec{x})\right]. \tag{C.2.19}$$

As for the $0^+ \to 2^+$ transition, the contribution from the m_ν part is at most of order of 10^{-3} in comparison with the $0^+ \to 0^+$ transition rate from the viewpoint of the kinematical factor, as obtained from the $S - D_{3/2}$ case in Table C.1. It is very hard to observe this contribution.

§C.2.2 The V+A part

Let us consider the M_{V+A} part of $R_{0\nu}$ in Eq.(C.2.7) by substituting Eqs.(3.3.17),

$$M_{V+A}(a) = \left(\frac{R}{2m_e}\right) \int d\vec{x}\, d\vec{y} \int \frac{d\vec{q}}{2\pi^2 \omega}\, e^{i\vec{q}\cdot(\vec{x}-\vec{y})} \cdot \left\{ \frac{1}{\omega + A_2}\left[u_{f\sigma}^L(\varepsilon_1 \vec{x}\,;\, \varepsilon_2 \vec{y})\, J_{LR}^{f\sigma}(\vec{x}, \vec{y}, a) + u_{f\sigma}^R(\varepsilon_1 \vec{x}, \varepsilon_2 \vec{y})\, J_{RL}^{f\sigma}(\vec{x}, \vec{y}, a)\right] - \frac{1}{\omega + A_1}\left[u_{\sigma f}^R(\varepsilon_1 \vec{y}\,;\, \varepsilon_2 \vec{x})\, J_{LR}^{f\sigma}(\vec{x}, \vec{y}, a) + u_{\sigma f}^L(\varepsilon_1 \vec{y}, \varepsilon_2 \vec{x})\, J_{RL}^{f\sigma}(\vec{x}, \vec{y}, a)\right] \right\}, \tag{C.2.20}$$

where Eq.(3.3.19) has been used. Note that the $\vec{q}$ integration should extend over the $\omega\,(=q^0)$ and $\vec{q}$ variable in $u^{\alpha}_{\rho\sigma}$ of Eq.(3.3.18).

It is observed from Eq.(C.2.20) that many terms cancel each other in contrast to the m_ν part, where the leading terms are retained. For example, the difference between $u^L_{\rho\sigma}$ and $u^R_{\rho\sigma}$ is only $(1\mp\gamma_5)$; namely, $(u^L_{\rho\sigma}+u^R_{\rho\sigma})$ has no γ_5 matrix, while $(u^L_{\rho\sigma}-u^R_{\rho\sigma})$ retains only the γ_5 part. On the other hand, $\tilde{J}^{\rho+}_R(x)$ in Eq.(C.1.4) can be obtained from $\hat{J}^{\rho+}_L(x)$ by replacing G_V and G_A by $\mathcal{E}_V$ and $-\mathcal{E}_A$, respectively. Therefore, each product of them, J_{LR} and J_{RL}, consists of the symmetric and antisymmetric parts under these replacements, $G_V \rightleftarrows \mathcal{E}_V$ and $G_A \rightleftarrows -\mathcal{E}_A$. If we define

$$\mathcal{G}_\pm = (\mathcal{G}_V\,\mathcal{E}_A \pm \mathcal{G}_A\,\mathcal{E}_V)/2\,, \qquad \text{(C.2.21)}$$

then the parts of J_{LR} with combinations $G_V\mathcal{E}_V$, $G_A\mathcal{E}_A$ and G_- should be the same as those of J_{RL} except the running suffix n, while the G_+ parts have the opposite signs. It is interesting to point out that if we accept the assumption $|x| \ll 1$, we find from Eq.(C.1.5) that

$$\mathcal{G}_V\,\mathcal{E}_V = (\lambda' V_{ej} + \eta V'_{ej})\,U_{ej}\,(g_V/g_A)^2, \qquad \mathcal{G}_A\,\mathcal{E}_A = (\lambda' V_{ej} - \eta V'_{ej})\,U_{ej},$$

$$\mathcal{G}_+ = \lambda' V_{ej}\,U_{ej}\,(g_V/g_A), \qquad \mathcal{G}_- = -\eta V'_{ej}\,U_{ej}\,(g_V/g_A). \qquad \text{(C.2.22)}$$

By contracting suffices ρ and σ, Eq.(C.2.20) becomes

$$M_{V+A}(a) = \{M_{V+A}(a)\}_n + \{M_{V+A}(a)\}_c\,, \qquad \text{(C.2.23)}$$

where $\{M_{V+A}(a)\}_n$ and $\{M_{V+A}(a)\}_c$ are the non-vanishing and vanishing parts of $M_{V+A}(a)$ in the closure approximations, respectively, as will be explained below Eq.(C.2.34) later;

$$\{M_{V+A}(a)\}_n$$

$$= \left(\frac{R}{m_e}\right) T_a \left\{ \begin{array}{l} (H_{\omega_2} - H_{\omega_1}) \left[\begin{array}{l} (X_3 + X_{5R})\,F^0_+ + Y_{3R}\,F^0_{5-} \\ + (X^\ell_{4R} + X^\ell_5)\,F^\ell_+ + (Y^\ell_4 - Y^\ell_{5R})\,F^\ell_{5-} \end{array} \right] \\ + (H^\ell_{g_2} + H^\ell_{g_1}) \left[\begin{array}{l} (X^\ell_{3R} + X^\ell_5)\,F^0_- + (Y^\ell_3 + Y^\ell_{5R})\,F^0_{5+} \\ + (X^{\ell k}_4 + X^{\ell k}_{6R})\,F^k_- + (Y^{\ell k}_{4R} + Y^{\ell k}_6)\,F^k_{5+} \end{array} \right] \end{array} \right\}, \qquad \text{(C.2.24)}$$

$$\{M_{V+A}(a)\}_c$$

$$= \left(\frac{R}{m_e}\right) T_a \left\{ \begin{array}{l} (H_{\omega_2} + H_{\omega_1}) \left[\begin{array}{l} (X_3 + X_{5R})\,F^0_- + Y_{3R}\,F^0_{5+} \\ + (X^\ell_{4R} + X^\ell_5)\,F^\ell_- + (Y^\ell_4 - Y^\ell_{5R})\,F^\ell_{5+} \end{array} \right] \\ + (H^\ell_{g_2} - H^\ell_{g_1}) \left[\begin{array}{l} (X^\ell_{3R} + X^\ell_5)\,F^0_+ + (Y^\ell_3 + Y^\ell_{5R})\,F^0_{5-} \\ + (X^{\ell k}_4 + X^{\ell k}_{6R})\,F^k_+ + (Y^{\ell k}_{4R} + Y^{\ell k}_6)\,F^k_{5-} \end{array} \right] \end{array} \right\}, \qquad \text{(C.2.25)}$$

where T_a is the part of the nuclear matrix element defined in Eq.(B.2.20), X and Y are nuclear tensor operators from the hadronic currents defined later, and $F^\mu_\pm$ and $F^\mu_{5\pm}$ with $\mu = 0,1,2,3$ are the electron currents

$$F^\mu_\pm(\varepsilon_1\vec{x};\,\varepsilon_2\vec{y}) = [u^\mu(\varepsilon_1\vec{x};\,\varepsilon_2\vec{y}) \pm u^\mu(\varepsilon_1\vec{y};\,\varepsilon_2\vec{x})]/2,$$

$$F^\mu_{5\pm}(\varepsilon_1\vec{x};\,\varepsilon_2\vec{y}) = [u^\mu_5(\varepsilon_1\vec{x};\,\varepsilon_2\vec{y}) \pm u^\mu_5(\varepsilon_1\vec{y};\,\varepsilon_2\vec{x})]/2, \qquad \text{(C.2.26)}$$

$$u^\mu(\varepsilon_1\vec{x};\,\varepsilon_2\vec{y}) = \bar{\psi}(\varepsilon_1\vec{x})\,\gamma^\mu\,\psi^c(\varepsilon_2\vec{y}),$$

$$u^\mu_5(\varepsilon_1\vec{x};\,\varepsilon_2\vec{y}) = \bar{\psi}(\varepsilon_1\vec{x})\,\gamma_5\gamma^\mu\,\psi^c(\varepsilon_2\vec{y}). \qquad \text{(C.2.27)}$$

Here four types of combinations of neutrino potentials appear: Two of them in $\{M_{V+A}(a)\}_n$ were defined already as

$$H_{\omega_2} - H_{\omega_1} = \left(\frac{\varepsilon_{12}}{R}\right) \rho_{0\omega}(\gamma_{nm}, E_a), \tag{C.2.28}$$

$$(H_{\vec{q}_2} + H_{\vec{q}_1})^\ell = i\left(\frac{2}{R\gamma_{nm}}\right) \rho_+'(\gamma_{nm}, E_a)(\hat{\gamma}_{nm})^\ell \tag{C.2.29}$$

in Eqs.(3.4.4) and (3.4.11), respectively, where $\vec{r}_{nm} = \vec{r}_n - \vec{r}_m$ $(= \vec{x} - \vec{y})$. Two new combinations are introduced in $\{M_{V+A}(a)\}_C$, Eq.(C.2.25):

$$H_{\omega_2} + H_{\omega_1} = \left(\frac{2}{R^2}\right) \rho_\omega(\gamma_{nm}, E_a), \tag{C.2.30}$$

$$(H_{\vec{q}_2} - H_{\vec{q}_1})^\ell = i\left(\frac{\varepsilon_{12}}{\gamma_{nm}}\right) \rho_0'(\gamma_{nm}, E_a)(\hat{\gamma}_{nm})^\ell, \tag{C.2.31}$$

where

$$\rho_\omega(\gamma, E_a) = \frac{R^2}{2\pi^2}\int d\vec{q}\, e^{i\vec{q}\cdot\vec{r}} \frac{\omega + \mu_a m_e}{(\omega + A_1)(\omega + A_2)}, \tag{C.2.32}$$

$$\rho_0'(\gamma, E_a) = -\frac{\gamma}{2\pi^2}\frac{d}{d\gamma}\int d\vec{q}\, e^{i\vec{q}\cdot\vec{r}} \frac{1}{\omega(\omega + A_1)(\omega + A_2)}. \tag{C.2.33}$$

Note that $h_\omega(r, E_a)$ is a divergent integral formally, but as discussed for $\vec{H}_{qk}$ below Eq.(3.4.7), it can be treated as a convergent integral, because the range of $\vec{q}$ variable is limited by the overlap of nuclear wave functions. These h_ω and h_0' are defined to be of the same order of magnitude of $h_{0\omega}$ and h_+' at $r_{nm} = R$, the nuclear radius. Therefore, when these h's are combined with the factor (R/m_e) in Eqs.(C.2.24) and (C.2.25), $(H_{\omega_2} + H_{\omega_1})$ and $(\vec{H}_{q2} + \vec{H}_{q1})$ have a large coefficient like $(1/m_e R) \sim 80$, while $(H_{\omega_2} - H_{\omega_1})$ and $(\vec{H}_{q2} - \vec{H}_{q1})$ have the smaller one such as $(\varepsilon_{12}/m_e) \sim 2$, which means the cancellation between main terms.

Next, the selection rules should be found by examining nuclear tensor operators X and Y;

$$X_3 = G_V \mathcal{E}_V - G_A \mathcal{E}_A (\vec{\sigma}_n \cdot \vec{\sigma}_m),$$

$$X_{3R}^\ell = G_A \mathcal{E}_A C_{\sigma+}^\ell - G_V \mathcal{E}_V D_+^\ell - i G_+ \varepsilon_{ik\ell} D_{\sigma-}^{ik},$$

$$X_4^{\ell k} = [G_V \mathcal{E}_V + G_A \mathcal{E}_A (\vec{\sigma}_n \cdot \vec{\sigma}_m)]\delta_{\ell k} - G_A \mathcal{E}_A (\sigma_n^\ell \sigma_m^k + \sigma_n^k \sigma_m^\ell) - i G_+ \varepsilon_{i\ell k} \sigma_+^i,$$

$$X_{4R}^\ell = G_A \mathcal{E}_A C_{\sigma+}^\ell - G_V \mathcal{E}_V D_+^\ell + i G_+ \varepsilon_{\ell ik} D_{\sigma-}^{ik},$$

$$X_5^\ell = -G_- \sigma_+^\ell, \qquad X_{5R} = G_-(C_+ + D_{\sigma+}^{kk}),$$

$$X_{6R}^{\ell k} = G_-[(C_+ - D_{\sigma+}^{ii})\delta_{\ell k} + (D_{\sigma+}^{\ell k} + D_{\sigma+}^{k\ell})],$$

$$Y_3^\ell = -i G_A \mathcal{E}_A (\vec{\sigma}_n \times \vec{\sigma}_m)^\ell + G_+ \sigma_-^\ell,$$

$$Y_{3R} = -G_+ (C_- + D_{\sigma-}^{kk})$$

$$Y_4^\ell = i G_A \mathcal{E}_A (\vec{\sigma}_n \times \vec{\sigma}_m)^\ell + G_+ \sigma_-^\ell,$$

$$Y_{4R}^{\ell k} = -i \varepsilon_{i\ell k}[G_A \mathcal{E}_A C_{\sigma-}^i - G_V \mathcal{E}_V D_-^i] - G_+[(C_- - D_{\sigma-}^{ii})\delta_{\ell k} + D_{\sigma-}^{\ell k} + D_{\sigma-}^{k\ell}],$$

$$Y_{5R}^\ell = i G_- \varepsilon_{ik\ell} D_{\sigma+}^{ik},$$

$$Y_6^{\ell k} = i G_- \varepsilon_{i\ell k} \sigma_-^i, \tag{C.2.34}$$

where $\sigma_\pm^\ell$, $C_{\sigma\pm}^\ell$, $D_\pm^\ell$ and $D_{\sigma\pm}^\ell$ are defined in Eq.(C.2.13), and X_{kR} and Y_{kR} with the suffix R mean the contributions from the nucleon recoil terms (C_n, $\vec{D}_n$ and so on) and, the products of two nucleon recoil terms like $C_n \vec{D}_m$ have been neglected.

Let us examine which terms vanish in the closure approximation. As already mentioned below Eq.(C.2.13), the closure approximation is expressed as vanishing the odd part of $M_{V+A}(a)$ under the exchange

of suffices n and m. Under this exchange, nuclear operators X's, electron currents F^{μ}_{+} and F^{μ}_{5+} and neutrino potential $H_{\omega k}$ are transformed as even, while Y, F^{μ}_{-}, F^{μ}_{5-} and $\vec{H}_{qk}$ as odd. By taking these characters into consideration, we can confirm that $\{M_{V+A}(a)\}_n$ in Eq. (C.2.24) is the non-vanishing part in the closure approximation, while $\{M_{V+A}(a)\}_c$ in Eq. (C.2.25) is the vanishing part.

Let us restrict our consideration to the $0^+ \to J^+$ transitions. Since the neutrino momentum $\vec{q}$ and the nucleon recoil terms C_n and $\vec{D}_m$ behave as odd parity operators, each of X_k, $(\vec{X}_k \cdot \vec{q})$, Y_k and $(\vec{Y}_k \cdot \vec{q})$ has a definite parity which is shown in Table C.2.

Now we examine each case where two emitted electrons have various partial waves. The finite de Broglie wave length correction (FBWC) is not taken into account, and will be discussed at the last part. Of course, the largest contribution should be the case where both electrons are in the S-wave state (the S-S case). This is the allowed transition in the terminology of the single β decay. In the S-S case with no FBWC, the electron wave function $\psi(\varepsilon, \vec{x})$ are independent of the vertex positions, so that $F^{\mu}_{-}(\varepsilon_1 0\,;\, \varepsilon_2 0) = F^{\mu}_{5-}(\varepsilon_1 0\,;\, \varepsilon_2 0) = 0$ from Eq. (C.2.26). It means also that we have no additional nuclear tensor operators such as $\vec{x} = \vec{r}_n$ and $\vec{y} = \vec{r}_m$ which come from the higher partial waves of electron. As long as we consider the $0^+ \to J^+$ transition, there is no contribution from the parity odd combinations like Y_{3R}, $(\vec{q} \cdot \vec{Y}_3)$ and so on. Thus, in the S-S case with no FBWC, we have for the $0^+ \to 0^+$ and 1^+ transitions,

$$\{M_{V+A}(a)\}_{n,S\text{-}S} = \left\{ \begin{array}{l} \left(\frac{\varepsilon_{12}}{m_e}\right) T_a \rho_{0\omega} \left[X_3 F^0_+(\varepsilon_1 0\,;\, \varepsilon_2 0) + X^k_5 F^k_+(\varepsilon_1 0\,;\, \varepsilon_2 0) \right] \\ + \left(\frac{2}{m_e R}\right) T_a \left(\frac{iR}{\gamma_{nm}}\right) \rho'_{1+}(\hat{\gamma}_{nm})^{\ell} \left[Y^{\ell}_{5R} F^0_{5+}(\varepsilon_1 0\,;\, \varepsilon_2 0) + Y^{\ell k}_{4R} F^k_{5+}(\varepsilon_1 0\,;\, \varepsilon_2 0) \right] \end{array} \right\}, \tag{C.2.35}$$

$$\{M_{V+A}(a)\}_{c,S\text{-}S} = \left\{ \begin{array}{l} \left(\frac{2}{m_e R}\right) T_a \rho_{\omega} \left[Y^k_4 F^k_{5+}(\varepsilon_1 0\,;\, \varepsilon_2 0) \right] \\ + \left(\frac{\varepsilon_{12}}{m_e}\right) T_a \left(\frac{iR}{\gamma_{nm}}\right) \rho'_0(\hat{\gamma}_{nm})^{\ell} \left[X^{\ell}_{3R} F^0_+(\varepsilon_1 0\,;\, \varepsilon_2 0) + X^{\ell k}_{6R} F^k_+(\varepsilon_1 0\,;\, \varepsilon_2 0) \right] \end{array} \right\}, \tag{C.2.36}$$

Among seven terms of M_{V+A} in the S-S case, only three operators X_3, $(\hat{r}_{nm} \cdot \vec{Y}_{5R})$ and $(\hat{r}_{nm} \cdot \vec{X}_{3R})$ contribute to the $0^+ \to 0^+$ transition and the others to the $0^+ \to 1^+$ transition, as shown in Table C.2.

Thus, in the S-S case with no FBWC, we have for the $0^+ \to 0^+$ transition

$$\sum_j \sum_a \left[M_{V+A}(a)\right]_{S\text{-}S} = g_A^2 \left\{ \begin{array}{l} \left(\frac{\varepsilon_{12}}{m_e}\right) \left[Z_3 + \{Z_{3R}\}_c \right] F^0_+(\varepsilon_1 0\,;\, \varepsilon_2 0) \\ + \left(\frac{4}{m_e R}\right) Z_{4R} F^0_{5+}(\varepsilon_1 0,\, \varepsilon_2 0) \end{array} \right\}, \tag{C.2.37}$$

corresponding to $M_{m_\nu}(a,L)$ in Eq. (C.2.15). Here the nuclear matrix elements are

$$Z_3 = \sum_j \sum_a \langle 0^+_f \| \rho_{0\omega}(\gamma_{nm}, E_a) X_3 \| 0^+_i \rangle, \tag{C.2.38}$$

$$Z_{4R} = \sum_j \sum_a \langle 0^+_f \| i \left(\frac{R}{2\gamma_{nm}}\right) \rho'_{1+}(\gamma_{nm}, E_a) (\hat{\gamma}_{nm} \cdot \vec{Y}_{5R}) \| 0^+_i \rangle, \tag{C.2.39}$$

$$\{Z_{3R}\}_c = \sum_j \sum_a \langle 0^+_f \| i \left(\frac{R}{2\gamma_{nm}}\right) \rho'_0(\gamma_{nm}, E_a) (\hat{\gamma}_{nm} \cdot \vec{X}_{3R}) \| 0^+_i \rangle, \tag{C.2.40}$$

where the abbreviation in Eq. (B.1.5) has been used. The second Z_{4R} ($\sim Y_{5R}$) due to the $\vec{q}$ term gives the recoil effect and has a large coefficient $(4/m_e R) \sim 320$, as seen from Eq. (C.2.37) and discussed in §3.3.2. Note that $\vec{Y}_{5R}$ in Eq. (C.2.34) is proportional to only $G_- \sim (-2)$ in Eq. (C.2.22). While Z_3 ($\sim X_3$) due to the ω term has a small coefficient $|\varepsilon_{12}|/m_e \sim 2$, because of the cancellation between two neutrino potentials given by $H_{\omega 2} - H_{\omega 1}$ in Eq. (C.2.28).

This term includes both the λ' and η right-handed parameters, as seen from Eqs.(C.2.34) and (C.2.22). The third $\{z_{3R}\}_C$ includes the nucleon recoil term and vanishes in the closure approximation, so that it can be safely neglected.

As we saw, the situation of the V+A part in the electron S-S case is quite different from the m_ν part, because of either the cancellation between two potentials or the nucleon recoil term. Therefore, we have to consider the case of the next partial waves of electrons, where one electron is in the P-wave state with $j = 1/2$, but the other is still in the S-wave, the $S - P_{1/2}$ case. According to the selection rule given in Table C.2, we have for the $0^+ \to 0^+$ transition,

$$\{M_{V+A}\}_{n,\,S-P\frac{1}{2}} = \left\{ \begin{array}{l} \left(\frac{2}{m_e R}\right) T_a \left(\frac{iR}{\gamma_{nm}}\right) R'_{+}(\hat{r}_{nm})^{\ell} \left[X_4^{\ell k} F_-^k + Y_6^{\ell k} F_{5+}^k \right] \\ + \left(\frac{\varepsilon_{12}}{m_e}\right) T_a \, R_{0\omega} \left[X_{4R}^{\ell} F_+^{\ell} - Y_{5R}^{\ell} F_{5-}^{\ell} \right] \end{array} \right\}, \qquad \text{(C.2.41)}$$

$$\{M_{V+A}\}_{C,\,S-P\frac{1}{2}} = \left\{ \begin{array}{l} \left(\frac{2}{m_e R}\right) T_a \, R_\omega \left[X_{4R}^{\ell} F_-^{\ell} - Y_{5R}^{\ell} F_{5+}^{\ell} \right] \\ + \left(\frac{\varepsilon_{12}}{m_e}\right) T_a \left(\frac{iR}{\gamma_{nm}}\right) R'_0(\hat{r}_{nm})^{\ell} \left[X_4^{\ell k} F_+^k + Y_6^{\ell k} F_{5-}^k \right] \end{array} \right\}. \qquad \text{(C.2.42)}$$

It may be expected from these equations that the leading terms in the $S - P_{1/2}$ case come from the first line of Eq.(C.2.41), because of the large coefficient $(2/m_e R)$ and the non-vanishing character in the closure approximation. Before concluding it, however, we have to check the features of electron current given by $F_\pm^k$ and $F_{5\pm}^k$ in Eq.(C.2.26). Let us consider F_-^k first. Concerning the electron current $u_{(5)}^\mu$ in Eq.(C.2.27), if the elctron with energy ε_1 is emitted

in the $P_{1/2}$-wave state, $F_-(\varepsilon_1 \vec{r}_n, \varepsilon_2 \vec{r}_m)$ is proportional to the relative coordinate $\vec{r}_{nm} = (\vec{r}_n - \vec{r}_m)$ and $\xi_\pm(\varepsilon_1) = \frac{1}{2}\alpha z + (\varepsilon_1 R \pm m_e R)/3$ which characterize the $P_{1/2}$-wave in Eq.(3.1.22). By combining the other case where the electron with ε_2 is in the $P_{1/2}$ state, F_- gives the kinematical factor like $\xi_+(\varepsilon_1) - \xi_-(\varepsilon_2) = (\varepsilon_{12} R + 2 m_e R)/3$. Thus, although the additive combination of two neutrino potential is obtained, the leading term of the electron $P_{1/2}$-wave gives the smaller coefficient like the ordinary P-wave, pr/3: Namely the coefficient of the first $X_4^{\ell k}$ term in Eq.(C.2.41) becomes $(2/m_e R) \times (\varepsilon_{12} R/3) \sim 1$ instead of $(2/m_e R) \sim 160$. On the other hand, the combination of $F_{5+}^k(\varepsilon_1 \vec{r}_n, \varepsilon_2 \vec{r}_m)$ in the second term of Eq.(C.2.41) gives the additive position vector such as $\vec{r}_{+nm} = (\vec{r}_n + \vec{r}_m)$ and the rather large constant coefficient like $\xi_+(\varepsilon_1) + \xi_-(\varepsilon_2) = \alpha z + (T_0 + 2) m_e R/3$. Thus, the second $Y_6^{\ell k}$ term in Eq.(C.2.41) has a large coefficient. This is the P-wave effect, which is discussed in §3.3.2.

Let us define four nuclear matrix elements corresponding to four terms in Eq.(C.2.41),

$$\begin{aligned} Z_5 &= \sum_j \sum_a \langle O_f^+ \| R'_+(\gamma_{nm}, E_a) (\hat{r}_{nm})^{\ell} (\hat{r}_{nm})^k \, X_4^{\ell k} \| O_i^+ \rangle, \\ Z_6 &= \sum_j \sum_a \langle O_f^+ \| \left(\frac{-1}{2\gamma_{nm}}\right) R'_+(\gamma_{nm}, E_a) (\hat{r}_{nm})^{\ell} (\hat{r}_{+nm})^k Y_6^{\ell k} \| O_i^+ \rangle, \\ Z_{5R} &= \sum_j \sum_a \langle O_f^+ \| \left(\frac{i}{2R}\right) R_{0\omega}(\gamma_{nm}, E_a) (\vec{r}_{+nm} \cdot \vec{X}_{4R}) \| O_i^+ \rangle, \\ Z_{6R} &= \sum_j \sum_a \langle O_f^+ \| \left(\frac{i}{2R}\right) R_{0\omega}(\gamma_{nm}, E_a) (\vec{r}_{nm} \cdot \vec{Y}_{5R}) \| O_i^+ \rangle, \end{aligned} \qquad \text{(C.2.43)}$$

where

$$\vec{r}_{+nm} = \vec{r}_n + \vec{r}_m \,, \qquad \vec{r}_{nm} = \vec{r}_n - \vec{r}_m \,. \qquad \text{(C.2.44)}$$

According to the estimations in the previous paragraph, Z_6 has a largest coefficient $(4\alpha z/m_e R) \sim 100$ which include only the right-

handed parameter $G_- \sim \eta$, as seen from Eq.(C.2.34). While Z_5, Z_{5R} and Z_{6R} have coefficients $(2\mathcal{E}_{12}/3m_e)$, $(\alpha Z \mathcal{E}_{12}/m_e)$ and $(\mathcal{E}_{12}/m_e)\times(\mathcal{E}_{12}R/3)$, respectively. Both right-handed parameters, λ' and η, appear in $Z_5 \sim X_4^{\ell k}$, while Z_{5R} includes the term of $G_+ \sim \lambda'$, so that we retain Z_5 and Z_{5R}. However, since the last Z_{6R} includes the nucleon recoil terms and their coefficients are small, we will ignore it hereafter. These results are summarized in Eqs.(C.3.5) and (C.3.6).

Returning to $\{M_{V+A}\}_{C,S\text{-}P_{1/2}}$ in Eq.(C.2.42), we should examine two terms, i.e., Y_{5R}^{ℓ} and $X_4^{\ell k}$. Their corresponding nuclear matrix elements are

$$\{Z_{6R}\}_C = \sum_j \sum_a \langle 0_f^+ \| \left(\frac{i}{2R}\right) R_\omega(r_{nm}, E_a)\,(\vec{Y}_{+nm}\cdot\vec{Y}_{5R}) \| 0_i^+ \rangle,$$

$$\{Z_5\}_C = \sum_j \sum_a \langle 0_f^+ \| \left(\frac{1}{r_{nm}}\right) R_0'(r_{nm}, E_a)\,(\hat{r}_{nm})^{\ell}(\vec{r}_{+nm})^{k} X_4^{\ell k} \| 0_i^+ \rangle. \tag{C.2.45}$$

Their coefficients are $\propto Z(2/m_eR) \sim 50$ and $\propto Z(\mathcal{E}_{12}/m_e) \sim 2/3$, respectively. The former $\{z_{6R}\}_C$ includes the nucleon recoil terms and only η parameter, as seen from Y_{5R}^{ℓ} in Eq.(C.2.34). Thus, $\{z_{6R}\}_C$ acts as a next correction term to the sum of Z_{4R} and Z_6. If there were a large cancellation between Z_{4R} and Z_6, as pointed out by Tomoda et al.,[32] this term might play some important contribution, although it is a vanishing term in the closure approximation. While, the second $\{z_5\}_C$ works as a correction term to Z_3 and Z_5 which include both λ and η. Thus, it is an unsolved problem how large $\{z_{6R}\}_C$ and $\{z_5\}_C$ are when the closure approximation is not assumed. In this sense, they are included in the final expression for $M_{V+A}(a)$ given in Eq. (C.3.7). But the remaining two terms, X_{4R}^{ℓ} and $Y_6^{\ell k}$ in Eq.(C.2.42) will be ignored hereafter,

because their order of magnitudes are $(4\mathcal{E}_{12}/3m_e) \times$ (the nucleon recoil term) and $(2\mathcal{E}_{12}^2 R/3m_e)$, respectively.

As we have seen, the large kinematical factors appear as a result of the large virtual neutrino momentum, where two neutrino potentials are additive, and the smaller ones by order of two are derived from their cancellation. Therefore, it is necessary to check the $P_{1/2}$-$P_{1/2}$ case in order to establish the reliability of our approximation. Since each electron P-wave gives the factor like $(\alpha Z/2)(r_n/R)$ shown in Eq.(3.1.22), there appears a suppression factor like $(r_n r_m/R^2)$ in the nuclear matrix elements. Therefore, the special attention should be paid for the cases where the neutrino potentials appear additively. Also it should be noticed that in the S-S case, we have no contribution from the $(H_{\omega 1} + H_{\omega 2})$ combination in Eq.(C.2.25). This is because $X_3 F_-^0$ and $X_5^{\ell} F_-^{\ell}$ vanish due to the S-wave character $(F_- = F_{5-}^{\ell} = 0)$, while $(\vec{Y}_4 \cdot \vec{F}_{5+})$ contributes only to the $0^+ \to 1^+$ transition. All others accompanied with $H_{\omega 1} + H_{\omega 2}$ do not give the $0^+ \to J^+$ transition, as seen from Table C.2.

Let us examine the $(H_{\omega 1} + H_{\omega 2})$ part in the $P_{1/2} - P_{1/2}$ case in detail, although this is the vanishing part in the closure approximation. The nuclear operator $X_3 F_-^0$ contributes only to the $0^+ \to 1^+$ transition. The reason is as follows: Since X_3 in Eq.(C.2.34) has the even property under the exchange of the running suffices n and m, there should be some term with the odd property under $n \rightleftarrows m$ to assure the vanishing character in the closure approximation. Such a term appears as one combination like $(\vec{r}_n \times \vec{r}_m)\cdot\vec{\sigma}_e$ from F_-^0, where $\vec{\sigma}_e$ is the spin operator acting on electrons. Thus, since X_3 is a rank 0 tensor operator, it contributes only to the $0^+ \to 1^+$ transition. Similarly, the $(\vec{Y}_4 \cdot \vec{F}_{5+})$ term in Eq.(C.2.25) gives only

the $0^+ \to 1^+$ trnsition. However, the $(\vec{X}_5 \cdot \vec{F}_-)$ term contributes to the $0^+ \to 0^+$ transition and its nuclear matrix element is

$$\{Z_7\}_C = \sum_j \sum_a \langle 0_f^+ \| \hat{P}_{ab}(r_{nm}, E_a) \left(\frac{i}{2R^2}\right)(\vec{r}_n \times \vec{r}_m) \cdot \vec{X}_5 \| 0_i^+ \rangle. \tag{C.2.46}$$

It is proportional to the ζ parameter through G_-. This term should be examined more carefully than $\{z_{6R}\}_C$, because of the large coefficient $(\propto z)^2 (1/m_e R) \sim 9$ with no nucleon recoil term. There are of course some contributions from $\{M_{V+A}(a)\}_n$ in Eq.(C.2.24). But all of them act as the correction terms to Z_3 and Z_{4R}. Therefore, only $\{Z_7\}_C$ will remain as a representative for these terms in the $P_{1/2}$-$P_{1/2}$ case.

Finally, let us consider the finite de Broglie wave length correction for the S-S case. As it is clear from Eq.(D.13) in Appendix D, this FBWC for Z_3 in Eq.(C.2.38) is of order of $(3/8)(\alpha z)^2 \times (r/R)^2$, so that we need not worry about it. However, the FBWC for Z_{4R} in Eq.(C.2.39) may give some problem, because its kinematical coefficient is the largest, $4/m_e R$. The nuclear matrix element due to FBWC for this case is expressed as

$$Z_{4RF} = \sum_j \sum_a \langle 0_f^+ \| i \left(\frac{R}{2r_{nm}}\right)\left(\frac{r_n^2 + r_m^2}{2R^2}\right) \hat{P}'_{1+}(r_{nm}, E_a)(\hat{r}_{nm} \cdot \vec{\tau}_{5R}) \| 0_i^+ \rangle. \tag{C.2.47}$$

Whether Z_{4RF} is important or not depends on the value of $|\chi'_F - C_{33}\chi'_R|$ in Eq.(8.2.1b), where χ'_F and χ'_R come from Z_6 and Z_{4R}, respectively. If $|\chi'_F - C_{33}\chi'_R| \sim O(10)$, then we have to calculate the FBWC for Z_{4R}, i.e. Z_{4RF} and also for Z_6. Furthermore, many terms in the $P_{1/2}$-$P_{1/2}$ case should be taken into consideration, because they are the same order of magnitude as Z_{4RF}, although Tomoda et al. do not estimate them.

§ C.3 The decay rate for the $0^+ \to 0^+$ transition

The decay rate for the $0^+ \to J^+$ transition ($J \neq 2$) takes the form,

$$d\Gamma_{0\nu}(0^+ \to J^+) = \frac{a_{0\nu}}{(m_e R)^2}\left\{ A_J^{(0\nu)} + (\hat{p}_1 \cdot \hat{p}_2) B_J^{(0\nu)} + \left[(\hat{p}_1 \cdot \hat{p}_2)^2 - \frac{1}{3}\right] C_J^{(0\nu)} \right\} d\Omega_{0\nu} \tag{C.3.1}$$

where

$$a_{0\nu} = (G g_A)^4 m_e^9 / (64\pi^5), \tag{C.3.2}$$

$$d\Omega_{0\nu} = m_e^{-5} p_1 p_2 \varepsilon_1 \varepsilon_2 \delta(\varepsilon_1 + \varepsilon_2 + E_f - M_i)\, d\varepsilon_1 d\varepsilon_2 d(\hat{p}_1 \cdot \hat{p}_2). \tag{C.3.3}$$

For the $0^+ \to 0^+$ transition in the 2n-mechanism, the coefficients are

$$A_0^{(0\nu)} = |N_1|^2 + |N_2|^2 + |N_3|^2 + |N_4|^2, \tag{C.3.4}$$

$$B_0^{(0\nu)} = -2\,\mathrm{Re}\,(N_1^* N_2 + N_3^* N_4), \tag{C.3.5}$$

$$C_0^{(0\nu)} = 0. \tag{C.3.6}$$

The matrix elements N's are given by some combinations of kinematical factors and reduced nuclear matrix elements which are defined in the previous subsections:

$$\begin{pmatrix} N_1 \\ N_2 \end{pmatrix} = \begin{pmatrix} \alpha_{-1}^* \\ \alpha_{11}^* \end{pmatrix} \begin{bmatrix} (Z_1 - Z_2) \\ \mp \left(\frac{4}{m_e R}\right)\left[Z_{4R} - \frac{1}{4}(\alpha z)^2 \{Z_7\}_C - \frac{3}{4}(\alpha z)^2 Z_{4RF} \right] \\ \pm \frac{2}{3}\left(\frac{3}{m_e R} \mp 2\right)\left[Z_6 - \{Z_{6R}\}_C \right] \end{bmatrix}, \tag{C.3.7a}$$

$$\begin{pmatrix} N_3 \\ N_4 \end{pmatrix} = \begin{pmatrix} \alpha^*_{1-1} \\ \alpha^*_{-11} \end{pmatrix} \begin{bmatrix} (Z_1 + Z_2) \\ \mp\left[\frac{\varepsilon_{12}}{m_e} Z_3 + \frac{1}{3}\left(\frac{\varepsilon_{12}}{m_e} \pm 2\right) Z_5\right] \\ \pm \frac{1}{3}\frac{\varepsilon_{12}}{m_e}\zeta\left(Z_{5R} - \frac{1}{2}\{Z_5\}_C\right) \end{bmatrix}, \tag{C.3.7b}$$

where ζ in Eq.(3.5.19) stands for the effect of the electron P-wave with J = 1/2, and the Coulomb correction $\alpha_{\lambda\chi}$ are defined as follows by using the normalization factor $A_\chi(\varepsilon)$ in Eq.(D.18) and the overall phase shift Δ^C_χ in Eq.(D.30):

$$\alpha_{\chi\lambda} = A_\chi(\varepsilon_1)\, A_\lambda(\varepsilon_2)\, e^{-i\Delta^C_\chi(\varepsilon_1) - i\Delta^C_\lambda(\varepsilon_2)} . \tag{C.3.8}$$

Now we shall assume in the m_ν part that $|Z_1| \gg |Z_2|$, because it is expected that $|\Sigma_j m_j G^2_{Aj}| \gg |\Sigma_j m_j \mathcal{E}^2_{Aj}|$ and $|\Sigma_j m_j G^2_V| \gg |\Sigma_j m_j \mathcal{E}^2_V|$. Concerning the V+A part, all terms with suffix C vanishing in the closure approximation will be neglected, and also the finite de Brogli wave-length correction terms like Z_{4RF} and the correction term due to the nucleon recoil (Z_{5R}) to the leading ω term are neglected.

Thus, within a good approximation, we have

$$\begin{pmatrix} N_1 \\ N_2 \end{pmatrix} = \begin{pmatrix} \alpha^*_{-1-1} \\ \alpha^*_{11} \end{pmatrix} \left[\left(Z_1 - \frac{4}{3}Z_6\right) \mp \left(\frac{4}{m_e R}\right)\left(Z_{4R} - \frac{1}{6}\zeta Z_6\right)\right], \tag{C.3.9a}$$

$$\begin{pmatrix} N_3 \\ N_4 \end{pmatrix} = \begin{pmatrix} \alpha^*_{1-1} \\ \alpha_{-11} \end{pmatrix} \left[\left(Z_1 - \frac{2}{3}Z_5\right) \mp \left(\frac{\varepsilon_{12}}{m_e}\right)\left(Z_3 + \frac{1}{3}Z_5\right)\right]. \tag{C.3.9b}$$

By using the definitions of nuclear parameters χ's in Eqs.(3.5.1) ~ Eq.(3.5.9) and the definitions of parameters in Eqs.(3.5.11)~ (3.5.13) and by neglecting the χ term as in Eq.(C.2.22), we have

$$\begin{aligned}
Z_1 &= (\langle m_\nu\rangle/m_e)(\chi_F - 1) e^{i\psi_0} M^{(0\nu)}_{GT}, \\
Z_3 &= \left[-\langle\lambda\rangle(\chi_{GT\omega} - \chi_{F\omega}) e^{i(\psi_0-\psi_1)} + \langle\eta\rangle(\chi_{GT\omega} + \chi_{F\omega}) e^{i(\psi_0-\psi_2)}\right] M^{(0\nu)}_{GT}, \\
Z_{4R} &= \langle\eta\rangle \chi'_R e^{i(\psi_0-\psi_2)} M^{(0\nu)}_{GT}, \\
Z_5 &= \frac{1}{3}\left[\langle\lambda\rangle\chi_{1+} e^{i(\psi_0-\psi_1)} - \langle\eta\rangle\chi_{1-} e^{i(\psi_0-\psi_2)}\right] M^{(0\nu)}_{GT}, \\
Z_6 &= \langle\eta\rangle \chi'_P e^{i(\psi_0-\psi_2)} M^{(0\nu)}_{GT}
\end{aligned} \tag{C.3.10}$$

where $\chi_{1\pm}$ are defined in Eq.(3.5.16), the CP violation phase ψ_0 is

$$\Sigma_j m_j U^2_{ej} = \langle m_\nu\rangle e^{i\psi_0} \tag{C.3.11}$$

and ψ_1 and ψ_2 are defined in Eq.(3.5.14). It is understood that if the neutrino mass m_j is greater than 10 MeV, then $\langle m_\nu\rangle$ is defined in Eq.(9.1.1) instead of Eq.(3.5.11), and accordingly $M^{(0\nu)}_{GT}$ in this section corresponds to $M^{(0\nu)}_{GT}(m_j = 0)$. By substituting Eq.(C.3.10) into Eqs.(C.3.9) and (C.3.4), we obtain Eq.(3.5.10). It is clear from Eqs.(C.3.4) and (C.3.8) that the Coulomb corrections appear as four combinations

$$\alpha_\pm = |\alpha_{-1-1}|^2 \pm |\alpha_{11}|^2, \quad \beta_\pm = |\alpha_{1-1}|^2 \pm |\alpha_{-11}|^2. \tag{C.3.12}$$

Their approximate expressions are given in Eq.(3.5.20).

If nuclear matrix elements are complex, combinations of χ's in Eq.(3.5.15) should be changed as follows:

$$\chi_k \longrightarrow Re[\chi_k^*], \quad \chi_k\chi_\ell \longrightarrow Re[\chi_k\chi_\ell^*], \tag{C.3.13a}$$

and the following additional terms should be added,

$$\begin{aligned}
C_{2I} &= Im(1-\chi_F)[\chi_{2-}^* b_{03} - \chi_{1+}^* b_{04}]\tan\psi_1, \\
C_{3I} &= -Im(1-\chi_F)[\chi_{2+}^* b_{03} - \chi_{1-}^* b_{04} - \chi_P'^* b_{05} + \chi_R'\chi_{06}]\tan\psi_2, \\
C_{6I} &= -2Im[\chi_{2-}\chi_{2+}^* b_{02} - \tfrac{1}{9}(\chi_{1+}\chi_{2+}^* + \chi_{2-}\chi_{1-}^*) b_{03} + \tfrac{1}{9}\chi_{1+}\chi_{1-}^* b_{04}]\tan(\psi_1-\psi_2),
\end{aligned} \tag{C.3.13b}$$

Within the same approximation, the correlation part $B_0^{(0\nu)}$ in Eq.(C.3.6) by substituting Eq.(C.3.9) is expressed as

$$B_0^{(0\nu)} = |M_{GT}^{(0\nu)}|^2 \left[\begin{array}{l} C_1^{(B)}\left(\frac{\langle m_\nu\rangle}{m_e}\right)^2 + C_2^{(B)}\left(\frac{\langle m_\nu\rangle}{m_e}\right)\langle\lambda\rangle\cos\psi_1 \\ + C_3^{(B)}\left(\frac{\langle m_\nu\rangle}{m_e}\right)\langle\eta\rangle\cos\psi_2 \\ + C_4^{(B)}\langle\lambda\rangle^2 + C_5^{(B)}\langle\eta\rangle^2 + C_6^{(B)}\langle\lambda\rangle\langle\eta\rangle\cos(\psi_1-\psi_2) \end{array}\right], \tag{C.3.14}$$

where six coefficients $C_i^{(B)}$ are defined as followes for the real nuclear matrix elements and $\sin\psi_1 = \sin\psi_2 = 0$,

$$C_1^{(B)} = -|1-\chi_F|^2 b_{01}^{(B)}, \tag{C.3.15a}$$

$$C_2^{(B)} = -Re[(1-\chi_F)\chi_{1+}^*] b_{04}^{(B)}, \tag{C.3.15b}$$

$$C_3^{(B)} = +Re[(1-\chi_F)\chi_{1-}^*] b_{04}^{(B)} - Re[(1-\chi_F)\chi_P'^*] b_{05}^{(B)}, \tag{C.3.15c}$$

$$C_4^{(B)} = |\chi_{2-}|^2 b_{02}^{(B)} - \tfrac{1}{9}|\chi_{1+}|^2 b_{04}^{(B)}, \tag{C.3.15d}$$

$$C_5^{(B)} = \left[\begin{array}{l} |\chi_{2+}|^2 b_{02}^{(B)} - \frac{1}{9}|\chi_{1-}|^2 b_{04}^{(B)} \\ \qquad + |\chi_R'|^2 b_{09}^{(B)} - Re(\chi_R'\chi_P'^*) b_{07}^{(B)} + |\chi_P'|^2 b_{08}^{(B)} \end{array}\right], \tag{C.3.15e}$$

$$C_6^{(B)} = (-2)\left\{Re[\chi_{2-}\chi_{2+}^*] b_{02}^{(B)} - \tfrac{1}{9}Re[\chi_{1+}\chi_{1-}^*] b_{04}^{(B)}\right\} \tag{C.3.15f}$$

If nuclear matrix elements are complex and $\sin\psi_K \neq 0$, the followings should be added,

$$\begin{aligned}
C_{1I}^{(B)} &= \left\{\begin{array}{l} Im[(1-\chi_F)\chi_{1+}^*]\tan\psi_1\ b_{04}^{(B)} \\ -\{Re[(1-\chi_F)\chi_{2-}^*]\tan\psi_1 + Im[(1-\chi_F)\chi_{2-}^*]\}\ b_{03I}^{(B)} \end{array}\right\}, \\
C_{3I}^{(B)} &= \left\{\begin{array}{l} -Im[(1-\chi_F)\chi_{1-}^*]\tan\psi_2\ b_{04}^{(B)} + Im[(1-\chi_F)\chi_P'^*]\tan\psi_2\ b_{05}^{(B)} \\ +\{Re[(1-\chi_F)\chi_{2+}^*]\tan\psi_2 + Im[(1-\chi_F)\chi_{2+}^*]\}\ b_{03I}^{(B)} \\ -\{Re[(1-\chi_F)\chi_P'^*]\tan\psi_2 + Im[(1-\chi_F)\chi_P'^*]\}\ b_{05I}^{(B)} \\ +\{Re[(1-\chi_F)\chi_R'^*]\tan\psi_2 + Im[(1-\chi_F)\chi_R'^*]\}\ b_{06I}^{(B)} \end{array}\right\}, \\
C_{4I}^{(B)} &= -\tfrac{2}{9}Im[\chi_{1+}\chi_{2-}^*]\ b_{03I}^{(B)}, \\
C_{5I}^{(B)} &= -\tfrac{2}{9}Im[\chi_{1-}\chi_{2+}^*] b_{03I}^{(B)} - Im[\chi_R'\chi_P'^*]\ b_{07I}^{(B)}, \\
C_{6I}^{(B)} &= 2\left[\begin{array}{l} \{-Im[\chi_{2-}\chi_{2+}^*]\ b_{02}^{(B)} + \frac{1}{9}Im[\chi_{1+}\chi_{1-}^*]\ b_{04}^{(B)}\}\tan(\psi_1-\psi_2) \\ +\frac{1}{9}\left\{\begin{array}{l}\{-Re[\chi_{1+}\chi_{2+}^*] + Re[\chi_{2-}\chi_{1-}^*]\}\tan(\psi_1-\psi_2) \\ \{+Im[\chi_{1+}\chi_{2+}^*] - Im[\chi_{2-}\chi_{1-}^*]\}\end{array}\right\} b_{03I}^{(B)} \end{array}\right].
\end{aligned} \tag{C.3.16}$$

Here kinematical factors $b_{0j}^{(B)}$ are

$$\begin{aligned}
b_{01}^{(B)} &= 2(\alpha_R+\beta_R), & b_{02}^{(B)} &= 2\left(\frac{E_{12}}{m_e}\right)^2\beta_R, \\
b_{03}^{(B)} &= \frac{16}{3}\alpha_R, & b_{04}^{(B)} &= \frac{8}{9}\beta_R, \\
b_{07R}^{(B)} &= \frac{32}{3}\frac{1}{(m_eR)^2}5\alpha_R, & b_{09}^{(B)} &= \frac{32}{(m_eR)^2}\alpha_R, \\
b_{08}^{(B)} &= \frac{8}{9}\left[\frac{5^2}{(m_eR)^2}-4\right]\alpha_R, & & \\
b_{03I}^{(B)} &= 4\left(\frac{E_{12}}{m_e}\right)\beta_I, & b_{05I}^{(B)} &= \frac{8}{3}\frac{1}{(m_eR)}5\alpha_I, \\
b_{06I}^{(B)} &= \frac{16}{(m_eR)}\alpha_I, & b_{07I}^{(B)} &= \frac{64}{3}\frac{1}{(m_eR)}\alpha_I.
\end{aligned} \tag{C.3.17}$$

and the combinations of the Coulomb normalization factors are

$$\alpha_R = \mathrm{Re}\,(\alpha_{-1-1}\alpha_{11}^{*}) \Rightarrow \tfrac{1}{4} p_1 p_2 \cos(\Delta_{-1-1} - \Delta_{11})\, C_{00},$$
$$\beta_R = \mathrm{Re}\,(\alpha_{1-1}\alpha_{-11}^{*}) \Rightarrow \tfrac{1}{4} p_1 p_2 \cos(\Delta_{1-1} - \Delta_{-11})\, C_{00},$$
$$\alpha_I = \mathrm{Im}\,(\alpha_{-1-1}\alpha_{11}^{*}) \Rightarrow -\tfrac{1}{4} p_1 p_2 \sin(\Delta_{-1-1} - \Delta_{11})\, C_{00},$$
$$\beta_I = \mathrm{Im}\,(\alpha_{1-1}\alpha_{-11}^{*}) \Rightarrow -\tfrac{1}{4} p_1 p_2 \sin(\Delta_{1-1} - \Delta_{-11})\, C_{00}. \quad \text{(C.3.18)}$$

The arrow means the approximation in Eq.(3.1.24), and $C_{K\lambda}$ is defined in Eq. (3.5.21).

§C.4 The $0^+ \to 2^+$ transition in the $(\beta\beta)_{0\nu}$ mode

The combination of the lowest electron partial waves for the $0^+ \to 2^+$ transition is the S-$P_{3/2}$ case, because the total angular momentum of two electron system should be $J_{2e} = 2$.

As it is clear from the selection rule for the m_ν part given in Table C.1, the parity odd nuclear operators are required in this S-$P_{3/2}$ case for the $0^+ \to 2^+$ transition, i.e. the nucleon recoil term Y^{ℓ}_{1R} in Eq.(C.2.12b). The rank 0 tensor operator, X in Eq.(C.2.12a), can not contribute, if one electron is the S-wave. Thus, the leading term from the m_ν part should come from the nuclear spin flip operator Y^{ℓ}_{1V} for the combination of the S- and $D_{3/2}$-electron waves. Therefore, we will ignore this contribution.

On the other hand, the situation becomes better for the V+A part, because of not only the large virtual neutrino momentum but also the rank 2 nuclear tensor operators like $X^{\ell k}_4$ and $Y^{\ell k}_6$ in Eq.(C.2.34), as seen from the selection rule for the V+A part in Table C.2.

It is easily seen from Table C.2 that Eqs.(C.2.41) and (C.2.42) for the $(0^+ \to 0^+)_{S\text{-}P_{1/2}}$ case can be used by reinterpreting the

electron currents $F^{\mu}_{\pm}$ and $F^{\mu}_{5\pm}$ as those for the $P_{3/2}$-wave instead of the $P_{1/2}$-wave. The parts from the ω term should include the nucleon recoil effect like X^{ℓ}_{4R} and Y^{ℓ}_{5R} similarly to the m_ν part mentioned above. Therefore they play only the minor correction to the contribution due to the $\vec{q}$ term, especially because of the neutrino potential difference, $H_{\omega 2} - H_{\omega 1}$. In addition, it should be noted that the $P_{3/2}$-wave is quite simple in comparison with the $P_{1/2}$-wave, because the leading term of the former is nothing but the first term of the spherical Bessel function $j_1(pr)$, cf. Eqs. (3.1.22) and (3.1.23). Therefore, there is no complication like the P-wave effect in the $P_{1/2}$-wave case.

Thus, for the $0^+ \to 2^+$ transition, it is enough to consider the first two terms, $X^{\ell k}_4 F^{k}_{-}$ and $Y^{\ell k}_6 F^{k}_{5+}$, in Eq.(C.2.41). Therefore, two following combinations of nuclear matrix elements enter as the leading contributions for the S-$P_{3/2}$ case in the $0^+ \to 2^+$ transitions;

$$(\mathcal{Z}_{21})^{k\ell} = \Sigma_j \Sigma_a \langle 2^+_f \,|\, h'_+(r_{nm}, E_a)(\hat{r}_{nm})^{j} X^{jk}_{4}(\hat{r}_{nm})^{\ell} \,|\, 0^+_i \rangle, \quad \text{(C.4.1)}$$

$$(\mathcal{Z}_{22})^{k\ell} = \Sigma_j \Sigma_a \langle 2^+_f \,|\, \left(\tfrac{i}{2 r_{nm}}\right) h'_+(r_{nm}, E_a)(\hat{r}_{nm})^{j} Y^{jk}_{6}(\hat{r}_{nm})^{\ell} \,|\, 0^+_i \rangle. \quad \text{(C.4.2)}$$

By using the definition of the reduced matrix element in Eq. (B.1.2) and the definitions of X^{jk}_4 and Y^{jk}_6 in Eq.(C.2.34), we find

$$\mathcal{Z}_{21} = \Sigma_j \Sigma_a \langle 2^+_f \| h'_+(r_{nm}, E_a)\, O_{12} \| 0^+_i \rangle$$

$$O_{12} \equiv \left\{ \begin{array}{l} [\hat{r}_{nm} \otimes \hat{r}_{nm}]^{(2)} (G_V \varepsilon_V + G_A \varepsilon_A (\vec{\sigma}_n \cdot \vec{\sigma}_m)) \\ - G_A \varepsilon_A \left([\hat{r}_{nm} \otimes \vec{\sigma}_n]^{(2)} (\hat{r}_{nm} \cdot \vec{\sigma}_m) + (\hat{r}_{nm} \cdot \vec{\sigma}_n)[\hat{r}_{nm} \otimes \vec{\sigma}_m]^{(2)} \right) \\ + i G_+ \left([\hat{r}_{nm} \otimes (\hat{r}_{nm} \times \vec{\sigma}_n)]^{(2)} + [\hat{r}_{nm} \otimes (\hat{r}_{nm} \times \vec{\sigma}_m)]^{(2)} \right) \end{array} \right\}, \quad \text{(C.4.3)}$$

$$Z_{22} = \sum_j \sum_a \langle 2_f^+ \| h_+(r_{nm}, E_a)\, O_{22} \| 0_i^+ \rangle,$$

$$O_{22} = -i\, G_-(r_{+nm}/r_{nm}) \left[\hat{r}_{+nm} \otimes \left(\hat{r}_{nm} \times (\vec{\sigma}_n - \vec{\sigma}_m) \right) \right]^{(2)}. \qquad \text{(C.4.4)}$$

which correspond to Z_5 and Z_6 in Eq.(C.2.43), respectively.

The Z_{21} and Z_{22} are obtained from the part of the additive neutrino potential, $(\vec{H}_{q2} + \vec{H}_{q1})$, and do not vanish in the closure approximation. Since there is no cancellation between leading terms, we need not consider other terms like 6 terms in Eqs.(C.2.41) and (C.2.42) and contributions from the higher spherical waves shown in Table C.2.

The coefficients of the partial decay rate for the $0^+ \to 2^+$ transition in Eq.(C.3.1) are

$$A_2^{(0\nu)} = \frac{1}{3} \left\{ |M_{2A}|^2 + |M_{2B}|^2 + |M_{2C}|^2 + |M_{2D}|^2 \right. \\ \left. + |N_{2A}|^2 + |N_{2B}|^2 + |N_{2C}|^2 + |N_{2D}|^2 \right\}, \qquad \text{(C.4.5)}$$

$$B_2^{(0\nu)} = -\frac{2}{3} Re \left\{ \left(M_{2A}^* M_{2B} + N_{2A}^* N_{2B} - M_{2C}^* N_{2D} - N_{2C}^* M_{2D} \right) \right. \\ \left. + \frac{1}{5} \left(M_{2A}^* N_{2A} + M_{2B}^* N_{2B} + M_{2C}^* N_{2C} + M_{2D}^* N_{2D} \right) \right\}, \qquad \text{(C.4.6)}$$

$$C_2^{(0\nu)} = \frac{1}{5} Re \left\{ M_{2A}^* N_{2B} + M_{2B}^* N_{2A} - M_{2C}^* M_{2D} - N_{2C}^* N_{2D} \right\}, \qquad \text{(C.4.7)}$$

where

$$\begin{pmatrix} M_{2A} \\ N_{2A} \end{pmatrix} = \begin{pmatrix} \alpha_{-2-1}^* \\ \alpha_{21}^* \end{pmatrix} \left(\frac{p_1}{m_e} \right) Z_{21}, \quad \begin{pmatrix} M_{2B} \\ N_{2B} \end{pmatrix} = \begin{pmatrix} \alpha_{-1-2}^* \\ \alpha_{12}^* \end{pmatrix} \left(\frac{p_2}{m_e} \right) Z_{21},$$

$$\begin{pmatrix} M_{2C} \\ N_{2C} \end{pmatrix} = \begin{pmatrix} \alpha_{-21}^* \\ \alpha_{2-1}^* \end{pmatrix} \left(\frac{p_1}{m_e} \right) Z_{22}, \quad \begin{pmatrix} M_{2D} \\ N_{2D} \end{pmatrix} = \begin{pmatrix} \alpha_{1-2}^* \\ \alpha_{-12}^* \end{pmatrix} \left(\frac{p_2}{m_e} \right) Z_{22} \qquad \text{(C.4.8)}$$

with $\alpha_{\kappa\lambda}$ defined in Eq.(C.3.8).

Thus, in the case where they are classified by the unknown parameters $\langle\lambda\rangle$ and $\langle\eta\rangle$ in Eqs.(3.5.12) and (3.5.13), we have

$$A_2^{(0\nu)} = b_{21} |Z_{21}|^2 + b_{22} |Z_{22}|^2, \qquad \text{(C.4.9)}$$

$$B_2^{(0\nu)} = -b_{21}^{(B)} |Z_{21}|^2 + b_{22}^{(B)} |Z_{22}|^2, \qquad \text{(C.4.10)}$$

$$C_2^{(0\nu)} = b_{21}^{(C)} |Z_{21}|^2 - b_{22}^{(C)} |Z_{22}|^2, \qquad \text{(C.4.11)}$$

where by using the definition of nuclear matrix elements in Eq. (3.5.24), Z_{21} and Z_{22} are reexpressed as in Eq.(3.5.23) and the kinematical factors are

$$b_{21} = \frac{1}{3} \left[\left(\frac{p_1}{m_e} \right)^2 \left(|\alpha_{-2-1}|^2 + |\alpha_{21}|^2 \right) + \left(\frac{p_2}{m_e} \right)^2 \left(|\alpha_{-1-2}|^2 + |\alpha_{12}|^2 \right) \right],$$

$$b_{22} = \frac{1}{3} \left[\left(\frac{p_1}{m_e} \right)^2 \left(|\alpha_{-21}|^2 + |\alpha_{2-1}|^2 \right) + \left(\frac{p_2}{m_e} \right)^2 \left(|\alpha_{1-2}|^2 + |\alpha_{-12}|^2 \right) \right], \qquad \text{(C.4.12)}$$

$$b_{21}^{(B)} = \frac{2}{3} Re \left\{ \left(\frac{p_1 p_2}{m_e^2} \right) \left(\alpha_{-2-1}^* \alpha_{-1-2} + \alpha_{21}^* \alpha_{12} \right) + \frac{1}{5} \left[\left(\frac{p_1}{m_e} \right)^2 \alpha_{-2-1}^* \alpha_{21} + \left(\frac{p_2}{m_e} \right)^2 \alpha_{-1-2}^* \alpha_{12} \right] \right\},$$

$$b_{22}^{(B)} = \frac{2}{3} Re \left\{ \left(\frac{p_1 p_2}{m_e^2} \right) \left(\alpha_{21}^* \alpha_{12} + \alpha_{2-1}^* \alpha_{1-2} \right) - \frac{1}{5} \left[\left(\frac{p_1}{m_e} \right)^2 \alpha_{21}^* \alpha_{2-1} + \left(\frac{p_2}{m_e} \right)^2 \alpha_{-12}^* \alpha_{1-2} \right] \right\}, \qquad \text{(C.4.13)}$$

$$b_{21}^{(C)} = \frac{1}{5} \left(\frac{p_1 p_2}{m_e^2} \right) Re \left(\alpha_{-2-1}^* \alpha_{12} + \alpha_{21}^* \alpha_{-1-2} \right),$$

$$b_{22}^{(C)} = \frac{1}{5} \left(\frac{p_1 p_2}{m_e^2} \right) Re \left(\alpha_{-21}^* \alpha_{1-2} + \alpha_{2-1}^* \alpha_{-12} \right), \qquad \text{(C.4.14)}$$

and their approximate forms are a little complicated as follows:

$$\begin{pmatrix} b_{21} \\ b_{22} \end{pmatrix} \Longrightarrow \frac{1}{6} \left(\varepsilon_1 \varepsilon_2 \pm m_e^2 \right) \left[\left(\frac{p_1}{m_e} \right)^2 C_{10} + \left(\frac{p_2}{m_e} \right)^2 C_{01} \right],$$

$$\begin{pmatrix} b_{21}^{(B)} \\ b_{22}^{(B)} \end{pmatrix} \Rightarrow \frac{1}{6}\left(\frac{p_1 p_2}{m_e^2}\right)\left[2(\varepsilon_1\varepsilon_2 \pm m_e^2)\sqrt{C_{10}\,C_{01}} \pm \frac{1}{5}(p_1^2 C_{10} + p_2^2 C_{01})\right],$$

$$\begin{pmatrix} b_{21}^{(C)} \\ b_{22}^{(C)} \end{pmatrix} \Rightarrow \frac{1}{10}\frac{(p_1 p_2)^2}{m_e^2}\sqrt{C_{10}\,C_{01}}\,, \qquad \text{(C.4.15)}$$

where $C_{\kappa\lambda}$ is defined in Eq. (3.5.21).

Appendix D

- Electron Coulomb wave functions -

In this Appendix, the relativistic lepton wave functions distorted by the Coulomb field of the daughter nucleus are summarized to explain notation and to be convenient for readers who wish to check numerical values of various quantities given in this paper. The detailed derivations have been given by Rose and many others.[163),164)] In the $\beta\beta$ decay, rigorously speaking, the Coulomb field due to the intermediate nucleus is different from the field of the daughter nucleus. This effect will be discussed at the last paragraph.

The lepton wave function $\psi_s(\varepsilon, \vec{r})$ is expressed as a superposition of Coulomb-distorted spherical waves,

$$\psi_s(\varepsilon, \vec{r}) = \sum_{\kappa,\mu} a_{\kappa\mu}(\hat{p}, s)\, \psi_{\kappa\mu}(\varepsilon, \vec{r}), \qquad \text{(D.1)}$$

where the partial waves $\psi_{\kappa\mu}$ are defined as

$$\psi_{\kappa\mu}(\varepsilon, \vec{r}) = \begin{pmatrix} \tilde{g}_\kappa(\varepsilon, r)\,\chi_{\kappa\mu}(\hat{r}) \\ i\,\tilde{f}_\kappa(\varepsilon, r)\,\chi_{-\kappa\mu}(\hat{r}) \end{pmatrix}, \qquad \text{(D.2)}$$

and the weight factor $a_{\kappa\mu}(\hat{p}, s)$ is introduced to describe the electron with a specific momentum direction $\hat{p}$ and a polarization s at infinity of r, that is,

$$a_{\kappa\mu}(\hat{p}, s) = 4\pi\, i^{\ell_\kappa}\, C(\ell_\kappa, \tfrac{1}{2}, j_\kappa\,;\, \mu - s, s)\, Y_{\ell_\kappa}^{\mu-s\,*}(\hat{p}). \qquad \text{(D.3)}$$

Here κ takes either positive or negative integers ($\pm k$), the total angular momentum is defined as $j_\kappa = |\kappa| - \frac{1}{2}$, and the orbital angular momenta are $\ell_\kappa = k$ for $\kappa = k > 0$, $\ell_\kappa = k-1$ for $\kappa = -k < 0$, and $\ell_{-\kappa} = \ell_\kappa - s_\kappa$ with $s_\kappa = \kappa/|\kappa|$.

The angular part $\chi_{\kappa\mu}(\hat{r})$ in Eq.(D.2) is expressed in the standard notation as

$$\chi_{\kappa\mu}(\hat{r}) = \sum_{\sigma=\pm\frac{1}{2}} C(\ell_\kappa, \tfrac{1}{2}, j_\kappa; \mu-\sigma, \sigma)\, Y_{\ell_\kappa}^{\mu-\sigma}(\hat{r})\, \chi_\sigma , \qquad (D.4)$$

where χ_σ is a two component Pauli spinor with the polarization σ, as used in Eq.(2.4.7). In the text, the partial waves are classified by ℓ_κ in $Y_{\ell_\kappa}^{\mu-\sigma}(\hat{r})$: Namely, $\ell_\kappa = 0$ and 1 stand for the S- and P-waves shown in Eqs.(3.1.20a) and (3.1.20b), respectively, and the D-wave with $j = 3/2$ is*)

$$\psi^{(D)}(\varepsilon, \vec{r}) = \begin{pmatrix} \tilde{g}_{+2}\,[-3(\vec{\sigma}\cdot\hat{r})(\vec{\sigma}\cdot\hat{r})(\vec{\sigma}\cdot\hat{p}) + 1]\,\chi_s \\ \tilde{f}_{-2}\,[3(\vec{\sigma}\cdot\hat{r})(\vec{\sigma}\cdot\hat{r}) - (\vec{\sigma}\cdot\hat{p})]\,\chi_s \end{pmatrix}_{j=3/2} . \qquad (D.5)$$

The modified radial wave functions in Eq.(D.2) are defined as

$$\begin{pmatrix} \tilde{g}_\kappa(\varepsilon, r) \\ \tilde{f}_\kappa(\varepsilon, r) \end{pmatrix} = e^{-i\Delta_\kappa^C} \begin{pmatrix} g_\kappa(\varepsilon, r) \\ f_\kappa(\varepsilon, r) \end{pmatrix}, \qquad (D.6)$$

where the overall phase shift Δ_κ^C is introduced to satisfy the boundary condition at $r = \infty$, a plane wave plus an incoming spherical wave, and given in Eq.(D.30) explicitly.

The screening correction due to the atomic charge depends on the assumption on the distribution of atomic electrons. Behrens and Jänecke have shown that it does not have the serious energy dependence (few percent reduction). Therefore, we do not take account of this correction in this paper. Thus, the non-zero phase shift Δ_κ^C depends in principle on the choice of the electrostatic

*) Note that the Pauli-Dirac representation of γ matrices is employed for the lepton wave functions: $\gamma^0 = \begin{pmatrix} 1 & 0 \\ 0 & -1 \end{pmatrix}$, $\vec{\gamma} = \begin{pmatrix} 0 & \vec{\sigma} \\ -\vec{\sigma} & 0 \end{pmatrix}$, $\gamma_5 = \begin{pmatrix} 0 & 1 \\ 1 & 0 \end{pmatrix}$.

potential $V(r)$ between the emitted electron and the daughter nucleus. Since the electron radial wave functions do not depend on $V(r)$ seriously,[165] the potential of the uniform charge distribution inside nucleus is used in this paper;

$$V(r) = \begin{cases} -\left(\frac{\alpha Z}{2R}\right)\left[3 - \left(\frac{r}{R}\right)^2\right] & \text{for } r \le R, \\ -\frac{\alpha Z}{r} & \text{for } r \ge R, \end{cases} \qquad (D.7)$$

where R denotes the nuclear radius $R = 3.108\cdot10^{-3}\, A^{1/3}(1/m_e)$.

The normalization of the radial wave functions $\tilde{g}_\kappa$ and $\tilde{f}_\kappa$ in Eq.(D.6) is chosen so that they reproduce the following spherical Bessel function in the limit $V(r) \to 0$;

$$\begin{pmatrix} \tilde{g}_\kappa(r) \\ \tilde{f}_\kappa(r) \end{pmatrix} \xrightarrow{\alpha Z \to 0} \sqrt{\frac{\varepsilon \pm m}{2\varepsilon}} \begin{pmatrix} j_{\ell_\kappa}(pr) \\ s_\kappa\, j_{\ell-\kappa}(pr) \end{pmatrix}, \qquad (D.8)$$

with $\exp(-i\Delta_\kappa^C) = 1$. By substituting Eq.(D.8), Eq.(D.1) is reduced to the well-known plane wave solution,

$$\psi_s(\varepsilon, \vec{r}) = \sqrt{\frac{\varepsilon + m}{2\varepsilon}} \begin{pmatrix} \chi_s \\ \frac{(\vec{\sigma}\cdot\vec{p})}{\varepsilon + m}\chi_s \end{pmatrix} e^{i\vec{p}\cdot\vec{r}} . \qquad (D.9)$$

For the neutrino radial wave functions, the right-hand side of Eq.(D.8) is used.

The inner regular solutions (inside nucleus, $r < R$) are expressed as a power series expansion of r:

$$\begin{aligned} \begin{pmatrix} g_\kappa(\varepsilon, r) \\ f_\kappa(\varepsilon, r) \end{pmatrix} &= A_\kappa \begin{pmatrix} g_\kappa^{(i)}(\varepsilon, r) \\ f_\kappa^{(i)}(\varepsilon, r) \end{pmatrix} \\ &= A_\kappa \frac{(pr)^{k-1}}{(2k-1)!!} \sum_{\ell=0}^{\infty} \begin{pmatrix} b_{\kappa,\ell} \\ a_{\kappa,\ell} \end{pmatrix} \left(\frac{r}{R}\right)^\ell . \end{aligned} \qquad (D.10)$$

Here the expansion coefficients ($a_{\kappa,n}$ and $b_{\kappa,n}$) are obtained by the recurrence relations given by Bühring,[164]

$$a_{\kappa,l+1} = \frac{-[(\varepsilon-m)R + \frac{3}{2}\alpha Z]\, b_{\kappa,l} + \frac{1}{2}\alpha Z\, b_{\kappa,l-1}}{l+1+k-\kappa},$$

$$b_{\kappa,l+1} = \frac{[(\varepsilon+m)R + \frac{3}{2}\alpha Z]\, a_{\kappa,l} - \frac{1}{2}\alpha Z\, a_{\kappa,l-1}}{l+1+k+\kappa}, \qquad \text{(D.11)}$$

where the initial values are

$$a_{k,0} = b_{-k,0} = 0,$$

$$a_{k,2l+1} = b_{-k,2l+1} = 0 \qquad \text{for } l \geq 0,$$

$$(a_{-k,2l} = b_{k,2l} = 0), \qquad \text{(D.12)}$$

$$a_{\kappa,-l} = b_{\kappa,-l} = 0 \qquad \text{for } l \geq 1.$$

Each partial wave of the inner regular solution up to the term of r^2 is as follows: The S-wave case is

$$\begin{pmatrix} g_{-1}(\varepsilon,r) \\ f_{+1}(\varepsilon,r) \end{pmatrix} \simeq A_{\mp 1}\left[1 - \frac{1}{6}(\bar{p}r)^2\right], \qquad \text{(D.13)}$$

where α is the fine structure constant ($\alpha^{-1} = 137.036$), and

$$(\bar{p}r)^2 = \left[\left(\frac{3}{2}\alpha Z\right)^2\left(\frac{r}{R}\right)^2 + 3\alpha Z\left(\frac{r}{R}\right)\varepsilon r + (pr)^2\right]. \qquad \text{(D.14)}$$

The $P_{1/2}$-wave case is

$$\begin{pmatrix} g_{+1}(\varepsilon,r) \\ f_{-1}(\varepsilon,r) \end{pmatrix}$$

$$\simeq \pm A_{\pm 1}\left(\frac{r}{3R}\right)\left\{\left[\frac{3}{2}\alpha Z + (\varepsilon \pm m)R\right]\left[1 - \frac{1}{10}(pr)^2\right] - \frac{3}{10}\alpha Z\left(\frac{r}{R}\right)^2\right\}. \qquad \text{(D.15)}$$

The $P_{3/2}$-wave case is

$$\begin{pmatrix} g_{-2}(\varepsilon,r) \\ f_{+2}(\varepsilon,r) \end{pmatrix} \simeq A_{\mp 2}\left(\frac{pr}{3}\right)\left[1 - \frac{1}{10}(\bar{p}r)^2\right]. \qquad \text{(D.16)}$$

The $D_{3/2}$-wave case is

$$\begin{pmatrix} g_{+2}(\varepsilon,r) \\ f_{-2}(\varepsilon,r) \end{pmatrix}$$

$$\simeq A_{\pm 2}\left(\frac{pr}{15}\right)\left(\frac{r}{R}\right)\left\{\left[\frac{3}{2}\alpha Z + (\varepsilon \pm m)R\right]\left[1 - \frac{1}{14}(\bar{p}r)^2\right] - \frac{4}{15}\alpha Z\left(\frac{r}{R}\right)^2\right\}. \qquad \text{(D.17)}$$

As easily seen, the convergence of $f_\kappa^{(i)}$ and $g_\kappa^{(i)}$ at the nuclear surface ($r = R$) is very slow, so that the higher order terms of $a_{\kappa,l}$ and $b_{\kappa,l}$ in Eq. (D.11) should be taken into account when the continuity conditions at $r = R$ are used for the numerical calculation.

The normalization factor A_κ of the inner regular solution is determined by the continuity condition at $r = R$ to the outer ($r > R$) solutions, $g_\kappa(R) = B_\kappa\left[g_\kappa^{(o)}(R) + H_\kappa \overline{g_\kappa^{(o)}}(R)\right]$ and $f_\kappa(R) = B_\kappa\left[f_\kappa^{(o)}(R) + H_\kappa \overline{f_\kappa^{(o)}}(R)\right]$;

$$A_{-k} = \left[g_{-k}^{(o)}(R) \Big/ g_{-k}^{(i)}(R)\right] B_{-k}\,(1 + \delta_{g,-k}),$$

$$A_{+k} = \left[f_k^{(o)}(R) \Big/ f_k^{(i)}(R)\right] B_k\,(1 + \delta_{f,k}). \qquad \text{(D.18)}$$

These expressions are convenient to see their characteristic features and to avoid the computational errors, because the leading terms of $g_{-k}^{(i)}(R)$ and $f_k^{(i)}(R)$ in the denominator of Eq. (D.18) are the first term of the corresponding spherical Bessel function $j_{k-1}(pR)$, as seen from Eq. (D.10) and the initial values $a_{k,0} = b_{-k,0} = 1$ in Eq. (D.12). The total normalization constant B_κ of the outer solutions for $r > R$ is $B_\kappa \approx 1$, as shown in Eq. (D.24), and the mixing

parameters $h_{g,-k}$ and $h_{f,k}$ between g_κ and f_κ are of order of $(\alpha Z)^2$, as will be confirmed from Eq.(D.26). Thus, the main characters of A_{-k} and A_{+k} are determined by the leading terms of the outer regular solutions $g_{-k}^{(0)}(R)$ and $f_k^{(0)}(R)$, namely N_{Fk} and $N_{Fk}\sqrt{(\varepsilon-m)/(\varepsilon+m)}$ in Eq.(D.20), respectively. Thus, we can easily see that the approximation of $A_{\pm k}$ in Eq.(3.1.24) has a good accuracy within the order of $(\alpha Z)^2$. This approximation is the one used by Konopinski and Uhlenbeck for their analysis on the single β decay. Of course, in principle, we can calculate A_{+k} by using $g_{+k}^{(0)}$ and $g_k^{(i)}$, the leading term of which are proportional to αZ, and in addition, $h_{g,k} \simeq -1 + (1/2)\sqrt{(\varepsilon-m)(\varepsilon+m)}$. Thus, from this choice, we can not see the features of A_k transparently.

Now, let us list various quantities related to the outer $(r > R)$ solutions. The radial wave functions $g_\kappa^{(0)}$ and $f_\kappa^{(0)}$ in Eq.(D.18) are the outer $(r > R)$ regular solutions for the point charge,

$$\begin{aligned}
g_{-k}^{(0)}(\varepsilon,\gamma,m) &= N_{Fk}\left(R_k\sqrt{1+\zeta_k} + I_k\sqrt{1-\zeta_k}\right)/\sqrt{2},\\
g_k^{(0)}(\varepsilon,\gamma,m) &= N_{Fk}\left(I_k\sqrt{1+\zeta_k} - R_k\sqrt{1-\zeta_k}\right)/\sqrt{2},\\
f_{-k}^{(0)}(\varepsilon,\gamma,m) &= -g_k^{(0)}(\varepsilon,\gamma,-m),\\
f_k^{(0)}(\varepsilon,\gamma,m) &= g_{-k}^{(0)}(\varepsilon,\gamma,-m),
\end{aligned} \tag{D.19}$$

which are obtained from Eqs.(5.76) and (5.77) of Ref.(163) by changing the normalization and by using the phase convention $\pi \le \eta_k < \frac{3}{2}\pi$ and $\frac{7}{4}\pi < \eta_{-k} \le 2\pi$. With this phase convention, $g_\kappa^{(0)}$ and $f_\kappa^{(0)}$ are reduced to the plane wave solution in Eq.(D.9) in the limit $\alpha Z \to 0$. Here the normalization N_{Fk} of the outer regular solution is

$$N_{Fk} = \sqrt{\frac{\varepsilon+m}{2\varepsilon}\,F_{k-1}(Z,\varepsilon)}\;\frac{(2\rho\gamma)^{k-1}}{(2k-1)!!}, \tag{D.20}$$

and the Fermi factor $F_{k-1}(Z,\varepsilon)$, y and γ_k are defined in Eqs.(3.1.25) and (3.1.26), and

$$\zeta_\kappa = \frac{\kappa\gamma_\kappa - y^2(m/\varepsilon)}{\gamma_k^2 + y^2}, \qquad \zeta_k = -\zeta_{-k}, \tag{D.21}$$

$$R_k + i\,I_k = \left(\frac{r}{R}\right)^{\gamma_k-k}\left(\frac{\gamma_k+iy}{k}\right)e^{i\rho\gamma}\,F(\gamma_k-iy,\,2\gamma_k+1;\,-2i\rho\gamma), \tag{D.22}$$

with F(a,c;x) being the confluent hypergeometric function.*)

The outer irregular solutions $\bar{g}_\kappa^{(0)}$ and $\bar{f}_\kappa^{(0)}$ are given by

$$\begin{aligned}
\bar{g}_{-k}^{(0)}(\varepsilon,\gamma,m) &= -\bar{N}_{Fk}\left(\bar{R}_k\sqrt{1-\zeta_k} + \bar{I}_k\sqrt{1+\zeta_k}\right)/\sqrt{2},\\
\bar{g}_k^{(0)}(\varepsilon,\gamma,m) &= \bar{N}_{Fk}\left(\bar{R}_k\sqrt{1+\zeta_k} - \bar{I}_k\sqrt{1-\zeta_k}\right)/\sqrt{2},\\
\bar{f}_{-k}^{(0)}(\varepsilon,\gamma,m) &= -\bar{g}_{+k}^{(0)}(\varepsilon,\gamma,-m),\\
\bar{f}_k^{(0)}(\varepsilon,\gamma,m) &= \bar{g}_{-k}^{(0)}(\varepsilon,\gamma,-m),
\end{aligned} \tag{D.23}$$

where $\bar{N}_{Fk}$ and $\bar{R}_k + i\,\bar{I}_k$ are obtained from N_{Fk} and $R_k + i\,I_k$ in Eqs.(D.20) and (D.22), respectively, by replacing γ_k with $-\gamma_k$. The corresponding phase convention for $\bar{\eta}_\kappa$ is $0 < \bar{\eta}_k < \pi/4$ and $\pi/2 \le \bar{\eta}_{-k} \le \pi$.

*) In the limit of $\alpha Z \to 0$, we get $\zeta_k \to 1$, $\zeta_k \to 1$, $F_{k-1} \to 1$ and $(R_k + i\,I_k) \to [(\rho r)^{1-k}(2k-1)!!][j_{k-1}(\rho r) + i\,j_k(\rho r)]$.

The total normalization factor B_κ of the outer solution is

$$B_\kappa = \left[1 + 2 H_\kappa \cos(\delta_\kappa - \bar{\delta}_\kappa) + H_\kappa^2 \right]^{-1/2} . \tag{D.24}$$

The mixing parameter between the outer regular and irregular solution is

$$H_\kappa = \rho_{g,\kappa} \left(\frac{g_\kappa^{(o)}(R)}{\bar{g}_\kappa^{(o)}(R)} \right) = \rho_{f,\kappa} \left(\frac{f_\kappa^{(o)}(R)}{\bar{f}_\kappa^{(o)}(R)} \right) , \tag{D.25}$$

and the mixing parameters between various $f_\kappa(R)$ and $g_\kappa(R)$ are

$$\rho_{g,\kappa} = \frac{\beta_\kappa - 1}{1 - \bar{\beta}_\kappa} , \quad \rho_{f,\kappa} = \frac{\beta_\kappa^{-1} - 1}{1 - \bar{\beta}_\kappa^{-1}} , \tag{D.26}$$

where

$$\beta_\kappa = \frac{f_\kappa^{(o)}(R) / g_\kappa^{(o)}(R)}{f_\kappa^{(i)}(R) / g_\kappa^{(i)}(R)} , \quad \bar{\beta}_\kappa = \frac{\bar{f}_\kappa^{(o)}(R) / \bar{g}_\kappa^{(o)}(R)}{f_\kappa^{(i)}(R) / g_\kappa^{(i)}(R)} . \tag{D.27}$$

The Coulomb phase shifts, δ_κ and $\bar{\delta}_\kappa$ appeared in Eq.(D.24), are defined by

$$\delta_\kappa = \eta_\kappa - \tfrac{1}{2}\pi\gamma_k - \arg \Gamma(\gamma_k + iy) , \tag{D.28a}$$

$$\bar{\delta}_\kappa = \bar{\eta}_\kappa + \tfrac{1}{2}\pi\gamma_k - \arg \Gamma(-\gamma_k + iy) , \tag{D.28b}$$

where phases η_κ and $\bar{\eta}_\kappa$ are defined as

$$\cos\eta_\kappa = -S_\kappa \sqrt{\frac{1 - S_\kappa}{2}} , \quad \sin\eta_\kappa = -\sqrt{\frac{1 + S_\kappa}{2}} , \tag{D.29a}$$

$$\cos\bar{\eta}_\kappa = S_\kappa \sqrt{\frac{1 - S_{-\kappa}}{2}} , \quad \sin\bar{\eta}_\kappa = \sqrt{\frac{1 + S_{-\kappa}}{2}} . \tag{D.29b}$$

The boundary condition at $r \to \infty$ determines the overall phase chift Δ_κ^c in Eq.(D.6)

$$\Delta_\kappa^c = \Delta_\kappa + \left(\frac{\pi}{2}\right)(\ell_\kappa + 1) , \tag{D.30}$$

$$\tan\Delta_\kappa = \frac{\sin\delta_\kappa + H_\kappa \sin\bar{\delta}_\kappa}{\cos\delta_\kappa + H_\kappa \cos\bar{\delta}_\kappa} . \tag{D.31}$$

Let us list the various approximations for the relativistic Fermi factor $F_{k-1}(Z,\varepsilon)$ in Eq.(3.1.23). It is reduced to the non-relativistic one (the NR case) by approximating $\gamma_k = \sqrt{k^2 - \alpha^2 Z^2} \to k$,

$$F_{k-1}^{NR}(Z,\varepsilon) \Rightarrow F_0^{NR} [(k-1)!]^{-2} \prod_{j=1}^{k-1} [(k-j)^2 + y^2] , \tag{D.32}$$

where

$$F_0^{NR}(Z,\varepsilon) = 2\pi y / [1 - \exp(-2\pi y)] , \tag{D.33}$$

y being defined in Eq.(3.1.26). In order to get the analytical expression of the half-life, Primakoff and Rosen have made a further approximation (the P-R case),

$$F_0^{PR}(Z,\varepsilon) = 2\pi y / [1 - \exp(-2\pi\alpha Z)] . \tag{D.34}$$

The factor $(2pR)^{2(\gamma_k - k)}$ in $F_{k-1}(Z,\varepsilon)$ gives the sizable enhancement in comparison with $F_{k-1}^{NR}(Z,\varepsilon)$, so that Eq.(D.32) is not recommended for the quantitative estimation, as Haxton et al.[34] and Nishiura[35] pointed out. For numerical calculation, it is worthwhile to mention that, although $F_{k-1} \sim (\varepsilon/p)^{2k-1}$ and the normalization factor in Eq.(D.20) $N_{Fk} \sim (\varepsilon/p)^{-1/2}$ in the limit of $p \to 0$, the momentum spectrum of electron is finite at $p = 0$, because of the

phase space factor,*) for example $d\Omega_{2\nu}$ in Eq.(B.3.4). The finite value of the electron spectrum at $p \simeq 0$ is due to this attractive Coulomb force.

Finally, let us consider the effect due to the Coulomb field of the intermediate nucleus with (Z-1) protons in the $(\beta\beta)_{0\nu}$ mode. While the virtual neutrino is propagating from the position of the first neutron decay to the second, the electron wave is distorted by the Coulomb field due to (Z-1) proton. After this neutrino is absorbed by the second neutron, this wave is distorted by Z protons in the daughter nucleus. Thus, the Coulomb wave function of the first emitted electron should be modified, because the solution in this Appendix has been obtained only in the Coulomb field of the daughter nucleus.

Since the first electron is travelling inside nucleus on an average during the time of the neutrino propagation, most of this modification should be made for the inner solution. Let us consider first the normalization A_κ defined in Eq.(D.18). This A_κ includes $g_{-k}^{(i)}(R)$ and $f_k^{(i)}(R)$ in the denominator. Their leading terms are given by the first term of $j_k(pR)$ similarly to the plane wave, as shwon in Eq.(D.10). Furthermore, the Coulomb correction to the outer regular solutions $g_{-k}^{(0)}(R)$ and $f_k^{(0)}(R)$ in A_κ appears mainly as $(\alpha Z)^2$, so that the replacement of Z with (Z-1) gives the correction of order of $\alpha^2 Z$. Thus we can conclude that A_κ in Eq.(D.10) does not depend on the change of the nuclear charge seriously, and its effect is less than 1% for the normalization A_κ.

---

*) The factor $(2pR)^{2\gamma_k}$ in F_{k-1} is cancelled by the term coming from $|\Gamma(\gamma_k + iy)|^2$ in the limit $p \to 0$.

Thus, the effect due to the change of the Coulomb field come from the inner solutions $g_k^{(i)}$ and $f_k^{(i)}$ themselves. This correction is not important for the electron partial waves $g_{-k}^{(i)}$ and $f_k^{(i)}$ like the S or $P_{3/2}$-wave, because their leading terms are independent of αZ, as shown in Eqs.(D.13) and (D.16). However, concerning $g_{+k}^{(i)}$ and $f_{-k}^{(i)}$ like the $P_{1/2}$ or $D_{3/2}$-wave, their leading terms are proportional to αZ, as seen from Eqs.(D.15) and (D.17), so that the correction due to the variation of nuclear charge is of oder of $1/Z$ for the first emitted electron. Since there is no such effect for the second emitted electron, the total correction due to this effect for the decay rate is at most about $1/Z$. Since this correction seems not to be serious for the $\beta\beta$ decaying nuclei, we did not take account of it in this paper.

In the $(\beta\beta)_{2\nu}$ mode, both electrons are emitted in the S-wave state mainly. Therefore, the effect due to the Coulomb field of the intermediate nucleus can not become large, because it appears through the normalization factor A_κ and the finite de Broglie wave length corrections as discussed before.

Appendix E

— Neutrino potentials and relative order of magnitudes of nuclear matrix elements —

In §3.4, it was shown that neutrino potentials h_+, $h_{0\omega}$, h'_+ and h_R appear in the nuclear matrix elements which are non-vanishing in the closure approximation. In addition, in Appendix C, new types of potentials h_ω and h'_0 in Eqs.(C.2.32) and (C.2.33) appeared in the vanishing matrix elements in the closure approximation.

In the small neutrino mass limit, potentials h_+, h_0, h'_+ and h_R are expressed in the analytic forms in Eq.(3.4.16), while h_ω and h'_0 are related to h_R in Eq.(3.4.16d) as

$$\begin{aligned} h_\omega(r, E_a) &= -(M/\mu_a m_e)\, h_R(r, E_a), \\ h'_0(r, E_a) &= -(Mr^2/\mu_a m_e R^2)\, h_R(r, E_a), \end{aligned} \tag{E.1}$$

where the approximation $A_1 \simeq A_2 \simeq \mu_a m_e$ is used.

For large m_ν, i.e., $m_\nu \gg A_K \approx \mu_a m_e$, potentials behave as

$$\begin{aligned} h_+(r, E_a) &= \left(\frac{R}{r}\right) e^{-m_\nu r}, \\ h_0(r, E_a) &= \frac{2}{\pi} K_0(m_\nu r) \to \sqrt{\frac{2}{\pi m_\nu r}}\, e^{-m_\nu r}, \\ h'_+(r, E_a) &= (1 + m_\nu r)\frac{R}{r}\, e^{-m_\nu r}, \\ h_R(r, E_a) &= -\left(\frac{m_\nu^2 R}{M}\right)\left(\frac{R}{r}\right) e^{-m_\nu r}, \\ h_\omega(r, E_a) &= \left(\frac{m_\nu R^2}{r}\right)\frac{2}{\pi} K_1(m_\nu r) \to \left(\frac{R}{r}\right)(m_\nu R)\sqrt{\frac{2}{\pi m_\nu r}}\, e^{-m_\nu r}, \\ h'_0(r, E_a) &= m_\nu r \frac{2}{\pi} K_1(m_\nu r) \to m_\nu r \sqrt{\frac{2}{\pi m_\nu r}}\, e^{-m_\nu r}. \end{aligned} \tag{E.2}$$

These potentials appear in the nuclear matrix elements and the relative coordinate of two nucleons $\vec{r}$ is integrated with the weight of overlapping of nuclear wave functions. As an approximation of the overlapping, we consider the uniform distribution of nucleons to obtain the average potentials,[27),31),65)]

$$f(r) = N\,\theta(r - r_c)\,\theta(\tilde{R} - r), \tag{E.3}$$

where

$$N = \left[\tfrac{4}{3}\pi\,(\tilde{R}^3 - r_c^3)\right]^{-1}. \tag{E.4}$$

Here r_c is the core radius of nucleon (~ 0.5fm) and $\tilde{R}$ is introduced to take into account the short range spin-spin interaction. Then we find the average potentials as[31),33)]

$$\begin{aligned} \langle h_+ \rangle &= \left(4\pi N R/(\mu_0 m_e)^2\right)\left[\phi(y) - y\phi'(y) + (2/\pi)y\right]_{y_c}^{\tilde{y}}, \\ \langle h_{0\omega} \rangle &= \langle h_+ \rangle - \mu_0 m_e R \langle h_0 \rangle, \\ \langle h'_+ \rangle &= \langle h_+ \rangle + \mu_0 m_e R \langle h_0 \rangle, \\ \langle h_R \rangle &= 4\pi N R^2 M \left[-\phi(y) + y\phi'(y)\right]_{y_c}^{\tilde{y}}, \\ \langle h_\omega \rangle &= (M/\mu_0 m_e)\langle h_R \rangle, \\ \langle h'_0 \rangle &= \left(4\pi N/(\mu_0 m_e)^3\right)\left[3(2 - y^2)\phi(y) - (6 - y^2)\phi' + \tfrac{12}{\pi} y\right]_{y_c}^{\tilde{y}}, \end{aligned} \tag{E.5}$$

where

$$\langle h_0 \rangle = \left(4\pi N/(\mu_0 m_e)^3\right)\left[(2 - y^2)\phi(y) - 2y\phi'(y) + \tfrac{4}{\pi} y\right]_{y_c}^{\tilde{y}}, \tag{E.6}$$

and $y_C = \mu_0 m_e r_C$ and $\tilde{y} = \mu_0 m_e \tilde{R}$. Here we denoted $\langle \mu_a \rangle_{av}$ by μ_0.

Let us evaluate the ratios of nuclear matrix elements from the average potentials in the case of light neutrinos by using the approximate relation in Eq.(7.2.5). In Fig. E.1, the $\tilde{R}/R$ dependences of $\langle h_+ \rangle$ are given for ^{76}Ge and ^{130}Te. The horizontal lines are the theoretical values of $[M_{GT}^{(0\nu)}]_C/[M_{GT}^{(2\nu)}]_C$ by Haxton et al. in Table 7.4. By using the relation $\langle h_+ \rangle \sim [M_{GT}^{(0\nu)}]_C/[M_{GT}^{(2\nu)}]_C$ in Eq.(7.2.5a), we find the effective radius $\tilde{R}$: $\tilde{R}/R =$ 0.720 and 0.665 for ^{76}Ge and ^{130}Te. The relatively small values of $\tilde{R}$ in comparison with R show the existence of the short range correlation. We show in Fig. E.2 the $\tilde{R}/R$ dependence of ratios of potentials $\langle h_+' \rangle/\langle h_+ \rangle$, $\langle h_0 \rangle/\langle h_+ \rangle$ and $\langle h_\omega \rangle/\langle h_+ \rangle$. The $\tilde{R}/R$ dependence of $\langle h_R \rangle/\langle h_+ \rangle$ is obtained by using the relation in Eq.(E.1). The vertical lines represent the values of $\tilde{R}$ determined in Fig. E.1. from which the ratios $\langle h_+' \rangle/\langle h_+ \rangle$, $\langle h_0 \rangle/\langle h_+ \rangle$ and $\langle h_R \rangle/\langle h_+ \rangle$ are determined. Since these values correspond to the ratio of nuclear matrix elements χ_{GT}', $\chi_{GT}^{(0)}$ and χ_R or χ_F' and $\chi_F^{(0)}$, we find the values of them for ^{76}Ge and ^{130}Te which are shown in the column denoted by pot. in Table 7.5. By repeating the same procedure for ^{48}Ca, ^{82}Se and ^{128}Te, we find the effective radius $\tilde{R}/R = 0.553(^{48}\text{Ca})$, $0.643(^{82}\text{Se})$ and $0.655(^{128}\text{Te})$ and the values of ratio of nuclear matrix elements in Table 7.5.

Appendix F

— Various lepton number violating processes —

In this appendix, the derivation of the transition formulae for the Majoron emitting process, the neutrinoless $\beta\beta$ decay between pairs of single β emitters and the $\mu^- e^+$ conversion by nucleus is presented.

§F.1. The Majoron emitting process : $(A, Z-2) \to (A, Z) + 2e^- + M^0$

The Majoron emitting process was first evaluated by Georgi, Glashow and Nussinov[39] and later by Vergados.[144] However, they used the nonrelativistic Coulomb wave function for the emitted electrons (Promokoff-Rosen approximation in Eq.(D.34)). Since this approximation is not a good approximation for the medium-heavy nuclei as mentioned in §1.3, we shall derive the half-life formula by using the relativistic Coulomb distortion.

Within the effective interaction in Eq.(5.2.1), the S matrix for the process in Fig. 1.7 is expressed as

$$S_{fi} = -i \frac{1}{2\sqrt{2}} \frac{1}{(2\pi)^2} \left(\frac{G}{\sqrt{2}}\right)^2 \sum_{j,k} g_{jk} U_{ej} U_{ek} \int dx\, dy\, dz \int dq_1\, dq_2 \frac{e^{-iq_1(x-z)}}{q_1^2 - m_j^2} \frac{e^{-iq_2(z-y)}}{q_2^2 - m_k^2} \langle N_f | T(J_L^{\rho\dagger}(x)\, J_L^{\sigma\dagger}(y)) | N_i \rangle \bar{\Psi}(\varepsilon_1, x) \gamma_\rho (1-\gamma_5)(\not{q}_1 + m_j)\gamma_5 (\not{q}_2 + m_k)(1-\gamma_5)\gamma_\sigma \Psi^c(\varepsilon_2, y)\, e^{ikz}/\sqrt{2k^0}, \tag{F.1.1}$$

where $\Psi(\varepsilon, x)$ is the relativistic Coulomb wave function of electron $\Psi(\varepsilon, x) = \psi(\varepsilon, \vec{x}) \exp(i\varepsilon x^0)$, $\psi(\varepsilon, \vec{x})$ is defined in Eq.(D.1) and $e^{ikz}/\sqrt{2k^0}$ is the wave function for the Majoron (M^0). The expression

corresponding to the old fashioned perturbation theory is derived by performing the integrations of x^0, y^0, z^0 and later q_1^0 and q_2^0. Instead of this procedure, we shall first perform the z integration and then q_2 integration. The result is

$$S_{fi} = -i\frac{a}{\sqrt{2}}\left(\frac{G}{\sqrt{2}}\right)^2 \sum q_{jk}\, U_{ej}\, U_{ek} \int dx\, dy \int \frac{dq}{(2\pi)^4} \frac{e^{-iq(x-y)}\, e^{iky}}{(q^2-m_j^2)((q+k)^2-m_k^2)} \frac{1}{\sqrt{2k^0}} \langle N_f|T(J_L^{\rho+}(x)\, J_L^{\sigma+}(y))|N_i\rangle$$
$$\bar{\Psi}(\varepsilon_1, x)\,\gamma_\rho\,(\not{q}\,(\not{q}+\not{k}) - m_j m_k)(1-\gamma_5)\gamma_\sigma\,\Psi^c(\varepsilon_2, y). \qquad \text{(F.1.2)}$$

By using the identity,

$$\not{q}(\not{q}+\not{k}) - m_j m_k = \frac{1}{2}\{q^2 - m_j^2 + (q+k)^2 - m_k^2\} + \frac{1}{2}\{[\not{q},\not{k}] + (m_j - m_k)^2\} \qquad \text{(F.1.3)}$$

the S-matrix is divided into two parts, where we used $k^0 = |\vec{k}|$ due to $m_M = 0$. The part from the first parenthesis is easily evaluated as

$$S_{fi}^{(1)} = -i\frac{a}{\sqrt{2}}\left(\frac{G}{\sqrt{2}}\right)^2 \sum g_{jk}\, U_{ej}\, U_{ek} \int dx\, dy \int \frac{dq}{(2\pi)^4} \frac{e^{-iq(x-y)}}{q^2 - m_j^2} \frac{1}{\sqrt{2k^0}} \langle N_f|T(J_L^{\rho+}(x)\, J_L^{\sigma+}(y))|N_i\rangle$$
$$\bar{\Psi}(\varepsilon_1, x)\,\gamma_\rho\,(1-\gamma_5)\gamma_\sigma\,\Psi^c(\varepsilon_2, y)\,\frac{1}{2}(e^{ikx} + e^{iky}). \qquad \text{(F.1.4)}$$

This form is essentially the same as the m_ν-part of the $(\beta\beta)_{0\nu}$ decay with the only difference by the factor $(e^{ikx} + e^{iky})$. By performing the integration with respect to x^0, y^0 and q^0, we find the R matrix in the closure approximation as

$$R_{fi}^{(1)} = \frac{1}{\sqrt{2}}\left(\frac{G}{\sqrt{2}}\right)^2 \sum g_{jk}\, U_{ej}\, U_{ek} \int d\vec{x}\, d\vec{y} \int \frac{d\vec{q}}{2(2\pi)^3\omega} e^{i\vec{q}(\vec{x}-\vec{y})} \frac{1}{\sqrt{2k^0}} \langle N_f|\, J_L^{\rho+}(\vec{x})\, J_L^{\sigma+}(\vec{y})\,|N_i\rangle$$
$$\left[e^{-i\vec{k}\vec{x}}\left(\frac{1}{\omega + A_2} + \frac{1}{\omega + A_2 + k^0}\right) + e^{-i\vec{k}\vec{y}}\left(\frac{1}{\omega + A_1} + \frac{1}{\omega + A_1 + k^0}\right)\right]$$
$$\bar{\Psi}(\varepsilon_1, \vec{x})\,\gamma_\rho\,(1-\gamma_5)\,\gamma_\sigma\,\Psi^c(\varepsilon_2, \vec{y}) \qquad \text{(F.1.5)}$$

where A_k is defined in Eq. (3.3.6). Since $k^0 = |\vec{k}|$ is at most a few MeV and thus $|\vec{k}\cdot\vec{x}| \sim |\vec{k}\cdot\vec{y}| \ll 1$, $k \ll \omega + A_k$, we can neglect all $\vec{k}$ and k^0 dependence in the above expression. Then we arrive at exactly the same expression as that of the m_ν-part in Eq. (3.3.2) aside from the normalization. Thus we can utilize the analysis of the m_ν-part for evaluating $R_{fi}^{(1)}$.

The evaluation of the part from the second parenthesis in Eq. (E.1.3) is rather complicated. The R matrix in the closure approximation is given by

$$R_{fi}^{(2)} = -\frac{1}{\sqrt{2}}\left(\frac{G}{\sqrt{2}}\right)^2\left(\frac{1}{m_e}\right)^2 \sum g_{jk}\, U_{ej}\, U_{ek} \int d\vec{x}\, d\vec{y} \int \frac{d\vec{q}}{2(2\pi)^3\,\omega_q\,\omega'_{q+k}} e^{i\vec{q}(\vec{x}-\vec{y})}\, e^{-i\vec{k}\vec{y}}$$
$$\bar{\Psi}(\varepsilon_1, \vec{x})\,\gamma_\rho \left\{ \begin{array}{l} [(m_j - m_k)^2 + [\not{q}_1, \not{q}_2]]\, L_+ L'_- \\ +[(m_j - m_k)^2 + [\tilde{\not{q}}_1, \tilde{\not{q}}_2]]\, K_- K'_+ \\ +[(m_j - m_k)^2 + [\tilde{\not{q}}_1, \not{q}_2]](L_+ + K'_+)[E_q + E'_{q+k} + k^0]^{-1} \\ +[(m_j - m_k)^2 + [\not{q}_1, \tilde{\not{q}}_2]](L'_- + K_-)[E_q + E'_{q+k} - k^0]^{-1} \end{array} \right\}$$
$$\cdot(1-\gamma_5)\,\gamma_\nu\,\Psi^c(\varepsilon_2, \vec{y})\,\langle N_f|\, J_L^\mu(\vec{x})\, J_L^\nu(\vec{y})\,|N_i\rangle, \qquad \text{(F.1.6)}$$

where $q_1 = (\varepsilon_q, \vec{q})$, $\tilde{q}_1 = (-\varepsilon_q, \vec{q})$, $q_2 = (\varepsilon'_{q+k}, \vec{q}+\vec{k})$, $\tilde{q}_2 = (-\varepsilon'_{q+k}, \vec{q}+\vec{k})$ with $\varepsilon_q = \sqrt{q^2 + m_j^2}$ and $\varepsilon'_{q+k} = \sqrt{(q+k)^2 + m_k^2}$, and

$$L_\pm = m_e[\varepsilon_q + \langle\mu_a\rangle_{av} m_e - \varepsilon_{12}/2 \pm k^0/2\,]^{-1},$$
$$K_\pm = m_e[\varepsilon_q + \langle\mu_a\rangle_{av} m_e + \varepsilon_{12}/2 \pm k^0/2\,]^{-1},$$
$$L'_\pm = L_\pm(\varepsilon_q \to \varepsilon'_{q+k}),\quad K'_\pm = K_\pm(\varepsilon_q \to \varepsilon'_{q+k}). \qquad \text{(F.1.7)}$$

This term was neglected in the previous articles.[39] We have made a careful examination of this contribution.[72] By expanding with respect to $\vec{k}$, we find that terms with $[g_2, g_2]$ etc. vanish in the limit $\vec{k} \to 0$, so that their contributions may be small. The terms involving $(m_j - m_k)^2$ vanish in the simple models where $g_{jk} \propto \delta_{jk}$. Here we only take into account the part from the first parenthesis in Eq.(F.1.3), $R_{fi}^{(1)}$, for simplicity. Then we arrive at the half-life formula in Eq. (5.2.2). It should be emphasized, however, that the second parenthesis part may not be neglecte for heavier neutrinos if there are nonvanishing off diagonal term in g_{jk}.

§F.2 The neutrinoless β-β decay between pairs of single β emitters

The decay rate due to the neutrino mass was first evaluated by Pacheco[146] by using the non-relativistic Coulomb wave function for electrons (Primakoff-Rosen approximation). Here we shall refine the formula by taking into account the relativistic Coulomb distortion and also by taking the right-handed current contributions into consideration.

The R matrix is given in terms of the m_ν and V+A parts, similarly to the $(\beta\beta)_{0\nu}$ decay. Since only the allowed β transition should be considered, electrons are taken to be in the S wave and the nucleon recoil terms in hadronic currents are neglected. Within these approximations, the $\vec{q}$ term in the V+A part does not contribute due to the parity selection rule, as discussed in §11.1.

Now the R matrix element is expressed as

$$R_{\beta\text{-}\beta} = \left(\frac{G}{\sqrt{2}}\right)^2 \frac{1}{2}\left(1 - P_{e_1 e_2}\right) \int d\vec{x}\, d\vec{y} \int \frac{d^4 q}{(2\pi)^3} \frac{e^{i\vec{q}(\vec{x}-\vec{y})}}{\vec{q}^2 - q_0^2 + m_j^2 - i\varepsilon} \delta(q_0 - \omega_0)$$

$$\left\{ m_j\, t^L_{\rho\sigma}(\varepsilon_1 0, \varepsilon_2 0)\, J^{\rho\sigma}_{LL}(\vec{x}, \vec{y}) + q^0 \left[\tilde{u}^L_{\rho\sigma}(\varepsilon_1 0, \varepsilon_2 0)\, J^{\rho\sigma}_{LR}(\vec{x}, \vec{y}) + (L \leftrightarrow R) \right] \right\}. \qquad \text{(F.2.1)}$$

Here $P_{e_1 e_2}$ represents the exchange of e_1 and e_2, $\omega_0 = Q + m_e - \varepsilon_1$, Q being the Q value of the β decaying nuclei, $t^L_{\rho\sigma}$ is defined in Eq.(3.3.5),

$$\tilde{u}^{L(R)}_{\rho\sigma}(\varepsilon_1 0, \varepsilon_2 0) = \bar{\psi}(\varepsilon_1 0)\gamma_\rho(1 \mp \gamma_5)\gamma^0\gamma_\sigma\psi^c(\varepsilon_2 0), \qquad \text{(F.2.2)}$$

$$\hat{J}^{\rho\sigma}_{\alpha\beta}(\vec{x}, \vec{y}) = \langle A_1' | \hat{J}^\rho_\alpha(\vec{x}) | A_1 \rangle \langle A_2' | \hat{J}^\sigma_\beta(\vec{y}) | A_2 \rangle + \langle A_2' | \hat{J}^\rho_\alpha(\vec{x}) | A_2 \rangle \langle A_1' | \hat{J}^\sigma_\beta(\vec{y}) | A_1 \rangle, \qquad \text{(F.2.3)}$$

where $\psi(\varepsilon_j, 0)$ is the electron wave function with the energy ε_j at $r = 0$ defined in Eq.(D.1), α, β = L or R, and A_i and A_i' $(i = 1, 2)$ are initial and final nuclear states of single beta emitters.

At this point, the following comments are in order : (i) The total energy conservation is expressed as $\varepsilon_1 + \varepsilon_2 = 2Q + 2m_e$ which implies that the events contain electrons with a kinetic energy higher than Q $(Q < \varepsilon - m_e < 2Q)$. This is the unique signal of the neutrinoless β-β decay between pairs of single β emitters. (ii) The virtual neutrino energy q^0 takes a fixed value, either $\omega_0 = Q + m_e - \varepsilon_1$ or $\omega_0' = Q + m_e - \varepsilon_2$ depending on 1 or $P_{e_1 e_2}$ part in the antisymmetrizer, because all nuclear states A_i and A_i' are physical states and thus the energy conservation at each vertex is satisfied.

Then the factor q^0 in the V+A part takes the constant value ω_0 or ω_0'. These terms contribute constructively by the relation $\omega_0 + \omega_0' = 0$ due to energy conservation, in contrast to the ω term of the $(\beta\beta)_{0\nu}$ mode where these contributions appear destructively. (iii) Now the neutrino potential is defined by

$$\tilde{H}(r) = \int \frac{d\vec{q}}{2\pi^3} \frac{e^{i\vec{q}\cdot\vec{r}}}{\vec{q}^2 - (\omega_0^2 - m_j^2) - i\varepsilon} = \frac{1}{r}\cos\left(\sqrt{\omega_0^2 - m_j^2}\, r\right), \tag{F.2.4}$$

with $\vec{r} = \vec{x} - \vec{y}$. (iv) The hadronic current part for the nuclear transition in Eq.(F.2.3) is determined by the nuclear matrix elements for the β decay. With the impulse approximation for hadronic currents in Eq.(C.1.4), we obtain

$$\int d\vec{x} \langle A_i' | \tilde{J}_L^\dagger(\vec{x}) | A_i \rangle = g_A \left\{ g^{\mu 0} G_V \langle A_i' | \sum_n \tau_n^+ L_n | A_i \rangle + g^{\mu k} G_A \langle A_i' | \sum_n \tau_n^+ \sigma_n^k | A_i \rangle \right\}, \tag{F.2.5}$$

$$\int d\vec{x} \langle A_i' | \tilde{J}_R^\dagger(\vec{x}) | A_i \rangle = g_A \left\{ g^{\mu 0} \varepsilon_V \langle A_i' | \sum_n \tau_n^+ L_n | A_i \rangle - g^{\mu k} \varepsilon_A \langle A_i' | \sum_n \tau_n^+ \sigma_n^k | A_i \rangle \right\}. \tag{F.2.6}$$

With the above preparation, the decay rate $d\Gamma_{\beta-\beta}$ is obtained from $R_{\beta-\beta}$ similarly to the $(\beta\beta)_{0\nu}$ case,

$$d\Gamma_{\beta-\beta} = \frac{G^4}{(2\pi)^5} g_A^4 \left(\tilde{H}(r)\right)^2 \left\{ \left|\sum_j m_j Z_1\right|^2 (\alpha_+ + \beta_+) + 2\left[(\varepsilon_1^2 + \varepsilon_2^2) - 2(Q+m_e)^2\right]\left[\left|\sum_j Z_2\right|^2 \beta_+ + \left|\sum_j Z_3\right|^2 \alpha_+\right] \right\} \tag{F.2.7}$$
$$\delta(\varepsilon_1 + \varepsilon_2 - 2(Q+m_e))\, p_1 p_2\, \varepsilon_1\, \varepsilon_2\, d\varepsilon_1\, d\varepsilon_2,$$

where nuclear matrix elements Z_1, Z_2 and Z_3 are defined in Eqs.(11.1.8a)-(11.1.8c), and the Coulomb corrections α_+ and β_+ are given in Eq.(C.3.12).

We remind that neutrino should propagate from one nucleus to the other so that the distance r must be larger than the atomic radius. Then, the neutrino potential $\tilde{H}(r)$ becomes a rapidly oscillating function of $\omega_0 = Q + m_e - \varepsilon_1$ or $\omega_0' = Q + m_e - \varepsilon_2$ because $\omega_0 r \sim 200$ for $\varepsilon \sim m_e$. Thus the approximation $\langle \tilde{H}^2 \rangle \approx \langle \cos^2(\sqrt{\omega_0^2 - m_j^2}\, r) \rangle / r^2 \sim 1/2\, r^2$ can be used. With this procedure, the decay rate formula in Eq.(11.1.2) is derived.

§F.3 The $\mu^- e^+$ conversion

The derivation of the capture rate is presented here because our result is somewhat different from previous works.

Let us start from the S-matrix in the second order perturbation using the current-current type weak interaction Hamiltonian of Eq.(3.1.3),

$$S_{\mu e} = \left(\frac{G}{\sqrt{2}}\right)^2 \sum_j \int dx\, dy \int \frac{dq}{(2\pi)^4} \frac{e^{iq(x-y)}}{q^2 - m_j^2 + i\varepsilon} e^{-i\varepsilon_f x_0} e^{i\varepsilon y_0}$$
$$\cdot \sum_{\alpha,\beta} \bar{\phi}(\varepsilon_f \vec{x})\, \gamma_\beta\, \alpha\, (q^\lambda \gamma_\lambda + m_j)\, \beta\, \gamma_\sigma\, \psi(\varepsilon \vec{y})$$
$$\cdot \sum_a \left\{ \begin{array}{l} \theta(x_0 - y_0)\, e^{i(E_f - E_a)x_0} e^{-i(E_i - E_a)y_0} \langle N_f | \tilde{J}_\alpha^\beta(\vec{x}) | N_a \rangle \langle N_a | \tilde{J}_\beta^\sigma(\vec{y}) | N_i \rangle \\ \theta(y_0 - x_0)\, e^{i(E_f - E_a)x_0} e^{-i(E_i - E_a)y_0} \langle N_f | \tilde{J}_\beta^\sigma(\vec{y}) | N_a \rangle \langle N_a | \tilde{J}_\alpha^\dagger(\vec{x}) | N_i \rangle \end{array} \right\}, \tag{F.3.1}$$

where α and β are either $(1-\gamma_5)$ or $(1+\gamma_5)$, and $\phi(\varepsilon_f \vec{x})$ and $\psi(\varepsilon \vec{y})$ are spinor wave functions for muon and positron with energies ε_f and ε, respectively. The θ-functions come from the time ordering for the hadronic currents and are not taken into account in the previous articles.[153] This will give some change in the capture rate formula as discussed later.

It may be worthwhile to note that the $\mu^- - e^+$ conversion is very similar to the $(\beta\beta)_{0\nu}$ mode and thus the calculation is performed almost parallel to the $(\beta\beta)_{0\nu}$ mode. In deriving the conversion rate, the following approximations are used: (i) We use the closure approximation which is rather safe because the energy difference between the intermediate and initial or final nuclei can be neglected in comparison with the muon mass. (ii) The muon wave function is taken as $\phi(\varepsilon_\mu, \vec{x}) = \phi_\mu(|\vec{x}|)u_\mu$ where $\phi_\mu(|\vec{x}|)$ is a bound state wave function in the K-orbit and u_μ is a spinor satisfying $\sum_{\text{spin}} u_\mu \bar{u}_\mu = (\gamma^0 + 1)\, m_\mu$. (iii) The non-relativistic impulse approximation for hadronic currents is used and the nucleon recoil terms are neglected. (iv) In contrast to the $(\beta\beta)_{0\nu}$ mode, the positron is emitted with the large energy $\varepsilon_\mu \sim O(m_\mu)$ so that the approximation $\psi(\varepsilon, \vec{y}) = \sqrt{F_0^{PR}(Z,\varepsilon)}\; e^{i\vec{p}\cdot\vec{y}}\, v(\vec{p})$ can be used, where $v(\vec{p})$ is a free spinor in Eq.(D.9) and F_0^{PR} is the Fermi factor due to Primakoff and Rosen[24] in Eq.(D.34). Also various nuclear final states are possible due to the energy supplied by muon and the angular momentum by positron. Under these approximations, the R-matrix element is given as follows,

$$R_{\mu e} = \frac{1}{4\pi}\left(\frac{G}{\sqrt{2}}\right)^2 \sqrt{F_0^{PR}(Z,\varepsilon)} \sum_j \left| m_j t_{p\sigma} T^{p\sigma} + \frac{1}{R}\left[U^L_{p\lambda\sigma}\, U_L^{p\lambda\sigma} + U^R_{p\lambda\sigma}\, U_R^{p\lambda\sigma} \right] \right|, \qquad \text{(F.3.2)}$$

where

$$t_{p\sigma} = \overline{u^c}(\vec{p})\, \gamma_p (1-\gamma_5)\gamma_\sigma\, u_\mu,$$

$$U^{L(R)}_{p\lambda\sigma} = \overline{u^c}(\vec{p})\, \gamma_p\, \gamma_\lambda (1 \mp \gamma_5)\, \gamma_\sigma\, u_\mu, \qquad \text{(F.3.3)}$$

$$T^{p\sigma} = \int d\vec{x}\, d\vec{y}\, \langle N_f | \bar{R}(|\vec{x}-\vec{y}|)\, \phi_\mu(|\vec{x}|)\, e^{-i\vec{p}\cdot\vec{y}}\, \tilde{J}_L^p(\vec{x})\, \tilde{J}_L^\sigma(\vec{y}) | N_i \rangle,$$

$$U^{p\sigma}_{L(R)} = \int d\vec{x}\, d\vec{y}\, \langle N_f | \bar{R}_\omega(|\vec{x}-\vec{y}|)\, \phi_\mu(|\vec{x}|)\, e^{-i\vec{p}\cdot\vec{y}}\, \tilde{J}^p_{L(R)}(\vec{x})\, \tilde{J}^\sigma_{R(L)}(\vec{y}) | N_i \rangle,$$

$$U^{pk\sigma}_{L(R)} = -i \int d\vec{x}\, d\vec{y}\, \langle N_f | \bar{R}(|\vec{x}-\vec{y}|)\, \phi_\mu(|\vec{x}|)\, e^{-i\vec{p}\cdot\vec{y}}\, \tilde{J}^p_{L(R)}(\vec{x})\, \tilde{J}^\sigma_{R(L)}(\vec{y})(x^k - y^k) | N_i \rangle. \qquad \text{(F.3.4)}$$

The neutrino propagating potentials are defined as

$$\bar{R}(r) = \frac{1}{m_e}\int \frac{d\vec{q}}{2\pi^3}\, e^{i\vec{q}\cdot\vec{r}}\, \frac{1}{\omega}\left(\frac{1}{m_\mu - \omega + i\varepsilon} - \frac{1}{m_\mu + \omega}\right) \approx \frac{2}{m_e r}\, e^{i m_\mu r}$$

$$\bar{R}_\omega(r) = R\int \frac{d\vec{q}}{2\pi^3}\, e^{i\vec{q}\cdot\vec{r}}\left(\frac{1}{m_\mu - \omega + i\varepsilon} + \frac{1}{m_\mu + \omega}\right) \approx \frac{-2}{m_e r}(m_\mu R)\, e^{i m_\mu r},$$

$$\bar{R}'(r) = \frac{d}{dr}\bar{R}(r) \approx \frac{-2}{m_e r}\left(\frac{R}{r} - i m_\mu R\right) e^{i m_\mu r}. \qquad \text{(F.3.5)}$$

By performing the similar calculations to the $(\beta\beta)_{0\nu}$ mode, we find the $\mu^- - e^+$ conversion rate,

$$\Gamma_{\mu e} = \left(\frac{G}{\sqrt{2}}\right)^4 \left(\frac{2}{8\pi}\right)^2 8(2\pi)^2 m_\mu^2 \left\{ \begin{array}{l} m_\mu\left[|T|^2 + |W_L|^2 + |W_R|^2 + T^{k*}T^k + W_L^{k*}W_L^k + W_R^{k*}W_R^k\right] \\ + 2 m_e R_e\left[W_L^* W_R - W_L^{k*} W_R^k\right] \\ + 2 R_e\left[T^*(m_e W_L + \varepsilon W_R) + T^{k*}(m_e W_L^k - \varepsilon_e W_R^k)\right] \end{array} \right\}, \qquad \text{(F.3.6}$$

where

$$T = T^{oo} - T^{kk},$$

$$T^k = T^{ko} - T^{ok} + i\varepsilon^{kij} T^{ij},$$

$$W_{L(R)} = U^{ooo}_{L(R)} + U^{joj}_{L(R)} + U^{ijo}_{L(R)} + U^{oij}_{L(R)} \pm i\varepsilon^{ikl} U^{ljk}_{L(R)},$$

$$W^k_{L(R)} = \left\{ \begin{array}{l} U^{koo}_{L(R)} + U^{ook}_{L(R)} \pm i\varepsilon^{kij} U^{ioj}_{L(R)} \\ + U^{ijk}_{L(R)} + U^{kjj}_{L(R)} + U^{ok o}_{L(R)} - U^{jkj}_{L(R)} \pm i\varepsilon_{qp}{}^{jk} U^{j\varepsilon p}_{L(R)} \end{array} \right\} \qquad \text{(F.3.7}$$

In order to obtain the rough estimate of the conversion rate, the nuclear matrix elements are evaluated by summing the final nuclear states with closure;

$$\sum_f \langle N_f|\sum_{nm} e^{-i\vec{p}\cdot\vec{r}_n}\Omega_{nm}|N_i\rangle^* \langle N_f|\sum_{n'm'} e^{-i\vec{p}\cdot\vec{r}_{n'}}\Omega'_{n'm'}|N_i\rangle$$

$$= \langle N_i|\sum_{\substack{nm\\(n=m)}}\Omega^+_{nm}\Omega'_{nm}|N_i\rangle + \langle N_i|\sum_{(n'm')\neq(nm)} e^{-i\vec{p}(\vec{r}_n-\vec{r}_{n'})}\Omega^+_{nm}\Omega_{n'm'}|N_i\rangle. \qquad \text{(F.3.8)}$$

where Ω_{nm} and Ω'_{nm} are appropriate nuclear operators. Next, according to Fujii and Primakoff[166], we take only the first term in Eq.(F.3.8) because the second term is expected to be small due to a rapidly oscillating factor $\exp(-i\vec{p}\,(\vec{r}_n - \vec{r}_{n'})$ with $p \sim \varepsilon \sim O(m_\mu)$.

It should be noted that in the approximation of neglecting nucleon recoil terms, the nuclear matrix elements $T^{p\sigma}$ and $U^{p0\sigma}_{L(R)}$ contain only the spin operators $\vec{\sigma}_n$ and/or $\vec{\sigma}_m$ aside from $\exp(-i\vec{p}\cdot\vec{y})$, while $U^{pk\sigma}_{L(R)}$ contains $\hat{r}_{nm}$ in addition. Thus the first term in Eq.(F.3.8) contains space dependence $\hat{r}_{nm}$ only when $U^{k}_{L(R)}$ appears in as Ω and/or Ω'. For these $\hat{r}_{nm}$, we require that they should form a rank 0 tensor for simplicity. With this approximation which is only needed for the V+A part, the $\mu^- - e^+$ conversion rate is given by

$$\Gamma_{\mu e} = \frac{\alpha^3}{2\pi} G^4 g_A^4 m_\mu^5 Z^4_{eff}(Z-1)\left[1-\exp(2\pi\alpha Z)\right]^{-1}$$
$$\cdot\Big\{ m_e^2\langle|\vec{R}|^2\rangle A + \langle|\vec{R}'/R|^2\rangle B + \langle|\vec{R}\omega/R|^2\rangle C + \mathrm{Re}\left(\langle(m_e\vec{R})^*(\vec{R}\omega/R)\rangle\right) D \Big\}, \qquad \text{(F.3.9)}$$

where, for example,

$$\langle(\vec{R})^2\rangle = (Z(Z-1))^{-1}\langle N_i|\sum_{\substack{nm\\(n\neq m)}}(\vec{R}(r_{nm}))^2|N_i\rangle, \qquad \text{(F.3.10)}$$

and the muon wave function squared is extracted from the nuclear matrix element as $\langle\phi_\mu^2\rangle = \frac{1}{\pi}(\propto m_\mu)^3 Z^4_{eff}$ Z with the effective nuclear charge Z_{eff}. Factors A, B, C and D are defined as follows.

$$A = \Big|\sum_j \frac{m_j}{m_e}(G_V'G_V - G_A'G_A S)\Big|^2 + 3\Big\{\Big|\sum_j \frac{m_j}{m_e}G_V'G_A\Big|^2 + \Big|\sum_j \frac{m_j}{m_e}G_A'G_V\Big|^2\Big\}$$
$$-2\,\mathrm{Re}\sum_j\Big(\frac{m_j}{m_e}G_V'G_A\Big)\Big(\frac{m_j}{m_e}G_A'G_V\Big)^* + \Big|\sum_j\frac{m_j}{m_e}G_A'G_A\Big|^2(9-S^2), \qquad \text{(F.3.11a)}$$

$$B = \Big|\sum_j(\varepsilon_V'G_V - \varepsilon_A'G_A S)\Big|^2 + \Big|\sum_j(G_V'\varepsilon_V - G_A'\varepsilon_A S)\Big|^2$$
$$+3\Big\{\Big|\sum_j\varepsilon_V'G_A\Big|^2 + \Big|\sum_j\varepsilon_A'G_V\Big|^2 + \Big|\sum_j G_V'\varepsilon_A\Big|^2 + \Big|\sum_j G_A'\varepsilon_V\Big|^2\Big\}$$
$$+\Big\{\Big|\sum_j\varepsilon_A'G_A\Big|^2 + \Big|\sum_j G_A'\varepsilon_A\Big|^2\Big\}(9-S^2)$$
$$-2S\,\mathrm{Re}\Big\{\Big(\sum_j\varepsilon_V'G_A\Big)^*\Big(\sum_j\varepsilon_A'G_V\Big) + \Big(\sum_j G_V'\varepsilon_A\Big)\Big(\sum_j G_A'\varepsilon_V\Big)\Big\}, \qquad \text{(F.3.11b)}$$

$$C = 3\Big\{\Big|\sum\varepsilon_V'G_A\Big|^2 + \Big|\sum\varepsilon_A'G_V\Big|^2 + \Big|\sum G_V'\varepsilon_A\Big|^2 + \Big|\sum G_A'\varepsilon_V\Big|^2\Big\}$$
$$+(9+S^2/3)\Big\{\Big|\sum\varepsilon_A'G_A\Big|^2 + \Big|\sum G_A'\varepsilon_A\Big|^2\Big\}$$
$$+\Big|\sum(\varepsilon_V'G_V + \varepsilon_A'G_A S)\Big|^2 + \Big|\sum(G_V'\varepsilon_V + G_A'\varepsilon_A S)\Big|^2$$
$$+\frac{2}{3}S\,\mathrm{Re}\Big\{\Big(\sum\varepsilon_V'G_A\Big)^*\Big(\sum\varepsilon_A'G_V\Big) + \Big(\sum G_V'\varepsilon_A\Big)^*\Big(\sum G_A'\varepsilon_V\Big)\Big\}$$
$$-\frac{4}{3}S\,\mathrm{Re}\Big\{\Big(\sum(\varepsilon_V'G_V + \varepsilon_A'G_A S)^*\Big(\sum\varepsilon_A'G_A\Big) + \sum(G_V'\varepsilon_V + G_A'\varepsilon_A S)^*\Big(\sum G_A'\varepsilon_A\Big)\Big\}, \qquad \text{(F.3.11c)}$$

$$D = 2\,\mathrm{Re}\Big\{\Big(\sum\frac{m_j}{m_e}(G_V'G_V - G_A'G_A S)\Big)^*\Big(\sum(G_V'\varepsilon_V - G_A'\varepsilon_A S)\Big)$$
$$+\Big(\sum\frac{m_j}{m_e}\varepsilon_V'G_A\Big)^*\Big(\sum(3G_V'\varepsilon_A - G_A'\varepsilon_V S)\Big)$$
$$+\Big(\sum\frac{m_j}{m_e}G_A'G_V\Big)^*\Big(\sum(3G_A'\varepsilon_V - G_V'\varepsilon_A S)\Big)$$
$$+\Big(\sum\frac{m_j}{m_e}G_A'G_A\Big)^*\Big(\sum G_A'\varepsilon_A\Big)(9-S^2)\Big\}, \qquad \text{(F.3.11d)}$$

where

$$G_V = [U_{\mu j} + \kappa' U'_{\mu j}]\,(g_V/g_A), \qquad \kappa' = \kappa\,(g'_V/g_V),$$
$$G_A = [U_{\mu j} - \kappa' U'_{\mu j}], \tag{F.3.12a}$$

$$\varepsilon_V = [\lambda' V_{\mu j} + \eta V'_{\mu j}]\,(g_V/g_A), \qquad \lambda' = \lambda\,(g'_V/g_V),$$
$$\varepsilon_A = [\lambda' V_{\mu j} - \eta V'_{\mu j}], \tag{F.3.12b}$$

and G'_V, G'_A, ε'_V and ε'_A are obtained from G_V, G_A, ε_V and ε_A by replacing μ with e. In the above expression S takes the value -3 if two protons are in the spin singlet state and S = 1 if they are in the spin triplet state.

Finally, we would like to comment on the relation between our result and the previous ones.[153),154)] At first, the previous articles are concerned with heavy neutrinos, while in our formalism, neutrinos are assumed to be light. If there is also a contribution from heavy neutrinos, the potentials for light neutrinos $e^{im_\mu r}/r$ should be modified to the Yukawa type $e^{-m_j r}/r$ for their propagations. Next, we explain the main differences. (i) Their decay rate is proportional to m_ν^4, while ours is to $|\Sigma_j m_j U_{ej} V_{ej}|^2$. (ii) Their nuclear matrix elements for the m_ν part include the tensor operator $\vec{r}_{nm}$ from $\vec{q}$ of the neutrino propagator, while ours do not contain $\vec{r}_{nm}$ as seen from $T^{\rho\sigma}$ in Eq.(F.3.4). The origin of these differences seems to come from their error in chiral projection when the mass insertion is operated. (iii) There are some other differences due to their ignorance of the time ordering.

References

1) J. C. Pati and A. Salam, Phys. Rev. D10 (1974), 275;
R. N. Mohapatra and J. C. Pati, Phys. Rev. D11 (1975), 566;
D11 (1975), 2599;
G. Senjanovic and R. N. Mohapatra, Phys. Rev. D12 (1975), 1502;
Riazuddin, R. E. Marshak and R. N. Mohapatra, Phys. Rev. D24 (1981), 1310.

2) C. Ryan and S. Okubo, Nuovo Ciment Suppl., 2 (1964), 234;
W. Pauli, Nuovo Cimento 6 (1957), 204;
F. Gürsey, Nuovo Cimento 7 (1958), 411.

3) K. M. Case, Phys. Rev. 107 (1957), 307;
R. N. Mohapatra and G. Senjanović, Phys. Rev. D23 (1981), 165;
T. P. Cheng and Ling-Fong Li, Phys. Rev. D22 (1980), 2860;
W. Pauli, Rev. Mod. Phys. 13 (1941), 203.

4) J. Schechter and J. W. Valle, Phys. Rev. D22 (1980), 2227.

5) M. Doi, M. Kenmoku, T. Kotani, H. Nishiura and E. Takasugi, Prog. Theor. Phys. 70 (1983), 1331.

6) T. Yanagida, Proc. *Workshop on Unified Theory and Baryon Number in the Universe*, ed. by Sawada and Sugamoto (KEK, 1979);
M. Gell-Mann, P. Ramond and R. Slansky, in "*Supergravity*", ed. by van Nieuwenhuizen and Freedman (North-Holland, Amsterdam, 1979).
G. Senjanovic and R. G. Mohapatra, Phys. Rev. Letters 44 (1980), 912.

7) J. L. Vuilleumier et al., Phys. Lett. 114B, (1982) 298;
F. Boehm, *Proc. 3rd Telemark Miniconf. on Neutrino Mass and*

Weak Interaction, ed. by Barger and Cline (AIP Conf. Series, 1985); Caltech preprint 63 - 436;
M. Shaevitz, *Proc. 1983 Int'l Symp. Lepton and Photon Int. at High Energies*, ed. by Cassel and Kreinick (Ithaca, 1983), p.132.

8) J. F. Cavaignac et al., Phys. Lett. 148B (1984), 387.

9) S. M. Bilenky, J. Hošek and S. T. Petcov, Phys. Letters 94B (1980), 495.
J. Schechter and J. W. F. Valle, Phys. Rev. D22 (1980), 2227; D23 (1981), 1666.

10) M. Doi, T. Kotani, H. Nishiura, K. Okuda and E. Takasugi, Phys. Lett. 102B (1981) 323.

11) M. Goeppert-Mayer, Phys. Rev. 48 (1935), 512.

12) W. H. Furry, Phys. Rev. 56 (1939), 1184.

13) E. J. Konopinski and H. Mahmoud, Phys. Rev. 92 (1953), 1045;
S. M. Bilenky and B. Pontecorvo, Phys. Letters, 102B (1981), 32.

14) B. Pontecorvo, Phys. Letters 26B (1968), 630.

15) N. Takaoka and K. Ogata, Z. Naturforschg, 21a (1966), 84.

16) T. Kirsten, AIP Conference Proceedings 96 (1983), 396;
T. Kirsten, *Proc. Conf. on Current Problems in Nuclear Physics*, Crete, Greece, June 1985; MPI Heidelberg, preprint.

17) W. C. Haxton and G. J. Stephenson, Jr., Progress in Particle and Nuclear Physics 12 (1984), 409.

18) W. C. Haxton, G. A. Cowan and M. Goldhaber, Phys. Rev. C28 (1983), 467.

19) L. Zanotti, Milano Univ. Preprint for ICOMAN 83 Conference, Frascati, January, 1983;
C. S. Wu, AIP Conference Proceedings 96 (1983), 374;

Yu. G. Zdesenko, Sov. J. Part. Nucl. 11 (1980), 542.

20) Ya. B. Zel'dovich and M. Yu Khlopov, JETP Lett. 34 (1981), 141.

21) M. Doi, T. Kotani, H. Nishiura and E. Takasugi, Prog. Theor. Phys. 69 (1983), 602.

22) J. Schechter and J. W. Valle, Phys. Rev. D25 (1982), 2951.

23) E. Takasugi, Phys. Letters 149B (1984), 372;
J. F. Nieves, Phys. Letters 147B (1984), 375.

24) H. Primakoff and S. P. Rosen, Rep. Prog. Phys. 22, (1959), 121; Proc. Phys. Soc. 78 (1961), 464.
S. P. Rosen, Proc. Phys. Soc. 74(1959), 350; Can. J. Phys. 37(1959), 780.

25) E. Greuling and R. C. Whitten, Ann. Phys. 11 (1960), 510.

26) M. Doi, T. Kotani, H. Nishiura, K. Okuda and E. Takasugi, Phys. Letters 103B (1981), 219; 113B (1982), 513(E); Prog. Theor. Phys. 66 (1981), 1739; 68 (1982), 347(E); 66 (1981), 1765, Appendix A; 68 (1982), 343(E).

27) H. Primakoff and S. P. Rosen, Phys. Rev. 184 (1969), 1925.

28) T. Kotani, *Proceedings of the Fourth Moriond Workshop*, ed. by J. Tran Thanh Van (Editions Frontieres, France, 1984), p. 397; *Proceedings of International Symposium on Nuclear Spectroscopy and Nuclear Interactions*, ed. by Egiri and Fukuda (World Scientific Pub., Singapore, 1984), p.259.

29) M. Doi, T. Kotani and E. Takasugi, Prof. Theor. Phys. 71 (1984), 1440.

30) S. P. Rosen, *Proceedings of Orbits Scietiae 1981*, Coral Gables (1981), p. 333.

31) M. Doi, T. Kotani, H. Nishiura and E. Takasugi, Prog. Theor. Phys. 70 (1983), 1353.
E. Takasugi, AIP Conference Proceedings 99 (1983), 207.

32) T. Tomoda, A. Faessler, K. W. Schmid and F. Grümmer, Phys, Letters 157B (1985), 4.

A. Faessler, private communication.

33) M. Doi, T. Kotani and E. Takasugi, Phys. Letters, 158B (1985), 164.

34) H. C. Haxton, G. J. Stephenson, Jr. and D. Strottman, Phys. Rev. Lett. 47 (1981), 153; Phys. Rev. D25 (1982), 2360.

35) H. Nishiura, Osaka University Thesis, Research Institute for Fundamental Physics, reprint RIFP-453 (1981).

36) K. Grotz and H. V. Klapdor, Phys. Letters 153B (1985), 1; H. V. Klapdor, Private Communication.

37) J. D. Vergados and R. N. Mohapatra, Phys. Rev. Letters 47 (1981), 1713.

38) L. Wolfenstein, Phys. Rev. D26 (1982), 2507;
W. C. Haxton, S. P. Rosen and G. J. Stephenson, Jr., Phys. Rev. D26 (1982), 1805;

39) M. M. Georgi, S. L. Glashow and S. Nussinov, Nucl. Phys. B193 (1981), 297.
G. B. Gelmini, S. Nussinov and M. Roncadelli, Nucl. Phys. B209 (1982), 157;
J. D. Vergados, Phys. Letters 109B (1982), 96; Nucl. Phys. B218 (1983), 109.

40) Y. Chikashige, R. N. Mohapatra and R. D. Peccei, Phys. Rev. Letters 45 (1980), 1926;
G. B. Gelmini and M. Roncadelli, Phys. Letters 99B (1981), 411.

41) E. Takasugi, *Proceedings of PANIC, Particles and Nuclei-Tenth International Conference,* Heidelberg, 1984; Nucl. Phys. A434 (1985), 457.

42) S. M. Bilenky and B. Pontecorvo, Phys. Rep. 41C (1978), 225.

43) T. Yanagida and M. Yoshimura, Prog. Theor. Phys. 64 (1980), 1870.

44) L. Wolfenstein, Phys. Lett. 107B (1981), 77.

45) S. Weinberg, Phys. Rev. 133B (1964), 1318; 134B (1964), 882.
P. A. Carruthers, *Spin and Isospin in Particle Physics,* Gordon and Breach, New York, 1971.
V. B. Berestetsii, E. M. Lifshitz and L. P. Pitaevskii, *Relativistic Quantum Theory* (Pergamon Press, 1971).

46) B. Kayser, Phys. Rev. D30 (1984), 1023.

47) J. Bernabeu and P. Pascual, Nucl. Phys. B228 (1983), 21.

48) J. M. Jauch, Helv. Phys. Acta 27 (1954), 89.
S. Kamefuchi and S. Tanaka, Prog. Theor. Phys. 14 (1955), 225.

49) L. Wolfenstein, Nucl. Phys. B185, (1981), 147.

50) S. T. Petcov, Phys. Lett. 110B (1982), 245.
C. N. Leung and S. T. Petcov, Nucl. Phys. 125B (1983), 461.
J. W. F. Valle, Phys. Rev. D27 (1983), 1672.
J. W. F. Valle and M. Singer, Phys. Rev. D28 (1983), 540.
D. Wyler and L. Wolfenstein, Nucl. Phys. B218 (1983), 205.

51) P. Herczeg, Proc. 3rd Telemark Miniconf. on Neutrino Mass and Weak Interaction, ed. by Barger and Cline (AIP Conf. Series, 1985), Los Alamos Preprint LA-UR-85-1345; Also Phys. Rev. D28 (1983), 200.

52) A. Halprin, S. Petcov and S. P. Rosen, Phys. Lett. 125B (1983), 335.

J. D. Vergados, Phys. Rev. D28 (1983), 2887.

S. P. Rosen, *Proceedings of the Fourth Moriond Workshop*, ed. by J. Tran Thanh Van (Editions Frontieres, France 1984), p.425.

53) M. Fukugita and T. Yanagida, Phys. Lett. 144B (1984), 386.

54) M. J. Dugan, G. B. Gelmini, H. Georgi and J. Hall, Phys. Rev. Lett. 54 (1985), 2302.

55) A. Zee, Phys. Lett. 93B (1980), 389.

56) B. W. Lee and R. E. Shrock, Phys. Rev. D16 (1977), 1444.

R. E. Shrock, Phys. Rev. D9 (1974), 743.

J. Kim, Phys. Rev. D14 (1976), 3000.

W. Marciano and A. I. Sanda, Phys. Lett. 67B (1977), 303.

57) K. Fujikawa and R. E. Shrock, Phys. Rev. Lett. 45 (1980), 963.

58) M. A. E. Beg and W. J. Marciano, Phys. Rev. D17 (1978), 1395.

59) S. T. Petcov, Yad. Foz. 25 (1977), 641 [Sov. J. Nucl. Phys. 25 (1977), 340]; 25 (1977), 698 (E)[25 (1977), 641]; Phys. Lett. 115B (1982), 401.

P. B. Pal and L. Wolfenstein, Phys. Rev. D25 (1982), 766.

B. Kayser, Phys. Rev. D26 (1982), 1662.

R. E. Shrock, Nucl. Phys. B206 (1982), 359.

J. F. Nieves, Phys. Rev. D26 (1982), 3152.

60) J. Schechter and J. W. F. Valle, Phys. Rev. D24 (1981), 1883; D25 (1982), 283 (E).

61) See for example, M. Morita, *Beta Decay and Muon Capture*, Benjamin, Mass., 1973.

62) E. J. Konopinski, *Theory of Beta Radioactivity* (Oxford Univ. Press, London, England, 1966).

63) A. Molina and P. Pascual, Nuovo Cim. 41 (1977), 756.

64) M. Doi, T. Kotani and E. Takasugi, *Proceedings of the third Telemark meeting on neutrino mass and weak interaction, Telemark, WI, 1984.*

65) A. Halprin, P. Minkowski, H. Primakoff and S. P. Rosen, Phys. Rev. D13 (1976), 2567.

66) J. D. Vergados, Phys. Rev. C24 (1981), 640.

67) J. D. Vergados, Phys. Rev. D25 (1982), 914.

68) Ching Cheng-rui and Ho Tso-hsin, Institute Theor. Physics at Beijing preprint, As-ITP-84-045.

G. A. Miller, Summary Talk at LAMPF Workshop on double charge exchange, Washington Univ. preprint, DOE/ER/40048-04-N5.

69) D. Smith, C. Picciotto and D. Brymann, Phys. Lett. 46B (1973), 157.

D. Bryman and C. Picciotto, Rev. Mod. Phys. 50 (1978), 11.

70) A. Halprin, Phys. Rev. D24 (1981), 2988.

71) C. E. Picciotto and M. S. Zahir, Phys. Rev. D26 (1982), 2320.

C. O. Escobar and V. Pleitez, Phys. Rev. D28 (1983), 1166.

72) M. Doi, T. Kotani and E. Takasugi, Osaka University preprint, OS-GE-85-04.

73) D. B. Reix, Phys. Lett. 115B (1982), 217.

D. Wilczek, Phys. Rev. Lett. 49 (1982), 1549.

G. B. Gelmini, S. Nussinov and T. Yanagida, Nucl. Phys. B219 (1983), 31.

74) L. Wolfenstein, Phys. Rev. Lett. 13 (1964), 562.

75) J. D. Vergados, Phys. Rev. C13 (1976), 865.

76) L. D. Skouras and J. D. Vergados, Phys. Rev. C28 (1983), 2122. See also Refs. (66)and (144).

77) L. Zamic and N. Auerbach, Phys. Rev. C26 (1982), 2185.

78) W. C. Haxton and G. J. Stephensen, Phys. Rev. C28 (1983), 458.

79) D. Bogdan, A. Faessler, A. Petrovici and S. Holan, Phys. Letters, 150B (1985), 29.

80) O. Scholten and Z. R. Yu, Michigan State Univ. preprint, MSUCL - 514 (1985).

81) H. F. Wu, H. Q. Song, T. T. S. Kuo, W. K. Cheng and D. Strottman, SUNY at Stony Brook preprint (1985).

82) A. H. Huffman, Phys. Rev. C2 (1970), 742.

83) K. Grotz, H. V. Klapdor and J. Metzinger, J. Phys. G9 (1983), L169; Phys. Lett. 132B (1983), 22.
H. V. Klapdor and K. Grotz, Phys. Lett. 142B (1984), 323; Phys. Rev. C30 (1984), 2098.
H. V. Klapdor, Prog. Part. Nucl. Phys. 10 (1983), 131.

84) P. Vogel and P. Fisher, Caltech preprint (1985).

85) T. Tsuboi, K. Muto and H. Horie, Phys. Lett. 143B (1984), 293.
K. Muto and H. Horie, private communication.

86) H. Nishiura, C. W. Kim and J. Kim, Phys. Rev. D31 (1985), 2288; C. W. Kim and H. Nishiura, Phys. Letters 139B (1984), 57.

87) M. Goeppert-Mayer, Naturwissen.17 (1929), 932; Ann. Phys. (Leipzig), 9 (1931), 273.
R. Korth et al., Proc. Int. Symp. on Nuclear Spectroscopy and Nuclear Interactions, ed. by Ejiri and Fukuda (World Scientific Pub., Singapore, 1984), P. 347.

88) J. D. Vergados, Nucl. Phys. B234 (1984), 213.

89) J. F. Richardson et al., Univ. of Missouri preprint (1981).

90) M. K. Moe, A. A. Hahn and S. R. Elliott, Univ. of California at Irvine preprint, UCI-Neutrino No. 133 (1984).

91) R. K. Bardin et al., Nucl. Phys. A158 (1970), 337.
B. Cleveland et al., Phys. Rev. Lett. 35 (1975), 757.

92) D. O. Caldwell et al., Santa Barbara-LBL preprint (1985).

93) F. Avignone et al., Phys. Rev. Lett. 54 (1985), 2309.

94) E. Bellotti et al., Phys. Lett. 146B (1984), 450.

95) A. A. Klimenko, A. A. Pomansky and A. A. Smolnikov, Paper present at "Neutrino 84", Nordkirchen, June 1984, INR-preprint INR-A-10.

96) E. Hennecke, O. Mannel and D. Sabu, Phys. Rev. C11 (1975), 1378.

97) P. Minkowski, Nucl. Phys. B201 (1982), 269.

98) T. Kirsten, H. Richter and E. Fessberger, Phys. Rev. Lett. 50 (1983), 474; Z. Phys. C16 (1983), 189.

99) H. Ejiri et al., *Proceedings of the third Telemark meeting on neutrino mass and weak interaction Telemark, WI, 1984.*

100) J. Simpson et al., Phys. Rev. Lett. 53 (1984), 141.

101) A. Forsten et al., Phys. Lett. 138B (1984), 301.

102) Yu. G. Zdesenko et al., Izv. Akad. Nauk. (USSR), Ser. Fiz. 45 (1981), 1856; *Proc. "Neutrino 82", Batafonfüred,* ed. by A. Frenkel (Budapest, 1982), Vol. 1, P. 209; JETP Letters 32 (1980), 58.

103) P. H. Hubert et al., Nuovo Cimento 85A (1985), 19.

104) E. Bellotti et al., AIP Conference Proceedings 99 (1983), 219

105) Particle Data Group, Rev. Mod. Phys. 56 (1984), S1.

106) K. E. Bergkvist, Nucl. Phys. B39 (1972), 317.
J. J. Simpson, Phys. Rev. D23 (1981), 649.

107) P. R. Burchat et al., Phys. Rev. Letters, 54 (1985), 2489.

108) V. A. Lubimov, *Proc. XXIIth Int. Conf. on High Energy Phys.* ed. A. Meyer and E. Wieczorek (Akad. der Wiss. der DDR. Zeuthen, 1984) Vol II, P. 108.

109) K. E. Bergkvist, Phys. Lett. 154B (1985), 224.

110) W. Kündig, private communication.

111) J. J. Simpson, Phys. Rev. Lett. 54 (1985), 1891.

112) J. Wotschack, *a talk given at XVI International Symposium on Multiparticle Dynamics*, Kiryat Anavim, Israel, 9-14 June, 1985.

113) N. J. Baker et al., Phys. Rev. Lett. 47 (1981), 1576.

114) N. Ushida et al., Phys. Rev. Lett. 47 (1981), 1694.

115) O. Erriques et al., Phys. Lett. 102B (1981), 73.

116) C. Santoni, *Proceedings of the fourth Moriond Workshop, ed.* by J. Tran Thanh Van (Editiors Frontieres, France, 1984), P. 207.
K. Winter, *Proceedings of the 1983 International Symposium on Lepton and Photon Interactions at High Energies, Ithaca, New York, ed.* by D. Cassel and D. Kreinick (Newman Lab. of Nucl. Studies, Cornell Univ. 1983), P. 177.
T. Yamazaki et al., Phys. Rev. Letters 52 (1984), 1089; KEK preprint 84-13 (1984).

117) J. U. Anderson et al., Phys. Letters, 113B (1982), 72.
S. Yasumi et al., *Proceedings of the third Telemark meeting on neutrino mass and weak interaction, Telmark, WI, 1984.*
F. X. Hartmann and R. A. Naumann, Phys. Rev. C31 (1985), 1594.

118) R. Cowsik and J. McClelland, Phys. Rev. Lett. 29 (1972), 669.

119) G. B. Gelmini and J. W. F. Valle, Phys. Lett. 142B (1984), 181.

120) M. J. Dugan, A. Manohar and A. E. Nelson, Phys. Rev. Lett. 55 (1985), 170.

121) M. Roncadelli and D. Weyler, Phys. Letters 113B (1983), 325.
P. Roy et al., Phys. Rev. Letters 52 (1984), 713; Phys. Rev. D30 (1983), 1949; D31 (1983), 2385 (E).
O. Shanker, Nucl. Phys. B250 (1985), 351.

122) M. A. B. Beg, R. V. Budny, M. Mohapatra and A. Sirlin, Phys. Rev. Letters 38 (1977), 1252.

123) J. Carr et al., Phys. Rev. Letters 51 (1983), 627.
D. P. Stoker et al., Phys. Rev. Letters 54 (1985), 1887.

124) M. Strovink, AIP Conference Proceedings 72 (1981), 46.
K. Mursula and F. Scheck, Nucl. Phys. B253 (1985), 189.

125) J. C. Pati and A. Salam, Phys. Letters 58B (1975), 333.
J. Maalampi and K. Enqvist, Phys. Letters 97B (1980), 217.
F. Wilczek and A. Zee, Phys. Rev. D25 (1982), 553.

126) K. Enqvist, K. Mursula and M. Roos, Nucl. Phys. B226 (1983), 121, and references therein.

127) J. van Klinken et al., Phys. Rev. Letters 50 (1983), 94.

128) J. van Klinken, Nucl. Phys. 75 (1966), 145.

129) F. P. Calaprice et al., Phys. Rev. Letters 35 (1975), 1566.

130) B. R. Holstein and S. B. Treiman, Phys. Rev. D16 (1977), 2369.

131) T. Vitale et al., unpublished. See also Ref. (130).

132) D. H. Wilkinson, Phys. Letters 67B (1977), 13.

133) F. Scheck, Phys. Reports 44 (1978), 187.

134) M. Doi, T. Kotani, H. Nishiura, K. Okuda and E. Takasugi, Prog. Theor. Phys. 67 (1982), 281, and Science Report (Col. Gen. Educ., Osaka Univ.) 30 (1981), 119.

135) R. E. Shrock, Phys. Rev. D24 (1981), 1275;

136) H. Burkard et al., Phys. Letters 150B (1985), 242.

137) R. S. Hayano et al., Phys. Rev. Letters 52 (1984), 329.

138) J. M. Fremlin and M. C. Walters, Proc. Roy. Soc. London A65 (1952), 911.

139) A. Berthelot et al., Compt. Rend 236 (1953), 1769.

140) R. G. Winter, Phys. Rev. 99 (1955), 88.

141) E. Bellotti et al., Lett. Nuovo Cimento 33 (1982), 273.

142) E. B. Norman and M. A. DeFaccio, Phys. Letters 148B (1984), 31.

143) E. B. Norman, Phys. Rev. C31 (1985), 1937.

144) J. D. Vergados, Nucl. Phys. B218 (1983), 109; Phys. Letters 109B (1982), 96.

145) C. W. Kim and K. Kubodera, Phys. Rev. D27 (1983),2765.

146) A. F. Pacheco, Phys. Rev. Letters 53 (1984), 979.

147) T. G. Rizzo, Phys. Letters 116B (1982), 23.

148) K. Enqvist, J. Maalampi and K. Mursula, Phys. Letters 124B (1983), 89.

149) J. N. Ng and A. N. Kamal, Phys. Rev. D18 (1978), 3412.

150) J. Abad, J. G. Esteve and A. F. Pacheco, Phys. Rev. D30 (1984), 1488.

151) A. Badertscher et al., Phys. Letters 79B (1978) 371; Nucl. Phys. A377 (1982), 406.

152) R. Abela et al., Phys. Letters 95B (1980), 318.

153) A. N. Kamal and J. N. Ng, Phys. Rev. D20 (1979), 2269.

154) J. D. Vergados and M. Ericson, Nucl. Phys. B195 (1982), 262.
G. K. Leontaris and J. D. Vergados, Nucl. Phys. B224 (1983), 137.

155) S. M. Austin et al., a paper presented at Int. Conference on Nuclear Phys. Frorence, Aug., 1983. Michigan State Univ. preprint.

156) J. J. Amato et al., Phys. Rev. Letters 21 (1968), 1709.

157) W. C. Barber et al., Phys. Rev. Letters 22 (1969), 902.

158) G. M. Marshall et al., Phys. Rev. D25 (1982), 1174.

159) A. Halprin, Phys. Rev. Letters 48 (1982), 1313.

160) B. Kayser and R. E. Shrock, Phys. Letters 112B (1982), 137.

161) T. Garavaglia, Phys. Rev. D29 (1984), 387.

162) S. P. Rosen, Phys. Rev. Letters 48 (1982), 842.

163) M. E. Rose, *Relativistic Electron* Theory (John Wiley & Sons, Inc., New York and London,1961).
C. P. Bhalla and M. E. Rose, Phys. Rev. 128 (1962), 774.

164) H. Behrens and J. Jänecke, *Numerical Tables for Beta-Decay and Electron Capture* (Springer, Berlin, 1969).
W. Bühring, Nucl. Phys. 40 (1963), 472.
L. Schülke, Z. Phys. 179 (1964), 331.

164) H. Behrens and W. Bühring, *Electron Radial wave functions and Nuclear Beta-Decay* (Clarendon Press, Oxford, 1982).

165) K. Koshigiri, M. Nishiura, H. Ohtsubo and M. Morita, Nucl. Phys. A319 (1979), 301.

166) A. Fujii and H. Primakoff, Nuovo Cimento 12 (1959), 1239.

167) C. W. Kim and H. Nishiura, Phys. Rev. D30 (1984), 1123;
H. Nishiura, Phys. Letters 157B (1985), 442.

168) M. Doi, M. Kenmoku, T. Kotani and E. Takasugi, Phys. Rev. D30 (1984), 626.

169) A. H. Wapstra and G. Audi, Nucl. Phys. A432 (1985), 55.

Table captions:

Table 1.1 Phase space estimates of the half-lives of the $(\beta\beta)_{2\nu}$ mode and the m_ν part of the $(\beta\beta)_{0\nu}$ mode for naturally occuring parent isotopes. The nuclear parameters $|M_{GT}^{[2\nu]}/\mu_0|$ and $|M_{GT}^{(0\nu)}(1-\chi_F)|$ are defined in Eqs.(3.2.9), (3.5.1) and (3.5.2). The total kinetic energy release T in units of keV defined in Eq. (3.2.6) is taken from the Table by Wapstra and Audi.[169]

* The single β decay is allowed kinematically.

\# The daughter nuclei are unstable against the α decay.

Table 1.2 *The selection rules for the* $\beta\beta$ decay. The circle, cross and triangle mean the dominant, forbidden and suppressed transitions, respectively. In the case of the N^*-mechanism, the static quark model has been used.

Table 3.1 The integrated kinematical factors of the $0^+ \to 0^+$ transition of the $(\beta\beta)_{2\nu}$ mode and the Majoron emitting process. The the values of $\langle \mu_a \rangle$ with asterisk are due to Haxton et al..[17] The definitions of T, $\langle \mu_a \rangle$, G_{GT} and G_B are given in Eqs. (3.2.6), (3.2.12), (3.2.11) and (5.2.4). The exact Coulomb factor in Eq. (B.3.6) is used.

Table 3.2 The integrated kinematical factors for the $0^+ \to 2^+$ transition of the $(\beta\beta)_{2\nu}$ mode in the 2n- and N^*-mechanisms. Here the value $\langle \mu_a \rangle = 10$ has been used for all nuclei. The definitions of G_{2n} and $G_{N^*2\nu}$ are given in Eqs. (3.2.18) and (4.5), respectively.

ble 3.3 Relative magnitudes of various contributions. Note that there is a cancellation of energy denominators for the ω-term so that the P-wave and recoil terms become dominant in the V+A part.

able 3.4 The integrated kinematical factors for the $0^+ \to 0^+$ transition of the $(\beta\beta)_{0\nu}$ mode. The values with asterisk for $\langle \mu_a \rangle$ are due to Haxton et al..[17]

Table 3.5 The integrated kinematical factors for the $0^+ - 2^+$ transition of the $(\beta\beta)_{0\nu}$ mode in the 2n- and N^*-mechanism.

Table 7.1 The theoretical predictions for $[M_{GT}^{(2\nu)}]_C$ and $\langle \mu_a \rangle_{av}$. The values of $\langle \mu_a \rangle_{av}$ with asterisk were derived by using the relation $|M_{GT}^{(2\nu)}/M_0| = |[M_{GT}^{(2\nu)}]_C| / \langle \mu_a \rangle_{av}$ in Eq. (3.2.14). The estimates by H.F. Wu et al. are not included because their values are not given explicitly.[81]

Table 7.2 The experimental data on the $(\beta\beta)_{2\nu}$ mode and the values of $|M_{GT}^{(2\nu)}/\mu_e|$ derived from the data which are compared with the theoretical predictions. See Eq. (3.2.13) and Table 3.1. The data underlined are due to the geochemical method.

HM : Heidelberg (Max-Planck) (16)
Col: Columbia (91)
BS : Battelle-South Carolina (93)
Irv: Irvine (90)
Mis: Missouri (89)
SB : Santa Barbara-LBL (92)
Mil: Milano (94)
Mos: Moscow (95)

H : Haxton et al. (34)
V : Vergados (75)
K : Klapdor et al.(36),(83)
VF: Vogel-Fisher(84)
SV: Skouras-Vergados (76)
Hu: Huffman(82)
T : Tsuboi et al.(85)

There are some additional theoretical estimates for 5 nuclei:

	^{100}Mo	^{128}Te	^{134}Xe	^{136}Xe	^{142}Ce
Klapdor et al.[36]		0.049	0.076	0.096	0.207
Vogel-Fisher[84]	0.23	0.10		0.098	

We thank sincerely Professor H.V. Klapdor and Professor P. Vogel for giving us their results before publication.

Table 7.3 The predictions of the nuclear matrix elements for the $0^+ \to 2^+$ transition (of the $(\beta\beta)_{2\nu}$ mode.) The values by Muto and Horie (MH) was obtained without using the closure approximation.[85] The symbol H means the values in the closure approximation by Haxton and Stephenson.[17]

Table 7.4 The theoretical predltions of the nuclear matrix elements. Here $\xi \approx M_{GT}^{(0\nu)}/[M_{GT}^{(2\nu)}]_C$ and χ_F are defined in Eq.(8.2.3) and Eq.(3.5.2). The scaled values for ^{82}Se and ^{130}Te are determined to repoduce the half-lives of the $(\beta\beta)_{2\nu}$ mode. The same scale factor is used for ^{76}Ge as for ^{82}Se, and for ^{128}Te as for ^{130}Te.

Table 7.5 The theoretical predictions of ratios of nuclear parameters defined in Eqs.(3.5.2)-(3.5.9). The "pot" represents the values are estimated by analyzing the neutrino potentials as discussed in § 7.2 and Appendix E.

Table 7.6 The predictions of the nuclear matrix elements for the $0^+ \to 2^+$ transition of the $(\beta\beta)_{0\nu}$ mode by Haxton et al.. We thank sincerely Professor W. C. Haxton for giving us his results before publications.

Table 8.1 The theoretical prediction for the $0^+ \to 2^+$ transition of the $(\beta\beta)_{2\nu}$ mode. The symbol H means that the nuclear matrix elements by Haxton et al.[17] are used together with the choice $\langle \mu_\alpha \rangle \approx 10$ and M represents the use of those by Muto et al.[86] For the N^*-mechanism, $P(\Delta)\,|\langle \text{要}_j | \text{要}_i \rangle|^2 \sim 10^{-3}$ is taken.

Table 8.2 The values of coeficients appeared in the $[T_{0\nu}(0^+ \to 0^+)]^{-1}$ defined in Eqs.(3.5.10) and (8.2.1). The ratios of nuclear matrix elements in Table 7.5 are used: the values by Haxton et al. for χ_F, χ'_F, χ'_{qT}, χ'_T and χ'_P, and the values by "pot" for $\chi^{(o)}_F$, $\chi^{(o)}_{qT}$ and χ'_R.

Table 8.3 The theoretical predictions for $\rho^{-1}_{2\nu}$ in Eq.(8.2.7) and the theoretical ratio of half-lives of ^{128}Te and ^{130}Te.

Table 8.4 The limits of neutrino mass and the right-handed parameters from various data. The values in the parenthesis for ^{128}Te/^{130}Te are obtained from the Missouri data.

Table 8.5 The experimental data on the $0^+ \to 0^+$ transition of the $(\beta\beta)_{0\nu}$ mode.

Col: Columbia (91)
SB : Santa Barbara-LBL (92)
Osa: Osaka (99)
Cal: Caltech (101)
UA : Ukrainian Academy (102)
Mil: Milano (94)
BS : Battelle-South Carolina (93)
Gue: Guelph (100)
Irv: Irvine (90)
Mos: Moskow (95)

Table 8.6 The experimental data on the $0^+ \to 2^+$ transition of the $(\beta\beta)_{0\nu}$ mode. The thoretical predictions are given by using nucler matrix elements by Haxton et al.[17] for the 2n-mechanism with $|\langle \eta \rangle| < 7 \cdot 10^{-7}$ and $|\langle \lambda \rangle| < 2 \cdot 10^{-5}$. For the N^*-mechanism, $P(\Delta)\,|\langle \text{要}_f | \text{要}_i \rangle|^2 \sim 10^{-3}$ is assumed.

SB : Santa Barbara-LBL (92)
Mil: Milano (94,104)
BZ : Bordeaux-Zaragoza (103)
Osa: Osaka (99)
Gue: Guelph (100)

Table 10.1 Constraints on the right-handed parameters imposed by the various experimental data. Here $\lambda_0' = \lambda_0 (\cos\theta'_c / \cos\theta_c)$ in Eq. (10.3.19), $\lambda_0'' = \lambda_0 (\sin\theta'_c / \sin\theta_c)$ in Eq. (10.4.4) and $a = \eta_0^2 + 1.26 \cdot 10^{-1} \lambda_0'^2 + 1.83 \lambda'_0 \eta_0$ from Eq. (10.2.20). The parameters $\bar{\nu}_e$ and $\bar{\nu}_\mu$ are small quantities of order θ_{LR}, the mixing angle between the left- and right-handed neutrinos, while $\bar{\nu}_{Me} \sim \bar{\nu}_{M\mu} \sim O(\theta_M)$, θ_M being the mixing between the left-handed and mirror neutrinos. $\lambda_0 \sim (M_{WL}/M_{MR})^2$, the squared mass ratio of the left and right gauge bosons and $\eta \sim -\tan\zeta$, ζ being their mixing. The H and S indicate that the limits are derived by using the nuclear matrix elements by Haxton et al. and by using the scaled values of them, respectively, from Table 8.4 and Eq.(8.2.13).

Table 11.1 Naturally occuring isotopes for the $\beta^+\beta^+$ decay, the electron capture to emit the positron (β^+/EC) and the double electron capture (EC/EC). Their available Q values denoted by T_j are taken from the Table by Wapstra and Audi.[169]

Table 11.2 Experimental data on the $\beta^+\beta^+$, β^+/EC and EC/EC decays.

Bir: Birmingham (138) BCLP: Berthelot et al. (139)
WRU: Western Reserve Univ. Mil: Milano (141)
Was: Washington (142) LBL: Laurence Berkley Lab. (143)

Table 11.3 The interplay of the CP phase β, the masses of Majorana neutrinos, m_1 and m_2, and their mixing angle θ. In the CP conserving case, two Majorana neutrinos contribute oppositely to the $\beta\beta$ decay and the μ^- - e^+ conversion.

Table A.1 Neutrino mixing schemes in various models. Rough order of mixing parameters are shown assuming the left-handed neutrino ($j \leq n$) are light, while the others (the right-handed neutrinos; the mirror neutrinos) are heavy.

Table B.1 The combinations of energy denominators for each nuclear operator X or Y in the $(\beta\beta)_{2\nu}$ mode, where all electrons and neutrinos are in the S-wave state and only the leading terms in the r expansion of the lepton wave functions are retained (no FBWC). See Eq.(B.2.21) for X and Y.

Table B.2 Order of magnitude of contributions from various lepton waves in the $0^+ \to 2^+$ transition of the $(\beta\beta)_{2\nu}$ mode. The terms proportional to $(pR)^2$ are not considered, where p represents one of lepton momenta. The (Q/2M) stands for the nucleon recoil effect, which is of order of (1/400).

Table C.1 The possible 0^+ - J^+ transitions in the m_ν part of the $(\beta\beta)_{0\nu}$ mode. The leading order of magnitude of their amplitudes for the $0^+ \to 0^+$ or $0^+ \to 2^+$ transitions are al shown by quantities which come from the lepton part. The factor (r/R) should be included in the nuclear matrix element, r being r_{nm} or the position of one of the decaying neutrons. The average electron momentum is expressed by p. The nucleon recoil effect is expressed by (Q/2M) symbolically. See Eq.(C.2.12) for X and Y.

Table C.2 The possible $0^+ \to J^+$ transition in the V+A part in the $(\beta\beta)_{0\nu}$ mode. The nuclear matrix elements are shown by z_k and z_{2k} in the parenthesis for the $0^+ \to 0^+$ and $0^+ \to 2^+$ transitions, respectively. The operator $\vec{r}$ means $\vec{r} = \vec{r}_n - \vec{r}_m$. See Eq.(C.2.34) for X and Y.

Figure captions:

Fig.1.1 The energy level structure for the ^{76}Ge $\beta^-\beta^-$ decay.

Fig.1.2 The diagram for the two neutrino mode $(\beta\beta)_{2\nu}$ of the $\beta\beta$ decay. in the 2n-mechanism.

Fig.1.3 The diagram for the neutrinoless mode $(\beta\beta)_{0\nu}$ of the $\beta\beta$ decay in the 2n-mechanism. Arrow represents the main helicity of the neutrino which is emitted or absorbed at each vertex.

Fig.1.4 The $\beta\beta$ decay in the N^*-mechamism. The wavy line represents the pion exchange or other strong interactions.

Fig.1.5 The $(\beta\beta)_{0\nu}$ mode by the transitions $\Delta^- \to \Delta^+ + 2e^-$ and $\Delta^0 \to \Delta^{++} + 2e^-$.

Fig.1.6 Mechanism for the $(\beta\beta)_{0\nu}$ mode by Higgs boson exchange. Here H_p^- represents the physical Higgs boson.

Fig.1.7 Mechanism for the $\beta\beta$ decay involving the Majoron emittion.

Fig.3.1 The pion exchange mechanism for the $(\beta\beta)_{2\nu}$ mode.

Fig.3.2 The μ_a (the energy of the intermediate nucleus) dependence of the integrated kinematical factor $G_{\pi\pi}(\mu_a)$ in Eq.(3.2.11). The virtical line indicates the μ_a corresponding to the first 1^+ state of the intermediate nuclei. The lines with arrow for ^{130}Te and ^{150}Nd mean the highest measured states, but not the 1^+ state.

Fig.3.3 The pion exchange mechanism for the $(\beta\beta)_{0\nu}$ mode.

Fig.3.4 The neutrino mass (m_ν) dependence of potentials.

Fig.3.5 The μ_a dependence of potentials. The zero neutrino mass is assumed, but the result is valid for $m_\nu \leq 1$MeV, as seen from Fig. 3.4.

Fig.3.6 The r dependence of potentials with $\mu_a = 18.5$l.

Fig.6.1 The single electron kinetic energy spectrum for the $(\beta\beta)_{2\nu}$ mode. ε_1 and Tm_e represent the electron energy and the maximum kinetic energy release, respectively.

Fig.6.2 The sum energy spectra for the $(\beta\beta)_{2\nu}$ and $(\beta\beta)_{0\nu}$ modes. $\varepsilon_1 + \varepsilon_2$ is the sum energy of two electrons.

Fig.6.3 The single electron kinetic energy spectra for the $(\beta\beta)_{2\nu}$ mode. The 2n- and N^*-mechanisms give the identical spectrum.

Fig.6.4 The sum energy spectrum for the $(\beta\beta)_{2\nu}$ and $(\beta\beta)_{0\nu}$ modes.

Fig.6.5 The single electron kinetic energy spectrum and the angular correlation of the m_ν^2 term for ^{76}Ge. The correlation coeficient α is defined in Eq.(6.2.1).

Fig.6.6 The single electron kinetic energy spectrum and the angular correlation of the λ^2 term for ^{76}Ge.

Fig.6.7 The single electron kinetic energy spectrum and the angular correlation of the η^2 term for ^{76}Ge and ^{48}Ca. For ^{76}Ge, the P-wave and recoil effects contribute constructively, while destructively for ^{48}Ca. The interplay of these two effects gives the sizable difference between ^{76}Ge and ^{48}Ca.

Fig.6.8 The single electron kinetic energy spectrum and the angular correlation for ^{76}Ge. The correlation coeficients α and β are defined in Eq.(6.2.2).

Fig.6.9 The single electron kinetic energy spectrum and the angular correlation for ^{76}Ge and ^{48}Ca. The large difference in the angular correlation is due to the difference of values of the nuclear matrix elements for ^{76}Ge and ^{48}Ca in Table 7.6.

Fig 6.10 The single electron kinetic energy spectrum for the Majoron emitting prosess. As a comparison, the spectrum for the $(\beta\beta)_{2\nu}$ mode is plotted by the broken line. The relative magnitude is obtained from the limit of the Majoron coupling in Eq.(8.2.11). The curve for the Majoron emitting process representes the upper limits and is magnified by the factor 35.

Fig.6.11 The sum energy spectrum of the Majoron emitting process in comparison with the $(\beta\beta)_{2\nu}$ and $(\beta\beta)_{0\nu}$ modes.

Fig.8.1 Limits on the neutrino mass $\langle m_\nu \rangle$ and the right-handed parameters $\langle\lambda\rangle$ and $\langle\eta\rangle$ imposed by the Heidelberg data on $(R_T)^{-1} \leq 3.29 \cdot 10^{-4}$. To derive the bounds, the values of ratios of nuclear matrix elements by Haxton et al. are used.[17] The cases $(\psi_1, \psi_2) = (0, \pi)$ and $(\pi, 0)$ are obtained from (a) and (b) by chainging $\langle\eta\rangle$ to $-\langle\eta\rangle$.

Fig.8.2 $\langle\lambda\rangle$ ($\langle\eta\rangle$) dependence of $(R_T)^{-1}$ with the fixed $\langle m_\nu \rangle$ in units of eV. Note that Fig.8.2a depends only on ψ_1, while Fig.8.2.b on ψ_2. The case $\psi_2 = \pi$ for (b) is obtained by changing $\langle\eta\rangle$ to $-\langle\eta\rangle$.

Fig.8.3 Limits on parameters imposed by the experimental bound on the $(\beta\beta)_{0\nu}$ mode for ^{48}Ca, $T_{0\nu}(0^+ \to 0^+) > 2 \cdot 10^{21}$ yr, with the value of $M_{GT}^{(0\nu)}$ by Haxton et al. and values in Table 8.2. Ellipsoids show the boundaries of the allowed domains.

Fig.8.4 Limits on parameters from ^{76}Ge, $T_{0\nu}(0^+ \to 0^+) > 1.2 \cdot 10^{23}$ yr, with the scaled value of $M_{GT}^{(0\nu)}$ in Table 7.4. If the value by Haxton et al.[17] is used, the limits become stronger by the factor 2.6.

Fig.8.5 Limits on parameters from ^{82}Se, $T_{0\nu}(0^+ \to 0^+) > 3.1 \cdot 10^{21}$ yr, with the scaled value of $M_{GT}^{(0\nu)}$. If the value by Haxton et al.[17] is used, the limits become stronger by the factor 2.6.

Fig.8.6 Limits on parameters from ^{130}Te, $T_{0\nu}(0^+ \to 0^+) > 1.2 \cdot 10^{21}$ yr, with the scaled value of $M_{GT}^{(0\nu)}$. If the value by Haxton et al.[17] is used the limits become stronger by the factor 13.

Fig.11.1 Quark diagrams for the $K^- \to \pi^+ + \mu^- + \mu^-$ decay. In order for this total lepton number violating decay to occur, the muon neutrino should be the massive Majorana particle.

Fig.11.2 The diagram for the μ decay (a), where N_i and $\bar{N}_j$ represent the mass eigenstate neutrino and antineutrino, respectively. If N_j's are Majorana particle ($\bar{N}_j = N_j$), then the diagram (b) is added. The interference between (a) and (b) shows the Majorana character of neutrino.

Fig.11.3 The diagram for the $\mu^- + e^+ \to \mu^+ + e^-$ transition. If ν_e and ν_μ are Dirac particle with mixing, then the transition occurs through the diagram (a). If neutrinos are Majorana particles, the diagram (b) is added. The triplet Higgs boson may mediate the transition through (c).

Fig.A.1 The diagram which leads to the Majorana mass term for the electron neutrino from the neutrinoless $\beta\beta$ decay (inside the boken lines). The black circle works as a filter to convert quarks and electrons to have the left-handed components, by the mass insertion if necessary.

Fig.A.2 The relation between the right-handed parameters η and λ in the $SU(2)_L \times SU(2)_R \times U(1)$ models. Here $\lambda = (M_1/M_2)^2$, where M_1 and M_2 ($M_1 < M_2$) are masses of gauge bosons.

Fig.E.1 The $\tilde{R}/R$ dependence of $\langle h_+ \rangle$, the average of h_+, for ^{76}Ge and ^{130}Te. The values 1.635 and 1.69 for ^{76}Ge and ^{130}Te are the theoretical estimates of $M_{GT}^{(0\nu)}/[M_{GT}^{(2\nu)}]_C$ by Haxton et al.,[17] from which the effective extension of nucleus $\tilde{R}$ is determined.

Fig.E.2 The $\tilde{R}/R$ dependence of ratios of the average potentials. The values of $\tilde{R}/R$, 0.72 and 0.655 for ^{76}Ge and ^{130}Te, are those determined from Fig.E.1, from which the values of ratios are obtained.

Transition	T (KeV)	$T_{2\nu} \cdot \left\lvert \frac{M_{GT}^{(2\nu)}}{\mu_0} \right\rvert^2$ (y)	$T_{0\nu} \left\lvert \frac{\langle m_\nu \rangle}{eV} M_{GT}^{(0\nu)} (1-\chi_F) \right\rvert^2$ (y)
$^{46}Ca \rightarrow {}^{46}Ti$	987 ± 4	8.71E21	7.16E26
$^{48}Ca \rightarrow {}^{48}Ti^*$	4271 ± 4	2.52E16	4.10E24
$^{70}Zn \rightarrow {}^{70}Ge$	1001 ± 3	3.17E21	4.27E26
$^{76}Ge \rightarrow {}^{76}Se$	2039.6±.9	7.66E18	4.09E25
$^{80}Se \rightarrow {}^{80}Kr$	130 ± 9	8.20E27	2.34E28
$^{82}Se \rightarrow {}^{82}Kr$	2995 ± 6	2.30E17	9.27E24
$^{86}Kr \rightarrow {}^{86}Sr$	1256 ± 5	3.00E20	1.57E26
$^{94}Zr \rightarrow {}^{94}Mo$	1145.3 ± 2.5	4.34E20	1.57E26
$^{96}Zr \rightarrow {}^{96}Mo^*$	3350 ± 3	5.19E16	4.46E24
$^{98}Mo \rightarrow {}^{98}Ru$	112 ± 7	1.03E28	1.49E28
$^{100}Mo \rightarrow {}^{100}Ru$	3034 ± 6	1.06E17	5.70E24
$^{104}Ru \rightarrow {}^{104}Pd$	1299 ± 2	1.09E20	8.32E25
$^{110}Pd \rightarrow {}^{110}Cd$	2013 ± 19	2.51E18	1.86E25
$^{114}Cd \rightarrow {}^{114}Sn$	534 ± 4	6.93E22	6.10E26
$^{116}Cd \rightarrow {}^{116}Sn$	2802 ± 4	1.25E17	5.28E24
$^{122}Sn \rightarrow {}^{122}Te$	364 ± 4	9.55E23	1.16E27
$^{124}Sn \rightarrow {}^{124}Te$	2288.1 ± 1.6	5.93E17	9.48E24
$^{128}Te \rightarrow {}^{128}Xe$	868 ± 4	1.18E21	1.43E26
$^{130}Te \rightarrow {}^{130}Xe$	2533 ± 4	2.08E17	5.89E24
$^{134}Xe \rightarrow {}^{134}Ba$	847 ± 10	1.16E21	1.30E26
$^{136}Xe \rightarrow {}^{136}Ba$	2479 ± 8	2.07E17	5.52E24
$^{142}Ce \rightarrow {}^{142}Nd$	1417.6 ± 2.5	1.38E19	2.31E25
$^{146}Nd \rightarrow {}^{146}Sm^\sharp$	56 ± 5	2.06E29	7.05E27
$^{148}Nd \rightarrow {}^{148}Sm^\sharp$	1928.3 ± 1.9	9.35E17	7.84E24
$^{150}Nd \rightarrow {}^{150}Sm$	3367.1 ± 2.2	8.41E15	1.25E24
$^{154}Sm \rightarrow {}^{154}Gd$	1251.9 ± 1.5	2.44E19	2.38E25
$^{160}Gd \rightarrow {}^{160}Dy$	1729.5 ± 1.4	1.51E18	7.99E24
$^{170}Er \rightarrow {}^{170}Yb$	653.9 ± 1.6	1.82E21	6.92E25
$^{176}Yb \rightarrow {}^{176}Hf$	1078.8 ± 2.7	3.26E19	1.75E25
$^{186}W \rightarrow {}^{186}Os^\sharp$	490.3 ± 2.2	7.68E21	6.95E25
$^{192}Os \rightarrow {}^{192}Pt$	417 ± 4	1.98E22	7.70E25
$^{198}Pt \rightarrow {}^{198}Hg$	1048 ± 4	1.63E19	8.74E24
$^{204}Hg \rightarrow {}^{204}Pb$	416.5 ± 1.1	1.23E22	5.06E25
$^{232}Th \rightarrow {}^{232}U^\sharp$	858.2 ± 6	1.68E19	3.97E24
$^{238}U \rightarrow {}^{238}Pu^\sharp$	1145.8 ± 1.7	1.47E18	1.68E24

Table 1.1

	$(\beta\beta)_{2\nu}$ mode		$(\beta\beta)_{0\nu}$ mode			
			m_ν-part		V+A part	
mechanisms	2n	N^*	2n	N^*	2n	N^*
nuclear transitions						
$0^+ \rightarrow 0^+$	○	×	○	×	○	×
$0^+ \rightarrow 2^+$	△	△	×	×	○	○

Table 1.2.

	^{48}Ca	^{76}Ge	^{82}Se	^{100}Mo	^{128}Te	^{130}Te	^{136}Xe	^{150}Nd
T	8.358	3.991	5.861	5.937	1.700	4.957	4.851	6.589
$\langle\mu_a\rangle$	15.10*	18.42*	19.73*	20	24.53*	25.98*	20	20
G_{GT}	$3.967\cdot10^{-17}$	$1.313\cdot10^{-19}$	$4.350\cdot10^{-18}$	$9.434\cdot10^{-18}$	$8.541\cdot10^{-22}$	$4.803\cdot10^{-18}$	$4.858\cdot10^{-18}$	$1.189\cdot10^{-16}$
G_R	$1.968\cdot10^{-15}$	$6.022\cdot10^{-17}$	$4.940\cdot10^{-16}$	$8.576\cdot10^{-16}$	$4.911\cdot10^{-18}$	$6.477\cdot10^{-16}$	$6.743\cdot10^{-16}$	$5.112\cdot10^{-15}$

Table 3.1

	^{48}Ca		^{76}Ge	^{82}Se	^{100}Mo	^{128}Te	^{130}Te	^{136}Xe	^{150}Nd
T	2_1^+ 6.435	2_2^+ 3.622	2_1^+ 2.900	2_1^+ 4.361	2_1^+ 4.879	2_1^+ 0.834	2_1^+ 3.908	2_1^+ 3.252	2_1^+ 5.936
G_{2n}	$1.131\cdot10^{-17}$	$6.848\cdot10^{-21}$	$1.182\cdot10^{-21}$	$2.151\cdot10^{-19}$	$1.895\cdot10^{-18}$	$3.223\cdot10^{-27}$	$2.906\cdot10^{-19}$	$3.646\cdot10^{-20}$	$1.182\cdot10^{-16}$
$G_{N^*2\nu}$	$3.707\cdot10^{-16}$	$2.244\cdot10^{-19}$	$3.872\cdot10^{-20}$	$7.049\cdot10^{-18}$	$6.210\cdot10^{-17}$	$1.056\cdot10^{-25}$	$9.523\cdot10^{-18}$	$1.195\cdot10^{-18}$	$3.872\cdot10^{-15}$

Table 3.2

	The $(\beta\beta)_{0\nu}$ mode : $0^+ \to 0^+$ transition G: in units of (1/yr)								
	^{48}Ca	^{76}Ge	^{82}Se	^{100}Mo	^{128}Te	^{130}Te	^{136}Xe	^{150}Nd
$\tau(m_e)$	8.359	3.994	5.881	5.935	1.700	4.957	4.855	6.589
$\langle\mu_a\rangle$	15.10^{*}	18.42^{*}	19.73^{*}	20	24.53^{*}	25.98^{*}	20	20
	$\cdot 10^{-14}$	$\cdot 10^{-15}$	$\cdot 10^{-14}$	$\cdot 10^{-14}$	$\cdot 10^{-15}$	$\cdot 10^{-14}$	$\cdot 10^{-14}$	$\cdot 10^{-13}$
G_{01}	6.369	6.400	2.817	4.575	1.827	4.435	4.729	2.096
G_{02}	$4.168 \cdot 10$	$1.062 \cdot 10$	9.860	$1.664 \cdot 10$	$5.658 \cdot 10^{-1}$	$1.181 \cdot 10$	$1.218 \cdot 10$	9.713
G_{03}	4.846	3.514	1.910	3.132	$4.829 \cdot 10^{-1}$	2.772	2.917	1.486
G_{04}	1.355	1.254	$5.825 \cdot 10^{-1}$	$9.498 \cdot 10^{-1}$	$2.938 \cdot 10^{-1}$	$9.074 \cdot 10^{-1}$	$9.664 \cdot 10^{-1}$	$4.427 \cdot 10^{-1}$
G_{05}	$9.303 \cdot 10$	$1.866 \cdot 10^{-2}$	$6.716 \cdot 10$	$1.208 \cdot 10^{-2}$	$9.908 \cdot 10$	$1.419 \cdot 10^{-2}$	$1.552 \cdot 10^{-2}$	$5.899 \cdot 10$
G_{06}	$1.021 \cdot 10^{-3}$	$1.429 \cdot 10^{-3}$	$4.774 \cdot 10^{-2}$	$7.087 \cdot 10^{-2}$	$4.942 \cdot 10^{-2}$	$6.886 \cdot 10^{-2}$	$7.278 \cdot 10^{-2}$	$2.478 \cdot 10^{-2}$
G_{07}	$8.177 \cdot 10^{-4}$	$8.876 \cdot 10^{-4}$	$3.879 \cdot 10^{-4}$	$6.641 \cdot 10^{-4}$	$3.041 \cdot 10^{-4}$	$6.563 \cdot 10^{-4}$	$7.029 \cdot 10^{-4}$	$3.191 \cdot 10^{-4}$
G_{08}	$4.017 \cdot 10^{-3}$	$5.965 \cdot 10^{-3}$	$2.846 \cdot 10^{-3}$	$5.884 \cdot 10^{-3}$	$3.077 \cdot 10^{-3}$	$6.970 \cdot 10^{-3}$	$7.719 \cdot 10^{-3}$	$3.948 \cdot 10^{-3}$
G_{09}	$4.166 \cdot 10^{-5}$	$3.304 \cdot 10^{-5}$	$1.322 \cdot 10^{-5}$	$1.875 \cdot 10^{-5}$	$7.516 \cdot 10^{-4}$	$1.546 \cdot 10^{-5}$	$1.601 \cdot 10^{-5}$	$6.453 \cdot 10^{-4}$

Table 3.4

Types of contributions		Contributions from electron wave functions and neutrino propagators: Coefficients	Relative magnitudes	Nuclear operators
m_ν part		$\frac{\langle m_\nu \rangle}{m_e} \frac{1}{2} \left(\frac{1}{\omega+A_1} + \frac{1}{\omega+A_2} \right)$	$\frac{1}{2}$	$\vec{\sigma}_n \cdot \vec{\sigma}_m \sim -3$
$V+A$ part	ω-term	$\left\{ \begin{matrix} \langle \eta_\nu \rangle \\ \langle \lambda \rangle \end{matrix} \right\} \frac{m_e}{\omega} \left\| \frac{1}{\omega+A_1} - \frac{1}{\omega+A_2} \right\|$	$\frac{m_e}{\omega} \frac{\lvert \epsilon_{12}' \rvert}{\omega} \sim \frac{\lvert \epsilon_{12} \rvert}{m_e}$ ~ 2	$\vec{\sigma}_n \cdot \vec{\sigma}_m \sim -3$
	q^+-term $\frac{pR}{\gamma}$	$\left\{ \begin{matrix} \langle \eta_\nu \rangle \\ \langle \lambda \rangle \end{matrix} \right\} \frac{m_e}{m_e} \left(\frac{pR}{\gamma} \right) \left(\frac{1}{\omega+A_1} + \frac{1}{\omega+A_2} \right) \left(\frac{r}{R} \right)$	$\frac{m_e q}{m_e} \frac{pr}{\gamma} \sim qr \left(\frac{p}{\gamma m_e} \right)$ ~ $\frac{1}{\gamma}$	$\vec{\sigma}_n \cdot \vec{\sigma}_m \sim -3$
	q^+- term $\frac{qR}{r^2}$	$\langle \eta_\nu \rangle \frac{m_e}{m_e} (qR) \left(\frac{1}{\omega+A_1} + \frac{1}{\omega+A_2} \right) \left(\frac{r}{R} \right)$	$\frac{m_e q_R r}{m_e R} \cdot qR \sim qr \left(\frac{qR}{m_e R} \right)$ ~ 30	$\frac{1}{2} \vec{r}_{nm} \cdot [\vec{r}_{nm} \times (\vec{\sigma}_n - \vec{\sigma}_m)]$ ~ $-\frac{2}{5}$
	Recoil	$\langle \eta_\nu \rangle \left(\frac{q}{m_e} \right) \left(\frac{1}{\omega+A_1} + \frac{1}{\omega+A_2} \right)$	$\left(\frac{m_e q}{m_e} \right) \sim \left(\frac{1}{m_e R} \right) (qR)$ ~ 80	$(D/M) (\vec{\sigma}_n \cdot \vec{\sigma}_m)$ $-4.7 \left(\frac{q}{M} \right) (\vec{\sigma}_n \cdot \vec{\sigma}_m) \sim \frac{4}{5}$

Table 3.3

	^{48}Ca		^{76}Ge	^{82}Se	^{100}Mo	^{128}Te	^{130}Te	^{136}Xe	^{150}Nd
T	2_1^+ 6.435	2_2^+ 3.622	2_1^+ 2.900	2_1^+ 4.361	2_1^+ 4.879	2_1^+ 0.834	2_1^+ 3.908	2_1^+ 3.252	2_1^+ 5.936
G_{21}	$1.476 \cdot 10^{-13}$	$7.629 \cdot 10^{-15}$	$4.499 \cdot 10^{-15}$	$3.374 \cdot 10^{-14}$	$9.146 \cdot 10^{-14}$	$1.631 \cdot 10^{-16}$	$5.577 \cdot 10^{-14}$	$2.746 \cdot 10^{-14}$	$7.358 \cdot 10^{-13}$
G_{22}	$1.292 \cdot 10^{-13}$	$5.732 \cdot 10^{-15}$	$3.128 \cdot 10^{-15}$	$2.704 \cdot 10^{-14}$	$7.584 \cdot 10^{-14}$	$0.6018 \cdot 10^{-16}$	$4.385 \cdot 10^{-14}$	$2.040 \cdot 10^{-14}$	$6.441 \cdot 10^{-13}$
$G_{N^*0\nu}$	$8.341 \cdot 10^{-11}$	$4.312 \cdot 10^{-12}$	$3.455 \cdot 10^{-12}$	$2.726 \cdot 10^{-11}$	$8.433 \cdot 10^{-11}$	$1.773 \cdot 10^{-13}$	$6.127 \cdot 10^{-11}$	$3.109 \cdot 10^{-11}$	$8.892 \cdot 10^{-10}$

Table 3.5

		^{48}Ca	^{76}Ge	^{82}Se	^{128}Te	^{130}Te	^{134}Xe	^{136}Xe	^{142}Ce	^{238}U
$\lvert M_{GT}^{(2\nu)}\rvert_C$ [$\langle u_a \rangle_{av}$] (Ref.)	Vergados (75)	0.14 [12.7]			0.56 [23.4]	0.49 [25.0]				
	Haxton et al. (17,34) (18,78)	0.444 [15.10]	2.556 [18.42] 2.78	1.876 [19.73]	2.948 [24.53]	2.966 [25.98]				3.28
	Zamic - Auerbach (77)	0.36	3.22							
	Skouras - Vergados (76)	0.25 [9]								
	Klapdor et al. (36)		1.93 [10.1]*	1.38 [11.0]*	0.52 [10.5]*	0.48 [10.6]*	0.77 [10.1]*	0.08 [0.84]*	1.30 [6.3]*	
	Tsuboi et al. (84)	0.424 [7.66]*								
	Scholten - Yu (80)				2.88	2.98				
	Bogdan et al. (79)		11.30							

Table 7.1

		^{48}Ca	^{76}Ge	^{82}Se	^{130}Te	^{150}Nd
Exp.	$T_{2\nu}$ (yr)			$(1.7\pm0.3)\cdot10^{20}$ (HM)	$(2.55\pm0.20)\cdot10^{21}$ (HM) $(1.0\pm0.1)\cdot10^{21}$ (Mis)	
	(Ref.)	$>3.6\cdot10^{19}$ (Col)	$>.2\cdot10^{20}$ (SB) $>2.8\cdot10^{19}$ (BS) $>4\cdot10^{18}$ (Mil)	$>4.1\cdot10^{19}$ (Irv)		$>1.3\cdot10^{19}$ (Mos)
	$\left\|\frac{M_{GT}^{(2\nu)}}{\mu_0}\right\|$			$3.6\cdot10^{-2}$	$0.90\cdot10^{-2}$ $1.4\cdot10^{-2}$	
		$<2.6\cdot10^{-2}$	$<2\cdot10^{-1}$ $<5.2\cdot10^{-1}$ $<14\cdot10^{-1}$	$<7.3\cdot10^{-2}$		$<2.5\cdot10^{-2}$
Theo.	$\left\|\frac{[M_{GT}^{(2\nu)}]_C}{\langle\mu_a\rangle_{av}}\right\|$	$2.94\cdot10^{-2}$ (H) $2.8\cdot10^{-2}$ (SV)	$1.39\cdot10^{-1}$ (H)	$9.51\cdot10^{-2}$ (H)	$11.4\cdot10^{-2}$ (H) $2.0\cdot10^{-2}$ (V)	
	$\left\|\frac{M_{GT}^{(2\nu)}}{\mu_0}\right\|$ (Ref.)	$5.54\cdot10^{-2}$ (T)	$1.91\cdot10^{-1}$ (K) $0.66\cdot10^{-1}$ (VF)	$12.5\cdot10^{-2}$ (K) $8.2\cdot10^{-2}$ (VF)	$10\cdot10^{-2}$ (Hu) $4.5\cdot10^{-2}$ (K) $9\cdot10^{-2}$ (VF)	$6.4\cdot10^{-2}$ (VF)

Table 7.2

	^{48}Ca		^{76}Ge
	2_1^+	2_2^+	2_1^+
$[M_2^{(2\nu)}]_C$	0.014 (H) 0.218 (MH)	0.64 (H)	0.10 (H)
$\left(\frac{M_2^{(2\nu)}}{\mu_2^3}\right)$	$8.00\cdot10^{-4}$ (MH)		

Table 7.3

		^{48}Ca	^{76}Ge	^{82}Se	^{128}Te	^{130}Te
Haxton et al. (17,34)	$\lvert[M_{GT}^{(2\nu)}]_C\rvert$	0.44	2.556	1.876	2.948	2.966
	$\lvert M_{GT}^{(0\nu)}\rvert$	1.00	4.18	3.45	4.98	5.02
	χ_F	-0.150	-0.201	-0.178	-0.227	-0.226
	ξ	2.27	1.64	1.84	1.69	1.69
Scaled from Haxton et al. (31)	$\lvert[M_{GT}^{(2\nu)}]_C\rvert$	0.44	0.974	0.715	0.233	0.235
	$\lvert M_{GT}^{(0\nu)}\rvert$	1.00	1.59	1.31	0.395	0.399
Klapdor et al. (36)	$\lvert[M_{GT}^{(2\nu)}]_C\rvert$		1.93	1.38	0.52	0.48
	$\lvert M_{GT}^{(0\nu)}\rvert$		10.40	8.20	10.03	9.44
	χ_P		-0.24	-0.23	-0.24	-0.24
	ξ		5.39	5.94	19.3	19.7

Table 7.4

Table 7.5

	^{48}Ca		^{76}Ge			^{82}Se		^{128}Te		^{130}Te	
	Haxton (17)	pot. (31,33)	Haxton (17)	Faessler (32)	pot. (31,33)	Haxton (17)	pot. (31,33)	Haxton (17)	pot. (31,33)	Haxton (17)	pot. (31,33)
χ_F	-0.150		-0.201			-0.178		-0.227		-0.226	
χ'_{GT}	1.087	1.10	1.141		1.16	1.142	1.16	1.175	1.19	1.179	1.20
χ'_F	-0.156	-0.165	-0.232		-0.233	-0.205	-0.206	-0.273	-0.270	-0.273	-0.271
χ'_T	-0.110		-0.013			-0.021		-0.030		-0.025	
$\chi^{(0)}_{GT}$		0.61		0.59	0.64		0.58		0.53		0.50
$\chi^{(0)}_F$		-0.09		-0.15	-0.13		-0.10		-0.12		-0.11
χ'_P	-0.191		0.270			0.440		0.338		0.227	
χ'_R		-0.021			-0.021		-0.025		-0.032		-0.034

		M_{2a}	M_{2b}	M_{2c}	M_{2d}	M_{2e}
^{48}Ca	2_1^+	-0.0721	-0.0178	0.0145	——	-0.1353
	2_2^+	0.0355	0.0469	-0.00474	——	-0.0202
^{76}Ge	2_1^+	0.0683	-0.000423	-0.0149	——	0.0138

Table 7.6

Theoretical Prediction of $T_{2\nu}(0^+ \to 2^+)$									
	^{48}Ca		^{76}Ge	^{82}Se	^{100}Mo	^{128}Te	^{130}Te	^{136}Xe	^{150}Nd
	2_1^+	2_2^+	2_1^+	2_1^+	2_1^+	2_1^+	2_1^+	2_1^+	2_1^+
2n	$4.6 \cdot 10^{26}$ (H) $1.4 \cdot 10^{23}$ (M)	$3.8 \cdot 10^{26}$ (H)	$8.5 \cdot 10^{28}$ (H)						
N^*	$2.70 \cdot 10^{24}$	$4.46 \cdot 10^{28}$	$2.58 \cdot 10^{28}$	$1.42 \cdot 10^{26}$	$1.61 \cdot 10^{25}$	$9.47 \cdot 10^{33}$	$1.05 \cdot 10^{26}$	$8.37 \cdot 10^{26}$	$2.58 \cdot 10^{23}$

Table 8.1

		^{48}Ca	^{76}Ge	^{82}Se	^{128}Te	^{130}Te
$< m_\nu >^2$	C_1 (1/y)	$8.422 \cdot 10^{-14}$	$9.232 \cdot 10^{-15}$	$3.909 \cdot 10^{-14}$	$2.750 \cdot 10^{-15}$	$6.667 \cdot 10^{-14}$
$< m_\nu >< \lambda >$	C_2/C_1	-0.3513	-0.3517	-0.4174	-0.1260	-0.3838
$< m_\nu >< \eta >$	C_3/C_1	-0.5708	-10.56	-12.55	-22.21	-10.39
	C_{31}	-0.06878	-0.1011	-0.05142	-0.2102	-0.1669
	C_{32}	-12.70	-24.27	-20.24	-44.20	-26.09
	C_{33}	10.98	7.661	7.109	4.988	4.854
$< \lambda >^2$	C_4/C_1	3.790	1.013	2.097	0.1576	1.460
$< \eta >^2$	C_5/C_1	1.528	117.6	271.8	275.4	156.9
	C_{51}	1.255	0.2265	0.5527	0.05429	0.2455
	C_{52}	476.9	646.1	728.2	1119	1045
	C_{53}	10.18	7.440	6.813	4.942	4.708
$< \lambda >< \eta >$	C_6/C_1	-4.199	-0.8007	-1.986	-0.03480	-0.9440

Table 8.2

		$[\rho_{2\nu}^{-1}]_C$	$\rho_{2\nu}^{-1}$	$(R_{2\nu})_{Th}^{-1} = \frac{T_{2\nu}(^{130}Te)}{T_{2\nu}(^{128}Te)}$
Theory	NM by Vergados (75)	1.2		$2.6 \cdot 10^{-4}$
	NM by Haxton et al. (34)	1.05		$1.97 \cdot 10^{-4}$
	NM by Klapdor et al. (36)		1.1	$2.1 \cdot 10^{-4}$

Table 8.3

	$T_{1/2}$ Exp. (yr)	$\langle m_\nu \rangle$ (eV)			$\langle \lambda \rangle \cdot 10^5$		$\langle \eta \rangle \cdot 10^6$	
		NM by Klapdor at al.	NM by Haxton at al.	scaled NM	NM by Haxton et al.	scaled NM	NM by Haxton at al.	scaled NM
^{48}Ca	$> 2 \cdot 10^{21}$		3.94		3.96		62.3	
^{76}Ge	$>1.2 \cdot 10^{23}$	1.48	3.67	9.66	0.714	1.88	0.663	1.74
^{82}Se	$>3.1 \cdot 10^{21}$	5.66	13.5	35.4	1.82	4.79	1.60	4.21
$\frac{^{128}Te}{^{130}Te}$	Ratio $3.04 \cdot 10^3$ $(1.59 \cdot 10^3)$	1.04 (1.97)	5.67 (10.3)		2.90 (5.45)		0.688 (1.21)	
^{130}Te	$>1.2 \cdot 10^{21}$	6.05	11.4	143	1.84	23.2	1.78	22.4

Table 8.4

Unit / Exp.	^{48}Ca 10^{21} y	^{76}Ge 10^{22} y	^{82}Se 10^{21} y	^{96}Zr 10^{19} y	^{100}Mo 10^{21} y	^{130}Te 10^{21} y	^{150}Nd 10^{21} y
$0^+ \to 0^+$	> 2 (Col)	> 12 (Mil)	> 3.1 (Col)	> (1.4 ~ 6.5) (UA)	> 2.1 (UA)	> 1.2 (UA)	> 1.2 (Mos) for $\langle m_\nu \rangle \neq 0$
		> 12 (SB)	> 1.4 (I)				> 0.8 (Mos) for $\eta \neq 0, \chi \neq 0$
		> 11.6 (BS)					
		> 5 (Osa)					
		> 3.2 (Gue)					
		> 1.9 (Cal)					
$0^+ \to 0^+_2$		(1122.3 KeV)					
		> 0.23 (SB)					
$\lvert 1-\chi_F \rvert \lvert M_{GT}^{0\nu} \rvert \cdot \langle m_\nu \rangle$ (eV)	<45.3	< 18.4	< 24.7	< 564	< 521	< 70.0	< 32.5

Table 8.5

		^{48}Ca		^{76}Ge	^{100}Mo	^{130}Te	^{148}Nd	^{150}Nd
Exp. (year)		2_1^+ (984 KeV)	2_1^+ (2421 KeV)	2_1^+ (559 KeV)	2_1^+ (540 KeV)	2_1^+ (536 KeV)	2_1^+ (550 KeV)	2_1^+ (334 KeV)
				$> 1.3 \cdot 10^{23}$ (SB) $> 4 \cdot 10^{22}$ (Osa) $> 2.2 \cdot 10^{22}$ (Mil) $> 0.55 \cdot 10^{22}$ (BZ) $> 0.5 \cdot 10^{22}$ (Gue)	$> 2 \cdot 10^{18}$ (Mil)		$> 3 \cdot 10^{18}$ (Mil)	$> 1 \cdot 10^{18}$ (Mil)
Theor.	2n η	$> 2.1 \cdot 10^{26}$	$> 6.5 \cdot 10^{28}$	$> 6.0 \cdot 10^{28}$				
	N* η	$> 2.4 \cdot 10^{25}$	$> 4.7 \cdot 10^{26}$	$> 5.9 \cdot 10^{26}$	$> 2.4 \cdot 10^{25}$	$> 3.3 \cdot 10^{25}$	$> 6.6 \cdot 10^{25}$	$> 2.3 \cdot 10^{24}$
	N* λ	$> 3.0 \cdot 10^{22}$	$> 5.8 \cdot 10^{23}$	$> 7.2 \cdot 10^{23}$	$> 2.9 \cdot 10^{22}$	$> 4.0 \cdot 10^{22}$	$> 8.0 \cdot 10^{22}$	$> 2.8 \cdot 10^{21}$

Table 8.6

	Model	$SU(2)_L \times SU(2)_R \times U(1)$			$SU(2)_L \times U(1)$ with mirror leptons
	Case / Input data	D	M - I	M - II	M - III
ββ decay	$^{128}Te/^{130}Te$	no constraint		$\lvert\lambda_0' \bar{\nu}_e\rvert < 2.9 \cdot 10^{-5}$ $\lvert\eta_0 \bar{\nu}_e\rvert < 6.7 \cdot 10^{-7}$	$\lvert\bar{\nu}_{Me}\rvert < 6.7 \cdot 10^{-7}$
	^{76}Ge			$\lvert\lambda_0' \bar{\nu}_e\rvert < \begin{cases} 0.71 \cdot 10^{-5} & (H) \\ 1.9 \cdot 10^{-5} & (S) \end{cases}$ $\lvert\eta_0 \bar{\nu}_e\rvert < \begin{cases} 0.65 \cdot 10^{-6} & (H) \\ 1.7 \cdot 10^{-6} & (S) \end{cases}$	$\lvert\bar{\nu}_{Me}\rvert < \begin{cases} 0.66 \cdot 10^{-6} & (H) \\ 1.7 \cdot 10^{-6} & (S) \end{cases}$
β decay	P_F/P_{GT}	$-7.8 \cdot 10^{-3} < \lambda_0'\eta_0 < 1.1 \cdot 10^{-2}$		$-7.8 \cdot 10^{-3} < \lambda_0'\eta_0\bar{\nu}_e^2 < 1.1 \cdot 10^{-2}$	$P_F/P_{GT} = 1$
	P_{GT}	$(\lambda_0' - \eta_0)^2 < 7.5 \cdot 10^{-3}$		$(\lambda_0' - \eta_0)^2 \bar{\nu}_e^2 < 7.5 \cdot 10^{-3}$	$\bar{\nu}_{Me}^2 < 7.5 \cdot 10^{-3}$
	A(O)	$-1.0 \cdot 10^{-4} < a < 1.0 \cdot 10^{-2}$		$-1.0 \cdot 10^{-4} < a\bar{\nu}_e^2 < 1.0 \cdot 10^{-2}$	$\bar{\nu}_{Me}^2 < 1.0 \cdot 10^{-2}$
μ decay	ρ	$\eta_0^2 < 2.7 \cdot 10^{-3}$		$\eta_0^2 (\bar{\nu}_\mu^2 + \bar{\nu}_e^2) < 5.4 \cdot 10^{-3}$	$\bar{\nu}_{Me}^2 + \bar{\nu}_{M\mu}^2 < 5.4 \cdot 10^{-3}$
	C_μ	$(\lambda_0' - \eta_0)^2 + \lambda_0^2 < 1.7 \cdot 10^{-3}$		$(\lambda_0' - \eta_0)^2 \bar{\nu}_\mu^2 < 1.7 \cdot 10^{-3}$	$\bar{\nu}_{M\mu}^2 < 1.7 \cdot 10^{-3}$
	ξ'	$\lambda_0^2 + \eta_0^2 < 4.6 \cdot 10^{-2}$		$\eta_0^2 \bar{\nu}_\mu^2 < 4.6 \cdot 10^{-2}$	$\bar{\nu}_{M\mu}^2 < 4.6 \cdot 10^{-3}$
K decay	P_μ	$(\lambda_0'' - \eta_0)^2 < 6.2 \cdot 10^{-2}$		$(\lambda_0'' - \eta_0)^2 \bar{\nu}_\mu^2 < 6.2 \cdot 10^{-2}$	$\bar{\nu}_{M\mu}^2 < 6.2 \cdot 10^{-2}$

Table 10.1

Transition	$\beta^+\beta^+$ decay	β^+/EC decay	EC/EC decay
	T_0 (KeV)	T_1 (KeV)	T_2 (KeV)
$^{36}Ar \rightarrow {}^{36}S$			433.1 ± 0.4
$^{40}Ca \rightarrow {}^{40}Ar$			192.7 ± 0.6
$^{50}Cr \rightarrow {}^{50}Ti$		146.3 ± 1.6	1168.3 ± 1.6
$^{54}Fe \rightarrow {}^{54}Cr$			680.2 ± 0.7
$^{58}Ni \rightarrow {}^{58}Fe$		905.2 ± 0.7	1927.2 ± 0.7
$^{64}Zn \rightarrow {}^{64}Ni$		74.3 ± 0.9	1096.3 ± 0.9
$^{74}Se \rightarrow {}^{74}Ge$		186.3 ± 0.9	1208.3 ± 0.9
$^{78}Kr \rightarrow {}^{78}Se$	833 ± 8	1855 ± 8	2877 ± 8
$^{84}Sr \rightarrow {}^{84}Kr$		769 ± 4	1791 ± 4
$^{92}Mo \rightarrow {}^{92}Zr$		626 ± 4	1648 ± 4
$^{96}Ru \rightarrow {}^{96}Mo$	677 ± 8	1699 ± 8	2721 ± 8
$^{102}Pd \rightarrow {}^{102}Ru$		176 ± 4	1198 ± 4
$^{106}Cd \rightarrow {}^{106}Pd$	734 ± 8	1756 ± 8	2778 ± 8
$^{108}Cd \rightarrow {}^{108}Pd$			261 ± 6
$^{112}Sn \rightarrow {}^{112}Cd$		906 ± 5	1928 ± 5
$^{120}Te \rightarrow {}^{120}Sn$		700 ± 19	1722 ± 19
$^{124}Xe \rightarrow {}^{124}Te$	821.6 ± 2.4	1843.6 ± 2.4	2865.6 ± 2.4
$^{126}Xe \rightarrow {}^{126}Te$			905 ± 7
$^{130}Ba \rightarrow {}^{130}Xe$	538 ± 8	1560 ± 8	2582 ± 8
$^{132}Ba \rightarrow {}^{132}Xe$			836 ± 9
$^{136}Ce \rightarrow {}^{136}Ba$	366 ± 50	1388 ± 50	2410 ± 50
$^{138}Ce \rightarrow {}^{138}Ba$			701 ± 11
$^{152}Gd \rightarrow {}^{152}Sm$			54.0 ± 1.6
$^{156}Dy \rightarrow {}^{156}Gd$		989 ± 7	2011 ± 7
$^{158}Dy \rightarrow {}^{158}Gd$			283 ± 3
$^{162}Er \rightarrow {}^{162}Dy$		821.9 ± 2.7	1843.9 ± 2.7
$^{164}Er \rightarrow {}^{164}Dy$			24.5 ± 2.2
$^{168}Yb \rightarrow {}^{168}Er$		399 ± 4	1421 ± 4
$^{174}Hf \rightarrow {}^{174}Yb$		82 ± 3	1104 ± 3
$^{184}Os \rightarrow {}^{184}W$		431.3 ± 1.6	1453.3 ± 1.6
$^{196}Hg \rightarrow {}^{196}Pt$			820 ± 3

Table 11.1

	$\beta^+\beta^+$ decay	β^+/EC decay	EC/EC decay
^{50}Cr		$>3.5\cdot10^{14}$ (Bir) $>1.8\cdot10^{17}$ $(0^+\rightarrow0^+(0))$ (LBL)	
^{58}Ni		$>3.2\cdot10^{17}$ (Bir) $>6.2\cdot10^{19}$ $(0^+\rightarrow0^+)_{0\nu+2\nu}$ $>5.3\cdot10^{19}$ $(0^+\rightarrow2^+)_{0\nu+2\nu}$ (Was)	$>4\cdot10^{19}$ $(0^+\rightarrow2^+)$ $(\beta^+/EC+EC/EC)$ (Mil) $>2.1\cdot10^{19}$ $(0^+\rightarrow0^+,2^+)_{0\nu}$ (Was)
^{64}Zn		$>1.9\cdot10^{15}$ (Bir) $>8\cdot10^{15}$ (BCLP) $>2.3\cdot10^{18}$ $(0^+\rightarrow0^+(0))$ (LBL)	
^{92}Mo		$>5.6\cdot10^{14}$ (Bir) $>3.0\cdot10^{17}$ $(0^+\rightarrow0^+(0))$ (LBL)	$>(3-6)\cdot10^{18}$ (Mil)
^{96}Ru	$>3.1\cdot10^{16}$ $(0^+\rightarrow0^+(0))$ (LBL)	$>6.7\cdot10^{16}$ $(0^+\rightarrow0^+(0))$ $>6.0\cdot10^{16}$ $(0^+\rightarrow2^+(778))$ $>4.5\cdot10^{16}$ $(0^+\rightarrow0^+(1148))$ $>5.5\cdot10^{16}$ $(0^+\rightarrow2^+(1498))$ $>5.3\cdot10^{16}$ $(0^+\rightarrow2^+(1626))$ $>5.3\cdot10^{16}$ $(0^+\rightarrow4^+(1628))$ (LBL)	
^{106}Cd	$>6\cdot10^{16}$ (WRU) $>2.6\cdot10^{17}$ $(0^+\rightarrow0^+)_{0\nu+2\nu}$ $>2.2\cdot10^{17}$ $(0^+\rightarrow2^+)_{0\nu+2\nu}$ (Was)	$>5.7\cdot10^{17}$ $(0^+\rightarrow0^+)_{0\nu+2\nu}$ $>4.9\cdot10^{17}$ $(0^+\rightarrow2^+)_{0\nu+2\nu}$ (Was)	$>1.5\cdot10^{17}$ $(0^+\rightarrow0^+,2^+)_{0\nu}$ (Was)

Table 11.2

	$m_1 \neq m_2$					$m_1 \propto m_2$				
β	$-\pi/2$	- - -	0	- - -	$\pi/2$	$\pi/2$ or $-\pi/2$				
CP property	conserved opposite sign	violated	conserved same sign	violated	conserved opposite sign	conserved opposite CP sign				
θ	arbitrary					$-\pi/4$	- - -	0	- - -	$\pi/4$
$\nu_{\alpha L}$	Majorana neutrinos					KM Dirac neutrinos ($m_1=m_2$)	PD ν	two Majorana neutrinos	PD ν	KM Dirac neutrinos ($m_1=m_2$)
$L_e - L_\mu$	not conserved					conserved	not conserved			conserved
$(\beta\beta)_{0\nu}$	destructive	+	constructive	+	destructive	forbidden	+	allowed	+	forbidden
$\mu^- - e^+$	constructive	+	destructive	+	constructive	allowed	+	forbidden	+	allowed

Table 11.3

Models		Multiplets	Type of Mass term	No of Neutrinos	Parametrization
$SU(2)_L \times U(1)$	I	$\begin{pmatrix}\nu_L\\ \ell_L\end{pmatrix}_{(n)}$, $\ell_{R\,(n)}$	M	n	$\kappa = \eta = \lambda = 0$ for $j \leq n$
	II A	$\begin{pmatrix}\nu_L\\ \ell_L\end{pmatrix}_{(n)}$, $\ell_{R\,(n)}$, $\nu_{R\,(m)}$	D + M	n + m	$U_{ej} \sim O(1)$
	III Mirror	$\begin{pmatrix}\nu_L\\ \ell_L\end{pmatrix}_{(n)}$, $\begin{pmatrix}\tilde{N}_R\\ L_R\end{pmatrix}_{(n)}$, $\begin{matrix}\ell_R\\ L_L\end{matrix}_{(n)}$	D + M	2n	$\kappa = \lambda = 0$, $\eta = 1$
	IV A Mirror	$\begin{pmatrix}\nu_L\\ \ell_L\end{pmatrix}_{(n)}$, $\begin{pmatrix}\tilde{N}_R\\ L_R\end{pmatrix}_{(n)}$, $\begin{matrix}\ell_R\\ L_L\end{matrix}_{(n)}$, $\begin{matrix}\nu_R\\ \tilde{N}_L\end{matrix}_{(m)}$	D + M	2(n + m)	$U_{ej} \sim O(1)$, $V'_{ej} \sim O(\theta_M)$ for $j \leq n$
$SU(2)_L \times SU(2)_R \times U(1)$	II B	$\begin{pmatrix}\nu_L\\ \ell_L\end{pmatrix}_{(n)}$; $\begin{pmatrix}\nu_R\\ \ell_R\end{pmatrix}_{(n)}$	D + M	2n	$\kappa = \eta = \eta_0 \sim -\tan\zeta$, $\lambda = \lambda_0 \sim (M_{W_L}/M_{W_R})^2$ $U_{ej} = U'_{ej} \sim O(1)$, $V_{ej} = V'_{ej} \sim O(\theta_{LR})$ for $j \leq n$
	IV B Mirror	$\begin{pmatrix}\nu_L\\ \ell_L\end{pmatrix}_{(n)}$, $\begin{pmatrix}\tilde{N}_R\\ L_R\end{pmatrix}_{(n)}$; $\begin{pmatrix}\nu_R\\ \ell_R\end{pmatrix}_{(n)}$, $\begin{pmatrix}\tilde{N}_L\\ L_L\end{pmatrix}_{(n)}$	D + M	4n	$U_{ej} \sim O(1)$, $\eta V'_{ej} \sim O(\theta_M, \eta_0\,\theta_{LR})$ $\kappa U_{ej} \sim O(\eta_0)$, $\lambda V_{ej} \sim O(\eta_0\,\theta_M, \lambda_0\,\theta_{LR})$ for $j \leq n$

Table A.1.

transition / nuclear operator	$0^+ \to 0^+$	$0^+ \to 1^+$	$0^+ \to 2^+$
$X_{+2\nu}$	$K_a + L_a$	——	——
$Y^{\ell}_{+2\nu}$	——	$K_{a-} + L_{a-}$ vanish by closure	——
$X_{-2\nu}$	$K_a - L_a$	——	——
$Y^{\ell}_{-2\nu}$	——	$K_{a-} - L_{a-}$ vanish by closure	——
$X^{k\ell}_{2\nu}$	$K_a - L_a$	$K_a - L_a$	$K_a - L_a$

Table B.1

Case	Two electron system	Two neutrino system	Order of magnitude of amplitude	
			Combination of energy denominator	lepton wave func.
1	S - S	S - S	$(K_a-L_a)\ \mu_a \simeq 2\mu_a^{-2}$	1
2	S - $P_{1/2}$	S - P	$(K_a+L_a)\ \mu_a \simeq 4$	$\alpha Z\,(\frac{r}{R})^2\,(pR)$
3	S - $D_{3/2}$	S - S		
4	$P_{1/2}$ - $P_{3/2}$	S - S		
5	$P_{1/2}$ - $P_{1/2}$	S - S	$(K_a-L_a)\ \mu_a \simeq 2\mu_a^{-2}$	$(\alpha Z)^2(\frac{r}{R})^2$
6	S - $P_{1/2}$	S - S	$(K_a+L_a)\ \mu_a \simeq 4$	$\alpha Z\,(\frac{r}{R})(\frac{Q}{2M})$
7	S - $P_{3/2}$	S - S		$(\frac{r}{R})(pR)(\frac{Q}{2M})$

Table B.2

Nuclear Operators	Parity	Partial Waves of Two Electrons									
		S - S	S - $P_{1/2}$	$P_{1/2}$ - $P_{1/2}$	S - $P_{3/2}$	S - $D_{3/2}$	$P_{1/2}$ - $P_{3/2}$				
X_{1S}	even	$0^+ \to 0^+$ h_+	———	$0^+ \to 0^+, 1^+$ $(\frac{\alpha Z}{2})^2 (\frac{\pi}{R})^2 h_+$	———	$0^+ \to 1^+, 2^+$ $(\frac{3\alpha Z}{10})(\frac{\pi}{R})^2 h_+$	$0^+ \to 1^+, 2^+$ $(\frac{\alpha Z}{2})(\frac{\pi}{R})^2 (pR) h_+$				
X_{1R}	odd	———	$0^+ \to 1^+$	———	$0^+ \to 1^+$	———	———				
Y^{λ}_{1V}	even	$0^+ \to 1^+$ $\frac{1}{2\sqrt{\pi}} \varepsilon_{12} R h_-$ vanish by closure	———	$0^+ \to 0^+, 1^+$ $(\frac{\alpha Z}{2})^2 (\frac{\pi}{R})^2 h_+$	———	$0^+ \to 1^+, 2^+$ $(\frac{3\alpha Z}{10})(\frac{\pi}{R})^2 h_+$	$0^+ \to 1^+, 2^+$ $(\frac{\alpha Z}{2})(\frac{\pi}{R})^2 (pR) h_+$				
Y^{λ}_{1R}	odd	———	$0^+ \to 0^+, 1^+$ $2\alpha Z (\frac{\pi}{R})(\frac{Q}{2M}) h_+$	———	$0^+ \to 1^+, 2^+$ $\frac{1}{3}(pR)(\frac{\pi}{R})(\frac{Q}{2M}) h_+$	———	———				

Table C.1

Table C.2

Nuclear Operator	Parity	Partial Waves of Two Electrons									
		S - S	S - $P_{1/2}$	$P_{1/2}$ - $P_{1/2}$	S - $P_{3/2}$	S - $D_{3/2}$	$P_{1/2}$ - $P_{3/2}$				
u only											
X^{λ}_{5R} $(\frac{r^{\lambda}}{R} \cdot \hat{r}_{5R})$	odd	———	$0^+ \to 1^+$	———	$0^+ \to 0^+, 1^+$ (z_6)	———	$0^+ \to 1^+, 2^+$ (z_{22})				
X^{λ}_{5} $(\frac{r^{\lambda}}{R} \cdot \hat{r}_{5R})(\frac{r^{\lambda}}{R} \cdot \hat{r}_{6R})$	even	$0^+ \to 1^+$	———	$0^+ \to 0^+, 1^+$ (z_7)	———	$0^+ \to 1^+, 2^+$	$0^+ \to 1^+, 2^+$				
X^{λ}_{5R} $(\frac{r^{\lambda}}{R} \cdot \hat{r}_{5R})$	even	$0^+ \to 0^+$ (z_4)	———	$0^+ \to 0^+, 1^+$	———	$0^+ \to 1^+, 2^+$	$0^+ \to 1^+, 2^+$				
X_{5R} $(\frac{r^{\lambda}}{R} \cdot \hat{r}_{5R})$	odd	———	$0^+ \to 1^+$	———	$0^+ \to 1^+$	———	———				
u and v											
X_3 $(\frac{r^{\lambda}}{R} \cdot \hat{r}_{3R})$	even	$0^+ \to 0^+$ (z_3)	———	$0^+ \to 0^+, 1^+$	———	$0^+ \to 1^+, 2^+$	$0^+ \to 1^+, 2^+$				
Y_{3R} $(\frac{r^{\lambda}}{R} \cdot \hat{r}_3)$	odd	———	$0^+ \to 1^+$	———	$0^+ \to 1^+$	———	———				
X^{λ}_{4R} $(\frac{r^{\lambda}}{R} \cdot \hat{r}^{\lambda}_4)$	odd	———	———	$0^+ \to 0^+, 1^+$ (z_5)	———	$0^+ \to 1^+, 2^+$ (z_{21})	———				
Y^{λ}_{4} $(\frac{r^{\lambda}}{R} \cdot \hat{r}^{\lambda}_{4R})$	even	$0^+ \to 1^+$	———	$0^+ \to 0^+, 1^+$	———	$0^+ \to 1^+, 2^+$	$0^+ \to 1^+, 2^+$				

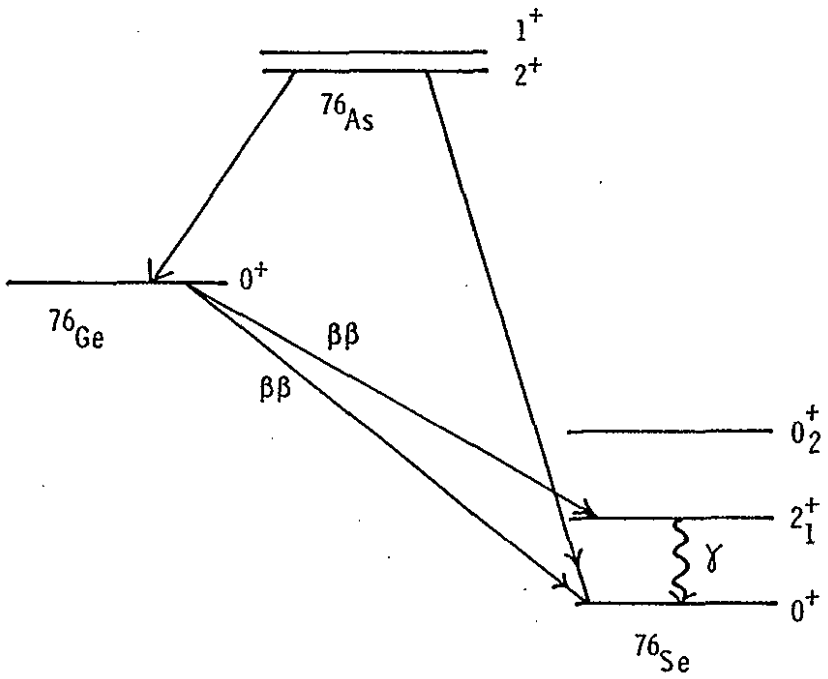

Fig. 1.1

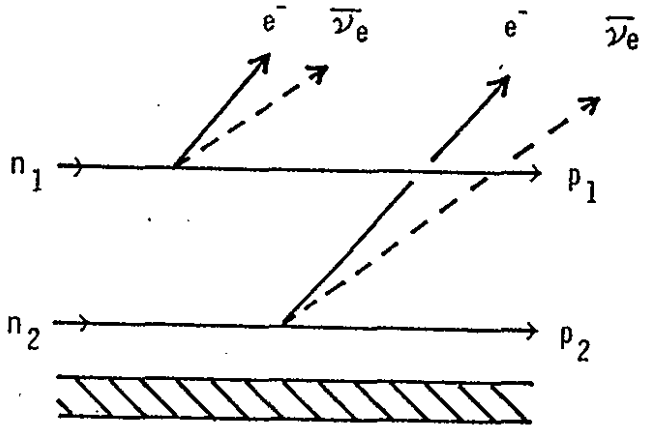

Fig. 1.2

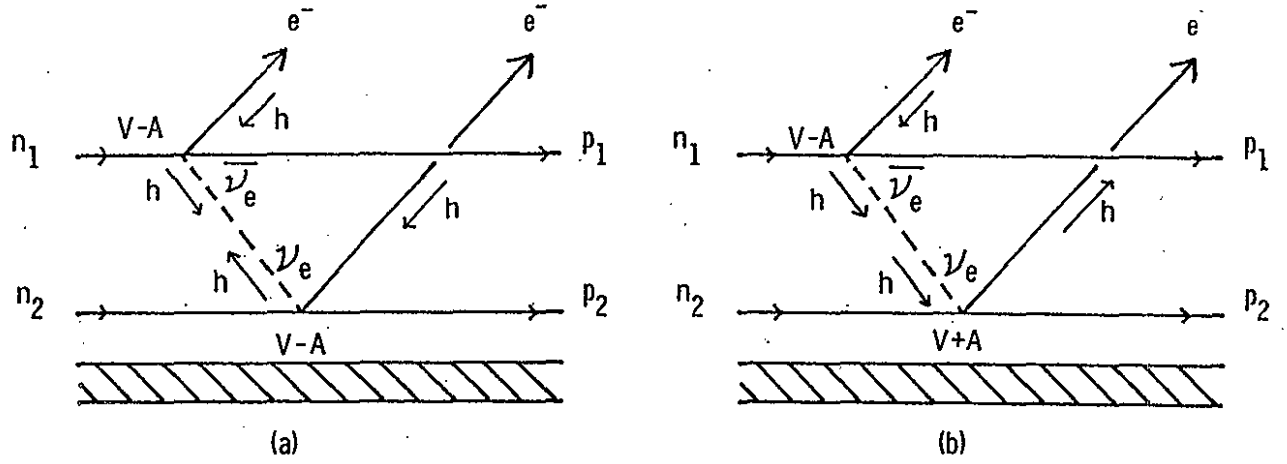
e⁻
e⁻
V-A
h
n1
p1
h
ν̄e
h
h
νe
n2
p2
V-A
(a)
e⁻
e
V-A
h
n1
p1
h
ν̄e
h
h
νe
n2
p2
V+A
(b)

Fig. 1.3

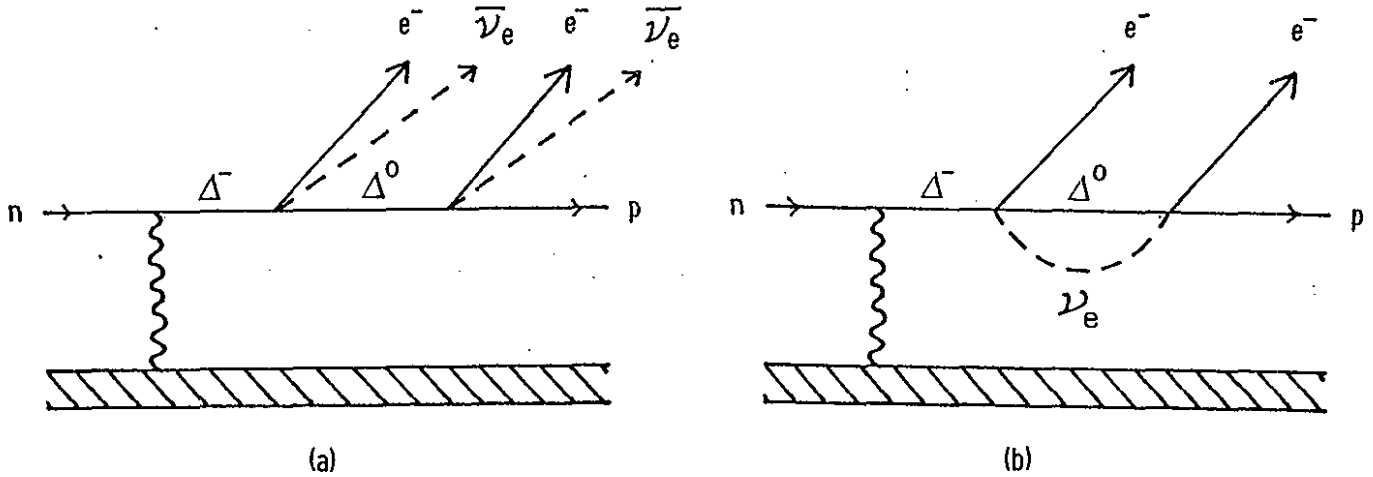
e⁻
ν̄e
e⁻
ν̄e
Δ⁻
Δ⁰
n
p
(a)
e⁻
e⁻
Δ⁻
Δ⁰
n
p
νe
(b)

Fig. 1.4

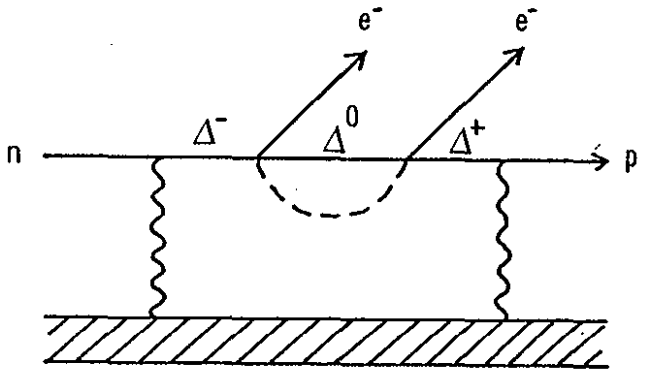

Fig. 1.5

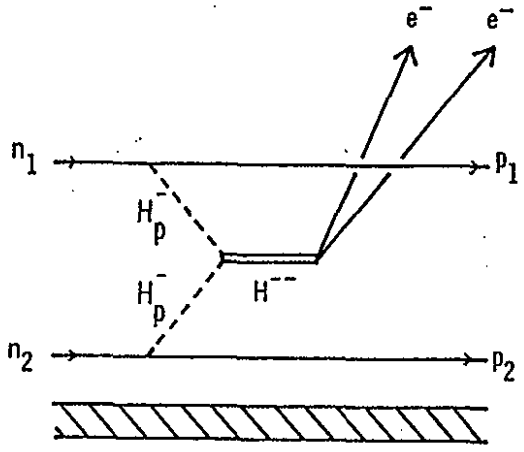

Fig. 1.6

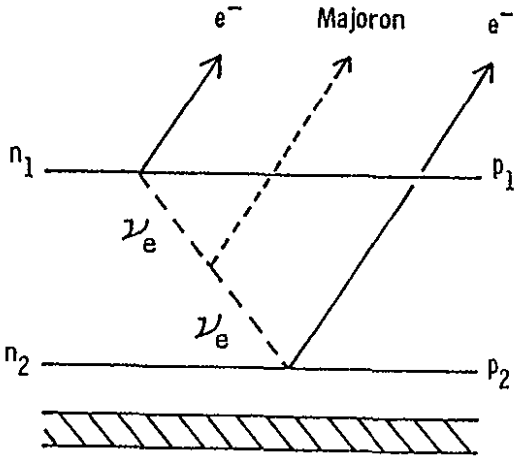

Fig. 1.7

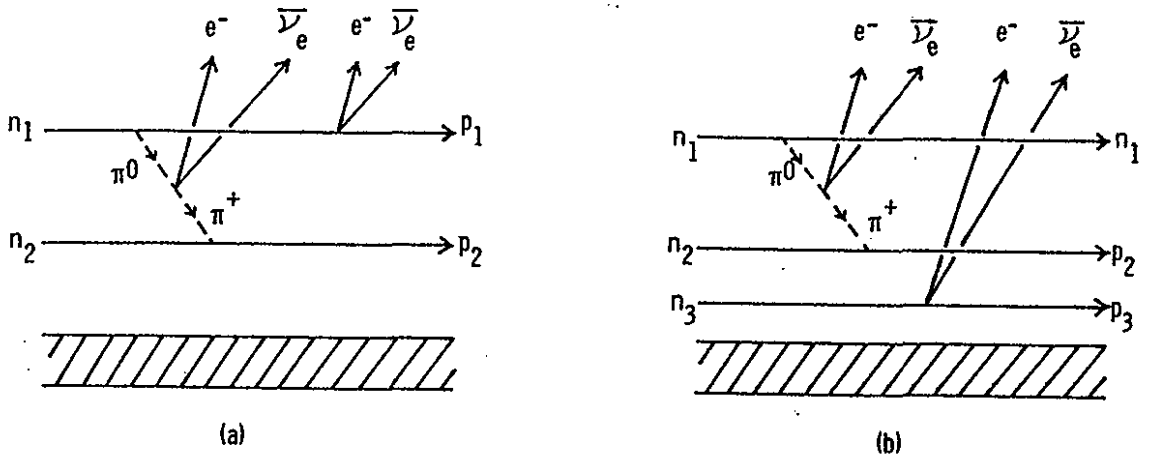
e⁻
ν̄e
e⁻
ν̄e
n1
p1
π0
π+
n2
p2
(a)
e⁻
ν̄e
e⁻
ν̄e
n1
n1
π0
π+
n2
p2
n3
p3
(b)

Fig. 3.1

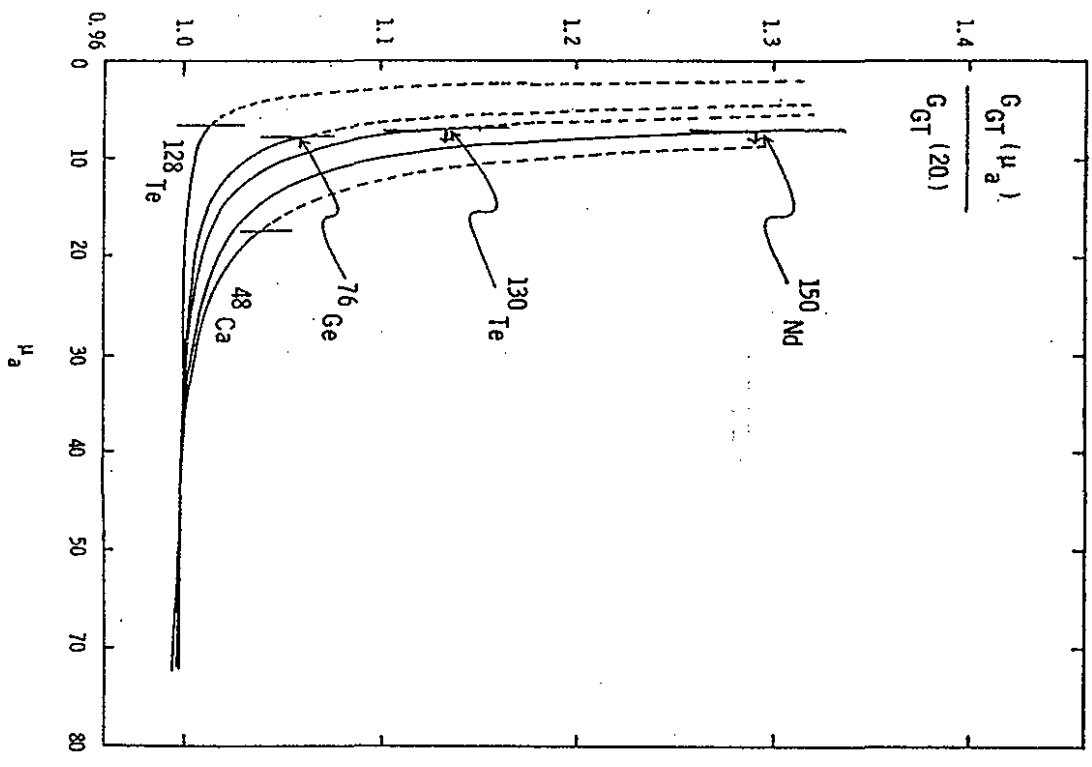
0.96
1.0
1.1
1.2
1.3
1.4
0
10
20
30
40
50
70
80
μa
GGT (μa) / GGT (20)
128 Te
48 Ca
76 Ge
130 Te
150 Nd

Fig. 3.2

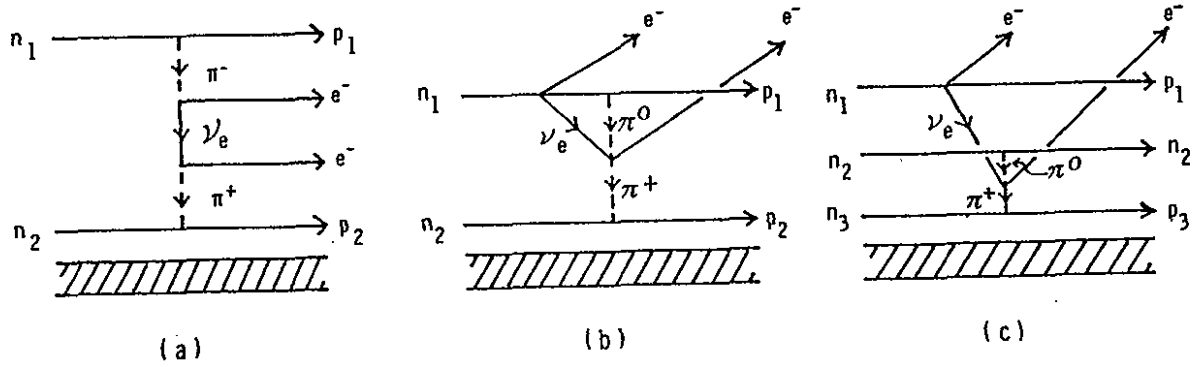
n1
p1
π⁻
e⁻
νe
e⁻
π⁺
n2
p2
(a)
e⁻
e⁻
n1
p1
νe
π⁰
π+
n2
p2
(b)
e⁻
e⁻
n1
p1
νe
n2
n2
π⁰
π⁺
n3
p3
(c)

Fig. 3.3

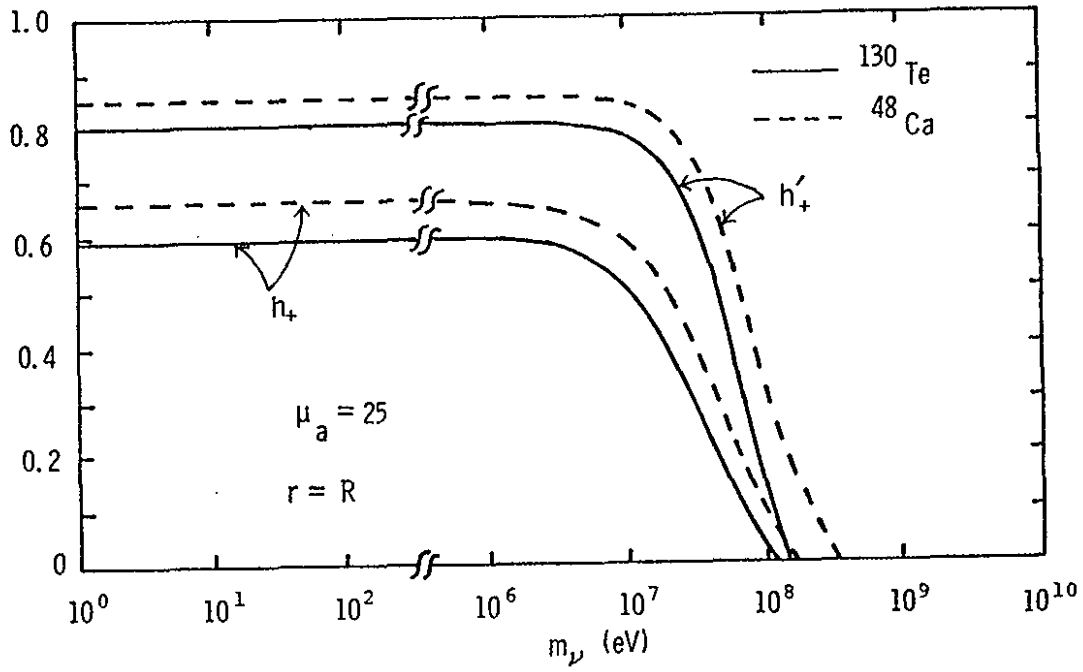
1.0
0.8
0.6
0.4
0.2
0
130 Te
48 Ca
h'+
h+
μa = 25
r = R
10⁰
10¹
10²
10⁶
10⁷
10⁸
10⁹
10¹⁰
mν (eV)

Fig. 3.4

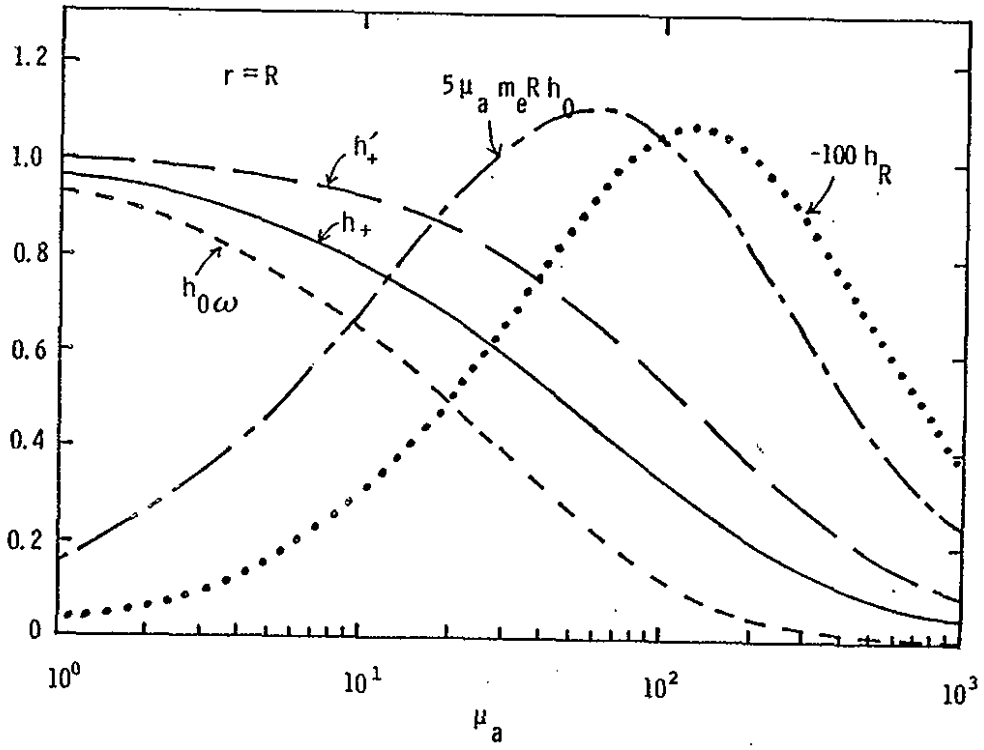
r = R
$5\mu_a m_e R h_0$
h'_+
h_+
$h_{0\omega}$
$-100\, h_R$
1.2
1.0
0.8
0.6
0.4
0.2
0
10^0
10^1
10^2
10^3
μ_a

Fig. 3.5

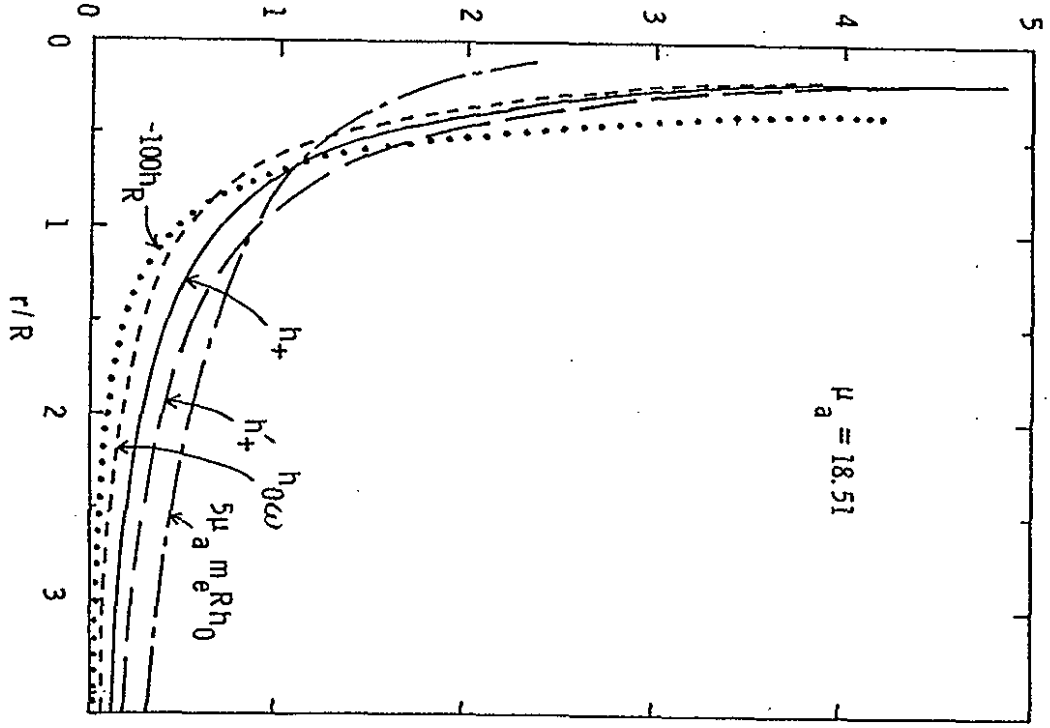
0
1
2
3
4
5
r/R
$-100h_R$
h_+
h'_+
$h_{0\omega}$
$5\mu_a m_e R h_0$
$\mu_a = 18.51$

Fig. 3.6

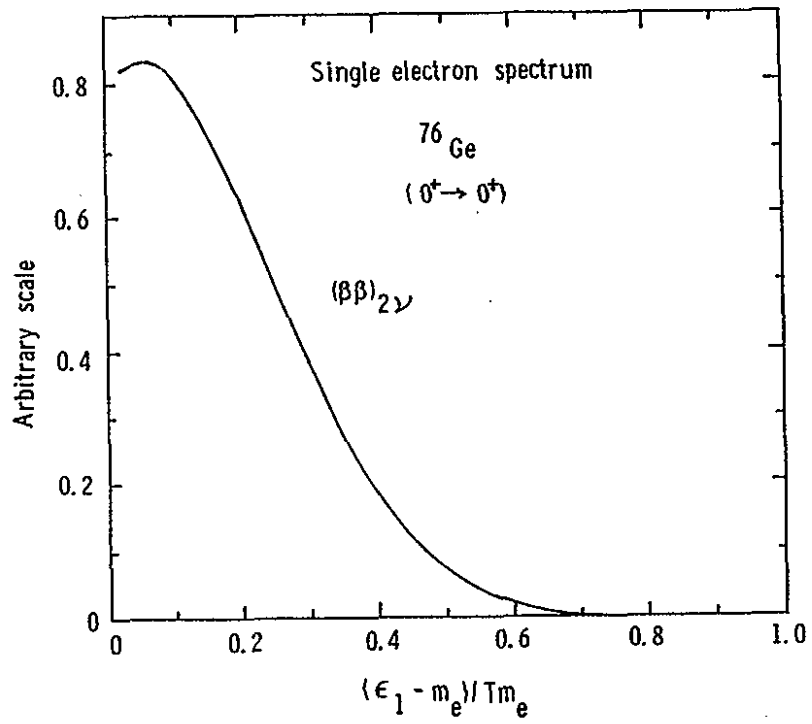
Single electron spectrum
^{76}Ge
$(0^+ \rightarrow 0^+)$
$(\beta\beta)_{2\nu}$
Arbitrary scale
0.8
0.6
0.4
0.2
0
0
0.2
0.4
0.6
0.8
1.0
$(\epsilon_1 - m_e)/Tm_e$

Fig. 6.1

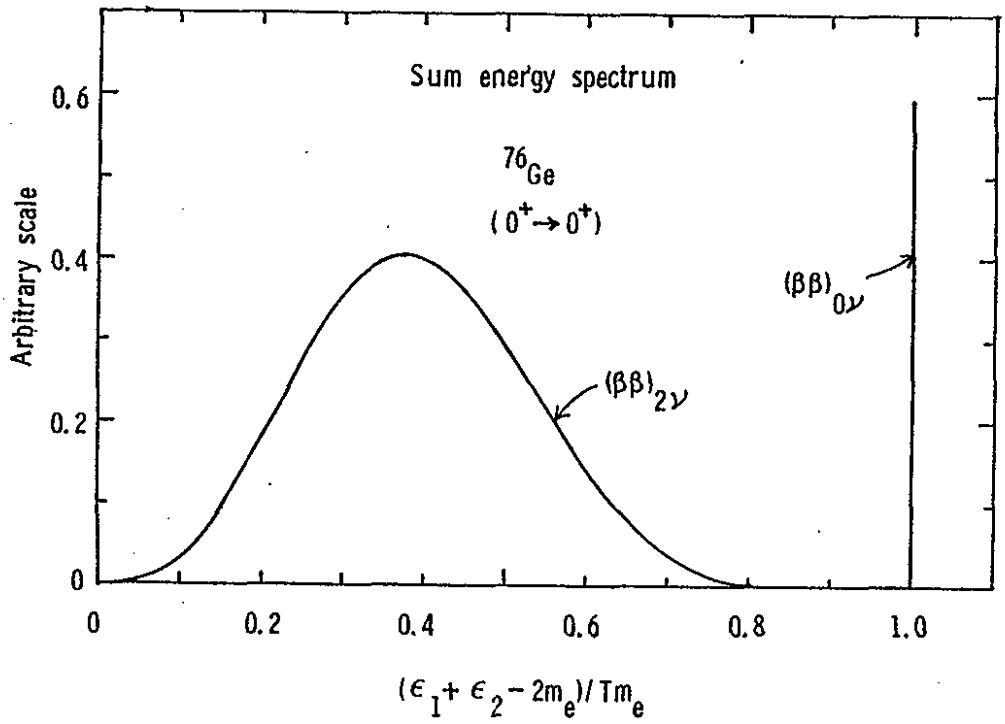
Sum energy spectrum
^{76}Ge
$(0^+ \rightarrow 0^+)$
$(\beta\beta)_{0\nu}$
$(\beta\beta)_{2\nu}$
Arbitrary scale
0.6
0.4
0.2
0
0
0.2
0.4
0.6
0.8
1.0
$(\epsilon_1 + \epsilon_2 - 2m_e)/Tm_e$

Fig. 6.2

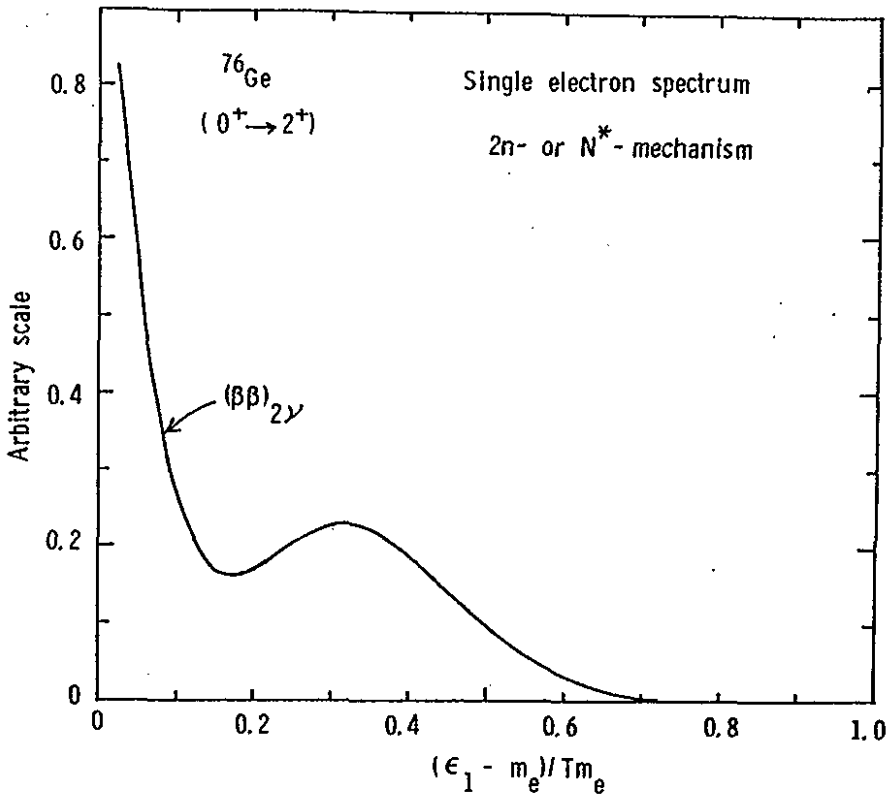
^{76}Ge
$(0^+ \rightarrow 2^+)$
Single electron spectrum
2n- or N*- mechanism
$(\beta\beta)_{2\nu}$
Arbitrary scale
0.8
0.6
0.4
0.2
0
0
0.2
0.4
0.6
0.8
1.0
$(\epsilon_1 - m_e)/Tm_e$

Fig. 6.3

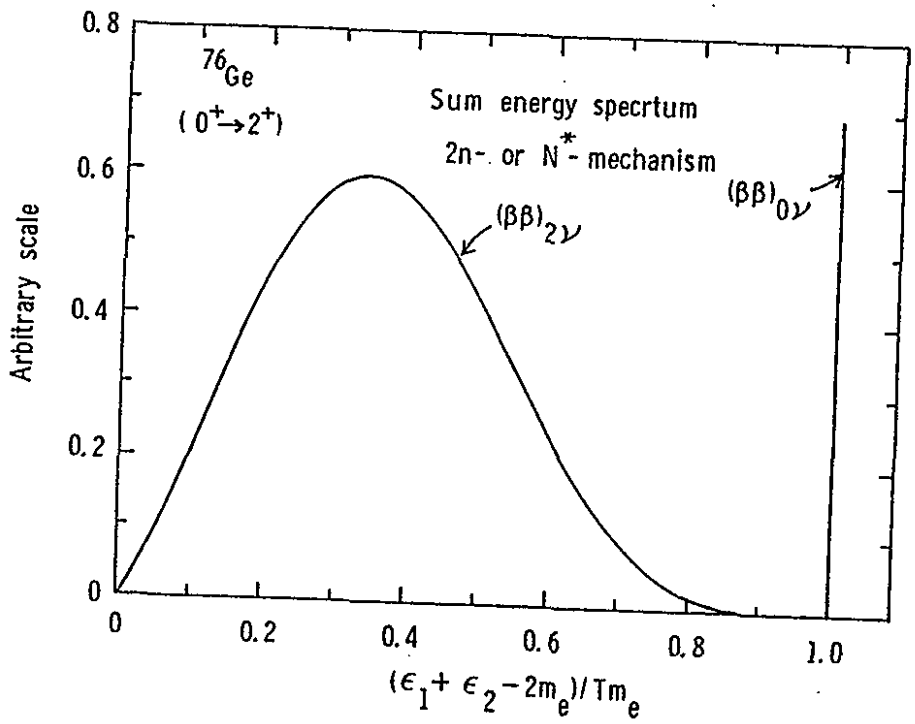
^{76}Ge
$(0^+ \rightarrow 2^+)$
Sum energy specrtum
2n- or N*- mechanism
$(\beta\beta)_{2\nu}$
$(\beta\beta)_{0\nu}$
Arbitrary scale
0.8
0.6
0.4
0.2
0
0
0.2
0.4
0.6
0.8
1.0
$(\epsilon_1 + \epsilon_2 - 2m_e)/Tm_e$

Fig. 6.4

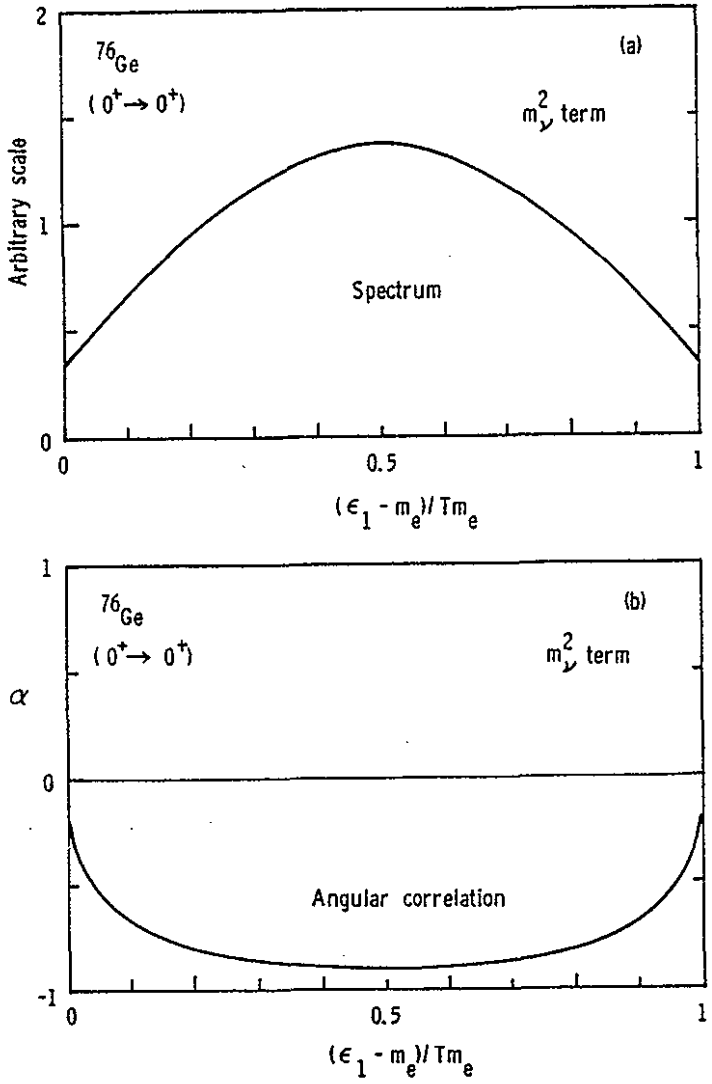
(a)
^{76}Ge
($0^+ \rightarrow 0^+$)
m_ν^2 term
Spectrum
Arbitrary scale
2
1
0
0
0.5
1
$(\epsilon_1 - m_e)/Tm_e$
(b)
^{76}Ge
($0^+ \rightarrow 0^+$)
m_ν^2 term
Angular correlation
α
1
0
-1
0
0.5
1
$(\epsilon_1 - m_e)/Tm_e$

Fig. 6.5

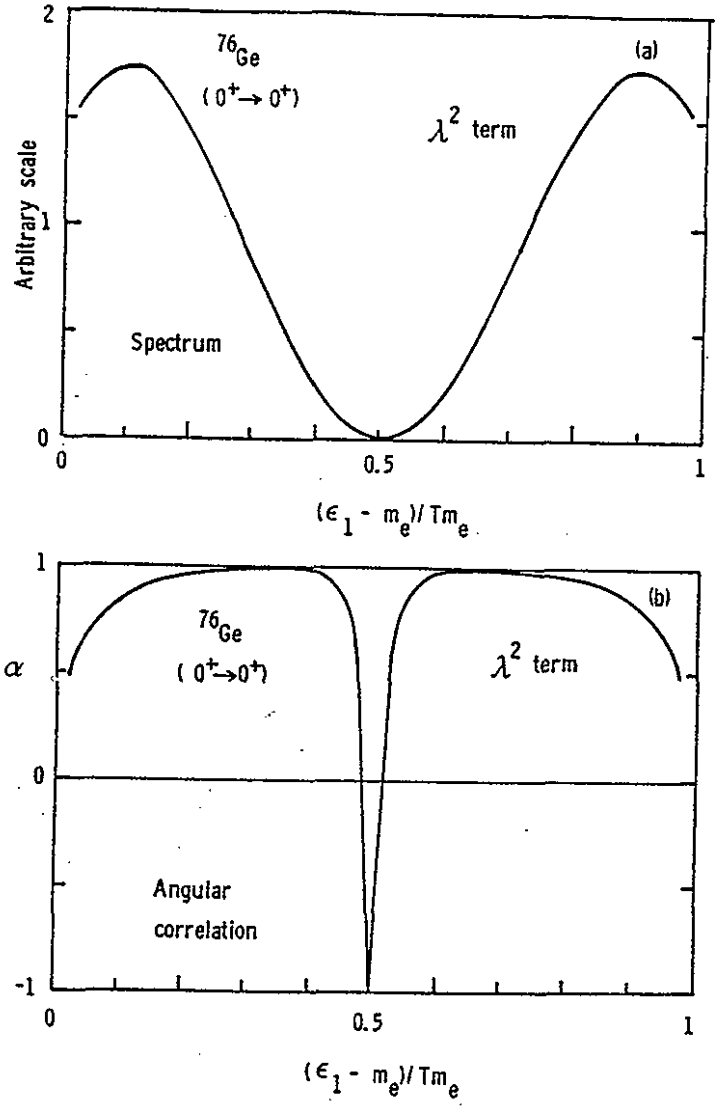
(a)
^{76}Ge
($0^+ \rightarrow 0^+$)
λ^2 term
Spectrum
Arbitrary scale
2
1
0
0
0.5
1
$(\epsilon_1 - m_e)/Tm_e$
(b)
^{76}Ge
($0^+ \rightarrow 0^+$)
λ^2 term
Angular correlation
α
1
0
-1
0
0.5
1
$(\epsilon_1 - m_e)/Tm_e$

Fig. 6.6

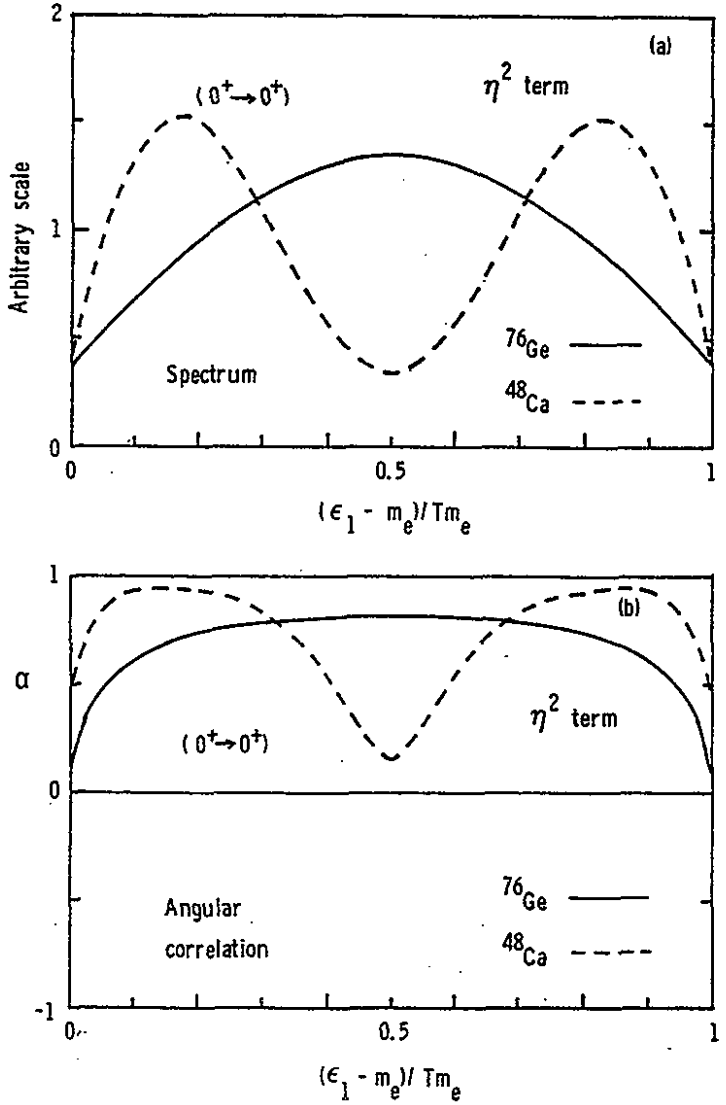
(a)
$(0^+ \rightarrow 0^+)$
η^2 term
Arbitrary scale
Spectrum
^{76}Ge
^{48}Ca
$(\epsilon_1 - m_e)/Tm_e$
(b)
α
$(0^+ \rightarrow 0^+)$
η^2 term
Angular correlation
^{76}Ge
^{48}Ca
$(\epsilon_1 - m_e)/Tm_e$

Fig. 6.7

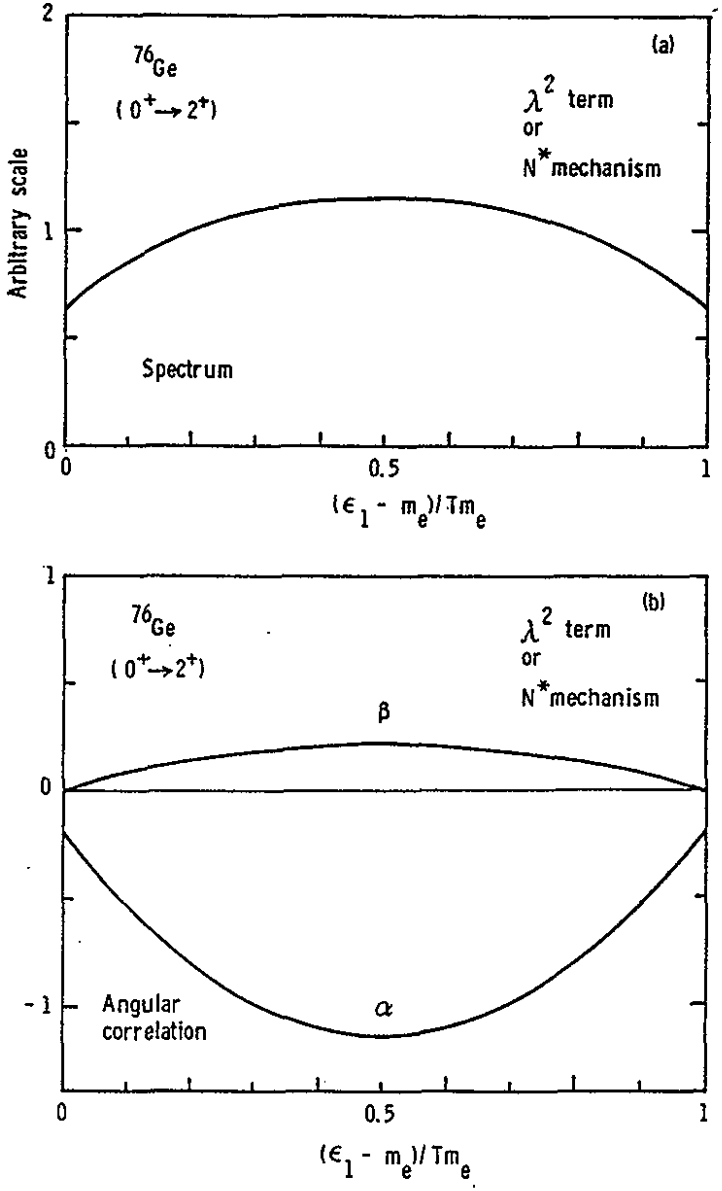
(a)
^{76}Ge
$(0^+ \rightarrow 2^+)$
λ^2 term
or
N^*mechanism
Arbitrary scale
Spectrum
$(\epsilon_1 - m_e)/Tm_e$
(b)
^{76}Ge
$(0^+ \rightarrow 2^+)$
λ^2 term
or
N^*mechanism
β
α
Angular correlation
$(\epsilon_1 - m_e)/Tm_e$

Fig. 6.8

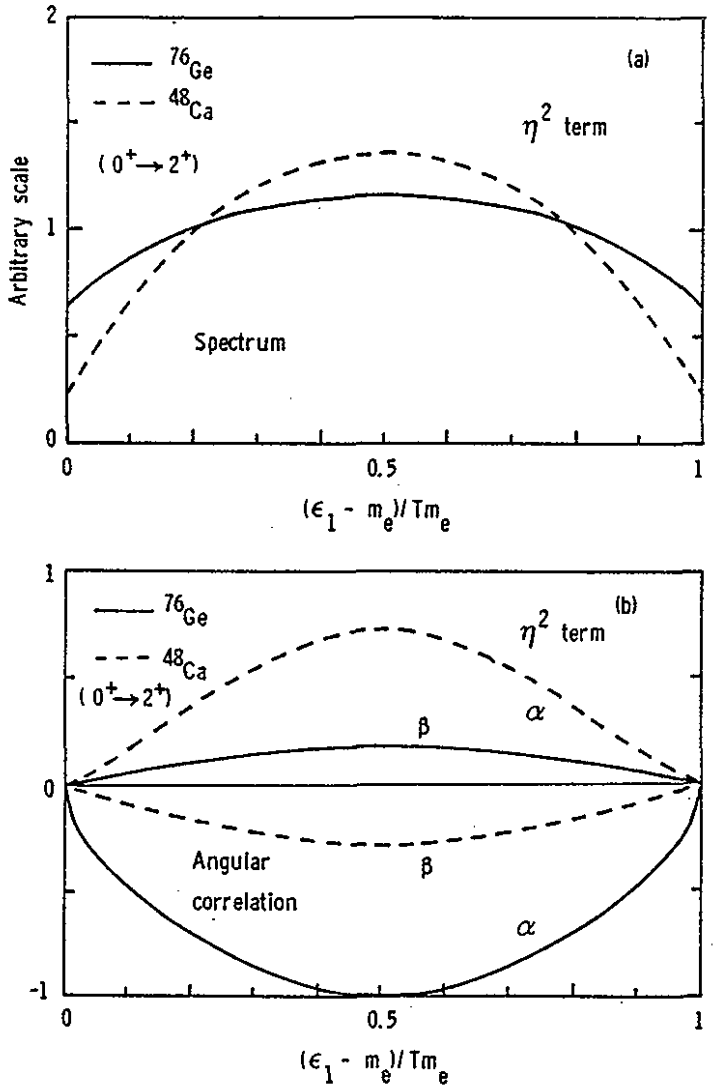

Fig. 6.9

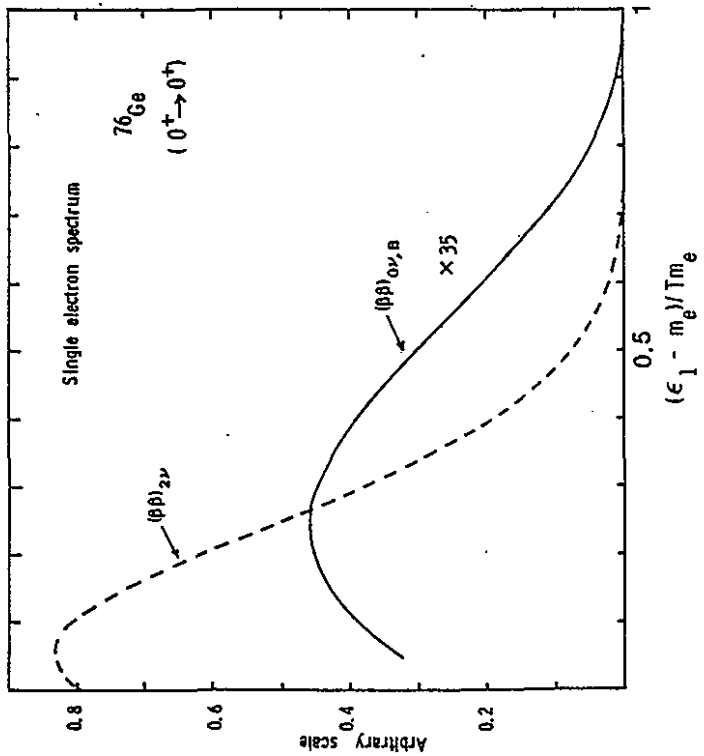

Fig. 6.10

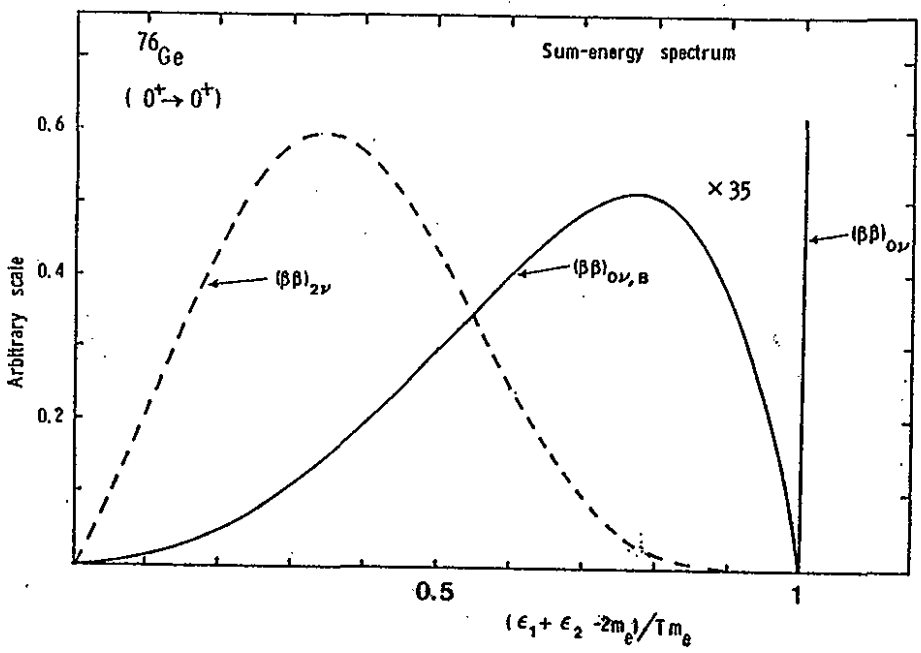

Fig. 6.11

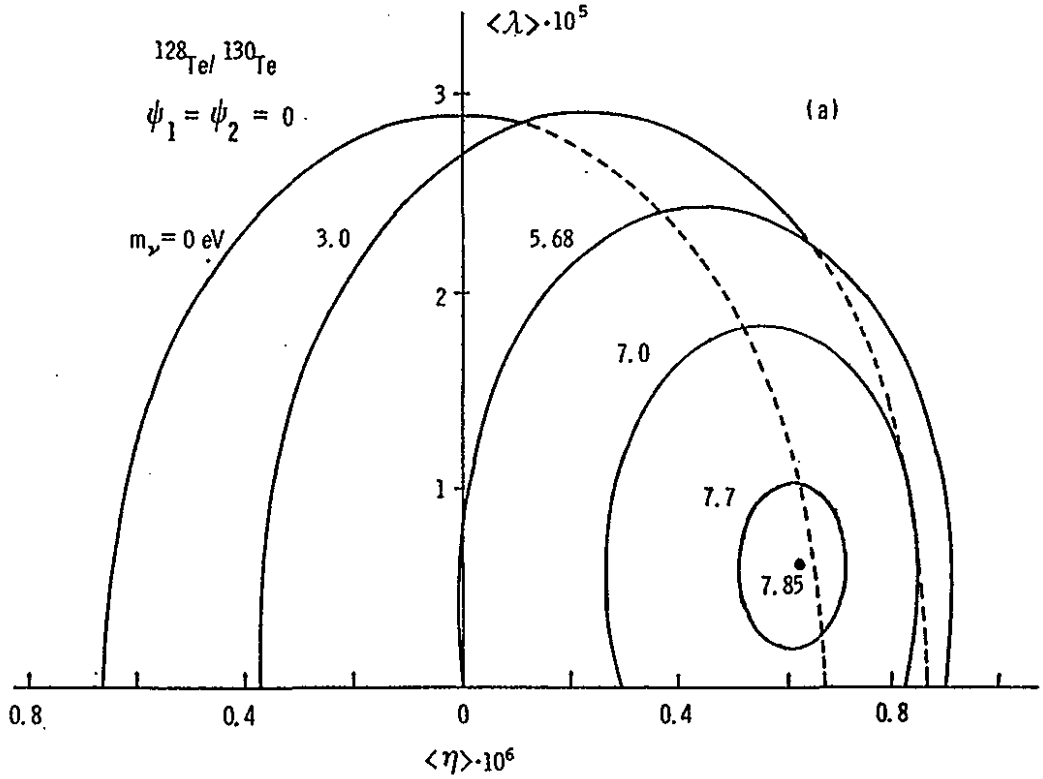

Fig. 8.1

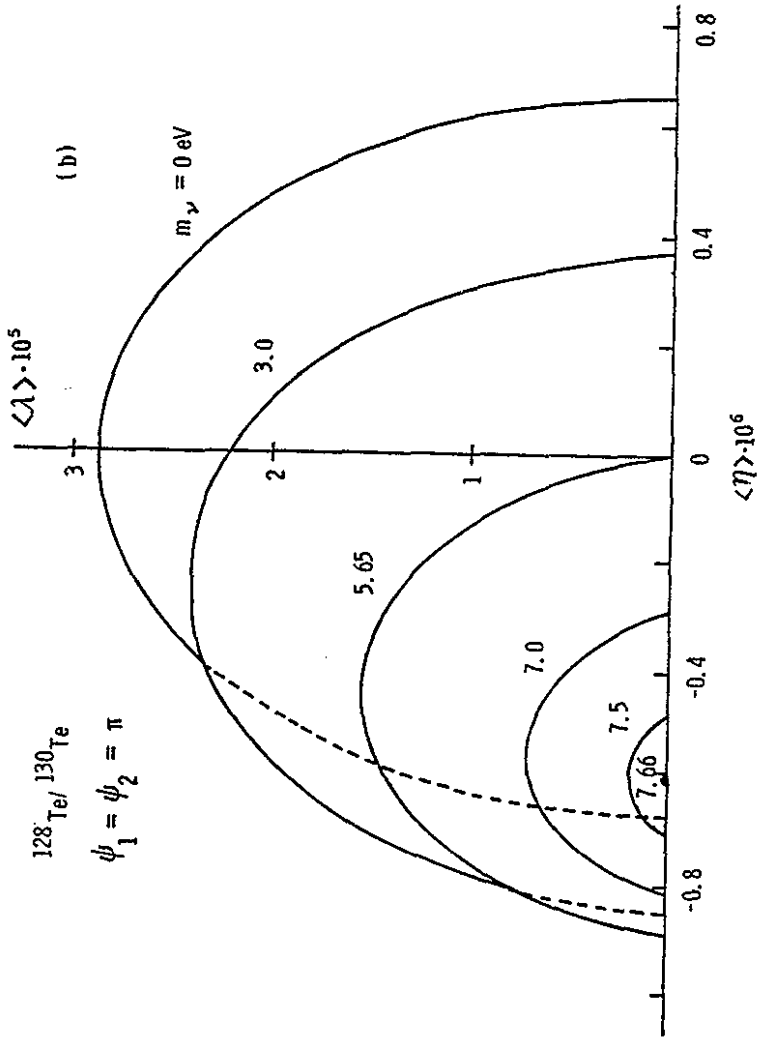
(b)
m_ν = 0 eV
3.0
5.65
7.0
7.5
7.66
$\langle\lambda\rangle\cdot10^5$
$\langle\eta\rangle\cdot10^6$
3
2
1
0
0.8
0.4
-0.4
-0.8
$^{128}Te/^{130}Te$
$\psi_1 = \psi_2 = \pi$

Fig. 8.1

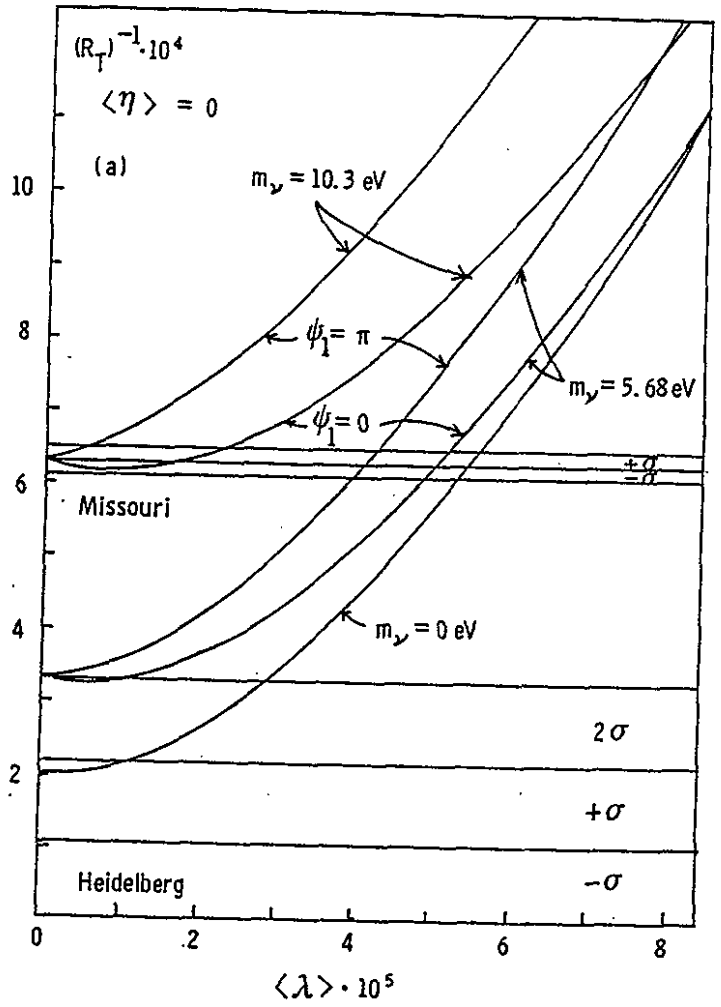
$(R_T)^{-1}\cdot10^4$
$\langle\eta\rangle$ = 0
(a)
m_ν = 10.3 eV
$\psi_1 = \pi$
$\psi_1 = 0$
m_ν = 5.68 eV
$\pm\sigma$
Missouri
m_ν = 0 eV
2σ
$+\sigma$
Heidelberg
$-\sigma$
10
8
6
4
2
0
2
4
6
8
$\langle\lambda\rangle\cdot10^5$

Fig. 8.2

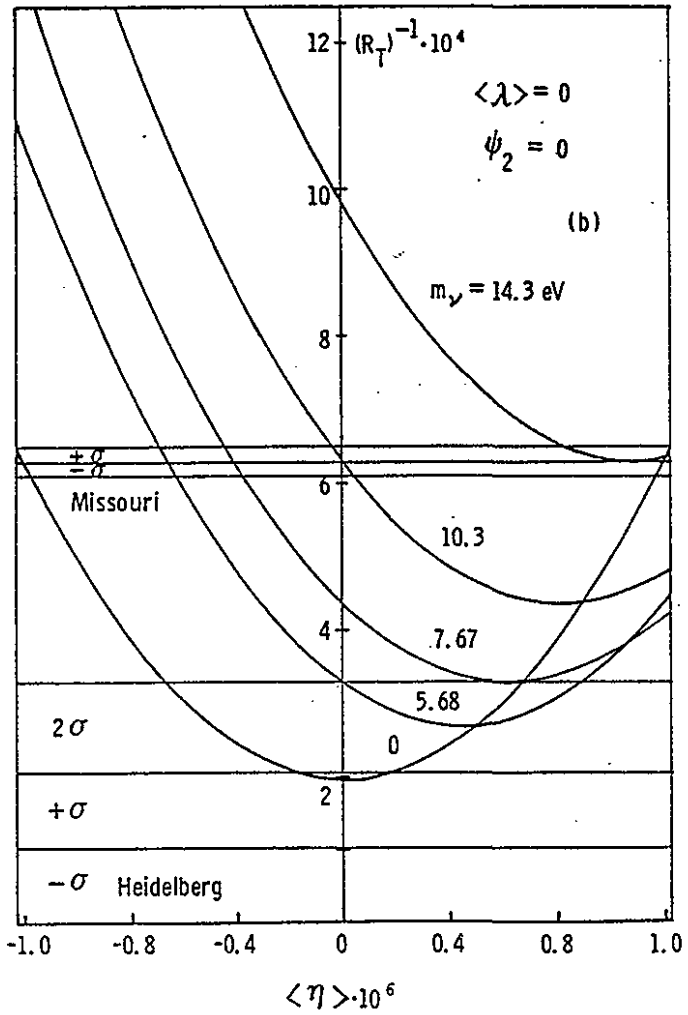
12
$(R_T)^{-1}\cdot 10^4$
$\langle\lambda\rangle = 0$
$\psi_2 = 0$
10
(b)
$m_\nu = 14.3$ eV
8
$\pm\sigma$
$\pm\sigma$
Missouri
6
10.3
4
7.67
5.68
2σ
0
$+\sigma$
2
$-\sigma$
Heidelberg
-1.0
-0.8
-0.4
0
0.4
0.8
1.0
$\langle\eta\rangle\cdot 10^6$

Fig. 8.2

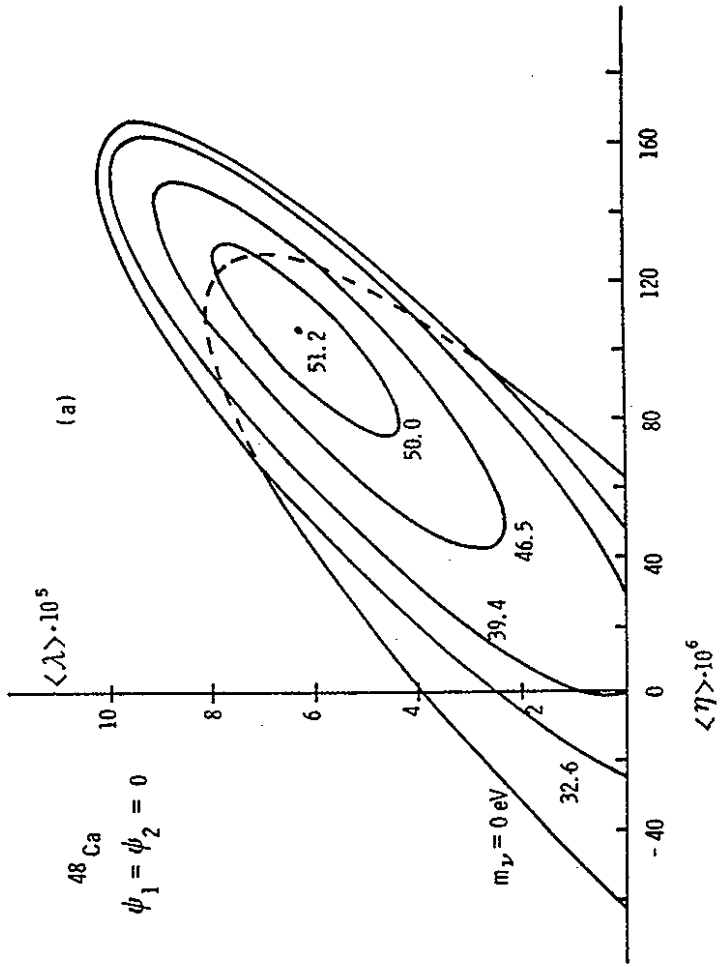
(a)
51.2
50.0
46.5
39.4
32.6
$m_\nu = 0$ eV
^{48}Ca
$\psi_1 = \psi_2 = 0$
$\langle\lambda\rangle\cdot 10^5$
10
8
6
4
2
0
$\langle\eta\rangle\cdot 10^6$
160
120
80
40
-40

Fig. 8.3

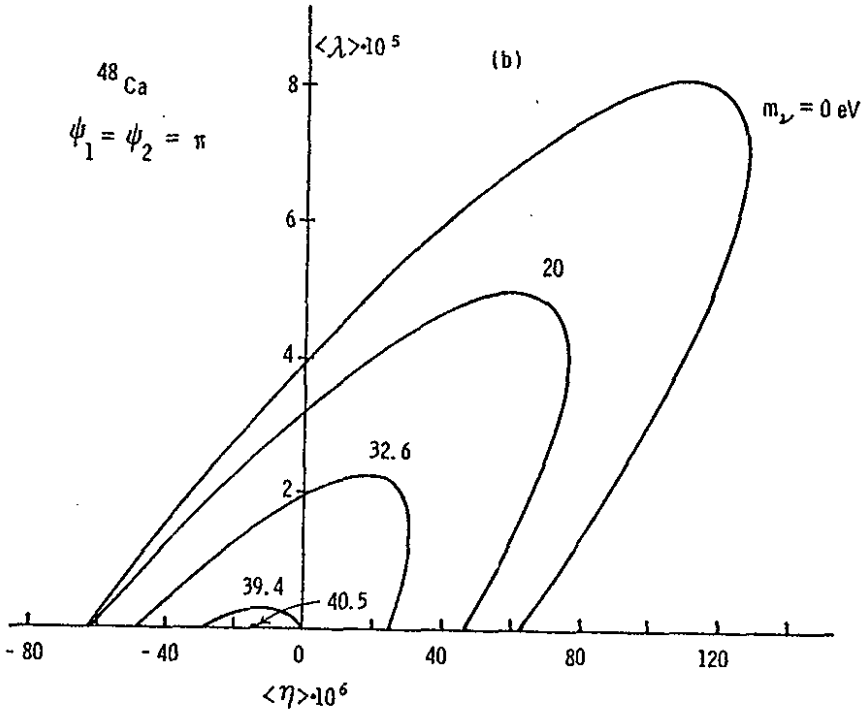
$\langle\lambda\rangle\cdot10^5$
(b)
^{48}Ca
$\psi_1 = \psi_2 = \pi$
$m_\nu = 0$ eV
20
32.6
39.4
40.5
8
6
4
2
-80
-40
0
40
80
120
$\langle\eta\rangle\cdot10^6$

Fig. 8.3

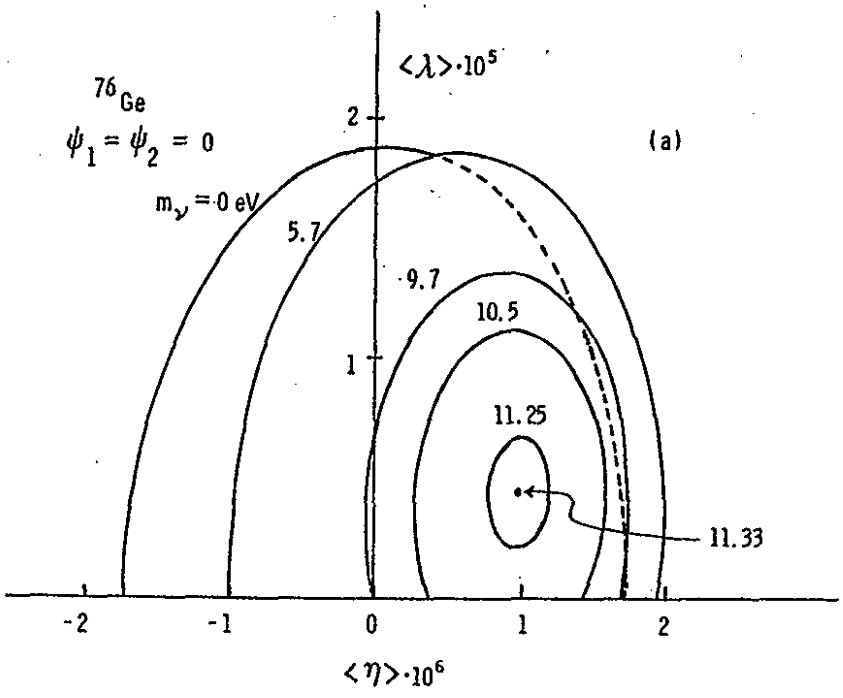
$\langle\lambda\rangle\cdot10^5$
^{76}Ge
$\psi_1 = \psi_2 = 0$
(a)
$m_\nu = 0$ eV
5.7
9.7
10.5
11.25
11.33
2
1
-2
-1
0
1
2
$\langle\eta\rangle\cdot10^6$

Fig. 8.4

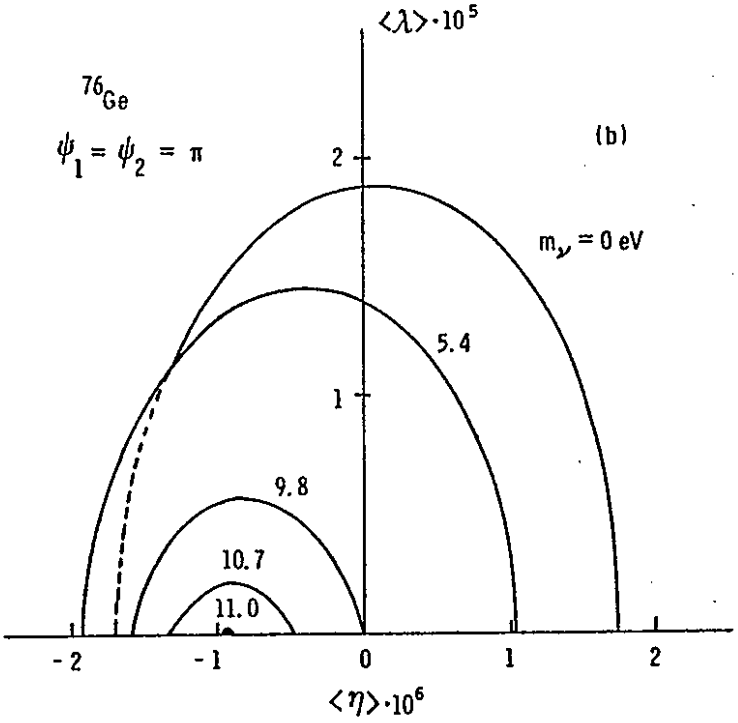
$\langle\lambda\rangle\cdot10^5$
^{76}Ge
$\psi_1 = \psi_2 = \pi$
(b)
$m_\nu = 0$ eV
5.4
9.8
10.7
11.0
2
1
-2
-1
0
1
2
$\langle\eta\rangle\cdot10^6$

Fig. 8.4

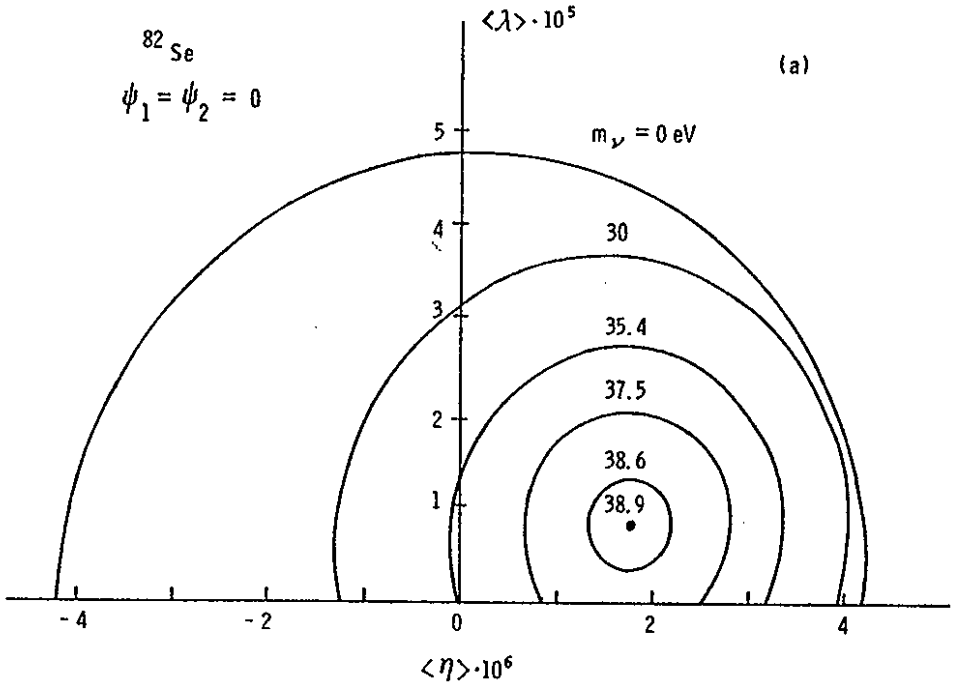
$\langle\lambda\rangle\cdot10^5$
^{82}Se
$\psi_1 = \psi_2 = 0$
(a)
$m_\nu = 0$ eV
30
35.4
37.5
38.6
38.9
5
4
3
2
1
-4
-2
0
2
4
$\langle\eta\rangle\cdot10^6$

Fig. 8.5

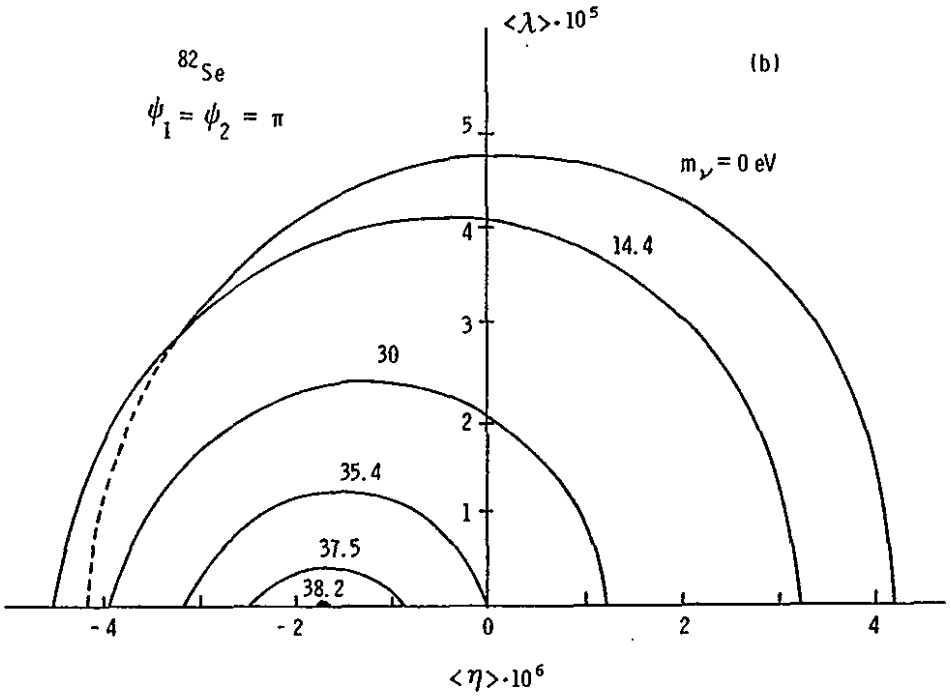
$\langle\lambda\rangle\cdot 10^5$
^{82}Se
$\psi_1 = \psi_2 = \pi$
(b)
$m_\nu = 0$ eV
14.4
30
35.4
37.5
38.2
5
4
3
2
1
-4
-2
0
2
4
$\langle\eta\rangle\cdot 10^6$

Fig. 8.5

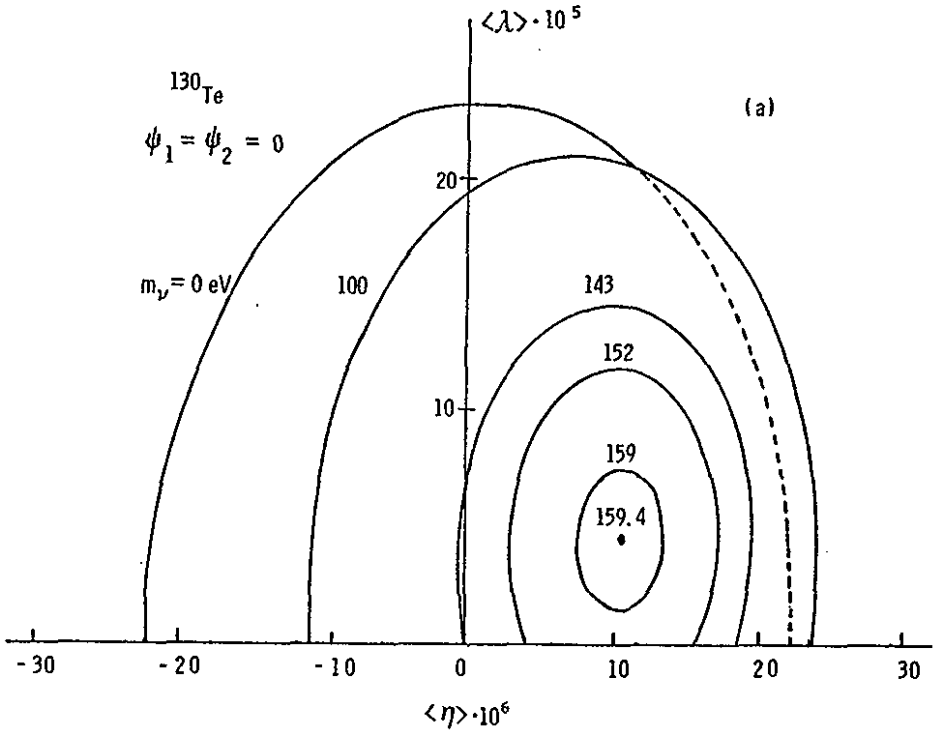
$\langle\lambda\rangle\cdot 10^5$
^{130}Te
$\psi_1 = \psi_2 = 0$
(a)
$m_\nu = 0$ eV
100
143
152
159
159.4
20
10
-30
-20
-10
0
10
20
30
$\langle\eta\rangle\cdot 10^6$

Fig. 8.6

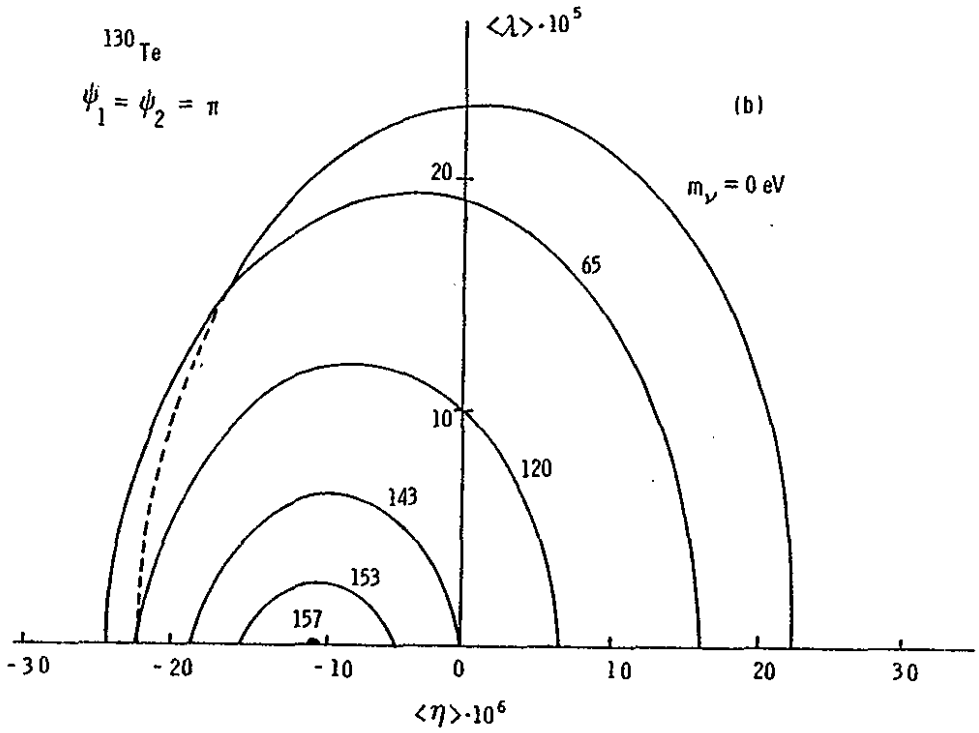

Fig. 8. 6

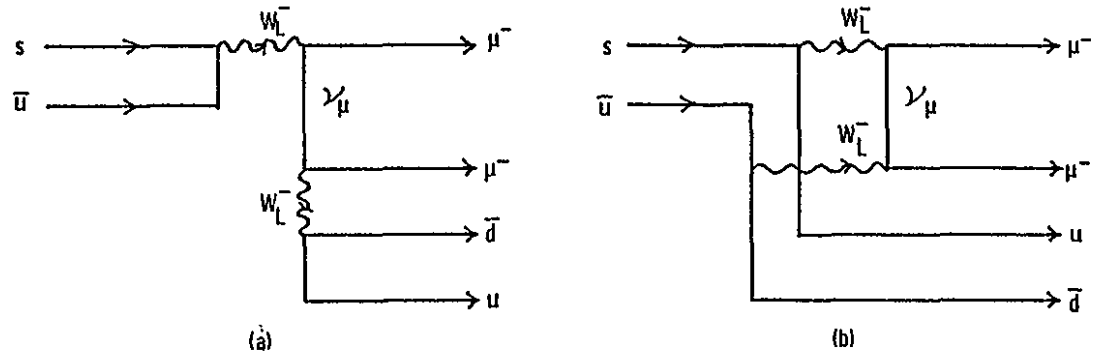

Fig. 11. 1

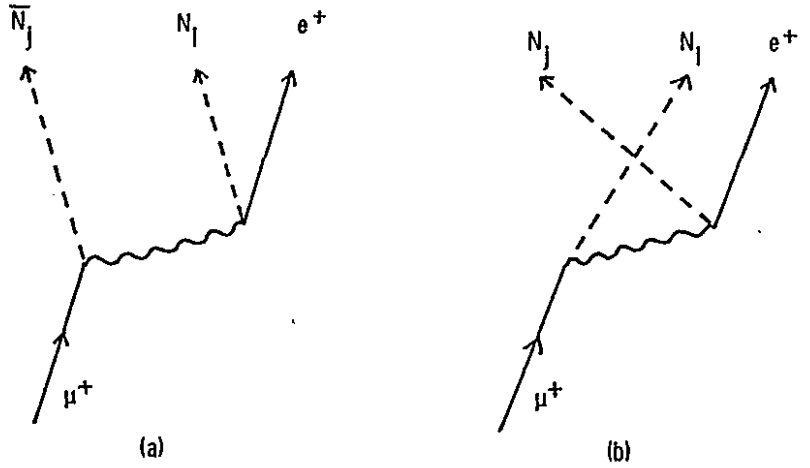

Fig. 11.2

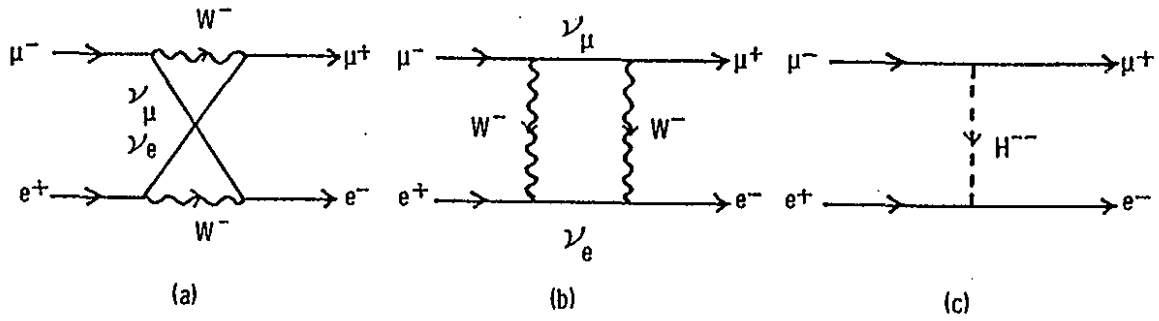

Fig. 11.3

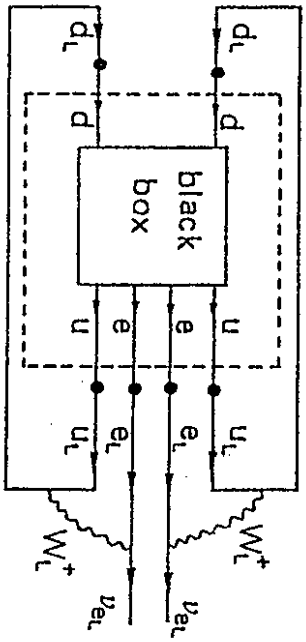
black box
d
u
e
d_L
u_L
e_L
W_L^+
ν_{eL}

Fig. A.1

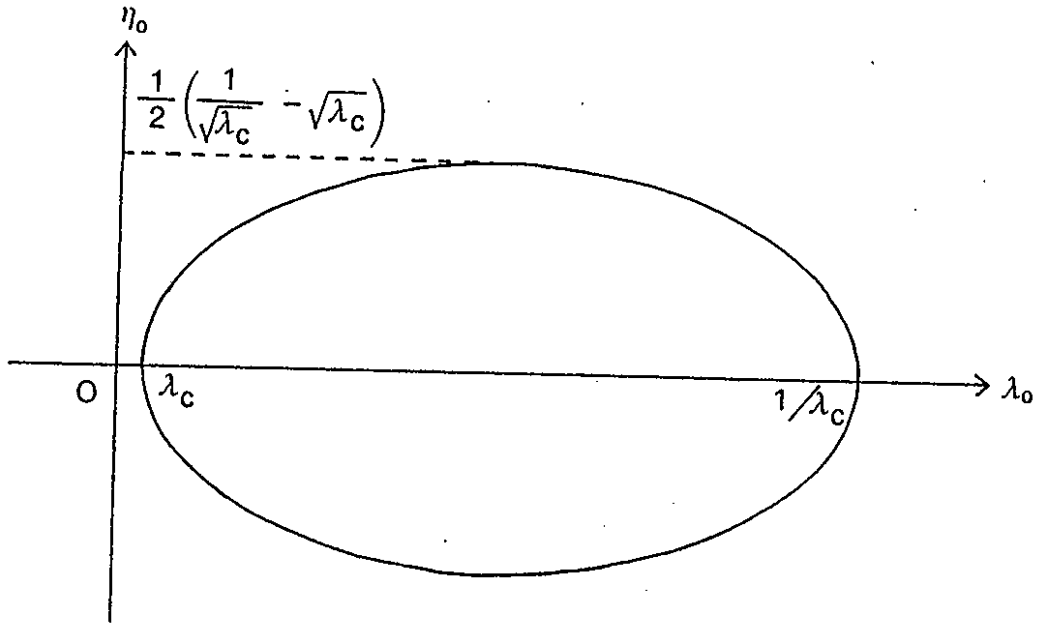
η_o
$\frac{1}{2}\left(\frac{1}{\sqrt{\lambda_c}} - \sqrt{\lambda_c}\right)$
O
λ_c
$1/\lambda_c$
λ_o

Fig. A.2

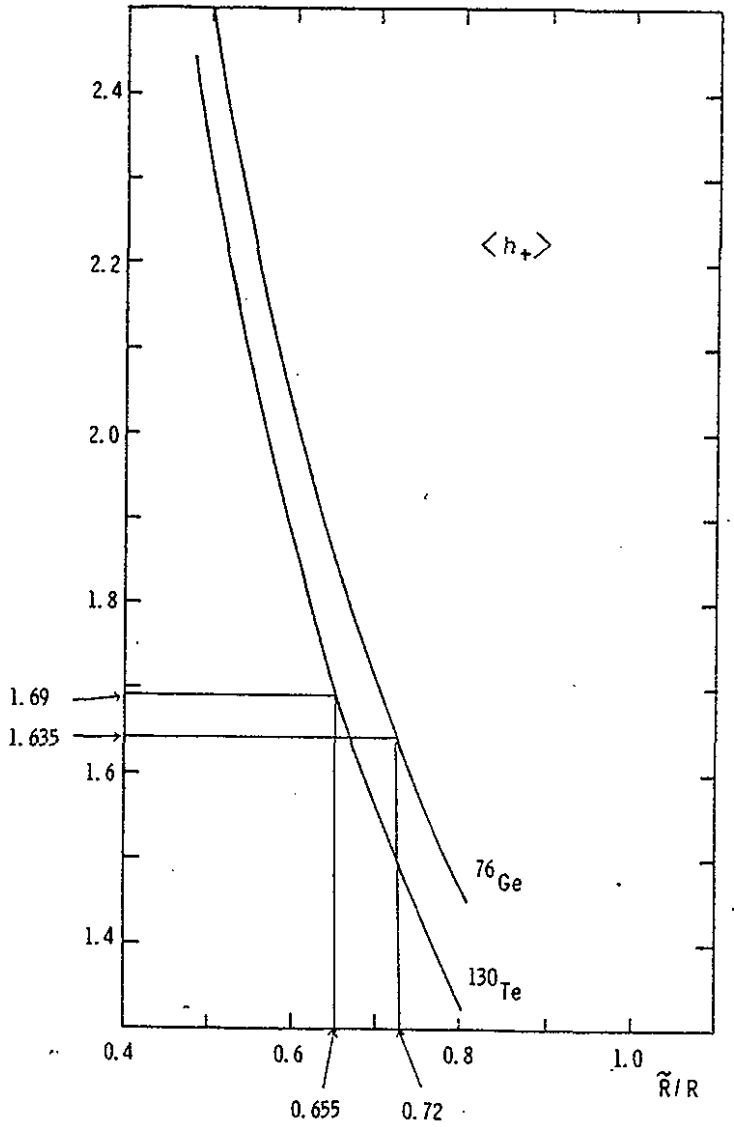
2.4
2.2
2.0
1.8
1.6
1.4
1.69
1.635
$\langle h_+ \rangle$
^{76}Ge
^{130}Te
0.4
0.6
0.8
1.0
$\tilde{R}/R$
0.655
0.72

Fig. E. 1

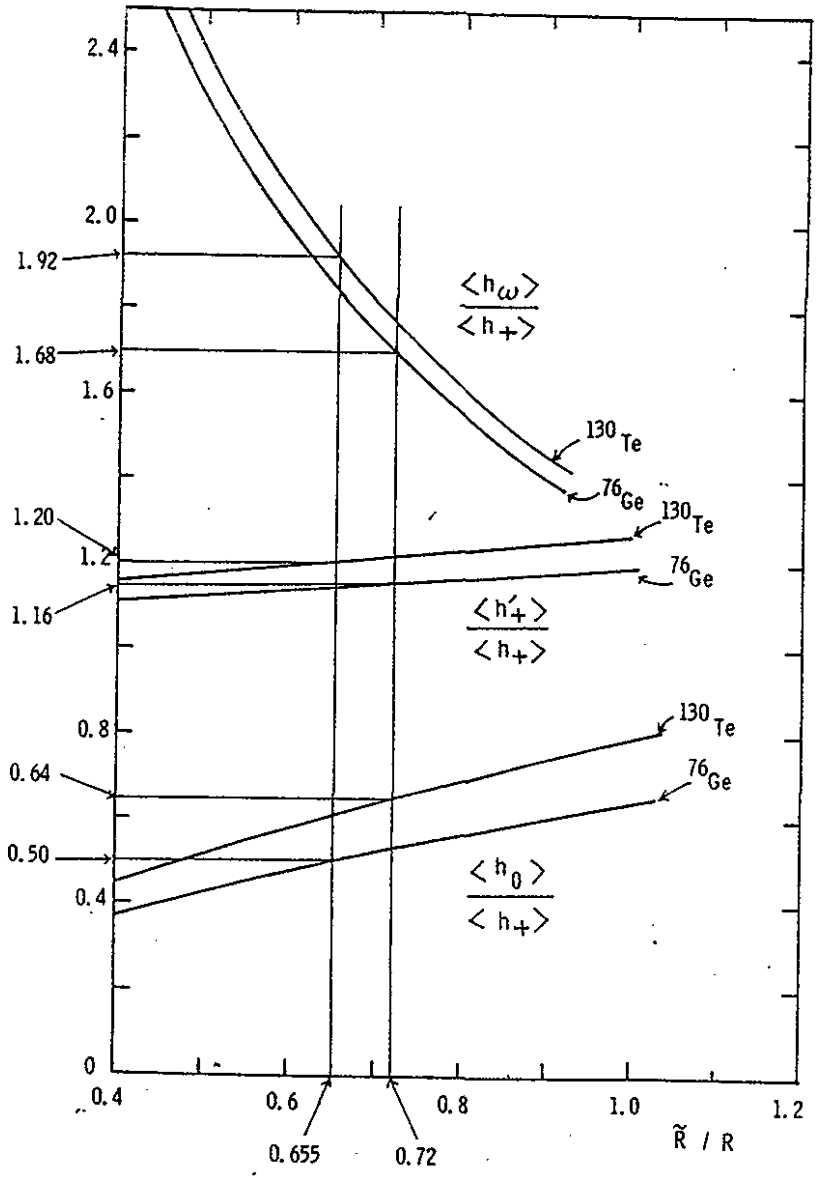
2.4
2.0
1.92
1.68
1.6
1.20
1.2
1.16
0.8
0.64
0.50
0.4
0
$\frac{\langle h_\omega \rangle}{\langle h_+ \rangle}$
^{130}Te
^{76}Ge
^{130}Te
^{76}Ge
$\frac{\langle h'_+ \rangle}{\langle h_+ \rangle}$
^{130}Te
^{76}Ge
$\frac{\langle h_0 \rangle}{\langle h_+ \rangle}$
0.4
0.6
0.8
1.0
1.2
$\tilde{R}/R$
0.655
0.72

Fig. E. 2

Note added: After submitting this review, we have received a preprint by the Tübingen-Jülich group[170] on the theoretical estimate of nuclear matrix elements appeared in the $(\beta\beta)_{0\nu}$ mode for ^{76}Ge. Their values of $M_{GT}^{(0\nu)}$, χ_F, χ_F', χ_{GT}' and χ_T' are similar to those by Haxton and Stephenson,[17] but the value due to the P wave effect, $\chi_P' = -0.218$, is opposite sign to $\chi_P' = 0.270$ by Haxton et al.[17] as shown in Table 7.5. They also evaluated the nucleon recoil term and obtained $\chi_R' = 0.403$ which is much larger than our estimate $\chi_R' = -0.021$ in Table 7.5. Note that the definition of χ_R' in their preprint is different from ours: $(\chi_R')_{our} = m_e R(\chi_R')_{Tübingen}$. They concluded that by their large value, the nucleon recoil term χ_R' dominates over the P wave term χ_P' and the much tighter bound on $\langle\eta\rangle$ was derived; $|\langle\eta\rangle| < 6\cdot10^{-8}$. Contrary to their new result, their previous paper[32] reported that χ_R' and χ_P' contribute destructively and moreover cancel each other completely. This means that their previous value seems to be $\chi_R' \sim \chi_P'/7.44 = -0.218/7.44 = -0.0293$ from Eq.(8.2.1) and Table 8.2, so that they obtained the much looser bound on $\langle\eta\rangle$. Since it is important whether the cancellation really occurs, we gave cautions in various places in this review.

Let us explain the origin of this sizable difference between their new value and ours. The neutrino potential h_R in χ_R' contains a singular part proportional to $\delta(\vec{r}_{nm})$, as seen from Eq.(3.4.15). In our evaluation, we have assumed that the relative distance between two decaying nucleons can not vanish, $\vec{r}_{nm} \neq 0$, because of the hard core and $\tau_n^+\tau_m^+ = 0$ for $n = m$. Therefore, the singular term $\delta(\vec{r}_{nm})$ did not contribute. In their new preprint, they assumed

the extended nucleon picture and thus the singular term gave the large contribution which dominated all others. Since the nucleon recoil term is important to get the information on $\langle\eta\rangle$, the further investigation is definitely needed.

We have also received a preprint by the Tokyo-KEK group[171] on the search of the heavy neutrino with the mass around 17 KeV which was reported by Simpson.[171] They made the precise measurement of the beta-ray spectrum of ^{35}S by using a Si(Li) spectrometer system. Their results were consistent with no heavy neutrino admixture and the upper limits for the mixing $\tan^2\theta \leq 0.3\%$ were determined in the mass range 10 ~ 50 KeV.

---

170) T. Tomoda et al., Tübingen preprint (1985).

171) T. Ohi et al., KEK preprint 85-17 (1985).